EXPLORATION OF POLYMER REPLACEMENTS FOR SF_6 IN CIRCUIT BREAKERS

Thesis submitted in accordance with the requirements of the University of Liverpool for the degree of Doctor in Philosophy

by

Ricky John Brookes

May 2010

ABSTRACT

Sulphur hexafluoride is a highly potent greenhouse gas that is primarily used in the power industry in switchgear. Its excellent thermal and dielectric properties mean that no equally effective environmentally friendly gasses exist. This thesis describes an investigation into the possible exploitation of micro-scale polymer particles in the circuit breaker arc quenching role. It was found that the complex interaction between arc plasma and polymer particles prompts mechanisms that enhance thermal energy extraction, which increases arc resistance and enables current interruption. The most significant quenching mechanisms were found to be: energy extraction from the polymer by their change of state and decomposition; increases in convective cooling and cool gas intermixing due to polymer reaction induced pressurisation; and improved thermal and dielectric properties of species around the arc due to polymer decomposition products.

CONTENTS

List of Figures

List of Tables

Acknowledgements

I would primarily like to thank my supervisor, Professor Joe Spencer, for giving me the opportunity to take part in this research and for his guidance and support throughout the project.

I would also like to express my appreciation to Dr. S. Taylor, Dr. H.M. Looe, Emeritus Professor G.R. Jones, Dr. A. Deakin, Mr. J. Humphries and the many members of the CIMS research group for their help throughout the course of this research.

I would like to acknowledge the contribution of the Engineering and Physical Sciences Council for supporting this project as part of the Supergen V program and like to thank the academic and industrial representatives for their interest in this work and their helpful opinions and ideas.

I would especially like to thank my parents, grandparents and brothers for their help and support over many years of study, and thank my girlfriend for her patience over the last few years of work.

Glossary

AC ..... Alternating Current
AEA ..... Atomic Energy Authority
AIS ..... Air Insulated Switchgear
CIGRE ..... International Conference on High Voltage Electric Systems
CO_2 ..... Carbon Dioxide
CTC ..... Complete Thermodynamic Equilibrium
DC ..... Direct Current
DP ..... Degree of Polymerisation
DSC ..... Differential Scanning Calorimetry
EPSRC ..... Engineering and Physical Sciences Research Council
GIS ..... Gas Insulated Substation
GWP ..... Global Warming Potential
HFC ..... Hydrofluorocarbon
HVDC ..... High Voltage Direct Current
IPCC ..... Intergovernmental Panel on Climate Change
LTE ..... Local Thermodynamic Equilibrium
M/Z ..... Mass to Charge Ratio
MCB ..... Miniature Circuit Breaker
NAEI ..... National Atmospheric Emissions Inventory
NIST ..... National Institute of Standards and Technology
PA6 ..... Polyamide 6
PBC ..... Polychlorinated Biphenyl
PE ..... Polyethylene
PFC ..... Perfluorocarbon
PMMA ..... Polymethylmethacrylate
PS ..... Polystyrene
PTFE ..... Polytetrafluoroethylene
PVC ..... Polyvinylchloride
RF ..... Radio Frequency
SEM ..... Secondary Electron Mutiplier

SF_6 ..... Sulphur Hexafluoride

TOFMS ..... Time of Flight Mass Spectrometer

UNEP ..... United Nations Environment Program

UNFCC ..... United Nations Framework Convention on Climate Change

VCB ..... Vacuum Circuit Breaker

VUV ..... Vacuum Ultraviolet

WMO ..... World Meteorological Organisation

Chapter 1

Introduction

CHAPTER 1 - INTRODUCTION

1.1 RESEARCH CONTEXT

Climate change is a growing issue both politically and socially. There is increasing focus on the effect that mankind has on the environment and the damage done by escalating industrialisation. One of the key issues regarding climate change is the release of greenhouse gasses into the atmosphere that lead to global warming. One of the most potent greenhouse gasses known is sulphur hexafluoride (SF_6), which is primarily used by the power industry as an insulating and arc quenching gas.

Sulphur hexafluoride is thousands of times more damaging to the environment than carbon dioxide and survives in the atmosphere for over three thousand years. The gas is increasingly popular for use in electricity switchgear due to its properties that allow smaller substations that are more suitable for citing in heavily populated areas and indoors. The 1997 Kyoto protocol of the United Nations Framework Convention on Climate Change set targets for its signatories to limit the release of environmentally harmful gasses, there are six gasses specified in the convention, one of which is sulphur hexafluoride [1]. The World Nuclear Association predicts the worldwide demand for electricity will double the 2006 level by 2030, reaching a predicted 33,265TWh [2]. This is due to increasing population, growing industrialisation of developing nations and an overall increased standard of living. In order to accommodate this, growing transmission and distribution obligations lead to an increase in electrical infrastructure, including SF_6 switchgear.

Sulphur hexafluoride is becoming increasingly popular in the power industry because of its excellent thermal and dielectric properties. This allows physically smaller substations, which are more convenient for citing in urban areas or indoors, at the present time there are no similarly performing alternatives.

1.2 RESEARCH OVERVIEW

This research is part of the Engineering and Physical Sciences Research Council (EPSRC) Supergen V program, a consortium of industrial and academic partners with the overall intention of improving the reliability and environmental sustainability of the power industry. Specifically, the objective of this research is to play a part in the development of future electrical plant that has the advantages of SF_6 switchgear but without the heavy environmental implications and so contribute to a more environmentally sustainable network.

Polymers are already commonly used in circuit breakers as nozzle materials to direct gas flow. Previous research has suggested the ablation of these polymers could play a part in arc control [3], however little is known of the complex interaction between the arc plasma and polymer material. Research is required to develop a fundamental understanding of the interaction and arc quenching mechanisms involved, such that they can be fully exploited in circuit breakers. Developing sufficient knowledge and experience at the fundamental level would then allow recommendations for future designs to be made that would enable the concept to be further developed.

To accomplish this, practical experimentation using circuit breaker type arc discharges was used along with various diagnostic apparatus. Polymer particulates were used so as to increase the reaction surface area, enhancing the interaction between polymer and plasma, thereby amplifying the arc quenching effects. Various types of polymer of different structures and compositions were selected to undergo test so as to gain a wide appreciation of the different mechanisms at work and move towards selecting the most efficient types of polymer quenchers for use in circuit breakers.

The development of a fundamental understanding of the complex particulate polymer-plasma interaction is an important stage in the longer-term development of the concept of polymeric circuit breaker interruption. This forms a foundation upon which further practical development work can be built.

1.3 THESIS CONTRIBUTIONS

The application of particulate polymers to arc plasma as a primary interruption medium has never been previously studied. This research has found that the interaction between micron-scale polymer particles and arc plasma causes mechanisms which enhance arc cooling, leading to increased resistance and subsequent current interruption. It has been found that the primary arc controlling features prompted by the polymer interaction are: turbulent changes of the arc physical shape; pressurisation effects leading to convective gas flows; arc induced polymer change of state leading to cooling; and the positive thermal and electronegative properties of polymer decomposition species.

This research has shown that polymers decompose in the arc to form mainly low molecular weight species due to the high plasma temperatures. The composition of chemical species around the arc generally consisted of monatomic polymer constituents, polymer chain fragments and the products of reactions between decomposition products and proximate gasses.

It has been found in this research that different types of polymer interact with the arc in distinct ways due to differences in structure and composition; as a result of this, the primary means of arc cooling differs between polymers. It has been found that vinyl and fluoropolymers cause effective cooling of the arc primarily by the processes of ablation and decomposition; it has also been found that polymers containing halogens produce a more electronegative post arc environment that can potentially lead to better dielectric recovery performance. Polyolefines were found to react with the plasma more violently, leading to arc cooling by convective gas flow and turbulence, as well as enhanced cool gas intermixing which can improve dielectric recovery. It was found that in an air environment, combustion of reactive hydrocarbons formed by polymer thermal degradation causes a significant volume of carbon dioxide to be formed. It is proposed that this may have a role in arc quenching due to superior thermal conductivity with respect to air and associated pressurisation effects.

1.4 THESIS STRUCTURE

This thesis describes the results of practical experimentation using polymer powders as arc quenching media in circuit breaker plasma discharges. The thesis is divided into a further seven chapters, which are outlined below.

In the next chapter a comprehensive literature review is made describing the scientific and political issues with SF_6 emissions from the power industry as well as the current research into alternatives, this forms a foundation of information that justifies the real world applications and relevance of the research. In **Chapter 3** a detailed background review describes all of the concepts and theory alluded to in the subsequent results and analysis, including information on dielectric breakdown and arc discharges; circuit breaker methodologies; polymer characteristics; as well as the operation and limitations of diagnostic apparatus. In **Chapter 4** the apparatus and methodology used in the experimentation is described in detail to enable an understanding of the way in which the results were obtained and how the polymer-plasma interaction was studied.

The experimental results are described in Chapters 5 and 6. **Chapter 5** describes the physical changes in the arc that occurred as a result of the polymer-plasma interaction in terms of electrical, morphological and pressurisation effects. In **Chapter 6** the results of atomic spectroscopy of the arc are described in terms of optical emission and mass spectroscopic analysis with the aim of understanding the influence of polymer micro-particles on the arc plasma. A comprehensive discussion is made in **Chapter 7**, where all of the results and analysis are brought together to form an overall impression of the polymeric arc quenching phenomena. Finally, in **Chapter 8** the main findings are combined to form a conclusion that fundamentally describes the main polymer arc quenching mechanisms. Given the knowledge and experience gained during the course of the research, recommendations for future work necessary to develop the concept are also made.

Chapter 2

Literature Review

CHAPTER 2 – LITERATURE REVIEW

2.1 SULPHUR HEXAFLUORIDE AND THE ENVIRONMENT

Sulphur hexafluoride is a synthetic greenhouse gas that is primarily used in power switchgear due to its excellent thermal and dielectric properties. Emissions of SF_6 contribute to climate change and consequently an alternative for this gas in the power industry is sought.

The Intergovernmental Panel on Climate Change (IPCC) was established by the World Meteorological Organisation (WMO) and the United Nations Environment Program (UNEP) in order to provide an objective and fair source of information on climate change [4]. The Fourth Assessment Report of IPCC Working Group I showed that human made PFCs, HFCs and SF_6 are very effective absorbers of infrared radiation [5]. Radiative forcing (RF) is the net difference in the incoming and outgoing radiation through the Earths atmosphere; it is used by the IPCC as the main measure of the global warming impact of a gas [6]. Gasses that contribute to positive radiative forcing, including SF_6, are those that lead to global warming.

The global warming potential (GWP) of a species is a measure of its contribution to climate change relative to carbon dioxide [7]. The UNFCCC data of the global warming potential of SF_6 over time is shown in Table 2-1. In all cases, the environmental impact of SF_6 is tens of thousands of times greater than that of CO_2, highlighting the atmospheric impact of the emission of such gas.

Table 2-1: Global warming potential of SF_6 with time [8]

GWP (CO_2 = 1)		
20 Years	100 Years	500 Years
16,300	23,900	34,900

The carbon dioxide equivalent of SF_6 is calculated by multiplying GWP by the ratio of atomic weights of carbon and CO_2 (12/44) [9]. Using this calculation, it can be found that 1t of SF_6 has the equivalent environmental impact of over 6,500t of CO_2. This means that even relatively small emissions of SF_6 from individual electrical plant can combine to have a significant cumulative effect on global warming.

The use of GWP by the IPCC as a means of comparing the relative effects of different types of gas on the environment is argued in some instances to be too simplistic because it does not take into account the complexity and non-linearity of the Earths atmospheric chemistry [10, 11, 12]. It is argued in some cases that GWP is not suitable because it was adapted from research on the behavior in the atmosphere of halocarbons [13], which behave in a more linear manner than other greenhouse gasses. Other criticism regards the relationship with CO_2 as the reference gas, reasoning that CO_2 itself behaves in a complex way, which has not been taken into account in the GWP calculation [14]. Although there is some debate in the scientific community over the precise definition of global warming potential, a detailed analysis into this is beyond the scope of this project. It can be considered that in this case the United Nations definition is appropriate and from this it is clear that SF_6 is significantly damaging to the environment this justifies the need to find a replacement.

Another important aspect that affects the impact of global warming gasses is atmospheric lifetime. Most industrial gasses released into the atmosphere, including CO_2, have relatively short lifetimes due to reactions with oxidants or photolyzation (molecular breakdown due to light). Fluorinated gasses such as SF_6 have low reactivity in the atmosphere and consequently may exist there for thousands of years. It is commonly stated in most literature, including that from the IPCC, that SF_6 has a typical lifetime in the atmosphere of 3,200 years [16, 17], other studies give the lifetime of SF_6 as 1937 +/- 432 years [18]. By way of contrast, CO_2 has an atmospheric lifetime of 50-100 years [20].

2.2 POLITICAL INTEREST

The level of SF_6 currently rises in the atmosphere at a rate of 5% per year [19]. Given the global warming impact and long atmospheric lifetime of the gas, the impact of SF_6 on global warming is becoming more significant and this has caused growing political interest.

The Kyoto protocol of the United Nations Framework Convention on Climate Change (UNFCCC) introduced targets for 37 industrialised nations that commit them to reducing emissions of greenhouse gasses by set and legally binding amounts. The environmental impact of the six gasses included in the Kyoto protocol is shown in Table 2-2, and shows SF_6 to be the most damaging.

Table 2-2: Properties of Kyoto greenhouse gasses [20]

Greenhouse Gas	Global Warming Potential (100 years)	Atmospheric Lifetime
CO_2	1	50-100
CH_4	21	12
NO_2	310	120
SF_6	**22,800**	**3200**
HFC's	140 – 11,700	6.6 – 264
PFC's	6,500 – 9,200	2,600 – 50,000

The European Commission began proposing legislation in 2003 to regulate fluorinated gas emission in order to help the EU meet its Kyoto commitments. The EU is required to reduce its greenhouse gas emissions by 336 million tonnes of CO_2 equivalent by 2012 (the end of the first commitment period) [21]. In 1995 the EUs fluorinated gas emissions were 65 million tonnes of CO_2 equivalent, which unchecked would mean emissions of 98 million tonnes of CO_2 equivalent in 2010 [22]. The 2009 UN Climate Change Conference did not result in new, binding emissions targets due to difficulties in negotiation. However, the non-binding 'Copenhagen Accord' encourages emissions targets to be submitted by countries and may potentially lead to firmer commitments in future, such as at the 2010 UN Climate Change conference in Mexico.

2.3 EMISSION AND MITIGATION

The amount of SF_6 in the atmosphere is increasing due to its continual emissions and long lifetime. High precision observations taken in the northern and southern hemisphere, in Antarctica and Tenerife respectively, showed that between 1970 and 1992, the amount of SF_6 in the atmosphere increased by two orders of magnitude [27]. By extrapolating this data with a quadratic curve, researchers found that the expected growth in SF_6 at that time was at a rate of 8% per year. Current data suggests an increase in atmospheric SF_6 of 5% per year [22]; which is lower than the Antarctica and Tenerife observations due to the implementation of SF_6 reduction strategies that came about in the mid 1990s. The change in annual atmospheric sulphur hexafluoride emissions since 1970 is highlighted in Figure 2-1.

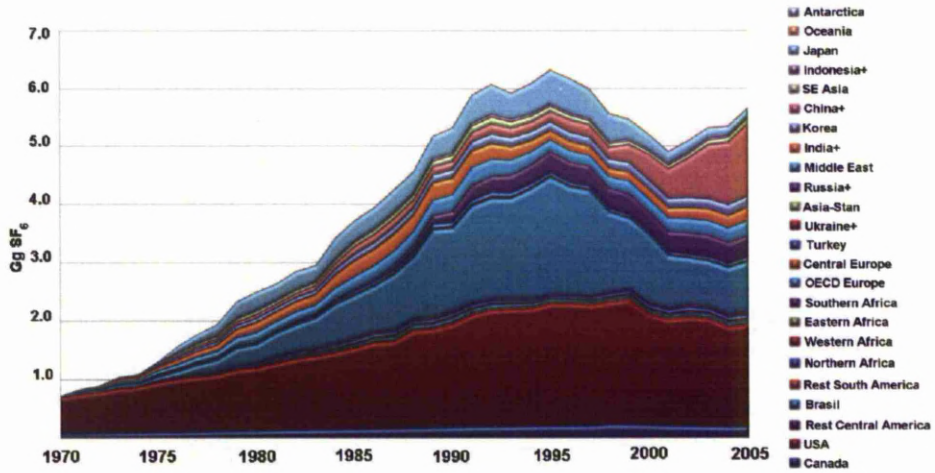

Figure 2-1: Change in atmospheric SF_6 release between 1970 and 2005 [15]

The global power industry uses 80% of all the SF_6 manufactured worldwide [28], and so it must shoulder the main burden of responsibility in reducing atmospheric leakage. Other uses of SF_6 and therefore sources of emission are from magnesium casting and insulation for windows; however the use of SF_6 in non-industrial roles is becoming rarer due to legislation.

In general there are four stages whereby SF_6 may be released into the atmosphere from electrical plant: in manufacture; during commissioning; from leaks during operation/maintenance; and from end of life destruction.

It is argued from some elements of the power industry that there is no need to replace SF_6 gas from electrical power infrastructure. In general there are two strands of argument against SF_6 replacement. The first is that the environmental impact of the gas is disputed; the second is that the environmental impact is acknowledged but it is argued that leakage is so small so as to not be significant. Research by the SF_6 switchgear manufacturer ABB claims that SF_6 contributes only <0.001% to the greenhouse effect and $<10^{-7}$ to stratospheric ozone destruction [23]. Similarly, research by CIGRE (Conference Internationale Des Grands Reseaux Electriques a Haute Tension/ International Conference on Large High Voltage Electric Systems) Working Group 23-10 argues that SF_6 does not contribute to global warming [24]. However, both sets of research only consider ozone depletion – of which SF_6 does not have a significant effect. The reason for this is because the constituent fluorine in SF_6 does not interact with O_3 due to its affinity with hydrogen. The major impact of SF_6 on the environment is via radiative forcing, which is not mentioned in the previous research. The studies also did not consider the cumulative effect of SF_6 on the environment.

In some cases it is argued that the release of SF_6 is sufficiently small so as to not be a significant problem. Research conducted using computational simulation compared leakages of SF_6 from AIS (145kV/63kA and 145kV/31.5kA) and GIS (145kV/40kA and 72.5kV/40kA) switchgear in normal service over a 20 year period [26]. It was found that for AIS switchgear, SF_6 losses contributed 10% to the global warming effect and for GIS SF_6 leakage contributed 30% to its global warming effect, concluding that the main contributor to climate change from circuit breakers was actually energy losses through inefficiency.

The United States Environmental Protection Agency found in a study of SF_6 leakage rates from newly manufactured circuit breakers [28] that of 2,329 circuit breakers between 1998 and 2005, 7.3% were classified as leaking. The study only considered leakages that triggered alarms, which only operated after a 10% loss of gas. Losses of less than 10% were not taken into account but would almost certainly drive up the overall leakage figure. It is argued in research by EDF Energy in France that the end of life disposal stage of switchgear, as opposed to in service, causes the most SF_6 losses and greatest environmental damage [25]. This is compounded by the fact that in future many electricity networks worldwide will require massive SF_6 switchgear replacement. It must also be noted that the most common way of disposing of SF_6 when decommissioning switchgear is incineration, which releases the harmful gas sulphur dioxide (SO_2).

The largest user of SF_6 in the UK is National Grid. The total amount of SF_6 lost through leakage by National Grid in 2007/08 was 14.53t [33], 3% of the total SF_6 inventory (422.32t) and the equivalent of 94,709t of CO_2. Due to the extremely high global warming potential of SF_6 and its accumulation in the atmosphere over thousands of years, these losses are a problem. The total SF_6 emissions from the UK between 1990 and 2006, estimated by the Atomic Energy Authority (AEA) an behalf of the National Atmospheric Emissions Inventory (NAEI) were 885.3t of SF_6 [34, 35], this corresponds to a CO_2 equivalent of over 5 million tonnes; all of which is still in the atmosphere.

Due to the lack of SF_6 replacements currently available, the favored approach by industry is the enhanced management of SF_6 in switchgear in order to reduce losses. A number of leak detection and mitigation systems have been developed and are in use with utilities worldwide [30,31,32]. Consolidated Edison in the USA in 2005 reduced its SF_6 emissions by 26% over its 5% per year reduction targets by the use of passive optical SF_6 detector cameras along with the priority deployment of new techniques in leak sealing [30]. Other types of SF_6 detectors used elsewhere use negative ion capture probes to analyse the type and quantity of gas around the apparatus [32].

Some leak monitoring involves the application of helium to systems to monitor output in conjunction with high precision leakage detectors, coupled with timely repairs to faulty equipment [36]. The disadvantage of leak detection and mitigation schemes is that they require manual operation and systematic surveying of the apparatus. This means leaks can only be detected during scheduled checking periods and also depends on the thoroughness of the operator.

Throughout the world there are increasing practices involved with SF_6 leakage reduction. In Germany leakage is minimised by improved SF_6 gas handling techniques at all stages of the switchgear lifecycle involving agreed targets, designated best practice for gas handling by SF_6 users and annual monitoring of emissions using the IPCC guidelines [37]. Until recently in China there was no government regulation or policy to control the emissions of SF_6 [38] and therefore was no real incentive to prevent losses. China manufactured 2,500t of SF_6 in 2005 (for all industries), of which 2,000t was used domestically [39]. Due to a 50% increase in electricity grid investment in 2006, the demand for SF_6 in China is expected to double domestic consumption. Analysis of Figure 2-1 shows that the post-2000 increase in atmospheric SF_6 was in large part due to increased emissions from China. The Australian government is committed to reducing its 1990 levels of greenhouse gasses by 2012 [40]. The measures used in Australia involve the development of best practice guides for the handling of SF_6 and guidelines on the reporting of SF_6 emissions. One of the emerging issues in Australia and worldwide is the disposal of sealed for life SF_6 units, these units have less operational leaks but are more difficult to dispose of.

The growing seriousness that utilities companies and governments are taking on the issue of SF_6 in recent years shows that it is becoming more and more of a concern. This means that there is a growing and increasingly urgent demand for the development of an effective alternative.

2.4 ALTERNATIVES TO SF_6 IN SWITCHGEAR

Mitigation of SF_6 leakage from power apparatus is a short term solution and does not completely eradicate release of the gas into the atmosphere. A more effective solution is to develop an alternative with the same advantages but without the environmental implications. Various types of research have been carried out with this intention, but to date no alternative has been developed.

2.4.1 OTHER GASSES

The plasma quenching efficiency in terms of temperature reduction of N_2, CO_2, O_2, air, He and H_2 gasses injected into thermal plasmas has been studied [42]. The best result found that 10% CO_2 caused a temperature decay equivalent to 2% SF_6, not sufficient to act as a replacement. The gas trifluoroiodomethane (CF_3I) has been studied because it has a higher dielectric strength than SF_6 but with a lower global warming potential (5), and shorter atmospheric lifetime [43]. The disadvantage of CF_3I is that at GIS pressures the boiling point of the gas is 25°C, so cannot be used in its normal state [44]. In order to use CF_3I in GIS, a mixture of 30%-70% CF_3I-CO_2 has been researched, which has a more practical boiling point of -12.5°C [45]. This gas mixture performance was 67% that of SF_6 for a breaker terminal fault and 32% that of SF_6 for a CF_3I-N_2 mixture. The performance and practicalities of operation mean Trifluoroiodomethane cannot be considered as a realistic alternative. In other research, 35 electronegative gasses were tested and many found to have dielectric strength greater than that of SF_6, but were restricted for use in switchgear due to the more limited pressure range they could operate in [46]. The most notable results showed that CF_3CN exceeded SF_6 in its insulating capability down to temperatures of 248K at its maximum usable pressure. At 202kPa, C_2F_5CN, $CF_3C{\equiv}CCF_3$ and CF_2Cl-CF_3 had better insulating performance than SF_6. It was found that at higher pressures (>> 202kPa) C_2F_6, CF_3Cl, CHF_3, CF_3NO and CF_4 can become competitive with SF_6 but for reasons of economy are not likely to be practical, for example C_2F_6 would need to be operated at 973kPa at 248K to exceed that of SF_6.

2.4.2 SF_6 GAS MIXTURES

For environmental and economic reasons, SF_6 gas mixtures have been developed that use lower percentage compositions of SF_6 along with environmentally benign gasses such as N_2. Using gas mixtures means the amount of SF_6 in the apparatus is minimized and consequently so is the amount of environmentally harmful gas released. The National Institute of Standards and Technology (NIST) have found that a mixture of SF_6 and nitrogen may be suitable for insulation and a mixture of SF_6 and helium potentially being used for circuit breakers [41].

2.4.3 VACUUM CIRCUIT BREAKERS

Vacuum interruption is a possible alternative to SF_6 and has become more popular in recent years. In Japan vacuum circuit breakers (VCB) are in the mainstream for distribution networks [47], especially pole mounted switches, which are used in large numbers. However, it has proved troublesome to develop VCBs for high voltage applications due to the difficulty in conducting heat away from the arc in a vacuum. The development of operational VCBs for networks above 168kV is limited by thermal conductivity and voltage-withstand capability compared with SF_6 gas [47]. Experimentally, it has been shown possible to connect two HV VCBs for application in transmission systems designed to interrupt a 40kA fault current in a 168kV system [48]. In China, a prototype 126kV, 2kA single break vacuum circuit breaker has been developed with a 40kA short circuit breaking current [49]. In order to enhance the environmental friendliness of the design, silicone oil was used as the external insulation as opposed to SF_6. As an alternative to silicone oil, compressed dry air has been suggested for external insulation [50]. An experimental 550kV VCB involving the connection of four interrupters serially has also been tested [51]; however the cost of this type of arrangement would currently be too prohibitive for utilities companies to use.

2.5 POLYMERS IN CIRCUIT BREAKERS

Research into nozzle ablation in high voltage circuit breakers has suggested that the ablated material may play a role in arc control [52]. Experiments carried out using a circuit breaker unit of 145kV and 60kA using various configurations of close fitting polytetrafluoroethylene (PTFE) sleeve around the electrode gap showed that although SF_6 remained superior, the PTFE sleeve with N_2 and CO_2 gas did perform in a manner approaching that of SF_6 at low pressures [53].

The magnitude of ablation of PTFE nozzles depends on the overall arc energy and research has shown that the main processes of heat loss from the arc were due to ablation from the radiation flux on the nozzle walls [54]. Investigations into the effect of the type of ablated material on dielectric recovery of a molded case circuit breaker voltage have been made [55]. It was found that Polyamide 6/6 (PA 6/6) and polyoxymethylene (POM) prompted a better recovery voltage performance than the reference ceramic (alumina) due to the larger pressurisation causing increased gas flow and faster deionization.

Computational investigations into the properties of ablated vapors of polymethylmethacrylate (PMMA), PA 6/6, polyethylene terephthalate (PETP), polyethylene (PE) and polyoxymethylene (POM) and the effect this has on the conduction of the arc have been made [56]. It was found that there were few polyatomic molecules at higher temperatures due to temperature related dissociation. This meant that at higher temperatures there were few molecules around the electrode gap that may have had a role in effecting electronegativity or temperature conduction. Research has also been carried out using the Chapman-Enskog method of computational simulation in the context of a plasma torch configuration with an argon carrier. The research calculated approximations of values of viscosity, thermal and electrical conduction, density, enthalpy, heat capacity and sonic velocity for PTFE, PMMA and PVC vapour [57,58] . It was found that PMMA caused the largest temperature decay due to having the highest specific heat of those polymers tested and therefore had the best plasma quenching efficiency.

In lower voltage experimental miniature circuit breakers (MCBs) and expulsion fuses the pressure rise caused by solid polymer wall ablation has been studied. Expulsion fuses have been used to interrupt low current [59] relying on the ablation of wall material in the presence of the arc to create a pressure rise and an intermixing of gasses that cool and de-ionize the gap. It has been found that the arc quenching ability of the surrounding material depended on several factors: the quantity and species of gas evolved; the endothermic nature of the reactions; the degree of turbulent intermixing; and the dielectric integrity of the gas formed [60]. In other research based on the arc interruption characteristics of polymers in expulsion fuses [61] it was found that the most promising materials were the cellulosic and polyacetal groups of polymers due to their production of large quantities of arc cooling gasses CO and H_2. The formation of these gasses is highly endothermic and so was effective at removing energy from the arc and electrode gap and hence quenching the arc.

Research into miniature circuit breakers has shown that the presence of polyester wall materials caused an increase in pressure with respect to ceramic, which aided in arc interruption [63]. A concern with using ablative wall materials was that vapour could settle on the electrodes and cause an increase in contact resistance and heat generation; however, it was found that this was not the case. Polyethylene ablation stabilized arcs have been studied with the intention of establishing the main factors in the ablation extinguishment process. It was concluded that the strong radiative aspect, more than two orders of magnitude higher than that of an air arc, coupled with the increased axial gas flow, was the main mechanism for energy loss from the arc [63]. Different research into ablation in MCBs tends to differ in terms of the significance placed on the effect of turbulence on interruption. Some studies found that turbulence played a part in the arc cooling effect [64] caused by the plasma-polymer interaction whereas in other papers arc is said to be more laminar in nature [65, 66]. The reason for this disparity could be due to the level of current used, with higher current arcs being more laminar.

Simulations have been conducted with argon thermal plasma torch configurations with the injection of PTFE finding that polymer injection reduced the plasma temperature [67], temperature reduction was also found to be enhanced by reducing the powder size or increasing the powder feed rate. Further simulations have been made using POM, PE and PMMA [68], and PTFE, PMMA, PE and POM [69] respectively. The arc temperature was found to decrease following powder injection, with PMMA having the most significant effect. These results corroborate those of the research mentioned previously that used solid polymer walls [58]. Polymers with higher values of specific heat over the other polymers for a given temperature were found to quench the arc with the greatest efficiency in the computations due to increased convection loss. A limitation with this research was that the thermal and transport properties of the ablated vapour were temperature and environment dependant and the argon ICTP configuration was of low energy and formed an arc only millimetres in length using an argon carrier gas; this did not accurately represent the type of arc evident in a high voltage circuit breaker.

The interaction between arc plasma and polymers is highly complex and currently there is only a limited understanding of the processes involved. So that polymers can be exploited for arc control in circuit breakers it is important to develop an understanding of the significant underlying quenching processes.

2.6 SUMMARY

Sulphur hexafluoride has a global warming potential 23,900 times that of CO_2 and a lifetime in the atmosphere of 3,200 years. There is an increasing amount of interest in the release of SF_6 and consequently growing legislature from organisations such as the EU and UN regarding limiting release. This has placed increasing pressure on the power industry to halt emissions.

At the present time there are no alternatives to SF_6 that provide the same advantages but without the environmental cost. For this reason, the power industry has focussed on mitigation schemes with the intention of minimising release whilst still enabling the use of the gas. These strategies mainly involve various leak detection and repair techniques, however it was shown that no scheme was completely effective and research has shown atmospheric SF_6 to continue to increase.

Previous research into finding replacements for sulphur hexafluoride has not been successful. Various gasses have been tested but none has been found to be as effective as SF_6 without the environmental implications. This has prompted the necessity to research less conventional means of circuit breaker interruption without SF_6.

Research into the behaviour of polymers in response to electric arcs has mainly focussed on polymer nozzle ablation and in particular the influence of ablated polymer vapour on arc control. In general it was found that ablated polymer vapour has an influence on arc quenching but little is known of the complex underlying mechanisms. In order to fully exploit the polymeric arc quenching phenomena for circuit breakers, research is necessary so as to improve knowledge of the mechanisms involved.

Chapter 3

Background

CHAPTER 3 - BACKGROUND

3.1 INTRODUCTION

The intention of this chapter is to provide background information on the principles of arc formation, extinguishment, plasma diagnostics and properties of polymers in the context of circuit breakers. The first section describes the ionisation and breakdown of gaseous media that lead to the formation of arcs between circuit breaker electrodes, which prevent proper circuit isolation. Subsequently the main processes of extracting energy from the arc in order to accomplish the change from conductor to insulator are described followed by an overview of different types of circuit breaker including oil, air, SF_6 and vacuum. Background information on the optical, chromatic and mass spectroscopic techniques utilised in this research are given to enable the reader to appreciate the advantages and limitations of the techniques when appraising the later results. Finally, the structure and properties of polymers are described with explanations of the main characteristics and terminology, particularly focussing on the polymers used in this investigation.

3.2 CONDUCTION AND BREAKDOWN OF GASSES

In the presence of strong electric fields gas molecules can become ionised and made to conduct. This is a particularly important consideration in circuit breakers, which are specifically designed to isolate an electrical circuit for maintenance or in the event of a fault. For this reason the design of circuit breakers is not merely the trivial act of mechanically separating two electrodes, but requires detailed consideration of the physics of the arc in order to incorporate methods of successful and lasting extinguishment that must act within a very short period of time.

3.2.1 IONISATION PROCESSES

In certain circumstances an electron may gain enough energy to be liberated from its parent atom or molecule, leaving a separate electron and a positively charged ion. Inside an electric field, the charged particles can then be made to conduct. There are several processes by which a gas may become ionised in circuit breakers, and these will now be discussed.

3.2.1.1 Collision Ionisation

The collision between a free electron and a neutral atom or molecule can lead to ionisation if the electron carries energy that exceeds the ionisation potential of the atom or molecule, this is summarised in 3-1.

$$e^- + A \xrightarrow{\varepsilon > V_i} e^- + A^+ + e^- \qquad (3\text{-}1)$$

Where:

ε – Energy of electron
A – Neutral atom/molecule
A^+ – Positive ion
e^- – Electron
V_i – Ionisation potential of A

Any free electrons within the electric field between open circuit breaker electrodes gain kinetic energy and are accelerated toward the anode. During this translation, the electron may undergo collisions with the surrounding neutral molecules and if there is enough kinetic energy involved ionisation of the neutrals will occur, forming more free electrons. Further ionising collisions produce additional free electrons, which are in turn accelerated leading to significant growth in electrons crossing the gap. Positively charged ions are also subject to movement in the opposite direction to the free electrons but are less likely to carry enough kinetic energy to cause ionisation due to their size.

3.2.1.2 Photo-Ionisation

If an atom or molecule absorbs electromagnetic radiation with energy greater than its ionisation potential, an electron can be liberated. As there is an association between wavelength of radiation and energy, a relationship can drawn, shown in 3-2.

$$\lambda \leq c.\frac{h}{V_i} \tag{3-2}$$

Where:

λ – Wavelength (nm)
h – Planks constant ($6.626\times10^{-34} J.s$)
c – Speed of light ($3\times10^{8} ms^{-1}$)
V_i – Ionisation potential of atom (eV)

Higher frequency radiation carries more energy; therefore, atoms with higher ionisation energy would require higher frequency radiation to be ionised. The proportion of radiation emitted from plasma in the vacuum ultra-violet (VUV) region has been shown to be a significant contributor to the ionisation of surrounding materials, such as polymeric nozzles [70].

3.2.1.3 Electrode Electron Emission

Ions in the electric field gain kinetic energy and if they reach the cathode may transfer this energy to the electrode material. In solid materials, the energy required to liberate electrons from the surface of the material is known as the work function. If the energy transferred from the positive ion exceeds the work function of the electrode material electrons may be liberated. Any remaining energy will go into adding kinetic energy to the liberated electron and to heating the surface of the electrode.

This type of emission can also occur due to photo-ionisation if the energy of the radiation exceeds the work function of the electrode material. The minimum, 'threshold frequency', of the incident radiation that can cause ionisation, is found from Equation 3-3:

$$\nu = \frac{\varphi}{h} \tag{3-3}$$

Where:

ν – Frequency (Hz)
φ – Work function of electrode material (J)
h – Planks constant ($6.626 \times 10^{-34} J.s$)

Electrons may also be emitted from the electrode by the impact of metastable particles. Metastable particles are excited (energetic) with lifetimes much longer than normal particles. If their energy exceeds the work function of the electrode material they can cause electron emission. There are also similar processes if neutral atoms with high kinetic energies impact the surface of the electrode.

3.2.1.4 Electron Attachment

Free electrons in the electrode gap may become attached to molecules that have an electron affinity. Particles with such characteristics have vacancies in their outer electron shells that mean electrons can be attached forming negative ions.

$$A + e^{-} \rightarrow A^{-} \tag{3-4}$$

Where:

A – Atom with electron affinty
e^{-} – Electron

The dielectric gasses used in circuit breakers tend to be composed electronegative molecules. The electron attachment process removes free electrons from the electrode gap meaning they cannot conduct and prevents them from performing further ionising collisions, reducing the overall number of free electrons in the gap. The negative ions formed by electron attachment are heavy and low in mobility and so do not attain enough energy to make ionising collisions.

The reason why molecules in electronegative gasses have an electron affinity is due to the strong attraction of their positively charged nucleus [71]. The electronegativity of a species is described by a relative quantity on the Pauling scale, which generally increases across the periodic table, with fluorine being the most electronegative with a value of 3.98 units [72].

3.2.2 FORMATION OF ARCS

In the past, the most commonly accepted hypothesis on the formation of arcs was the Townsend theory; however it was found to have limitations that led to the development of streamer theory.

Townsend theory of current growth describes a process dominated by collision ionisation. Townsend current growth shows the average current in the gap as a function of the number of ionising collisions and gap distance. The initial electron avalanche causes further secondary avalanches due to additional electrons being liberated – a 'snowball' effect.

The Townsend theory is intuitive but was found to have two main drawbacks. Firstly, it does not consider the effects of pressure in the electrode gap and so is only valid for low pressures of less than 133kPa. As well as pressure, the Townsend theory predicts the time lags before breakdown – caused by the time taken for ionisation processes to occur – to be much longer than those observed in reality. As both of these factors notably affect the breakdown process it was necessary for streamer theory to be developed.

Streamer theory predicts the liberation of an electron from the cathode, which then moves in the electric field. This starts an electron avalanche due to the continual ionising collisions and consequent liberation of more electrons that repeat the process. The low-mobility positive ions formed by ionising collisions remain in the gap and form a space charge, enhancing the field. Photo-ionisation in the space charge region liberates further electrons that then form secondary avalanches.

Secondary avalanches form further positive ions that add to the original number and cause the space charge region to extend from the anode to the cathode – a streamer. At the instant the streamer approaches the electrode, a cathode spot forms, liberating a stream of electrons to neutralise the positive streamer space charge – this is a spark breakdown, shown graphically in Figure 3-1.

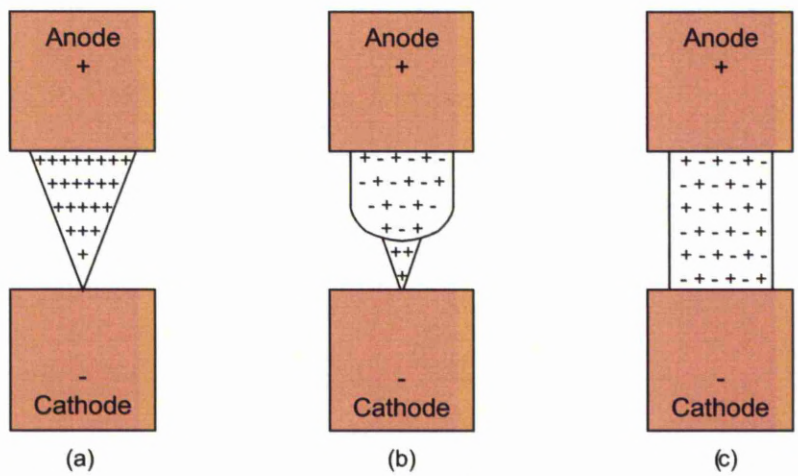

Figure 3-1: Formation of a cathode streamer [73]

(a) avalanche has crossed the electrode gap

(b) streamer crosses over half of the gap length

(c) gap crossed by a conductive channel

After the initial breakdown, glow and arc discharges occur depending on the current flowing. As the current increases, a glow discharge forms, develops into abnormal glow and above 1A transitions into a very high temperature and very high current density arc discharge.

An arc discharge is in the plasma state, which consists of a high density of energetic ions and electrons. The mixture of electrons and ions extending across the electrode gap means a conductive path is present between the electrodes and proper circuit isolation is not achieved.

The amount of ionised particles available in the gap (and therefore conductivity) is related to temperature. As a result of this, the main method of arc quenching incorporated in circuit breakers is rapid cooling of the arc and post arc electrode gap in order to reduce ionisation and increase resistance.

3.2.3 VACUUM BREAKDOWN

It is logical to think that removing particles from the electrode gap by forming a vacuum should prevent the formation of arcs, but in reality this is not the case. In vacuum arcs conductive particles are formed from the electrode material, which means characteristics such as the voltage drop and current density are dependant on the type of material, as opposed to the dielectric medium. Metals with high boiling and thermal conductivity tend to cause arcs with higher current density [74].

Metal vapour from cathode spots provides both the electrons and metal ions that contribute to the arc [75]. There are various hypothesise to explain the process of vacuum breakdown yet there is still no definitive theory that explains all of the phenomena observed. Particle exchange mechanism describes the cumulative to and fro of charged particles moving in the electrode gap under the influence of the electric field. Impact of the particles leads to further emissions in a chain reaction that leads to breakdown of the gap. Field emission theory describes the emission of electrode vapour into the gap as a result of the influence of ions or electrons on the opposing electrode which causes local temperature rises. Other theories describe the acceleration of loosely bonded electrode 'clumps' of material in the field and their subsequent electrode bombardment.

3.3 CIRCUIT BREAKER INTERRUPTION

3.3.1 INTERRUPTION CHARACTERISTICS

The role of the circuit breaker is to break normal currents in an expected operating range and under fault conditions, such as when short circuits develop. As well as this, the breaker must be able to carry nominal and abnormal currents when closed and must be a good conductor in order to reduce losses through Joule heating at the connection between the electrodes. Finally, when the circuit breaker is open, it must be able to withstand the voltage between the open contacts and prevent breakdown, both when the breaker is operating normally and in the post arc environment.

The conductivity of an arc is a function of plasma temperature and a circuit breaker design aims to control the change of the arc medium from conductor to insulator by cooling. Following current zero, the electrode gap must be cooled and de-ionised sufficiently to recovery dielectric integrity and withstand the voltage transients that occur.

If left alone, circuit breaker arc plasmas tend to an equilibrium condition where the input energy is in balance with energy losses that occur, to enable current interruption the energy loss mechanisms must be enhanced by cooling. There are four main processes involved in cooling the arc plasma [76]:

1. Isentropic cooling: adiabatic expansion during the flow of plasma along the pressure gradient that cools the arc internally
2. Cooling by thermal conduction: transfer of thermal energy due to the temperature gradient and depends on gas state
3. Cooling by mixing with cool background gas: caused by the difference in temperature between the masses flowing in and out
4. Cooling by radiation loss: radiated energy in the form of light, which is absorbed by the surrounding gas

The objective of a circuit breaker is not to prevent the arc occurring in the first place but to control the point at which it changes from conductor to insulator. High voltage and high current interruption can only be accomplished by the exploitation of the arc as a rapidly variable impedance that does not require the large scale energy dissipation of conventional resistances [77].

In a.c. circuits, it is simpler and more effective to extinguish the arc during the time of current zero. If the arc is extinguished outside of the current zero period, current chopping occurs leading to serious transient recovery voltages due to the inability of an inductive circuit to abruptly change. The behaviour of the arc around current zero is complex and the arc resistance does not rapidly change from conductor to insulator. At a point approaching current zero, the arc voltage rises rapidly relative to the decrease in the current, forming a voltage extinction peak. An example of the voltage and current characteristics for the interruption of an ac inductive circuit is shown in Figure 3-2.

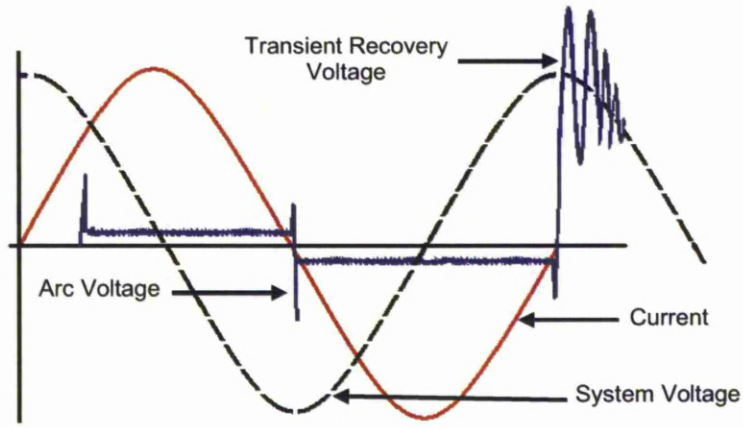

Figure 3-2: Circuit breaker interruption voltage and current waveforms

After current interruption the two sides of the circuit adjust to different voltage levels and transients on both sides of the circuit breaker exist, this stresses the electrode gap and can mean the post arc current will increase rather than fade out leading to arc re-ignition.

High voltage direct current (HVDC) transmission is becoming increasingly popular, because it is more efficient for longer distance transmission, both in terms of operation and cost [78]. As there is no natural current zero, the apparatus must use some means to reduce the current, it is also necessary to dissipate the inductive energy in the circuit so as to reduce high over-voltages. As a dc circuit breaker increases arc resistance, it causes the voltage to increase until it reaches a value greater than the system voltage, at which point the arc extinguishes because it cannot be maintained. A diagram showing the main features of a dc interruption is shown in Figure 3-3.

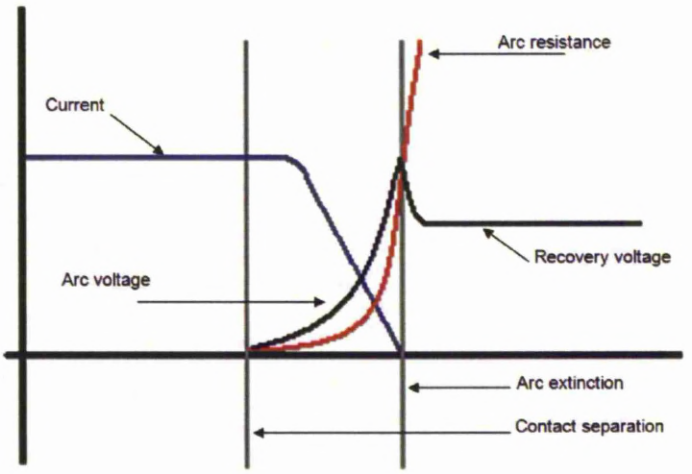

Figure 3-3: Electrical characteristics of a dc interruption

There are various interruption schemes used in dc breakers with the general aims of: forcing the current to zero, dissipating the inductive energy in the circuit and limiting the resulting over-voltages to safe levels. Lower voltage systems of a few kV can utilise arc chutes to lengthen and cool the arc but this is not suitable for high voltages. Some examples of oil [79], compressed air [80], vacuum [81, 82] and SF_6 [83] direct current interrupters exist which use the extinguishing media to raise the arc voltage along with a surge arrestor type resistor to dissipate the inductive energy from the circuit. Other designs cause self or forced oscillations to bring the current to zero.

3.3.2 TYPES OF CIRCUIT BREAKER

3.3.2.1 Oil

Oil circuit breakers have been used since the early part of the 20th century [84] and continue to be common today. In a simple plain break circuit breaker, when an arc forms oil is dissociated into carbon compounds and hydrogen. This effect cools the arc, lowering its conductivity and plays an important part in interruption [85]. Liquids are much denser than gasses and consequently conduct heat away from the arc more efficiently, for example mineral oil is better at conducting heat away from the arc than nitrogen [86].

Liquid dielectrics used in circuit breakers are almost universally forms of hydrocarbons and need to be purified to remove water contamination, which can have a significant effect on reducing dielectric strength. Further disadvantages of oil insulation are that it undergoes aging due to prolonged heating and forms sludge that reduces the circulation of the oil and therefore its ability to conduct heat. There are also concerns over the environmental impact of the oil when the apparatus is decommissioned or reconditioned. It is known that insulating oil in use often contains varying degrees of polychlorinated biphenyls (PCBs), which are harmful to health [87]. On the positive side, if properly maintained, the robust nature of oil filled circuit breakers means that they are still commonly in use today, some of which have been in service for 70-80 years [88]. Operating older oil filled switchgear requires careful assessment and diagnostics, especially in light of the fact that increases in the electricity demand since when they were installed means that they are often required to break and carry larger currents than originally designed.

Although there are still many oil filled circuit breakers in service, oil based interrupters have become less fashionable for new installations, with SF_6 and vacuum becoming more popular [88].

3.3.2.2 Air Insulation

Air is the most common type of circuit breaker insulation in high voltage systems due to its dielectric and heat conducting ability and particularly because of its low cost [89]. The voltage breakdown strength of gasses is related to pressure and gap distance by Paschens law, shown in Equation 3-5.

$$V = \frac{a(pd)}{\ln(pd) + b} \tag{3-5}$$

Where:

V - Breakdown volatge (V)
p - Pressure (Torr)
d - Gap distance (cm)
a, b - Gas composition constants

Paschens law shows that for a given gap distance, larger pressure increases the breakdown strength of the medium. Air at atmospheric pressure is often used, with the required breakdown strength achieved by using large gap distances. This is economically favourable, but for high voltage switching it requires a large amount of space and so is not suitable for citing in heavily populated areas or indoors.

Introducing a gas flow around the arc enhances the interruption capability of gasses further. Air blast interrupters were first developed that used compressed air fired into the arc so as to achieve a higher dielectric strength due to pressurisation [90] and cause cooling of the arc and electrode gap leading to deionisation. Compressed air flow can be introduced axially or perpendicular to the arc (cross flow). The benefit of cross flow is that it lengthens the arc and increases its resistance. Examples of the two schemes are shown in Figure 3-4.

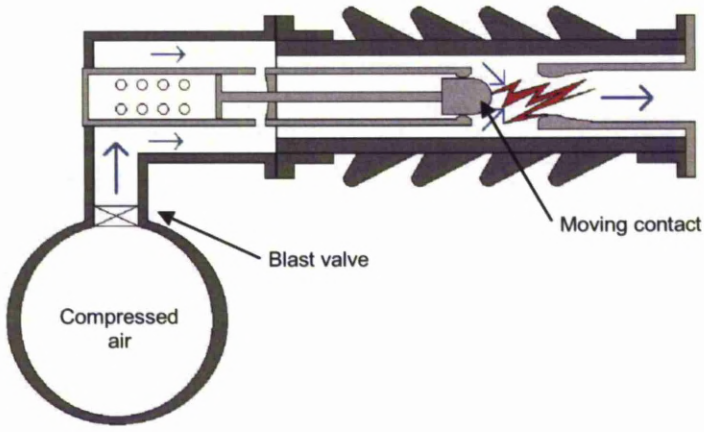

(a)

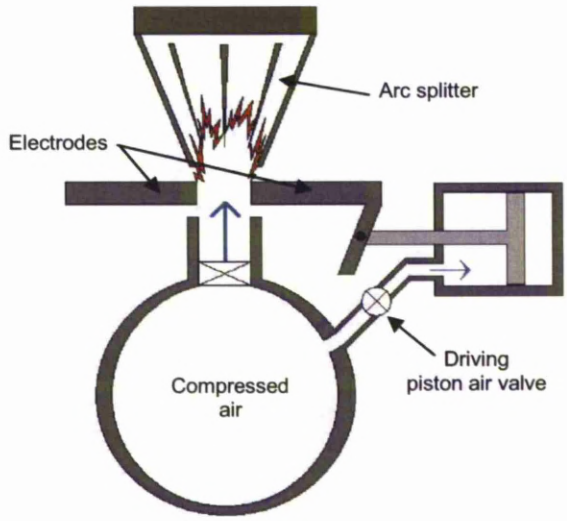

(b)

Figure 3-4: Compressed air axial and cross blast interruption schemes: [91]

(a) Axial

(b) Cross-blast

Eventually circuit breakers with a higher breaking capacity were required due to increases in transmission and distribution voltages. This led to the research and development of circuit breakers that used gasses with superior dielectric and thermal properties to air.

3.3.2.3 Enhanced Circuit Breaker Gasses

Properties such as specific heat and thermal conductivity determine the efficiency that a gas removes energy from the arc. Also, the electronegative properties of the gas determine its ability to attract electrons and form heavy, low mobility ions, which do not conduct in the field easily and do not develop enough kinetic energy to cause ionising collisions. Other important considerations for the selection of circuit breaker gas are [92]:

- High dielectric strength
- Thermal stability and chemical inertness to construction materials
- Non-flammable
- Physiologically inert
- Low condensation temperature
- Good heat transfer
- Readily available at moderate cost

Although air is still very popular as insulation, replacing it with other gasses can improve interruption capability. Historically, electronegative gasses such as oxygen, SF_6, Freon, CO_2 and fluorocarbons have been researched, with SF_6 becoming extremely popular due to its outstanding properties. Gas blast circuit breakers that use SF_6 have been shown to be particularly effective due to both the dielectric strength of SF_6 and its highly effective ability to remove energy from the arc.

Early SF_6 designs used compressed gas in cylinders but this was mainly superseded by the 'puffer' style design, which used pistons to cause gas flow. In 'puffer' interrupters gas is injected into the arc by a mechanical compression device linked to the electrode movement in order to cause a gas flow and increase convective cooling. This removes energy from the arc as well as flush ionised gas away from the electrode gap to improve its recovery of post arc dielectric integrity.

Other schemes are self-blast circuit breakers that use the energy of the arc to cause a pressure differential and gas flow. These designs utilise certain nozzle geometries with expansion volumes that pressurise due to the thermal energy from the arc and act as a means of causing convective cooling and flushing ionised gas from the electrode gap around the current zero period.

3.3.2.4 Vacuum Circuit Breakers

Vacuum circuit breakers have been in existence for more than 80 years [93]. Due to the necessity to maintain a vacuum the conventional methods of arc extinguishment using oil or gas flow cannot be used. The benefit of this is a simpler design that requires less energy for operation and is generally maintenance free. Arc extinguishment is achieved by deliberately diffusing the plasma by the use of a magnetic field. The disadvantage of vacuum is the relatively low voltage of operation of existing technology, with production units not being able compete with SF_6 circuit breakers for high voltage applications. A diagram of a typical basic vacuum interrupter design is given in Figure 3-5.

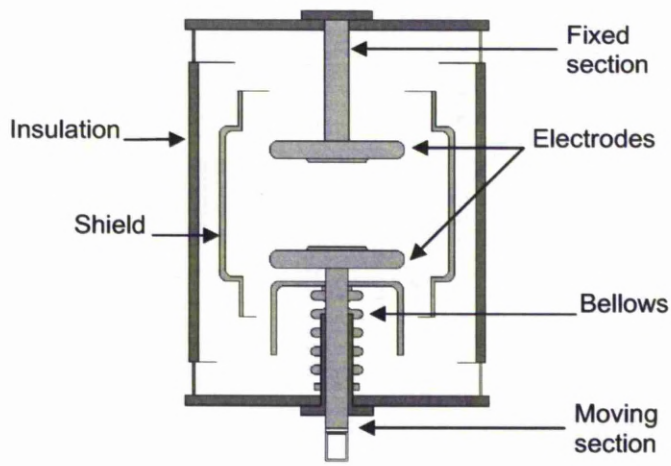

Figure 3-5: Vacuum interrupter design with plane electrodes [94]

At low current, a diffuse arc is observed with several columns; as the current increases the arcs gather together into a single column, which stresses the metal of the anode, causing significant melting and vapour production. This causes the dielectric integrity of the electrode gap to become very weak, hence reducing the interruption capability.

The objective of most of the research into this type of circuit breaker is to enhance interruption capability by developing strategies to prevent the anode melting. Plane electrodes can be used for currents of less than 10kA; however for higher currents more complex designs are required. Greater interruption capacity can be achieved by utilising a magnetic field to move the cathode spot around, or by spreading the arc energy over the entire face of the electrode, rather than just an intense spot. This has necessitated the development of more complex spiral type electrode designs, but spiral designs have also seemed to reach a limit of interrupting capacity of about 40kA [95]. More recently, research has focussed on developing axial magnetic fields, rather than the transverse ones used previously, with the intention of interrupting larger currents. After interruption there is the same problem with recovery voltages as is present in other types of circuit breaker.

As a replacement for SF_6, vacuum technology is currently limited to some applications and will only be suitable if in the future higher breaking capacities can be achieved at reasonable cost.

3.3.2.5 SF_6 Circuit Breakers

The worldwide electric power industry currently uses 80% of all of the SF_6 manufactured globally per year [97]. Sulphur hexafluoride was first discovered in 1901 by the French chemists Paul Lebeau and Nobel Prize winner Henry Moissan [96]. It is a dense gas that is normally inert and non-toxic, it remains in a gaseous state at elevated pressures over a wide temperature range, which makes it suitable for high voltage applications.

Sulphur hexafluoride was first used in circuit breakers in the 1950s in a three-inch plain break gap where it was found to provide superior performance over air [98]. The thermal and dielectric properties of SF_6 mean that its breaking capacity is significantly larger than that of air and it is capable of rapidly changing a conductive arc into an insulator. Some properties of SF_6 are given in Table 3-1 and its enhanced dielectric ability over air is shown in Figure 3-6.

Table 3-1: Properties of SF_6 [99]

Property	Value
Molecular Weight (g/mol)	146.05
Latent Heat of Fusion (KJ/kg)	39.75
Boiling Point (sublimation) (°C)	-63.9
Latent Heat of Vaporisation (KJ/kg)	162.2
Thermal Conductivity (mW/mK)	12.058
Specific Heat (at 21°C) (KJ/mol.K)	0.097
Global Warming Potential	23900
Atmospheric Lifetime (years)	3200

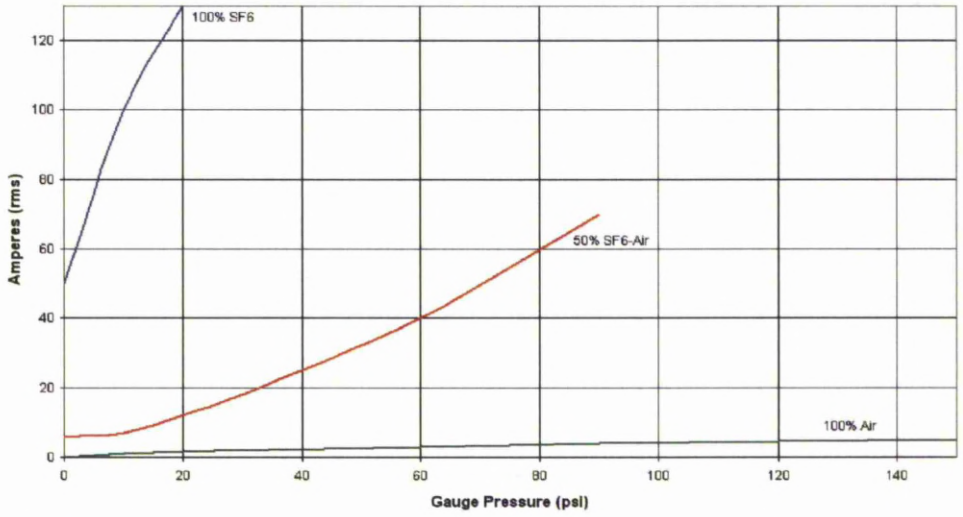

Figure 3-6: Dielectric strength of SF_6 versus air for 2,300V at 60Hz [98]

The dielectric ability of a mixture of SF_6 and air is also shown in Figure 3-6, this has been exploited in recent times in gas mixes aimed at reducing the amount of SF_6 used in circuit breakers because of environmental and cost considerations.

The thermal conduction mechanism in SF_6 is particularly efficient due to its unusual dissociation characteristics. The peak in thermal conductivity of SF_6 occurs at around 2,000K, below the peak conduction temperature of 4,000-5,000K. This means SF_6 will cool the arc via dissociation before the arc reaches its peak conductivity and therefore when it is harder to interrupt. Due to SF_6 containing fluorine it has a high value of electronegativity. This means that some of the conducting electrons in the arc can be removed, initially forming low mobility negative ions and then recombining into neutral molecules.

The absence of carbon from the SF_6 molecule is advantageous as it means there is no need to consider the problems caused by the build up of solid carbon deposits [101]. The excellent properties of SF_6 also extend beyond arc quenching period and allow SF_6 to withstand high recovery voltages in the system. This is due to the ability of SF_6 to very rapidly recover its dielectric strength following current zero.

The first production SF_6 circuit breakers went into service in 1956, and were rated at 115kV and 400A [102]. It was three years later before the first fully fledged high voltage SF_6 circuit breakers were brought about, with ratings of 230kV, 10,000MVA [103]. These used similar schemes to existing breakers of the time, by using compressed gas flow from a reservoir to blow the arc axially. The first 'puffer' style SF_6 interrupters were developed by Westinghouse in 1965 [105]. The technique was to attach a piston to the moving contact in order to force gas through an orifice into the arc column and designs of this era still form the basis of modern puffer circuit breakers [106]. Simple expansion volumes were later developed and incorporated to force gas flow as a result of arc heating, reducing the energy of operation over puffer devices. Other designs used a blast valve with compressed SF_6, which was triggered by contact separation. Diagrams of the main types are shown in Figure 3-7.

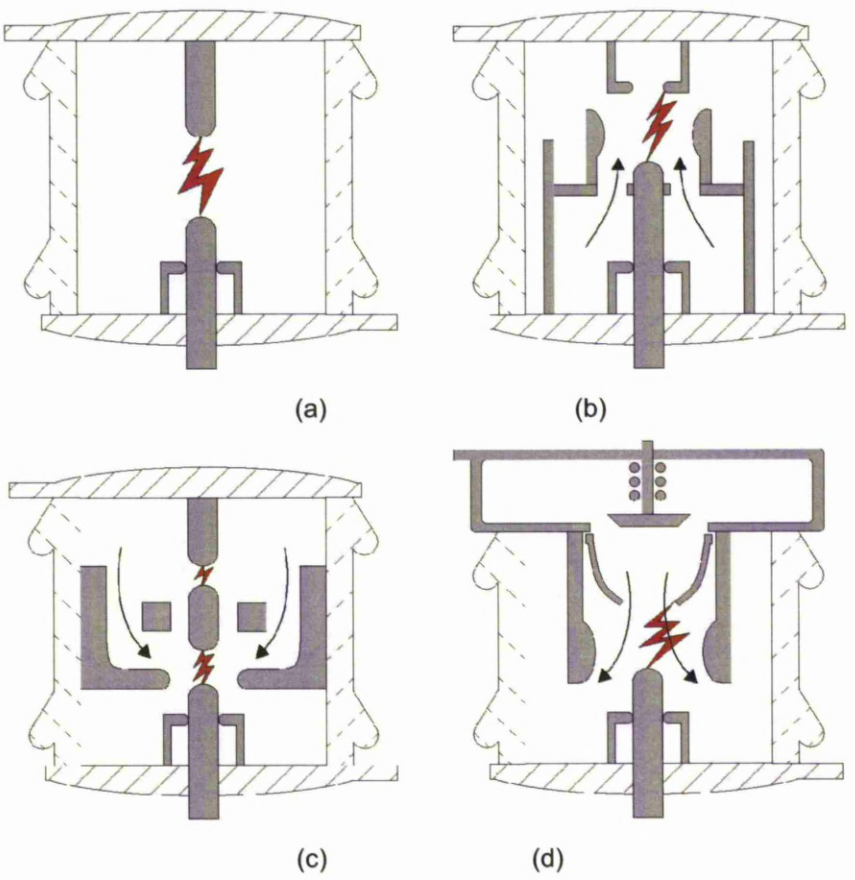

Figure 3-7: Designs of SF_6 Interrupters [104]:

(a) Plain break
(b) Puffer
(c) Self-pressurising
(d) Blast (double pressure)

It is clear that sulphur hexafluoride is a highly effective circuit breaker gas and is becoming increasingly popular, indeed in modern times it is used almost exclusively used for new systems from 72.5kV/25kA up to 800kV/63kA [107], as well as lower capacity apparatus. This popularity is understandable as it has allowed the introduction of GIS apparatus that are more conveniently cited in areas of population and therefore demand. However these advantages carry an environmental cost that must still be considered.

3.4 CIRCUIT BREAKER DIAGNOSTICS

The main aim of this investigation was to develop a deeper understanding of the complex plasma-polymer interaction on a fundamental level, to achieve this diagnostic apparatus that could extract the maximum amount of information from each polymer-arc discharge were used. Optical spectrometry, chromatic processing, mass spectroscopy, pressure sensing, current and voltage probes and high-speed imaging were used. Atomic spectroscopic techniques in the context of plasma diagnostics are more involved and so some background detail is given in this section.

3.4.1 OPTICAL EMISSION SPECTROSCOPY

3.4.1.1 Introduction

Spectroscopy is a powerful and versatile diagnostic technique and in this case is intended to be used to highlight the main changes in the arc as a result of the plasma-polymer interaction. Optical emission occurs due to energetic plasma causing the outer electron of the proximate species to become excited enough to move into a higher energy level. However, the electron is unstable in this state and after a short lifetime drops back to the ground state, simultaneously releasing a corresponding amount of energy in the form of a photon, whose wavelength corresponds to the energy drop by Planks law; this is shown in Equation 3-6.

$$E = \frac{hc}{\lambda} \tag{3-6}$$

Where:

E = energy (J)

h = Planks constant (6.6×10^{-34}Js)

c = speed of light (3×10^{6}ms^{-1})

λ = wavelength (m)

The central wavelength of emission corresponds to the energy gap between the upper energy level p and the lower energy level k, a basic representation of this is given in Figure 3-8.

$$E = E_p - E_k \tag{3-7}$$

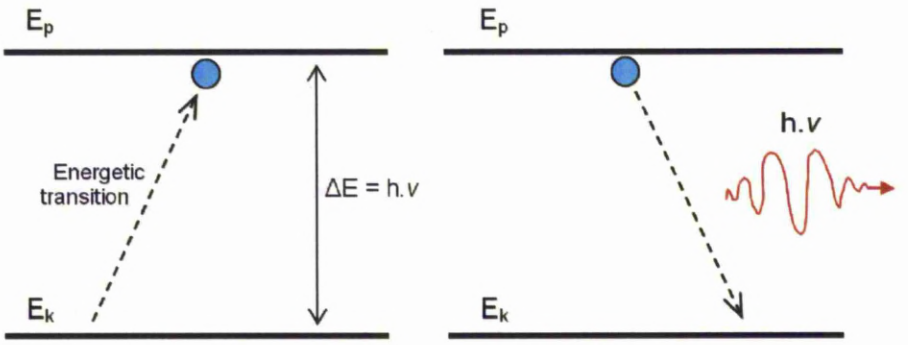

Figure 3-8: Electron excitation and downward transition emitting a photon

Due to the fact that the energy gap E is characteristic of the emitting species, each element emits an individual set of wavelengths of photons and so the light spectrum emitted from the arc contains spectral peaks at different wavelengths. Analysis of the wavelengths of the emission lines can be used to identify the species present in the arc.

Identification of particle species using emission spectroscopy is relatively simple by referring to published wavelength tables. Care must be taken in wavelength interpretation because in some cases the Doppler Effect can cause shifts in wavelength. However in general, this effect is very small and cannot be detected without a high-resolution spectrometer [108], which is not used in this case.

The main characteristics that can be interpreted from a plasma spectral emission line are highlighted in Figure 3-9.

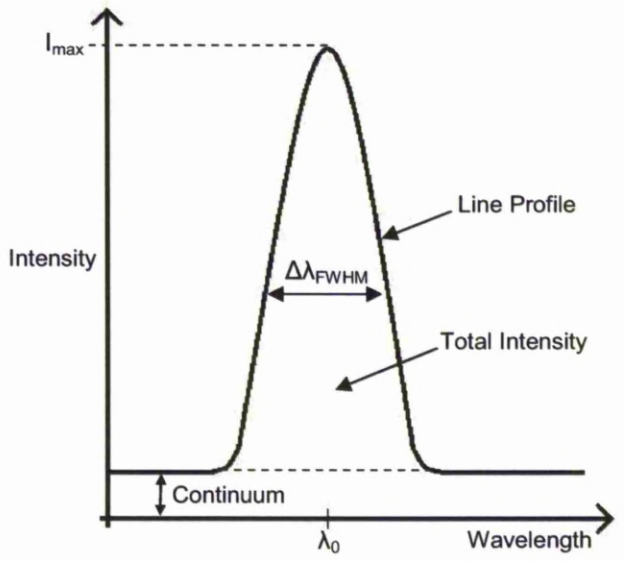

Figure 3-9: Information characteristics of a spectral line

Analysis of spectral line characteristics allows information on the state of the plasma to be found. The total energy emitted in the line allows conclusions to be drawn regarding the excitation temperature and particle density of the emitting species. The central wavelength λ_0 refers to the emitting species described previously; the continuous background radiation can allow determination of the electron temperature. The line profile (shape) gives information on the kinetic temperature of the emitting atom (from Doppler broadening) or the density of perturbing particles (from pressure broadening). The value of intensity of a spectral line is obtained from the integral of the line around its centre. Due to this reason, the best lines for analysis should not be disturbed (overlapped due to broadening) by other lines and should not be located inside areas of heavy continuum radiation.

The spectroscopic apparatus used to capture optical emissions generally consist of an entrance slit, diffraction grating and detector element; the specification of the constituent parts determines the resolving ability and limitations of the system.

At the spectrometer, the light emitted from plasma enters the entrance slit, usually through coupling by an optical fibre. The intensity of light detected is proportional to the size of the entrance slit and inversely proportional to the spectral resolution. This means that because plasma generally has a high intensity already, a smaller slit is desirable to enhance resolution. The diffraction grating splits the incident light into constituent wavelengths and is measured in terms of lines per mm. The specification of the grating determines the wavelength range and sensitivity of the spectrometer. The detector element can either be a photo-multiplier or a CCD. When a photo-multiplier is used it is mounted behind an exit slit, the width of which determines the spectral resolution. In the cases where a CCD array is used, the pixel size influences resolution. In all cases, the combination of slit size, diffraction grating and detector determines the spectroscopic ability of the device.

The benefit of emission spectroscopy is that it allows real-time monitoring of the plasma providing an insight into the processes being undertaken and the plasma parameters. It is non-invasive, such that information about the state of the plasma can be found without any direct contact thus preventing any disturbing effects. Another advantage is that because it is an optical system, interference from the strong electromagnetic fields present around electrical plant does not disturb the results.

3.4.1.2 Temperature Determination

The estimation of temperature is one of the most common spectroscopic techniques used in plasma diagnostics. There are various methods that can be used to estimate the temperature of plasma and the type used depends on the form of the spectral data and assumptions on the state of the plasma.

In this project, optical emission spectroscopy was performed, which is particularly suitable for use in arc analysis. This is because absorption spectroscopy techniques are not recommended for single shot experiments with relatively low repetition rates [109] as in this case.

An important concept in this context is optical thickness. Photons emitted by species in the plasma can be reabsorbed by other species before exiting the plasma body and therefore before reaching the detector. Optically thin plasmas are those where, for the purposes of analysis, the effect of this absorption is considered negligible. The method of temperature estimation used requires the assumption of whether the plasma is optically thin or thick.

Another important consideration is thermodynamic equilibrium. Complete thermodynamic equilibrium (CTE) occurs when the plasma is uniform and homogenous in kinetic and chemical equilibrium such that the plasma properties are unambiguous functions of temperature [110]. This means that in the plasma, ionisation must be balanced by recombination, bremsstrahlung effect by absorption, line radiation by line absorption etc. If this is the case, then the distribution functions of particle energies and excited energy levels of the atom can be obtained from the Maxwell-Boltzmann distribution – which is a function of temperature alone. In reality the vast majority of laboratory plasma does not achieve this state so a more realistic state has been described, known as local thermodynamic equilibrium (LTE).

Plasma in local thermodynamic equilibrium is considered optically thin such that the plasma radiation does not need to be in equilibrium. The requirement for collision processes in the plasma to be in equilibrium are still needed but can be considered locally as opposed to the whole plasma body, that is, it is acceptable for them to differ from point to point in space and time. In most cases the normal analysis procedure is to assume the plasma is in LTE and then proceed to analyse the spectra to find the temperature and then assess the results for consistency.

By considering the plasma as optically thin and in local thermodynamic equilibrium there are several methods of using the spectral lines in order to find the temperature. One of the most common methods uses the relative intensities of spectral lines from the same atomic species, outlined in Equation 3-8 [111].

$$\frac{I_1}{I_2} = \frac{A_1 g_1 \lambda_2}{A_2 g_2 \lambda_1} \exp\left(-\frac{E_1 - E_2}{kT}\right) \quad (3\text{-}8)$$

Where:

I_n = relative intensity of line n

A_n = transition probability of n

g_n = statistical weight of n

λ_n = wavelength of line n (nm)

k = Boltzmann constant ($1.38 \times 10^{-23} m^2 kg\ s^{-1} K^{-1}$)

E = energy of upper level

T = temperature (K)

The transition probability, statistical weights and energy of upper levels can be found in most cases by reference to published tables [112]. The greater the difference between the energies of the upper levels of the spectral lines leads to more accurate temperature estimation. As a result of this, when considering spectral lines for analysis, they should be selected that maximise this difference. A limitation is the condition that the lines of the species must be in the same ionisation stage. A larger E_1-E_2 difference can be found from species in different ionisation stages but this complicates the analysis and requires more data on the ionisation states of the lines.

3.4.2 CHROMATIC PROCESSING

3.4.2.1 Introduction

An electrical discharge is a complex system whose characteristics depend on a number of interrelated parameters which may change simultaneously. An optical emission spectrum of plasma contains many features which may alter to different extents relative to each other depending on the characteristics of the arc. This makes it extremely difficult to accurately compare spectra from different environments by visual interpretation alone, chromatic processing allows easier analysis of the data.

The chromatic methodology was originally developed to access trends in emergent features in complex data so as to allow quantification of the interaction between features and parameters, which would not be possible by conventional interpretation [113]. Chromaticity is particularly useful in this investigation to enable comparison between differences in arc characteristics in different polymer environments that would otherwise not be seen.

3.4.2.2 Chromatic Algorithm

The chromatic technique utilises three detectors with overlapping responsivities that integrate the whole optical signal within each bandwidth. The non-orthogonal nature of these is exploited to allow simple quantification of the complex spectral signature without being subject to variation as a result of uniform signal changes across the whole bandwidth. An example of an optical spectrum with filters in place is shown in Figure 3-10.

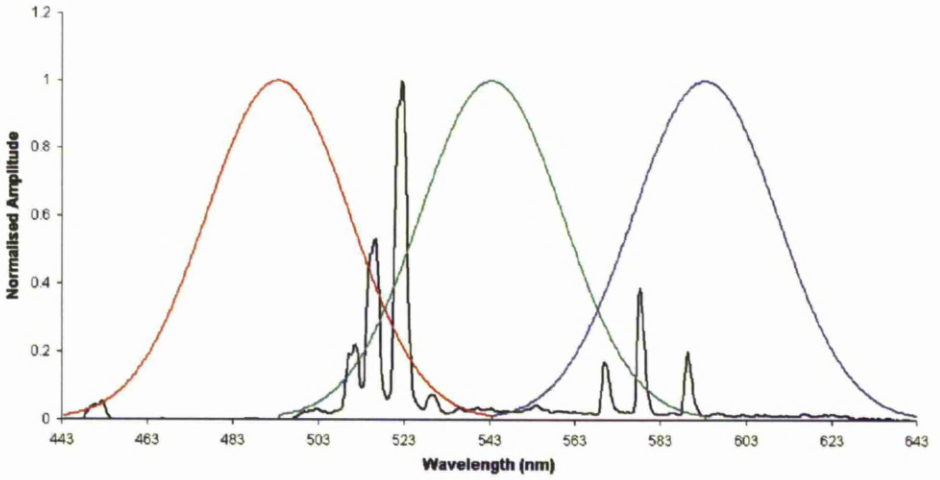

Figure 3-10: Processing a complex spectrum with Gaussian RGB filters

The outputs of the non-orthogonal processors, known as R, G, B, can be converted into hue, lightness and saturation (H, L, S) values by the use of existing colour science algorithms to allow plotting on HL and HS polar plots, which allows comparison and interpretation.

Hue is representative of the dominant wavelength of the signal; saturation refers to the spectral spread; and lightness the energy of the original spectrum. Hue is plotted as an angular quantity, whilst L and S are radial values. The chromatic parameters are calculated from the R, G, B processors by the relationships shown in Equations 3-9 (hue), 3-10 (lightness) and 3-11 (saturation) and shown in Figure 3-11.

$$\left.\begin{array}{ll} \mathrm{H} = 240 - 120\dfrac{g}{g+b} & r = 0 \\ \mathrm{H} = 360 - 120\dfrac{b}{b+r} & g = 0 \\ \mathrm{H} = 120 - 120\dfrac{r}{r+g} & b = 0 \end{array}\right\} \quad \begin{array}{l} r = R - \min(R,G,B) \\ g = G - \min(R,G,B) \\ b = B - \min(R,G,B) \end{array} \qquad (3\text{-}9)$$

$$\mathrm{L} = \frac{(R+G+B)}{3} \quad \text{--- (3-10)}$$

$$\mathrm{S} = \frac{[\max(R,G,B) - \min(R,G,B)]}{[\max(R,G,B) + \min(R,G,B)]} \qquad (3\text{-}11)$$

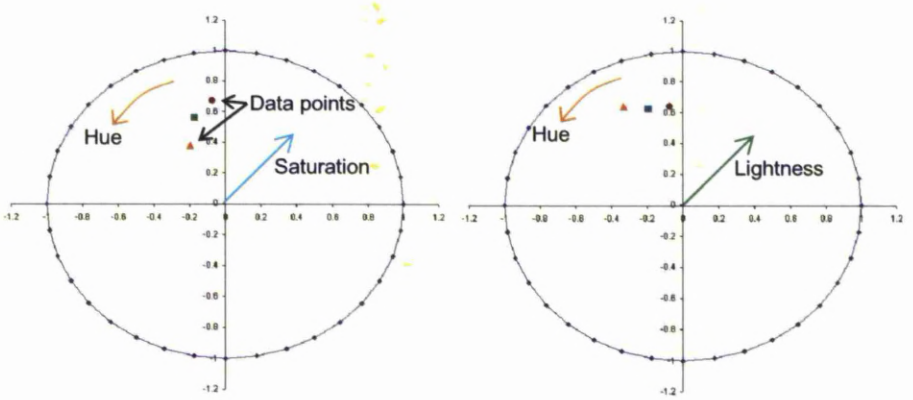

(a) (b)

Figure 3-11: Polar plots of three chromatically processed spectra: (a) HS; (b) HL

In this investigation the chromatic methodology is utilised as a tool amongst other techniques, in the interpretation of differences in optical spectra from arcs formed in different polymeric environments. This allows a quantitative comparison between spectra with the intention of playing a part in the development of deeper understanding of the plasma-polymer interaction and its role in quenching. It is beyond the scope of this thesis to go into a more detailed exposition on chromaticity, but more information can be found from other publications [114].

3.4.3 MASS SPECTROMETRY

3.4.3.1 Introduction

Mass spectrometry allows the chemical composition of a sample to be determined to a very accurate level. In a mass spectrometer, the sample is ionised then separated and detected. The separation of the different species in the sample is achieved due to differences in the mass to charge (m/z) ratio.

The mass to charge ratio is the atomic mass of the species divided by its charge achieved through ionisation. The charge acquired by the species is usually equal to one because it is rare multiply charged ions are produced. Separation of the species is attained because in electrodynamics, species with different mass to charge ratios move in different paths in a vacuum when subjected to the same electric and magnetic forces. By applying different fields, different species can be detected. A summary diagram of the main stages involved in mass spectrometry is shown in Figure 3-12.

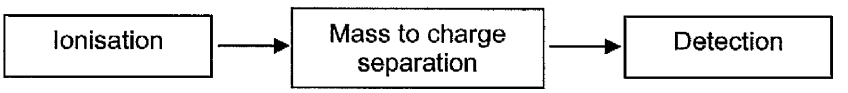

Figure 3-12: Block diagram of mass spectrometry methodology

There are different types of mass spectrometer and they usually differ in terms of how they create and separate the ions. Examples of different types of mass spectrometer are time of flight (TOFMS), quadrupole and ion traps. In this project a quadrupole mass spectrometer was used. The spectrometer sampled gas from the chamber continuously during an experiment and the samples entering the device were ionised by the impact of a high energy electron beam whose electrons carried enough energy to ionise each sample molecule. This is known as electron impact ionisation and is a 'hard' ionisation technique that forms ions with a single charge and because z = 1, the m/z of each detected species corresponds with the atomic mass of the molecule. The resultant positive ions could then be accelerated towards the detector, whilst any species that were not ionised were easily separated and removed.

The quadrupole refers to the way in which the ions are separated. The system contains two pairs of rods, each pair connected and sited opposite each other, the ionised sample travels to the detector between the rods. A radio frequency (RF) voltage is applied between the pairs of rods with a superimposed direct current (dc) voltage. For a given ratio of RF and dc voltages, only ions with a certain mass to charge ratio could travel between the rods to the detector, the other ions would follow different trajectories. A diagram of the quadrupole system is shown in Figure 3-13.

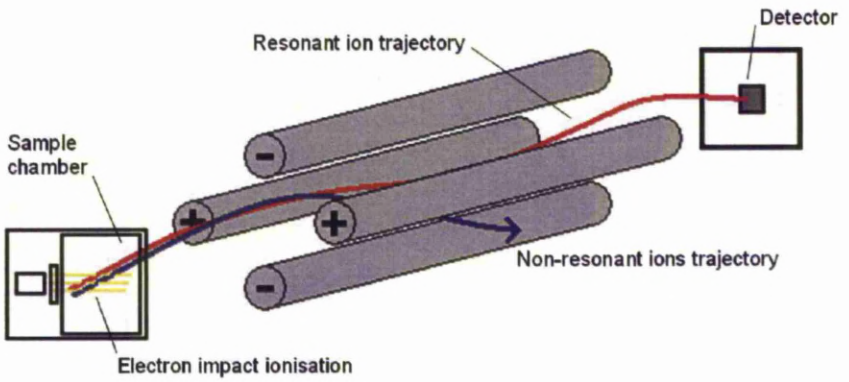

Figure 3-13: Quadrupole mass spectrometer configuration

By continuously altering the ratio of voltages over certain values, scanning of a range of m/z values could be performed. The separation is conducted in a vacuum in order to prevent collisions between the ions and the surrounding neutrals.

The detector coordinates the scanning voltages (corresponding m/z values) with the signals detected, allowing the abundance of each m/z to be measured. A greater degree of ion impacts to the detector with each voltage ratio (and therefore m/z) indicate a more abundant species. Substantial amplification at the detector is needed as the number of ions reaching the detector at a particular instant is usually very small.

3.4.3.2 Data Interpretation

The interpretation of mass spectral data is not trivial due to the interference between different species with the same mass-charge ratio and due to fragmentation. This means the analysis of mass spectral data requires careful consideration and knowledge of all the data available. Mass spectrometry can be used for analysis of the chemical species present in a sample, molecular structure or test for the presence of impurities.

The mass spectrometer ionisation procedure can cause fragmentation of the sample molecules, which must be considered in the interpretation of results. A sampled molecule that is not fragmented by ionisation is known as the molecular fragment; the ions that do gain sufficient energy to fragment form a combination of other ions and neutrals from the original molecule. It is also possible that the secondary ions (labelled B and C below) can further fragment into smaller species.

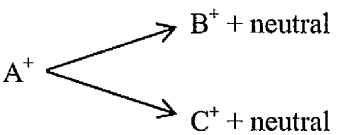

In a mass spectrum there will generally be a peak at the m/z of the molecular atom and then subsequent peaks at smaller values that represent the fragmented ions. A difficulty in sampling the circuit breaker environment is the wide abundance of different chemical species that mean there can be more than one molecular ion and its fragments. Due to this, mass spectral interpretation requires careful investigation and consideration of fragmentation and reaction mechanisms.

3.5 POLYMERS

3.5.1 OUTLINE

The utilisation of solid nozzle polymer ablation has been found to assist in the performance of lower concentration SF_6 gas mixes [100]. This section aims to provide background information on the properties of polymers.

Synthetic polymers are long chain molecules, comprised of a basic repeating unit called a monomer. The monomer is usually an alkene, a molecule containing a double carbon bond. The polymerisation process uses heat, pressure and a catalyst to break the double bonds in the monomer molecules and allow them to bond to each other. A simple diagram explaining this process is given in Figure 3-14.

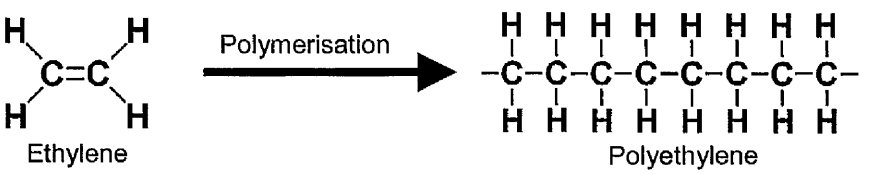

Figure 3-14: Polymerisation of ethylene into polyethylene

Polymers consist of many long chains grouped together in either regular (crystalline) of irregular (amorphous) structures, usually a solid polymer contains a mixture of crystalline and amorphous chains.

3.5.2 PROPERTIES

The attributes of the polymer are affected by several factors, including the composition of the monomer it was made up from and the structure of the chains and types of bond.

The length of the chain relates to the number of monomers joined together, also called the degree of polymerisation (DP). One of the most important properties of the polymer that is affected by the degree of polymerisation is the melting temperature [115], where a longer chain length causes a higher melting point. A higher DP also causes a higher amount of tensile strength [115]. These effects are due to longer chains being subject to larger degrees of Van der Waals forces between them and so more strength is achieved.

The linearity of the polymer chain is also important. There are many different types of branching configuration, such as star, comb or a network of linked polymer chains. The type of branching affects the strength of the polymer, with long chain branches increasing strength due to an increase in entanglement, but short branching of chains reducing strength because of a larger degree of disorder. The degree of cross-linking of the polymer chain is important with regard to strength. Cross-linking refers to the formation of chemical bonds between polymer chains which causes an increase strength, this is the process by which vulcanisation strengthens rubber for tyres. On the other hand, a polymer can be made more flexible by the inclusion of plasticisers. Plasticisers are molecules that go in-between the polymer chains to reduce the chain interaction thereby making the polymer less rigid.

The energy involved in changes of state is dependant on the structure and composition of the polymer chain linkages. These characteristics are generally found by using differential scanning calorimetry (DSC). In DSC, the energy input into a sample is measured and compared to a reference. At the points where the sample changes state, more energy input is required for the sample than the reference and is shown on the DSC heat flow trace.

An example DSC curve is shown in Figure 3-15 showing the main transitions undertaken by polymers when heated.

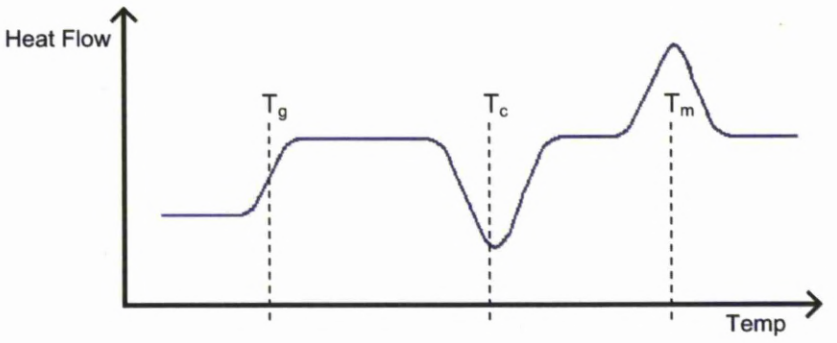

Figure 3-15: DSC trace of polymer change of state: T_g – glass transition; T_c – crystallisation; T_m – melting

When a polymer is heated the first phase change occurs at the glass transition temperature, T_g. Glass transition is only undertaken by amorphous or semi-amorphous polymers and occurs due to the increase in kinetic energy gained by the molecules. The glass transition period is shown as an increase in heat flow in Figure 3-16; the gradient of the line at this point depends on the polymer heat capacity. Above T_g, the polymer chains become more mobile, altering the mobility of the polymer chains causes the solid polymer to become softer. Below the glass transition temperature the polymer becomes brittle and hard.

After the glass transition stage, the heat capacity of the polymer is greater and so the overall heat flow is higher. At a certain point beyond T_g the extra mobility of the polymer chains mean they become crystalline, this causes the DSC heat flow to drop because an exothermic reaction occurs. The lowest point of the heat flow trough indicates the crystallisation temperature T_c.

If the polymer is continued to be heated it will eventually reach its melting point, T_m. This is signified in Figure 3-15 by a peak in the heat flow, because melting an endothermic reaction, meaning extra energy is required to be input into the system.

In polymers, the melting point does not signify a change into a liquid as is the case conventionally; rather it refers to the point at which the intra-chain bonds break allowing polymer chains to freely move. If the polymer is continued to be heated there would not be a transition into a gas as is the case conventionally due to the fact that polymers will decompose before reaching any theoretical boiling point. Polymer decomposition involves the breakage of the polymer chains into smaller molecules, which is known as de-polymerisation. Depending on energy input into the system, the decomposition products can also be further dissociated into their constituent atoms.

In the case of this research, polymers were applied to the arc plasma in powder form. The benefit of this was that it increased the surface area available for reaction and meant the effect of the polymer-arc interaction – and so any arc quenching – was enhanced. As well as the differences in structure and composition, the polymers were also chosen to be common and readily available at reasonable cost in order to make any future design commercially viable. The mean particle radius for the six polymers was 195μm and the density varied from 0.94 to 2.20gcm^{-1} amongst the polymer types. It was expected that the distribution of powder sizes would have a Gaussian nature around the mean radius for each type, although this was not tested and this variation was not considered to have any effect on the results. Each particle in the powder was considered to be spherical but in reality there would be inconsistencies in shape. Again, this variation was not considered to have any measurable effect on the plasma-polymer interaction or on the arc quenching ability.

3.5.3 DESCRIPTION OF POLYMERS USED

Polymers are grouped into general groups based on their composition and structure. In order to test the arc quenching effect most widely, polymers from a variety of different groups were selected. These are shown in Table 3-2.

Table 3-2: Polymers selected for test [116]

Polymer Group	Polymer Name	Abbreviation	Structure
Polyolefines	Polyethylene	PE	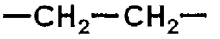
Vinyl Polymers	Polystyrene	PS	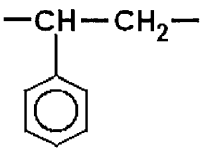
	Polyvinyl chloride	PVC	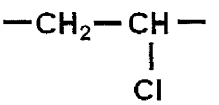
Fluoropolymers	Polytetrafluoroethylene	PTFE	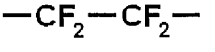
Polyacrylics	Polymethyl-methacrylate	PMMA	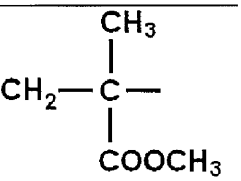
Polyamides	Polyamide 6	PA6	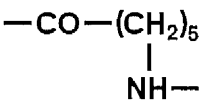

A summary of some of the most relevant properties of the polymers used in this project is given in Table 3-3. It was hoped to be able to draw a relationship between the properties of polymers and their effectiveness in circuit breakers.

Table 3-3: Summary of polymer properties [116]

Property	PE	PMMA	PS	PVC	PA6	PTFE
Glass Transition Temperature (K)	163	377	368	358	328	400
Melting Point (K)	419	473	513	500	493	608
Decomposition Temperature (K)	573	543	633	513	673	773
Specific Heat (KJ/ kg K)	1.90	1.45	1.20	1.25	1.70	1.00
Thermal Conductivity (W/ m K)	0.41	0.19	0.16	0.16	0.29	0.25
Density (g/cm)	0.94	1.19	1.05	1.40	1.13	2.20
Enthalpy of Fusion (KJ/mol)	4.01**	X	8.68	7.53**	4.85**	3.42

X = no data available

** = Reference [117]

In addition to the properties already described previously, Table 3-3 shows two properties not discussed; namely specific heat and enthalpy of fusion. Specific heat is defined as the energy required to increase a given amount of sample by a certain temperature interval. Enthalpy of fusion refers to the energy input required for the change of state that occurs on melting and describes an endothermic process that absorbs energy from the surroundings.

It must be noted that in all cases the values given in Table 3 are for tests under standard conditions of 25°C and 100kPa. Different conditions of temperature and pressure cause variations on the values listed in the table. It is common for peaks in values to occur at different temperature or pressure due to association or dissociation of certain molecules.

3.6 SUMMARY

Arcs are formed in circuit breakers because of the ionisation of the insulating medium due to the strong electric field between the electrodes. Further ionisation and electron avalanches lead to the formation of arcs - plasmas with high temperatures and current densities. This prevents current interruption and proper circuit isolation. There are various circuit breaker schemes that aim to extinguish the arc at the proper time to enable circuit isolation for maintenance or in the event of a fault.

Three common circuit breaker diagnostic techniques are used in this investigation, namely optical emission spectroscopy, mass spectrometry and chromatic processing. These techniques allow the analysis of changes in plasma characteristics which can indicate the quality of various interruption schemes.

Differences in the structure and composition of polymers are the reason why they display individual physical properties. This means that various polymers react differently when subjected to the arc plasma and consequently influence interruption by the use of a variety of mechanisms.

Chapter 4

Apparatus and Methodology

CHAPTER 4 – APPARATUS & METHODOLOGY

4.1 CHAPTER INTRODUCTION

This research used experimentation to provoke reactions between arc plasma and polymer micro-particles that could be studied. The data obtained could then be used to understand the complicated physical and chemical processes involved in quenching electrical discharges using polymeric material.

To accomplish this, a representation of a circuit breaker was used in which an arc could be drawn between the electrodes. A mechanism was designed so that polymeric powder could be injected into the arc by means of pressurised nitrogen propellant. The arc discharge was then studied by the use of current and voltage measurements, optical spectrometry, high speed imaging, mass spectrometry, and pressure monitoring.

4.2 APPARATUS

4.2.1 MAIN TEST CHAMBER

The test chamber comprised a steel cylinder with four cylindrical ports set 90° from each other that contained windows made of 18mm thick toughened glass, which allowed monitoring of the arc. The ports could also be fitted with special brackets to allow the fitting of other apparatus, such as the injector mechanism. The lid of the chamber was steel and secured using sixteen 15mm diameter bolts and sealed with a rubber o-ring allowing pressurisation of the vessel with air, N_2, CO_2 or SF_6 and which prevented leakage of potentially harmful arc by-products. The lid of the chamber contained a central mounting for the initiation electrode mechanism and radial screw mounts for internal sensor attachment. The main external features of the test chamber are shown in Figure 4-1.

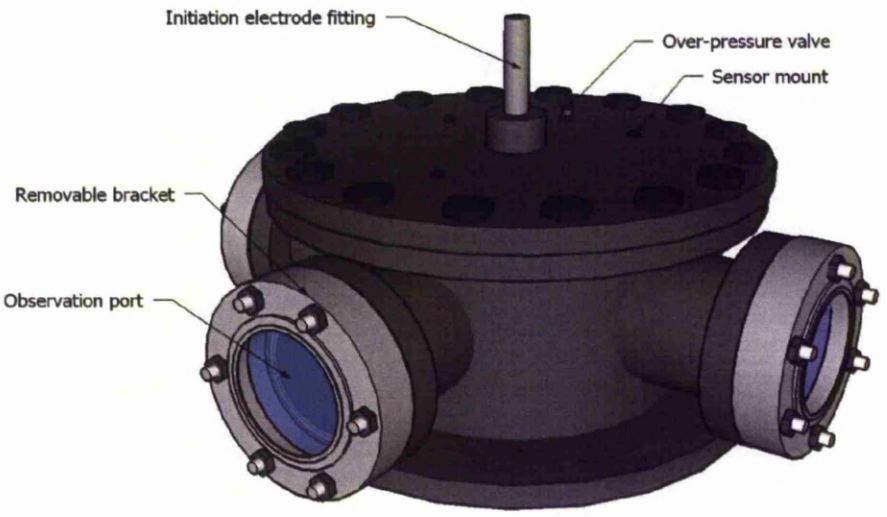

Figure 4-1: Main external features of experiment chamber

The design of the apparatus was such that it provided a realistic environment but still allowed easy access for diagnostic apparatus and faster experiment turnaround time than would be experienced with a full scale circuit breaker. The total volume, including the central chamber and observation arms, was $0.017m^3$, which was large enough to minimise pressurisation effects from the nitrogen propellant. The external dimensions of the chamber are shown in the Appendix.

The electrodes were copper and cylindrical in shape with a length of 50mm and diameter 20mm, mounted centrally in the chamber and spaced 30mm apart. The anode was the lower electrode and fed via a high voltage cable connected to a capacitor bank; ground and experimental earth were connected to the body of the chamber and the second electrode, which also contained the arc initiation mechanism. The cathode was the upper electrode with the same dimensions as the anode but with a central hole of diameter 7mm, through which a copper initiation electrode retracted. The cathode and initiation electrode mechanism were directly connected to the chamber and therefore earthed. The internal features of the test chamber are shown in Figure 4-2.

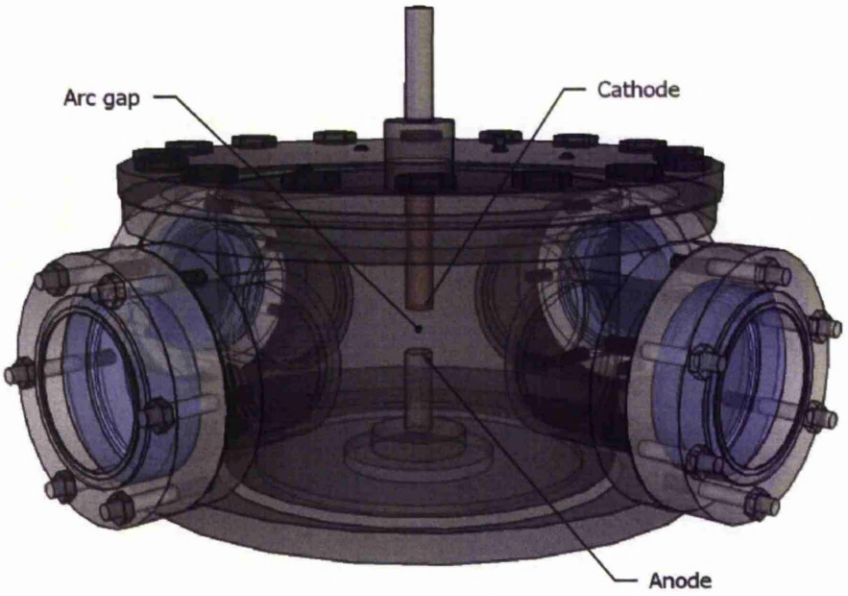

Figure 4-2: Internal arc chamber arrangement showing electrode gap

Both electrodes were screw mounted into the chamber allowing replacement when worn. The formation of the arc centrally in the chamber meant its characteristics could be observed more easily by spectroscopy and high speed video imaging via the observation ports.

4.2.2 CAPACITOR BANK CIRCUIT

Arcs were formed by the implementation of energy from a capacitor bank to the test chamber electrodes via a series resistor and inductor. The simultaneous application of this energy with the separation of the test chamber electrodes was sufficient to cause ionisation and dielectric breakdown that established into an arc discharge between the anode and cathode.

The capacitor bank consisted of a 33mF bank and an ignitron based control circuit. The ignitrons were used as switching devices in order to control the discharge of the capacitor bank into the test chamber and its deactivation at the end of each experiment in accordance with the control signals.

The experiment circuit consisted of an 184μH inductor in series with a 4.5Ω resistor; a current shunt was a further 1mΩ in series. The circuit diagram of the capacitor bank circuit is shown in Figure 4-3.

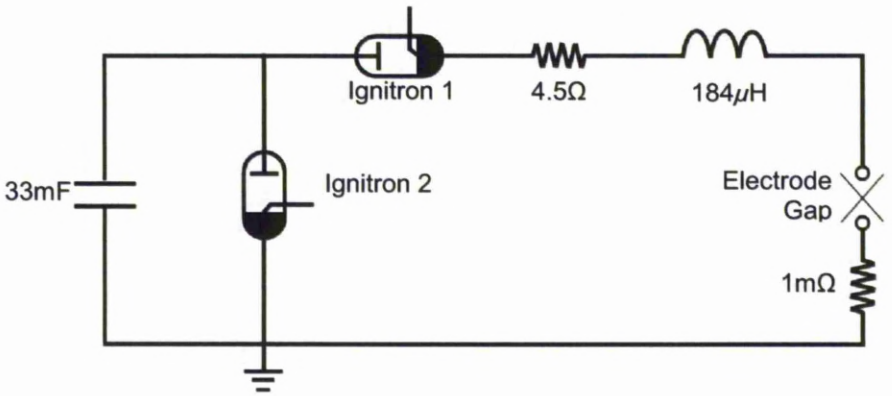

Figure 4-3: Capacitor bank discharge circuit diagram

In each experiment the capacitor bank was charged to 2.5kV, subsequently the first ignitron was triggered in synchronism with the activation of the initiation electrode and triggering of other apparatus, discharging the capacitor bank via the resistor and inductor circuit and forming the arc. The apparatus was configured to form a 50A, 2.5kW pseudo-dc arc on initiation for a maximum duration of 220ms. The discharge of energy from the capacitor bank meant the arc current reduced at a mean rate of 0.15A/ms. Fluctuations in voltage during the first part of initiation occurred due to the transfer of the plasma from the initiation rod and establishment of the arc on the upper electrode.

Configuration of the timing and control unit determined when the second ignitron was activated, which discharged the remaining capacitor bank energy to earth and extinguished the arc (if it had not already been extinguished by the interruption medium). In all tests the maximum time period was set to be 220ms in order to: enable a stable arc to be formed between the electrodes to allow experimental consistency; allow the injection the polymeric material into the plasma; and to permit the interaction to be monitored in detail.

A photograph of the main capacitor bank elements used in the formation of the arcs is shown in Figure 4-4.

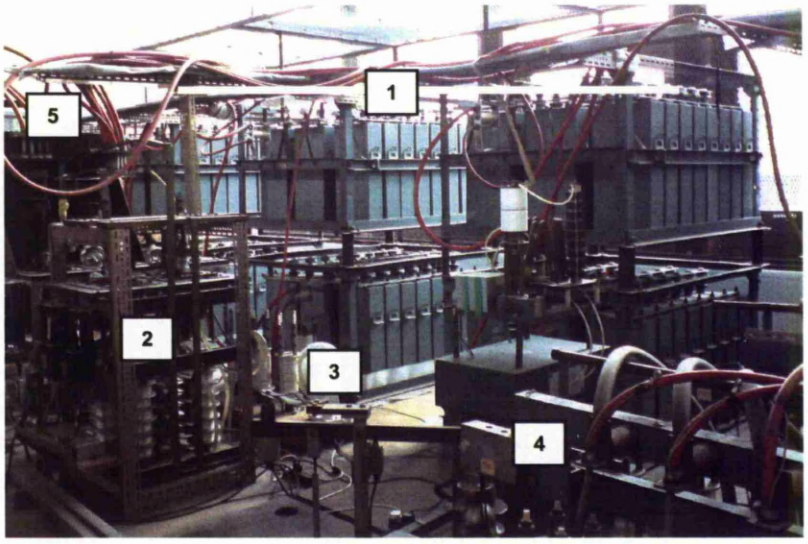

Figure 4-4: Photograph of capacitor bank and associated circuitry

1. Capacitor bank
2. Ignitrons and control signal interface
3. Resistor stack
4. Discharge mechanism
5. Bank output cabling

4.2.3 ARC INITIATION AND TIMING CONTROL

The arc formation mechanism consisted of a cylindrical copper initiation electrode 300mm long and 6mm in diameter that retracted into the cathode, driven by a solenoid. The solenoid was powered by an 115V/5A dc power supply supplemented by booster capacitors of total capacitance 2.94mF. The initiation electrode was driven by the solenoid at a speed of $0.86ms^{-1}$ and therefore the arc reached its full length between the electrodes 35ms after activation. At the start of the experiment, the initiation electrode was in contact with the anode. The solenoid was triggered by the timing and control system to move in synchronism with the discharge of the capacitor bank energy, drawing an arc between the anode and the initiation electrode.

When the initiation electrode was fully retracted the arc was established between the anode and cathode and was at full length. A cut away view of the initiation apparatus is shown in Figure 4-5.

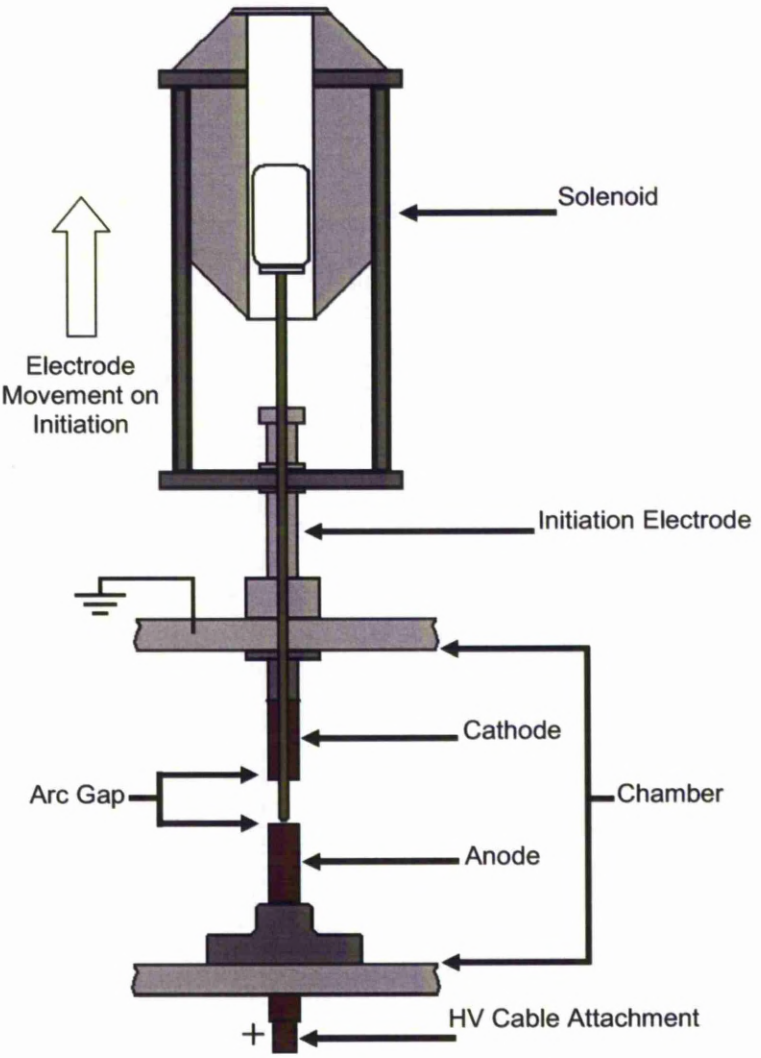

Figure 4-5: Cut-away view of initiation electrode solenoid mechanism

The correct synchronisation between the capacitor bank discharge and movement of the initiation electrode was important to ensure arc formation. The timing and control unit needed to be configured to account for the mechanical delay due to inertia in the solenoid movement so as to discharge the capacitor bank simultaneous to when the initiation electrode began to move.

Trigger signals for all of the apparatus and diagnostic equipment emanated from a central control unit. In the first instance the control unit was used to set the ultimate capacitor bank energy and charge it via a manually operated variac. The trigger signals for all of the apparatus consisted of 200V microsecond pulses that emanated from the control unit; the sequence of each trigger was adjusted based on the results of calibration tests performed initially in the absence of an arc. This was necessary in order to ensure that the arc initiation apparatus and diagnostic equipment activation occurred in the correct sequence.

The delay between the solenoid trigger and the movement of the initiation electrode was found to be 20ms; as a result of this the capacitor bank was not triggered until 20ms after the solenoid trigger. The polymer injector was operated 40ms after arc initiation in order to account for the initiation rod movement between the electrodes and inject the powder into a fully formed arc. The second ignitron, used to end the experiment by discharging the remaining capacitor bank energy to earth, was triggered last and configured to cause a maximum arc duration of 220ms. A timing diagram showing the triggering and operation of the apparatus is shown in Figure 4-6.

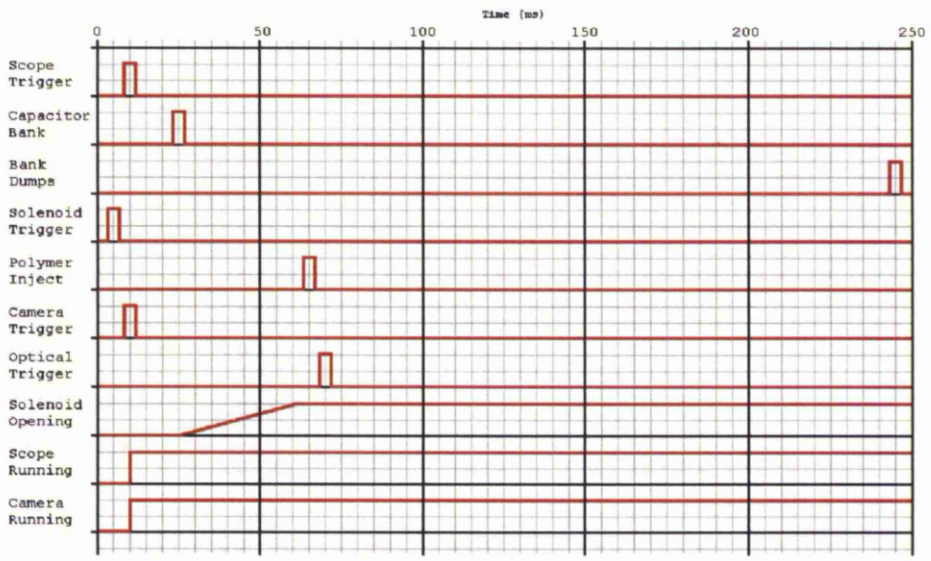

Figure 4-6: Timing diagram of apparatus operation

4.2.4 EXPERIMENTAL ARC CHARACTERISTICS

The discharge was pseudo-dc in nature, but in many ways the character of the arc, either dc or ac, in this fundamental analysis is irrelevant. The intention of the investigation is not to conduct operational tests on circuit breakers or represent real life fault conditions. The arc is in the most part a medium in which to apply the polymers and allow study of the elementary nature of the plasma-polymer interaction. As such, the data obtained in this project intends to provide the essential groundwork for the development of future prototypes that can be used in operational tests. With that said, the changes in the electrical characteristics of the arc are of interest and as such will be studied.

4.2.5 POLYMER POWDER INJECTION MECHANISM

The purpose of injecting powder into the arc discharge was to enhance the reaction between the arc plasma and powder. The polymer powders were deployed via an injection of pressurised nitrogen gas, which was activated by the opening of a solenoid valve triggered by the timing and control circuitry. In the experiments that used polymers, four grams were weighed using a chemical balance and loaded into the polymer injection apparatus.

The powder injection apparatus consisted of a size W nitrogen bottle (11m^3, 230bar) with a 500kPa (5bar) regulator that fed into a smaller 0.001m^3 (1L) gas storage pressure cylinder via a control valve. The powder was weighed before loading with a Sartorius ISO9001 compliant chemical balance and the system initialised by loading the powder into a chamber at the front of the equipment and pressurising the smaller gas storage cylinder to 172kPa (25psi) from the larger nitrogen bottle. The outlet of the injector was fitted into a custom metal cover that fitted over one of the observation port brackets and allowed injection of gas and polymer whilst maintaining the pressure integrity of the chamber. The outlet was 270mm from the electrode gap and in line with its centre, ensuring the powder would be injected directly into the arc. A diagram of the polymer injection mechanism is shown in Figure 4-7.

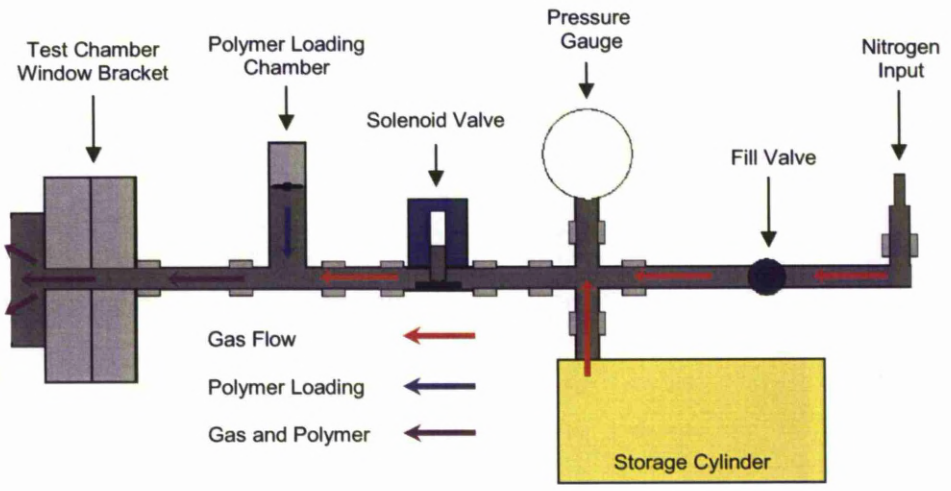

Figure 4-7: Diagram of polymer injection mechanism

A solenoid valve, powered by the same 115V/5A power supply used to operate the initiation solenoid and triggered by the timing and control unit determined the point at which the polymers were applied to the arc. When triggered, the $0.001m^3$ nitrogen cylinder discharged through the solenoid valve and polymer storage chamber, carrying the gas/polymer mix into the arc plasma, forcing a strong interaction. The quantity of nitrogen propellant stored in the storage cylinder at the start was $0.00344m^3$ (3.44L), and discharged in 6ms causing an average flow rate of gas and polymer of $0.034m^3$/min (34L/min).

The characteristics of the rate of flow versus time were assumed to be Gaussian in nature. Polymer injection was triggered by the timing and control apparatus 40ms after arc initiation in order to account for the delay in displacement of the initiation electrode so as to inject the polymer into a full length arc, peak flow was found to occur 43ms after arc initiation. Features of the nitrogen/polymer flow are given in Figure 4-8.

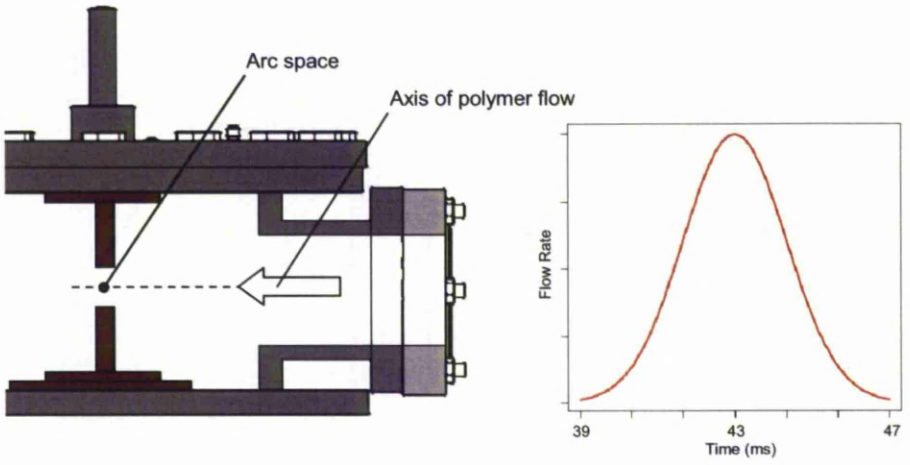

Figure 4-8: Polymer flow features: (a) flow direction; (b) expected flow rate

Analysis of the high-speed images of the test chamber following an arcing shot allowed the flow characteristic of the polymer injection to be estimated. It was found the apparatus applied the material at an angle of approximately 6° to the central axis of the electrode gap, which meant the spread diameter of the injected polymers at the arc was 50mm, with the electrode gap being 30mm long and 20mm wide.

4.2.6 GAS HANDLING APPARATUS

A gas handling plant was used to both add different gasses such as CO_2 to the chamber and also, importantly, to flush out potentially harmful arcing by-products. In cases where only a gas was used, such as with SF_6, the chamber was reduced to a vacuum before being re-filled with the test gas to 101kPa. After each test the chamber was twice reduced to a vacuum and flushed with N_2 in order to remove any gaseous by-products of the reaction and prevent contamination of later tests. Following experiments where polymer micro-particles were used, the chamber was thoroughly cleaned of any residual solid material before the next experiment. A diagram showing the gas handling system is shown in Figure 4-9.

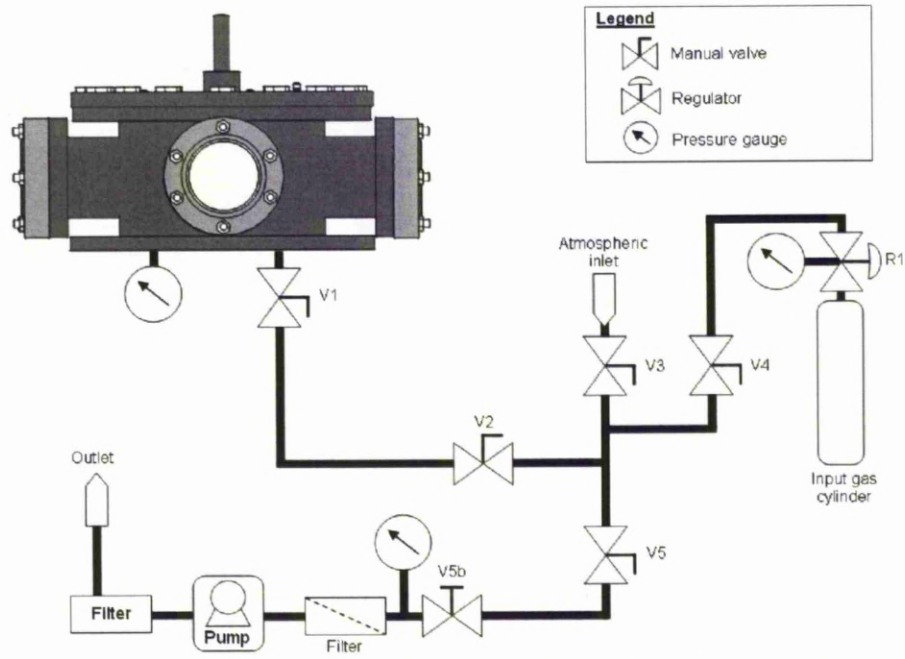

Figure 4-9: Gas handling apparatus for input and output of gaseous media

The flow of gas into the chamber was controlled by a 500kPa regulator (R1) attached to the source compressed gas cylinder. Gasses N_2, CO_2 and SF_6 were used in the course of the project provided by $11m^3$, 230bar gas cylinders. When the test chamber was at the desired pressure, valve V1 was closed before the experiment commenced. The chamber could be refilled with atmospheric air following cleaning or flushing by opening valve V3. Following a test, an electric 0.16kW Edwards 5 two stage rotary vacuum pump was used to pump the gas from the chamber. In order to remove harmful species, two filters were used, a carbon pellet type prior to the gas entering the pump and a liquid sodium variety before the gasses were emitted into the atmosphere. To ensure the removal of harmful gasses or contaminants that could alter the accuracy of test results the chamber was flushed with nitrogen following the gas extraction.

When SF_6 gas was used, a Dilo Type B048R01 SF_6 recovery system was utilised attached via a filter following valve V5 in Figure 4-9 to replace the pump and atmospheric outlet system. This prevented the environmentally damaging gas escaping into the atmosphere after it was used.

4.3 DIAGNOSTIC APPARATUS

4.3.1 CURRENT AND VOLTAGE MEASUREMENT

The changes in electrical characteristics of the arc as a result of the polymer-plasma interaction were studied to determine the arc quenching efficiency and mechanisms that occurred. A high voltage probe and current shunt were used, interfaced with an oscilloscope. The voltage probe was an ISO9001 compliant Tektronix P6015A passive high voltage probe and corresponding compensation box with a 7 – 49pF range. The probe had a 1000x attenuation effect such that the voltage displayed on the oscilloscope was understated by a factor of 1000. The specification of the probe is shown in Table 4-1.

Table 4-1: High voltage probe specification [118]

Bandwidth (MHz)	Typical Rise Time (ns)	Loading (MΩ/pF)	Maximum Input Voltage	Attenuation
75	4.0	100 / 3	20kV (rms), 40kV-100ms	1000X

Current was measured by use of a Thomas type current shunt, using a 1mΩ manganin resistor with a 1000:1 ratio connected via a coaxial cable to the oscilloscope. The shunt was considered to have an accuracy of 0.5% with a de-rating factor of 66% for continuous use, defined as being greater than 2mins, so was not a factor in any of these tests. Thermal drift was considered to start to occur at temperatures greater than 80°C and become significant at temperatures greater than 120°C. The current shunt was low side mounted on the ground side of the load, shown in Figure 4-3. This is a common configuration in power applications in order to eliminate any common mode voltages that could damage the oscilloscope measuring device. The voltage and current probes were connected to a Tektronix 2230 100MHz two-channel oscilloscope, which in turn was connected to a data-logging computer running the Tektronix WaveStar software. The oscilloscope was triggered externally by a signal from the timing and control unit via a 2kV/2μs isolation pulse transformer.

4.3.2 PRESSURE MEASUREMENT

Pressure differentials are often used in circuit breakers to force a gas flow that increases convective cooling of the arc. Any pressure increases caused by the polymer reaction with the arc were considered to be potentially useful in quenching, and were monitored via a sensor screw mounted in the chamber lid. However, the quenching effect in this configuration would be limited due to the absence of a nozzle around the electrodes to direct gas flow across the arc.

The pressure sensing apparatus consisted of a Kistler Type 601A piezoelectric sensor connected to a Kistler type 5001 charge amplifier. The sensor specification is given in Table 4-2.

Table 4-2: Specification of Kistler piezoelectric sensor

Pressure Range (bar)	Sensitivity (pC/bar)	Linearity (%FSO)	Operating Temperature Range (°C)	Capacitance (pF)
0 - 250	-16.55	± 0.3	-150 - 240	5

The sensor utilised the piezoelectric effect via a quartz crystal with the measured pressure acting through a diaphragm facing into the test chamber. This type of sensor is ideal for the dynamic pressure measurement and rapid changes expected in arcing experiments. The charge amplifier converted the small charge from the sensor crystal into a proportional voltage that could be monitored and stored via a Tektronix 2230 oscilloscope. It consisted of an inverting voltage amplifier with a high open loop gain and extremely high input impedance, being such that the capacitance of the sensor and cable could be neglected. A diagram indicating the position of the pressure sensor is shown in Figure 4-10.

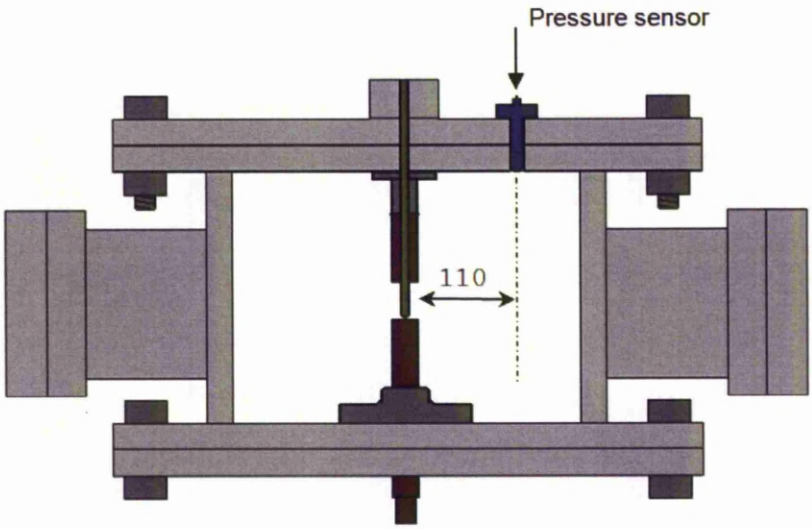

Figure 4-10: Pressure sensor mounting position

The pressure monitoring oscilloscope was triggered directly from the timing and control unit via a 2kV/2μs isolation pulse transformer. Voltage calibration of the pressure sensor was achieved by use of a Druck DPI500 digital pressure indicator and compressed nitrogen, allowing the voltage displayed on the oscilloscope to be directly attributed to a value of pressure.

4.3.3 OPTICAL SPECTROMETER

Optical emission spectroscopy is a common plasma diagnostic technique and provides many clues as to how the arc is changed by the application of the polymers and so can aid in the understanding of the reaction and quenching mechanisms observed. A Stellarnet EPP2000-LT14-VIS-10 optical spectrometer was used interfaced with the Spectrawiz software, the specification of which is shown in Table 4-3.

Table 4-3: Specification of optical spectrometer [119]

Wavelength Range (nm)	Grating (g/mm)	Slit Size (nm)	Slit Resolution (nm)
350 - 1150	600	14	0.8

The device used a CCD detector with a 1000:1 signal to noise ratio and pixel size 14um x 200um. The dynamic range of the system was 2000:1 with 6 decades. The software integration time was adjusted in order to maximise the detector output whilst avoiding saturation and maximising signal to noise ratio. The light emitted from the arc plasma was of high intensity and therefore the integration time was set to a low value of 4ms, a low value of integration time also enhanced the wavelength resolution. The Spectrawiz software was configured with smoothing and averaging switched off in order to allow more accurate determination of lower intensity spectral features with respect to the dominant copper emission lines formed from evaporated electrode material.

The input of the spectrometer was connected to an SMA905 0.22na optical fibre that was clamped facing into one of the chamber windows and pointing at the centre of the electrode gap. The critical angle of the fibre was 12.7° and so the acceptance angle was 25.4°. The fibre input was located 255mm from the arc; the positioning is shown in Figure 4-11.

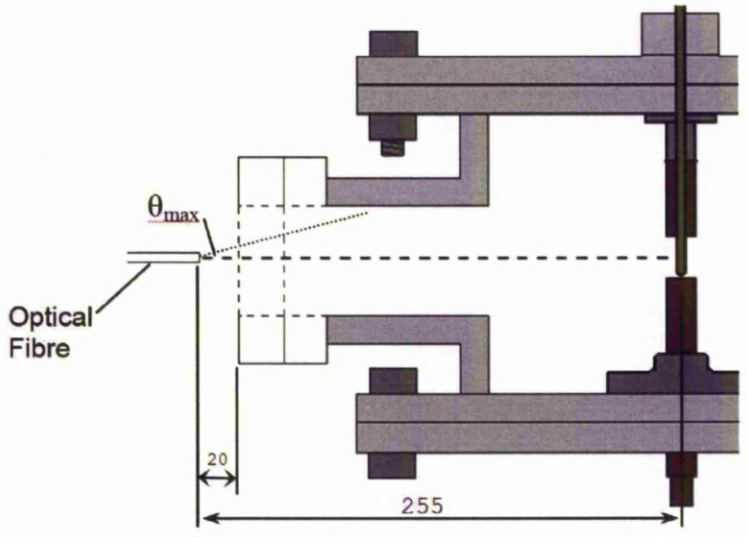

Figure 4-11: Optical fibre positioning into test chamber

The spectrometer was factory calibrated but was tested for wavelength and intensity by analysis of the main features of a test spectrum and reference to published spectral data. The spectrometer was found to be accurate to ±0.28nm for wavelength and ±13.5% for relative intensity. The larger error in intensity is due to an inherent difficulty in performing relative intensity calibration because published data is less accurate due to different scales being used in different publications [120]. In terms of both wavelength and intensity the spectrometer was considered sufficiently accurate to be used.

4.3.4 MASS SPECTROMETER

The thermodynamics of the change of state of polymers and subsequent chemical reactions was speculated to play a part in arc quenching by increasing the extraction of thermal energy from the arc, reducing plasma conductivity. The use of mass spectrometry made it possible to develop a greater appreciation of how polymers interact with the arc plasma in terms of decomposition and chemical reactions between decomposed species.

An MKS Cirrus quadrupole residual gas analyser was used, controlled by a PC running the Process Eye Professional software. This apparatus could monitor gas compositions over a wide range – from parts per billion up to percentage levels and used a heated inlet capillary to 150°C in order to allow a fast response to changes in composition after an arc event. The silica lined capillary was inert in order to prevent contamination or alteration of the sample. The mass spectrometer specification is given in Table 4-4.

Table 4-4: Specification of MKS Cirrus mass spectrometer [121]

Mass Range (amu)	Detection Limit (ppb)	Capillary	Gas Consumption Rate (ml/min)	Detector
1 – 300 variable	<100	Heated inert silica	20	Dual Faraday - SEM

The sampling inlet was linked to the chamber by a capillary tube of 1mm internal diameter which entered the test chamber via a 2mm hole in a circular bracket that fitted over one of the observation ports in place of the window. The access hole and sampling tube was sealed with epoxy resin externally in order to maintain chamber pressure integrity. Inside the chamber the tube was positioned 50mm from the arc gap and located 30mm above it and held in position by a support attached to the chamber lid. The sampling capillary positioning is shown in Figure 4-12.

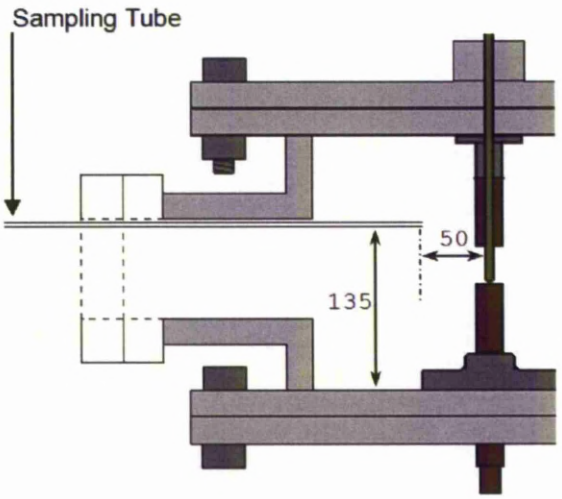

Figure 4-12: Position of mass spectrometer sampling tube

In order to reduce collisions that would inhibit the transit of ions in the mass spectrometer, it utilised a high compression turbo-molecular pump/diaphragm combination. The operating pressure inside the chamber was controlled by the Process Eye software to maintain 0.001kPa during experiments in order to allow accurate comparison in intensity between specific masses in each different test. The gas was sampled at a rate of 20ml/min before being input into the mass spectrometer ionisation source. The ionisation source was a twin heated filament that ionised the sample before it was applied to the quadrupole mass filter by means of emitted energetic electrons.

The quadrupole was configured by the Process Eye software to scan 1-100amu by variation of the ratio of voltages over the four rods. It was decided to limit the scanning range to less than the 300amu maximum as it was expected the energy of the plasma would render the presence of any high molecular weight species to be unlikely. The sample chamber and inlet interface could be baked via a radiant heater to 180°C to avoid vapour condensation inside.

Dual detectors consisting of Faraday and secondary electron multiplier (SEM) types were used in the system in order to optimise sensitivity and long-term stability of performance. The Faraday cup detector detects incident ions by measuring the charge it gains as a result of collisions and then using the generated current to form the mass spectrum. A secondary electron multiplier uses the incident charges from the ions to bombard a metal surface to emit electrons that are then accelerated by an electric field to cause more energetic collision with a second metal surface, emitting further electrons in a process called secondary emission, which increases the detection of small quantities of ions.

The detected mass spectrum was displayed on a computer via the Process Eye Professional software, which was connected to the mass spectrometer by a LAN connection. This allowed configuration of the mass spectrometer settings; status monitoring of parameters such as chamber pressure and filament status; and real time observation and storage of the mass spectrum.

4.3.5 HIGH SPEED IMAGING

High-speed imaging provided a qualitative indication of the effect the presence of polymers had on the arc in terms of such things as arc shape, length, turbulence and to a certain extent, presence of vapour. A Photron Fastcam SA-1 high speed camera was used, triggered by the timing and control unit via a TTL signal converter, which changed the 200V, 1μs trigger pulse into a 5V TTL signal that was compatible with the cameras.

The Photron Fastcam used a 12-bit CMOS sensor, allowing a maximum resolution of 1024 x 1024. The camera was fitted with a Nikon 24-85mm f2.8 zoom lens. For experimentation, the resolution was set to 1024 x 1024 at 5,400 frames per second, with a shutter speed of either 400μs or 200μs depending on the type of test, and aperture set to f22. A photograph of the camera in its experiment position is shown in Figure 4-13. Due to the intensity of the light emitted from the arc an 8X neutral density filter was fitted to the lens in each case in order to attenuate the light and prevent detector saturation. In all cases the camera was positioned on axis with the centre of the electrode gap and positioned outside the chamber 255mm from the arc. This kept the camera a safe distance from the discharge and prevented detector saturation but afforded sufficient proximity to allow detailed arc imaging.

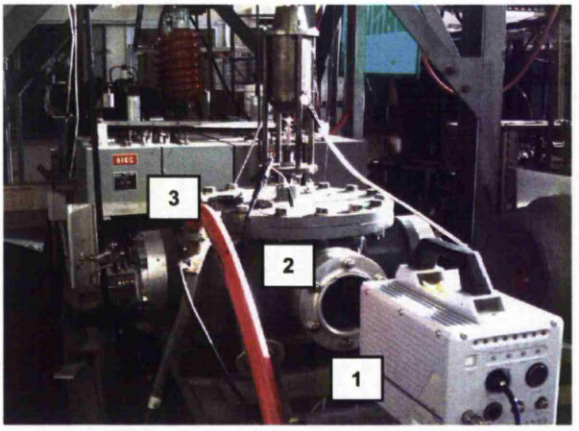

Figure 4-13: Photron SA1 high speed video camera in test position

1. High speed camera
2. Observation port
3. High voltage cable

The exposure time could be configured by the camera operating software and was used at two different settings during the course of the experimentation. Longer exposure times produced imagery with a more representative colour tone in the outer parts of the discharge and were acceptable for imaging the arc with no polymer. A shorter exposure time of 200μs allowed more detailed observation in the region of the arc allowing better resolution of the polymer particulates and the vapour formed, but with a pinkish hue to the images.

4.4 OVERALL CONFIGURATION

In most cases all of the apparatus and diagnostic equipment operated simultaneously so that direct comparisons between results could be made in the knowledge that they were all representing the same occurrence. This caused a complex procedure of pre-configuration and triggering for each test, and meant a long process of data download and subsequent analysis. A photograph of the test set up is shown in Figure 4-14. A diagram showing the entire experimental set up is shown in Figure 4-15, which shows the test chamber, capacitor bank circuit and control system, diagnostics triggering lines and outputs.

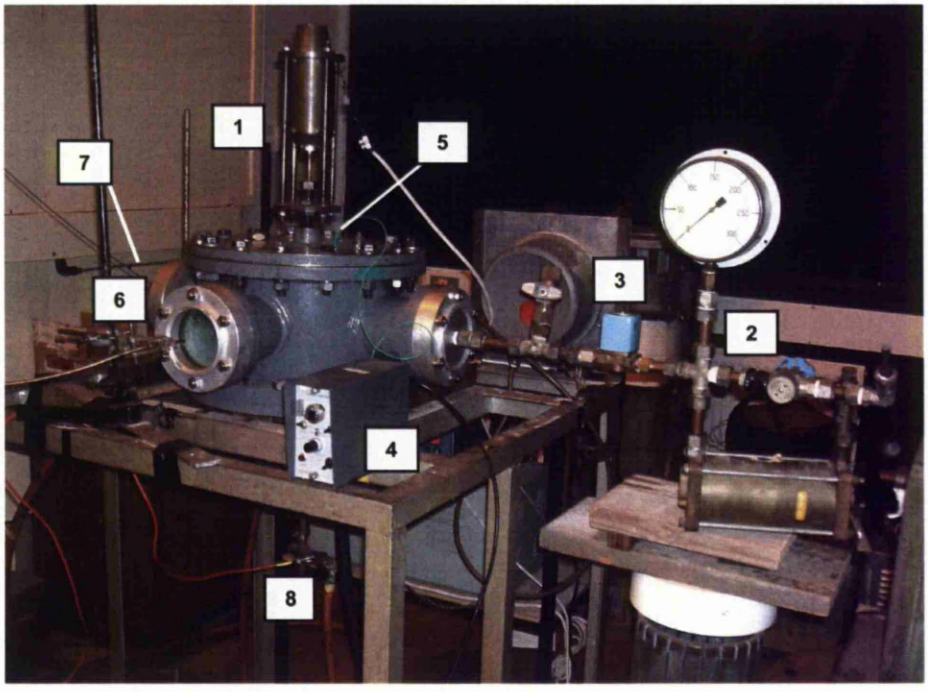

Figure 4-14: Full arc formation and diagnostic apparatus configuration

1. Initiation electrode drive solenoid
2. Polymer injection apparatus
3. Polymer injection control solenoid
4. Pressure sensor charge amplifier
5. Pressure sensor
6. Optical fibre linked to optical spectrometer
7. Mass spectrometer sampling tube
8. High voltage cable input

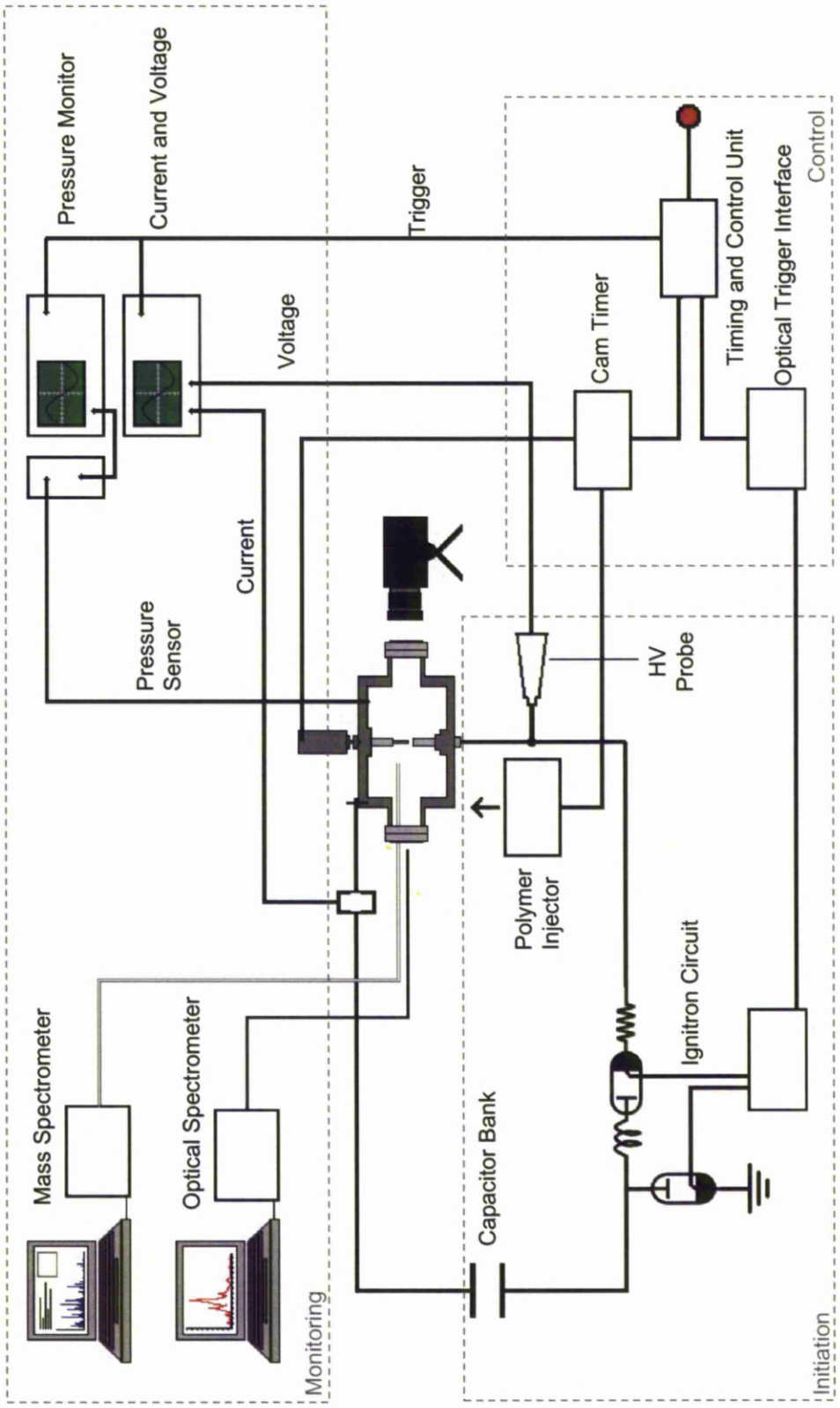

Figure 4-15: Overall experimental configuration

4.5 SUMMARY

Experimentation was the primary means of obtaining the results necessary to achieve the project aims; therefore the apparatus and diagnostic equipment used were vital. This type of arrangement was necessary to obtain the wide variety of experimental data needed to aid in the understanding of the complex processes involved.

The test chamber was such that it allowed diagnostic observation of the arc plasma and its interaction with polymer particulates. The energy for the arc was provided by a capacitor bank and operated by a timing and control system; this was vital in synchronising the application of capacitor bank energy with the separation of the electrodes and triggering of the diagnostic apparatus.

The polymer injection apparatus consisted of a solenoid valve mechanism, operated from a central control unit. It used pressurised nitrogen to propel the particulate polymers into the arc plasma, prompting an intense reaction.

The diagnostic apparatus consisted of an optical spectrometer, mass spectrometer, pressure sensor, high speed camera and two oscilloscopes. The aim was to monitor the plasma-polymer interaction so as to measure quenching efficiency and develop an understanding of the complex reactions taking place.

Chapter 5

Physical Characteristics

CHAPTER 5 – PHYSICAL CHARACTERISTICS

The physical characteristics of the arc are defined in this case to be related to its electrical properties, physical shape and size and properties related to convective gas flow and pressurisation. This chapter describes the results of experiments that aim to understand how polymer micro-particles influence the physical characteristics of the arc and lead to quenching.

5.1 ARC ELECTRICAL CHARACTERISTICS

The electrical characteristics of the arc were studied to asses the extent to which particulate polymers influenced arc current control and therefore interruption. In the first instance, arc discharges in various gaseous environments were tested so as to form a baseline of information that would allow comparison with the polymeric-arc characteristics. The gasses air, CO_2, SF_6 and N_2 were chosen for test as they already have applications in operational and experimental switchgear. The primary changes in arc electrical characteristics due to the plasma-polymer interaction were studied with a range of polymer types. The results provided a basis of fundamental understanding that then formed a foundation for further investigation.

5.1.1 ARC IN AIR

The fundamental characteristics of discharges in air with this experimental configuration in the absence of polymers were studied so as to establish a baseline for comparison with other arcing environments. A representative oscilloscope trace highlighting the main features of the current and voltage characteristics is shown in Figure 5-1.

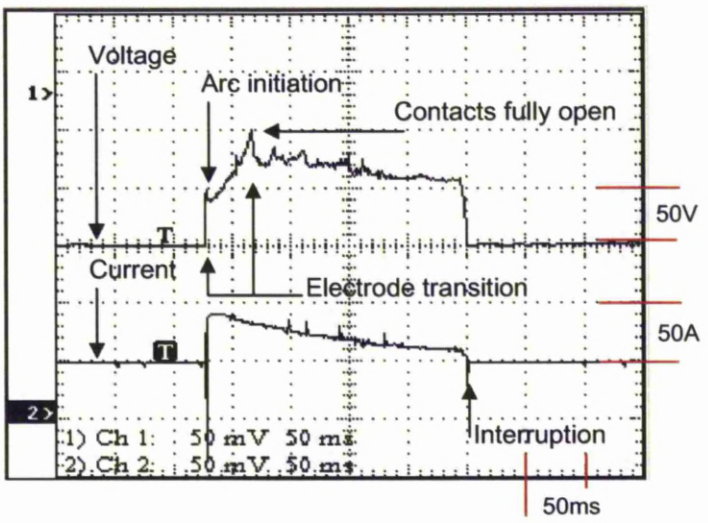

Figure 5-1: Voltage and current characteristics of an arc in air

The initiation electrode took 35ms to transition the electrode gap and establish between the anode and cathode. The arc voltage shows a gradual incline for this period due to lengthening as a result of the change in electrode separation and a consequent increase in resistance. A voltage peak can be observed on 35ms as the arc is established between the anode and cathode, before reducing at an approximate rate of 0.15A/ms as a result of the discharge of capacitor bank energy. After 220ms (from the point of initiation), the plasma was extinguished by the control apparatus to end the test. No signs of current interruption were observed and the arc was stable in character.

5.1.2 ENHANCED ARCING CONTROL GASSES

The arc quenching performance of CO_2, SF_6 and N_2 gas were tested so as to form a basis for comparison with the polymer-arc characteristics. Some relevant properties of these gasses are shown in Table 5-1. The three gasses were chosen for test due to having been used in operational or experimental circuit breaker applications previously, because of the different favourable aspects of their properties.

Table 5-1: Fundamental gas properties [122]

	CO_2	SF_6	N_2
Molecular Mass	44.01	146.06	28.01
Density (kg/m^3)	1.8	5.9	1.1
Dielectric Strength (%)	34	100	25
Arcing Time Constant	15	0.8	220

The properties of SF_6 have been discussed at length in previous chapters. Carbon dioxide has been used in experimental circuit breakers in various circumstances due to having relatively benign environmental characteristics and reasonable insulating and thermal properties [123, 124]. Nitrogen was used because of its relative low cost and favourable qualities for circuit breaker use such as being non-flammable and non-toxic.

5.1.2.1 Sulphur Hexafluoride and Carbon Dioxide

Representative oscilloscope traces showing changes in electrical characteristics of the arc in CO_2 and SF_6 are shown in Figures 5-2 and 5-3. In both cases, the presence of these gasses around the arc caused greater voltage and current fluctuations than observed in a purely air environment.

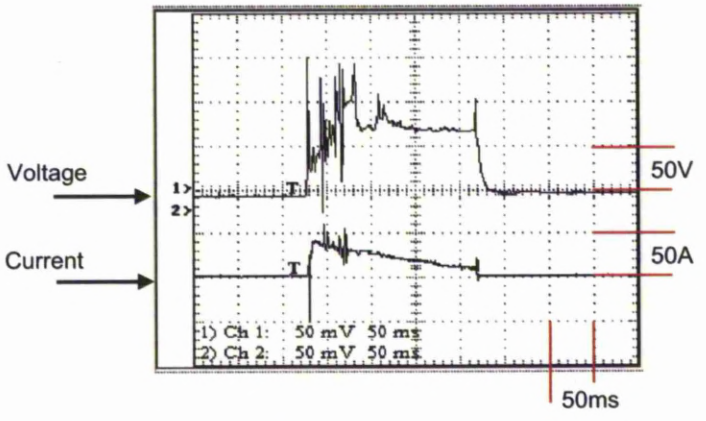

Figure 5-2: Voltage and current characteristics of an arc in CO_2

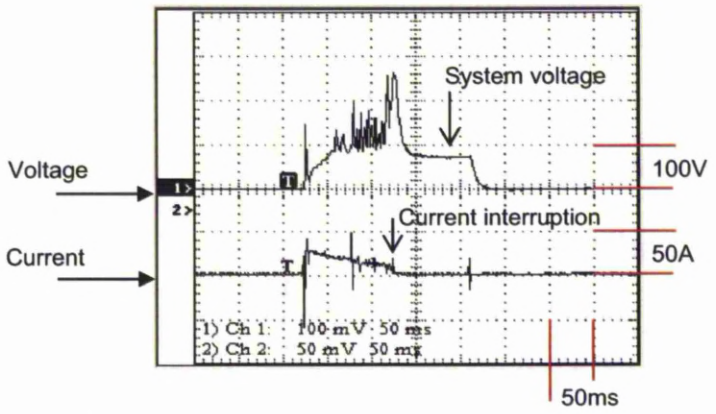

Figure 5-3: Voltage and current characteristics of an arc in SF_6

In the case of CO_2 the presence of the gas caused increased arc resistance but not to the extent that could cause extinction. The arc in an SF_6 environment caused interruption 103ms after initiation, with voltage and current fluctuations occurring with increasing amplitude until the arc was interrupted. This is due to the excellent thermal and dielectric properties of SF_6 [125].

5.1.2.2 Nitrogen Propellant

Polymer powder was propelled into the arc plasma via pressurised nitrogen. This gas was used due to its comparatively neutral arc quenching properties that allowed the polymer-quenching mechanisms to take precedence. It was important to quantify the effect of nitrogen flow across the arc on its own so that in subsequent polymer-arc tests, any improvement in quenching efficiency could be recognised as being due to the influence of the polymer and not solely due to the gas flow. Nitrogen was applied at a rate of $0.034m^3$/min for 6ms in the manner described in Chapter 4. A representative current and voltage trace for N_2 injection alone is shown in Figure 5-4. The N_2 gas flow results form a baseline that mean in the polymeric tests, any increases in energy dissipation from the arc above this level can be attributed to the effect of the polymer interaction and not the gas flow.

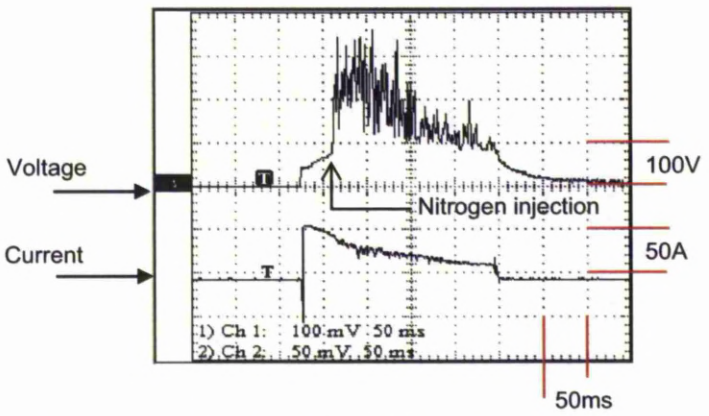

Figure 5-4: Oscilloscope trace of N_2 injection alone

For the first 40ms the discharge formed normally with an increasing voltage due to arc lengthening because of electrode separation. On 40ms nitrogen injection was triggered by the timing and control apparatus, ensuring the gas flow was applied to a fully formed arc. Significant voltage fluctuations occurred and a small alteration in current was also observed. These effects were partly due to morphological changes in shape and length of the arc but primarily due to an increase in convective cooling, causing an increase in arc resistance. The voltage peaks suggested an increase in arc resistance that was most likely caused by gas flow extracting energy from the arc leading to an increase in input energy to maintain the energy balance.

A convective flow of gas or oil is one of the main processes used in arc quenching in modern circuit breakers [126], usually by utilising an axial flow and is one of the three main energy emission processes, with conduction and radiation being the other two [126]. By increasing convection the dissipation of energy from the arc is increased and cooling occurs, this also prompts an increase in input energy as the system tends to an equilibrium condition in order to maintain the energy balance between input and losses. Another effect of a radial gas flow is the development of changes in the length and shape of the plasma between the electrodes which can alter the conductive path and lead to a higher resistance.

5.1.3 POLYMERIC ARC CHARACTERISTICS

Representative oscilloscope traces showing current and voltage changes with time as a result of the application of different polymers to the arc plasma are shown in Figure 5-5.

Figure 5-5: Voltage and current characteristics of polymeric arcs: (a) PS; (b) PA6; (c) PMMA; (d) PVC; (e) PTFE; (f) PE

In the cases of PS, PVC, PTFE and PE (Figures 5-6(a), (d), (e) and (f)) the application of the polymers caused extinguishment of the arc and a corresponding large voltage peak. The current and voltage formed normally until 40ms after initiation when the particulate polymers were injected into the plasma. The interaction between the polymer particulates and the arc plasma caused changes that impeded conductivity and ultimately interrupted the current altogether.

The polymers PA6 and PMMA failed to interrupt the arc current. In the case of PA6 a notable drop in current was seen in Figure 5-6(b) at around 50ms; however it seems the resulting voltage spike allowed the arc to re-strike. The injection of PMMA caused some voltage fluctuation shown in Figure 5-6(c) to a maximum of 150V in a manner similar to that of the nitrogen alone case but did not lead to current interruption.

A summary of the time periods to extinguishment after repeated experiments with polymeric arcs are given in Table 5-2.

Table 5-2: Mean time period to interruption[**]

Type	*Set 1*	*Set 2*	*Set 3*	*Set 4*	Mean	*Standard Deviation*	*Standard Error*
Air	220	220	220	X	220	0.0	0.0
CO_2	220	220	220	X	220	0.0	0.0
SF_6	103	94	110	X	102	8.0	2.7
N_2 (Inj.)	220	220	220	220	220	0.0	0.0
PMMA	220	220	220	220	220	0.0	0.0
PVC	220*	65	47	58	57	9.1	3.0
PS	50	55	42	197*	49	6.6	2.2
PE	50	103	220*	55	69	26.8	8.9
PA6	220	220	220	220	220	0.0	0.0
PTFE	50	52	180*	55	52	2.5	0.8

* = anomalous, excluded from mean, X = test not performed

[**] Note that the data shown in Table 5-2 is a representative sample, taken from four sets of experiments. During the course of the research many more measurements of current and voltage were taken, but are not included here for brevity, however the mean values can be considered to be typical.

The results in Table 5-2 show consistency from set to set with only a few easily recognised anomalies, most likely due to normal experimental error. The unpredictable nature and complexity of arc discharges means that some experimental variation was to be expected, but the overall impression is that the arc extinguishing characteristics of the polymers could be consistently applied. The most significant degree of variation came from the polyethylene tests due to a wider range of results over the four sets; however this does not significantly change the overall trends observed. By comparison to the case of nitrogen injection alone, it is clear that the presence of the polymers cause changes to the arc electrical characteristics that lead to quenching.

The mean time from initiation (designated t=0) shown in Table 5-2 does not take into account the fact that the polymers were not injected until 40ms later. Therefore the actual interruption times due to the effect of the polymer interaction are the above values minus 40ms. The mean time period to current eradication from t=0, and that from t=40ms, is shown graphically in Figure 5-6.

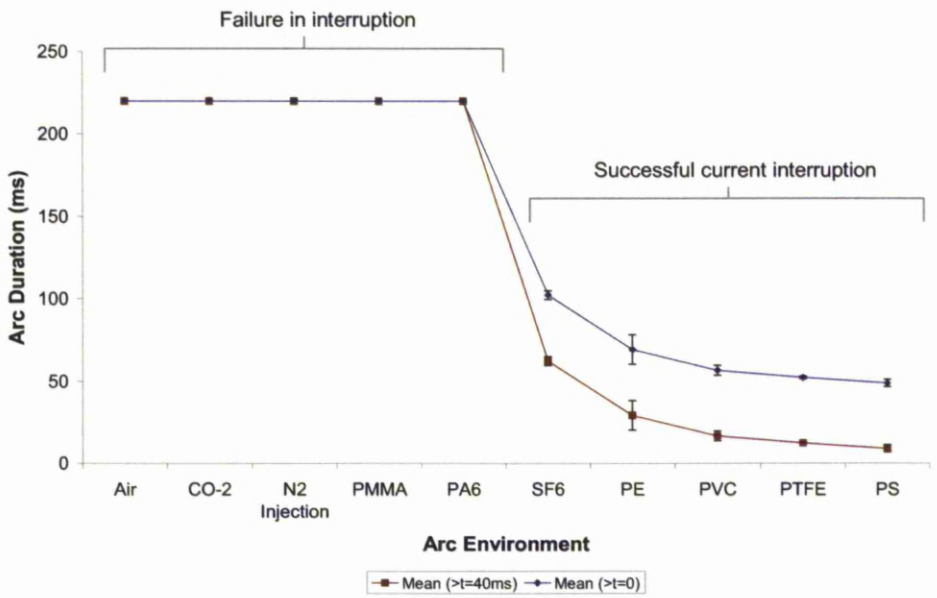

Figure 5-6: Mean time period to arc interruption

The quenching of the arc current was also accompanied by a large voltage peak due to the rapid increase in resistance as a result of the polymer-plasma interaction. The increase in arc voltage was due to the enhancement of the input energy to the electrode gap in order to maintain the energy balance of the discharge [128] and was limited by the energy stored in the circuit. Over-voltages are a feature of this type of interruption as the energy stored in the circuit is dissipated and in operation must be forced to a low enough value so as not to harm the system or apparatus [127]. This showed that the polymers increased energy losses from the plasma, leading to arc extinction occurring.

A table detailing interruption voltage peak from a range of polymer tests and the corresponding mean values and standard errors are shown in Table 5-3. The maximum recorded voltage is in the region of 800V due to oscilloscope range saturation.

*Table 5-3: Voltage peak at interruption***

Type	*Set 1*	*Set 2*	*Set 3*	*Set 4*	Mean	*SD*	*SE*
Air	62	58.3	56.7	X	59	2.7	0.9
CO_2	98	107	102	X	102	4.5	1.5
SF_6	271	257	261	X	263	7.2	2.4
N_2 (Inj.)	107	113	93.3	102.3	104	8.3	2.1
PMMA	127	200	130	55	152	41.3	13.8
PVC	143*	767	813	804	795	24.4	8.1
PS	798	807	807	790	801	8.2	2.0
PE	801	813	57*	793	802	10.1	3.4
PA6	120	123	130	105	120	10.5	2.6
PTFE	807	813	807	802	807	4.5	1.1

The mean voltage peak on interruption for each polymer and gaseous test environment are shown in Figure 5-7. The polymers that interrupted the arc within the designated time formed the larger voltage peaks due to their ability to increase resistance sufficiently rapidly to cause current eradication. The mechanisms used by the polymers to accomplish this type of interruption are the focal point of this investigation.

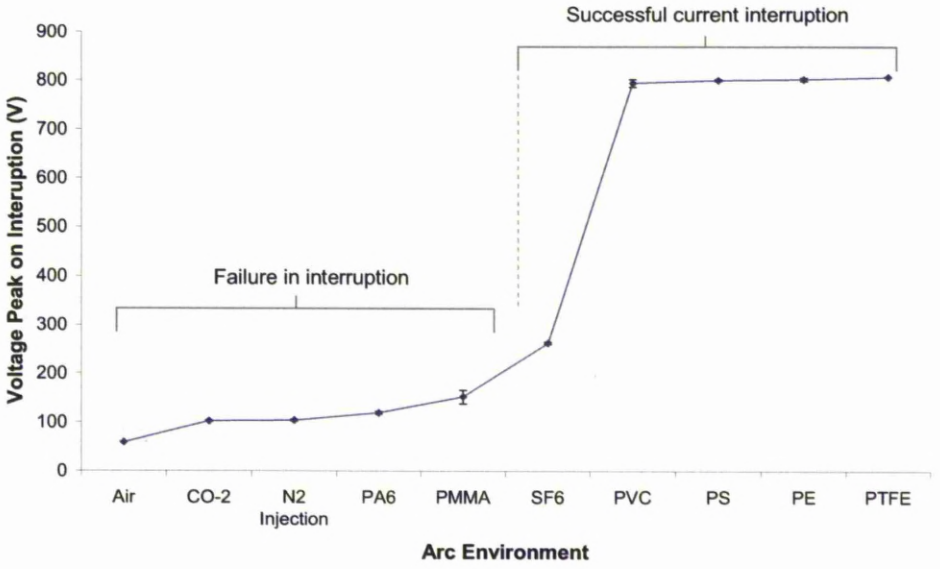

Figure 5-7: Mean voltage peak on interruption

An inverse relationship can be observed between the time period to current interruption and the corresponding voltage spike, shown in Figure 5-8. The relationship between time period and voltage peak shows that the polymers which were more capable of quenching the arc reduced the current to zero in the shortest time and produced larger voltage peaks on extinction.

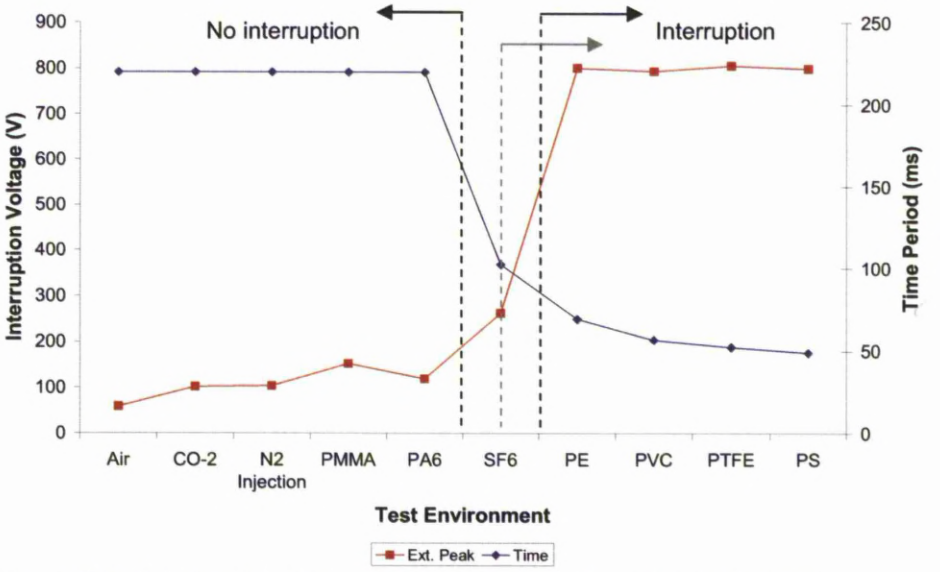

Figure 5-8: Relationship between time period to interruption and voltage

Changes in arc current and voltage can be brought together in order to demonstrate the overall effect polymers had on the arc. The polymers that were successful at quenching did so because of their ability to extract thermal energy from the arc by some means. As the conductivity of plasma is strongly related to temperature, it seems some types of polymer were likely to be more effective than others due to their ability to more efficiently cool the arc, increasing resistance, shown in Figure 5-9.

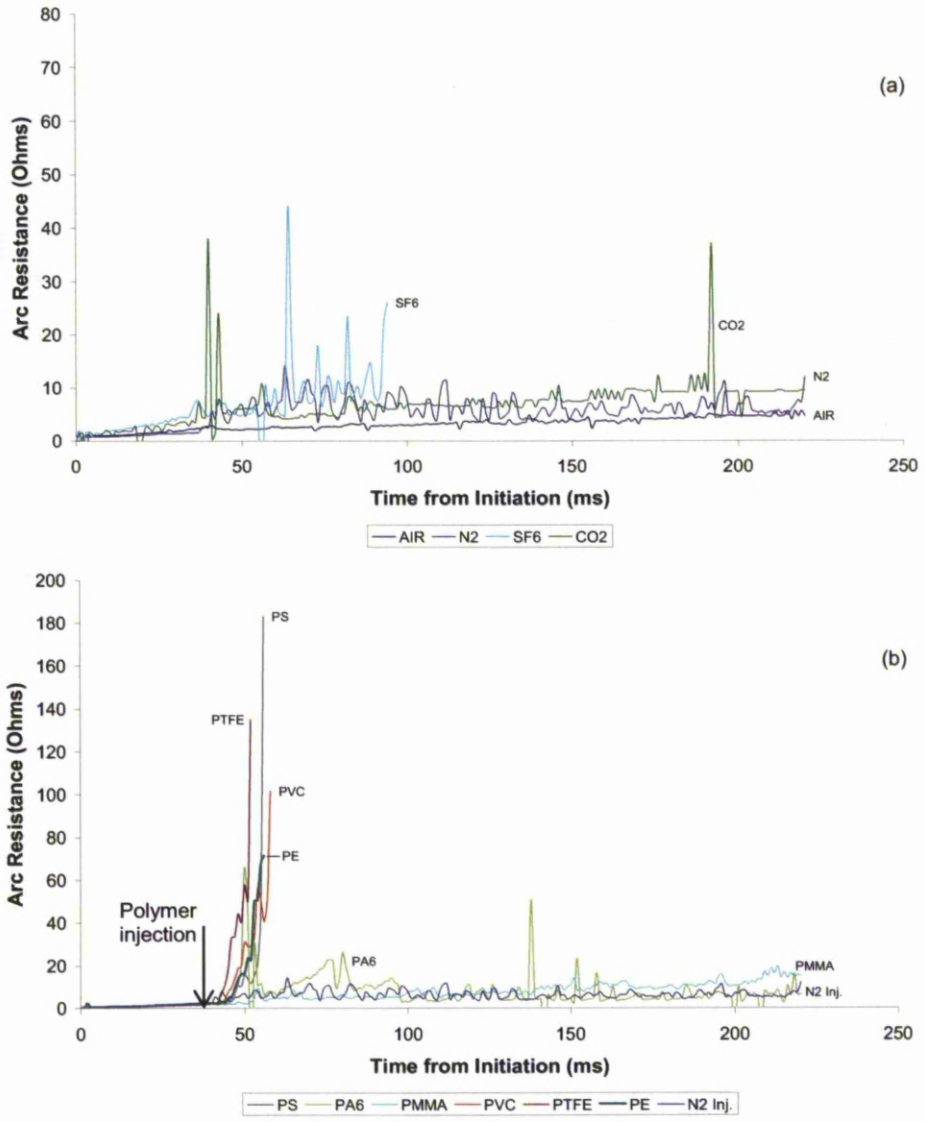

Figure 5-9: Changes in arc resistance with time in different environments: (a) Quenching gasses; (b) Polymers (Note differences in ordinate scale)

Both carbon dioxide and sulphur hexafluoride caused fluctuations in the arc resistance shown in Figure 5-9(a). Nitrogen did so to a lesser extent and the arc in air formed a relatively smooth line. Of those gasses tested, only SF_6 caused arc extinguishment, although the performance of CO_2 suggested it also impeded the arc current to a notable extent. This was likely due to the ability of the gasses to both inhibit current flow due to electronegativity and more efficiently extract thermal energy than air or nitrogen. In comparison to Figure 5-9(b), the changes in arc characteristics with gasses were less significant than was observed with polymers.

In Figure 5-9(b) there can be seen a sharp increase in the resistance of the arc when the polymers PTFE, PS, PVC and PE were applied, especially in comparison to the case of nitrogen injection alone. This was due to the reduction in arc current as a result of the cooling of the arc and consequent increase in resistance. The application of the other polymeric material, PMMA and PA6, did not increase resistance as notably. Polyamide 6 was observed to cause some fluctuation but not enough to affect interruption, and in all sets of tests PA6 was not seen to quench the arc before the end of the designated time.

So as to highlight more clearly the changes in the arc as a result of the interaction with the particulate polymers, a chart of resistance versus time for the first 65ms of arc duration for the most effective polymer quenchers is shown in Figure 5-10. The effect of the polymers in increasing arc resistance over N_2 gas flow alone can be clearly seen. The results suggest that the more successful polymer quenchers were those that were able to rapidly and efficiently extract energy from the arc. The complexity of the plasma-polymer interaction makes it difficult to be able to accurately describe the mechanisms in place that are responsible for polymeric-arc extinction. It seems clear that at a basic level the polymers extract energy from the arc, cooling it and reducing conductivity. However the exact mechanisms and the particular properties of certain polymers that make them more effective than others are not currently known and are the subject of the investigation in the following chapters.

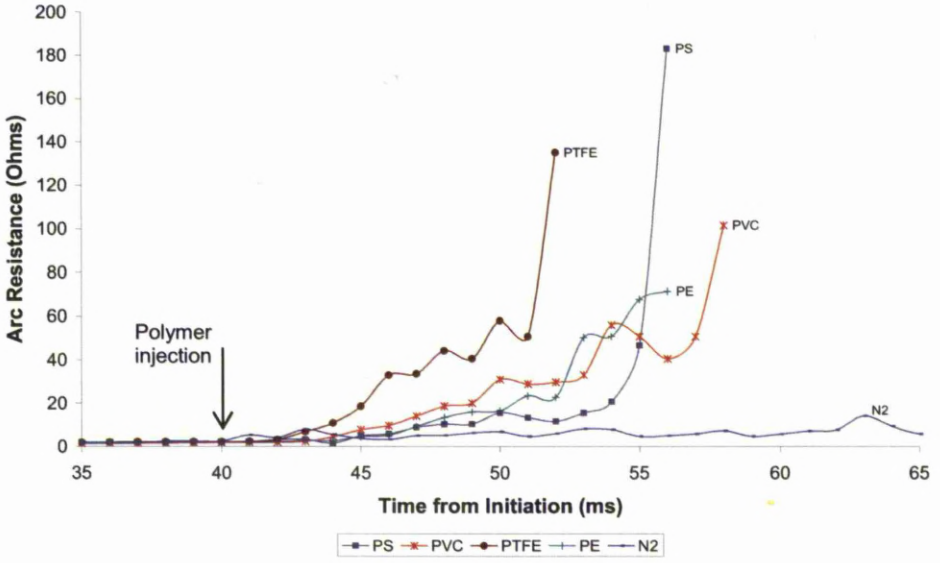

Figure 5-10: Arc resistance changes for efficient quenchers for the first 65ms

The polymer interaction could be responsible for interruption by utilising mechanisms such as: energy extraction by ablation and decomposition; favourable changes in thermal and/or electrical conductivity of the gas around the arc; and beneficial thermodynamics of chemical reactions between ablated gas species. The increase in resistance could also be due to morphological changes to the plasma as a result of violent reactions between the plasma and polymer causing changes in arc length and shape, turbulence could also add to convection losses and has been previously considered in some research as being a significant process in arc extinction [129]. The more efficient polymer quenching materials were likely to better utilise one or more of these schemes in order to increase arc resistance; it is likely that a combination of factors were at play in a highly complex interaction.

The aim of further investigation shown in subsequent chapters was to explain the polymer-quenching phenomena, the reasons for the difference in efficiency between materials and ways in which to enhance these effects.

5.1.4 SUMMARY OF ELECTRICAL PROPERTIES

A series of tests were performed with the aim of exploring the changes in the electrical characteristics of circuit breaker discharges caused by the application of polymeric particulates. Of particular interest was the ability of different types of polymer to quench electric arcs due to the nature of the interaction mechanism. The polymers PTFE, PS, PVC and PE all caused arc current interruption by their presence in the nitrogen gas flow, which enhanced energy losses from the plasma. The polymers PA6 and PMMA did not cause significant enough changes to extinguish the arc; however PA6 did cause fluctuations in arc resistance that suggested some positive aspects of its interaction. The quenching ability of the polymers is speculated to be due in the most part to the increase in energy losses from the arc as a result of the plasma-polymer interaction. The more effective quenchers were those whose properties meant they more efficiently extracted energy.

5.2 HIGH SPEED IMAGING

High-speed video gives a qualitative impression of the interaction between the polymeric particles and the arc plasma. The nature of discharges in gasses and with nitrogen-polymer axial flows was studied so as to observe changes in the plasma when interacting with polymer particulates. A visual impression of the changes in the arc in various environments provides an interesting and intuitive means of aiding in the overall understanding of the phenomena.

5.2.1 AIR, SF_6 AND CO_2 ARC IMAGING

Imagery of an arc in air in the absence of any polymer is shown in Figure 5-11. The image sequences shown start at 35ms - the point at which the initiation electrode first reached full retraction and the arc was at full length. The positions of the electrodes are marked with white dashed lines.

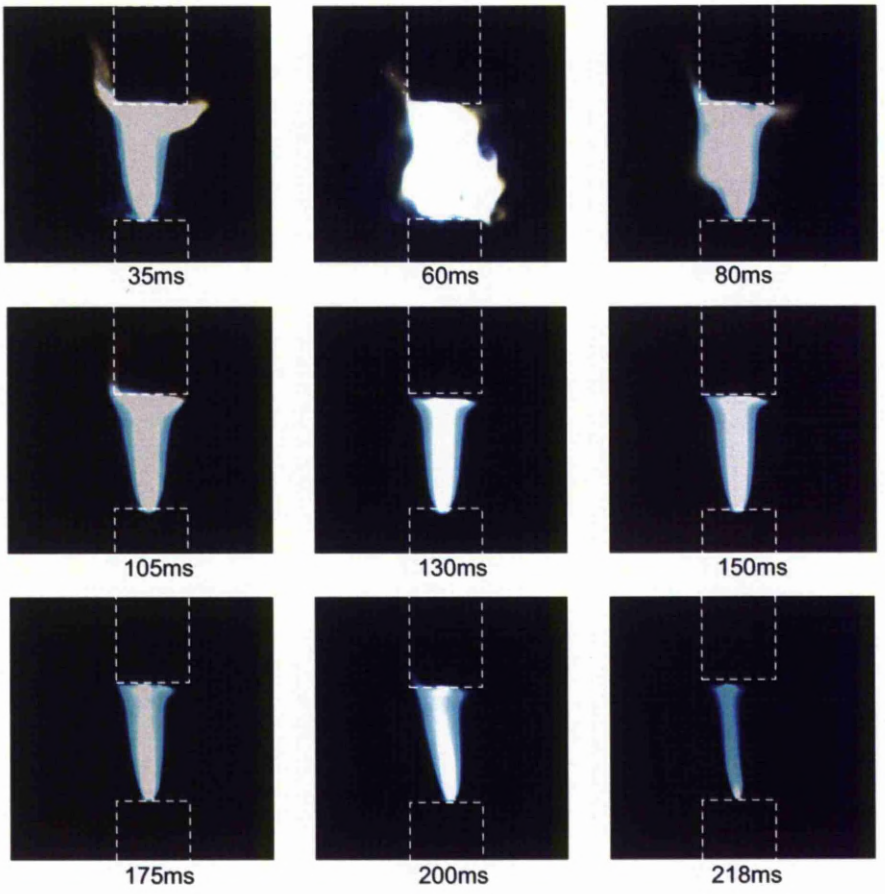

Figure 5-11: Time series of images from an arc in air

The first image in Figure 5-11 at 35ms shows the presence of vapour at the upper electrode, most likely copper, as the arc transferred to the cathode from the initiation electrode. Further instability is observed as the arc establishes before a very laminar flow occurs for the remainder of the time and shows the arc energy balance to be in equilibrium. The final frame shows a thinning and dimming of the arc immediately prior to extinguishment (caused by the system).

The arc formed in an SF_6 environment is shown in Figure 5-12. After initiation the arc is seen to increasingly perform loops and spirals with time, which significantly increase length and resistance of the arc and ultimately force interruption. A thinner and brighter arc core is observed in SF_6 than compared to that of air and is a common feature of SF_6 arcs. This effect is due to the combination of a high arc core temperature and steep radial temperature gradient with the surrounding gas due to poor thermal conductivity at arc temperatures; this effect in combination with the high electron affinity of the gas creates a non-conductive region around the outside of the arc core [130].

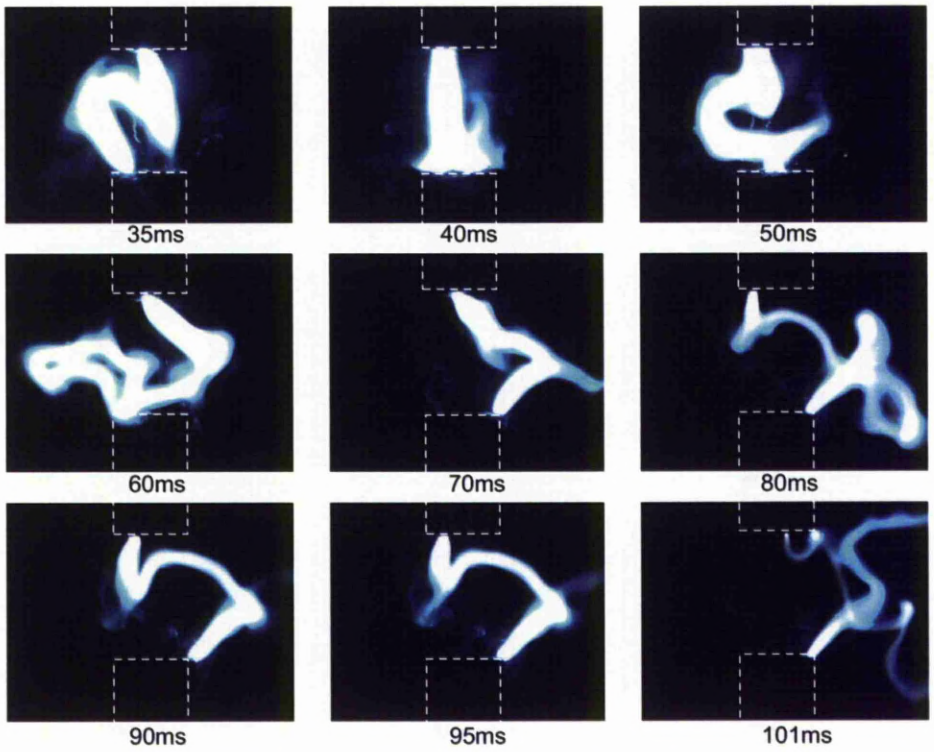

Figure 5-12: High speed imaging time series of an arc in sulphur hexafluoride

The arc in carbon dioxide shown in Figure 5-13 shows a slightly turbulent arc that does not gain stability and form into a laminar flow. Visual interpretation alone seems to suggest a greater quenching performance over air because of the enhanced energy losses and increase in resistance caused by the instability.

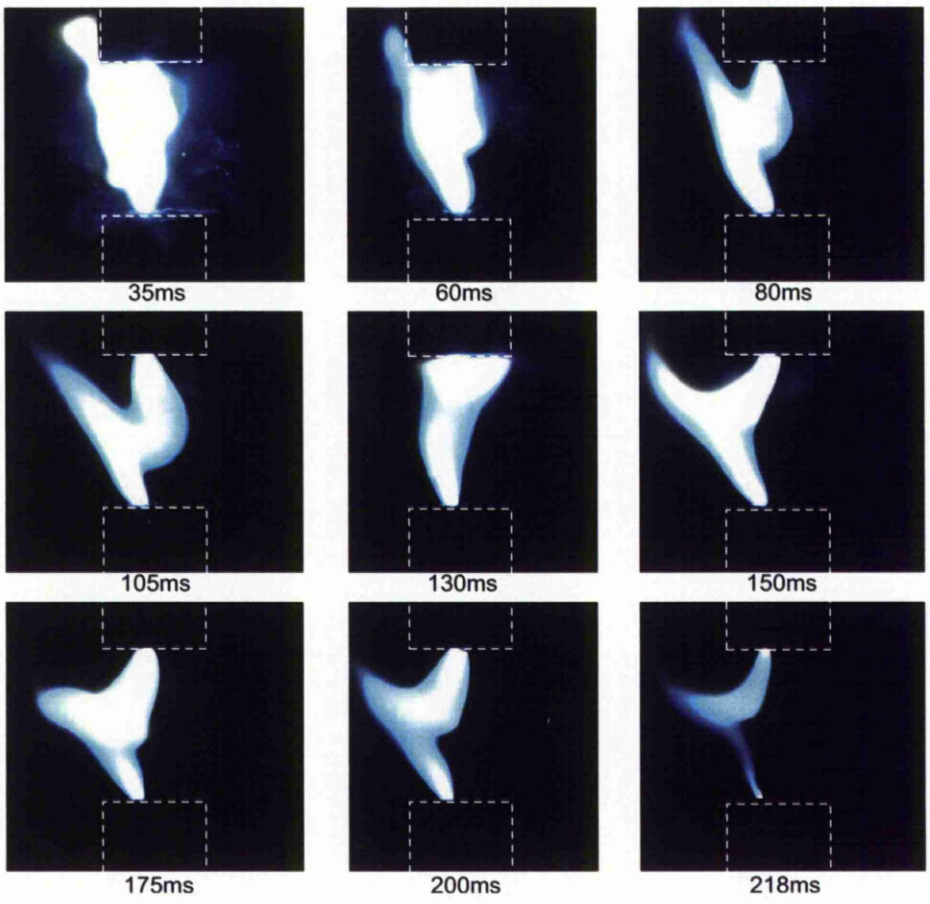

Figure 5-13: Arc imaging series of an arc on a CO_2 environment

A larger diameter arc can be observed in Figure 5-13 with respect to SF_6 because of the larger thermal conductivity of CO_2 at arc temperatures forming a lower temperature gradient; also, the outer layers of the plasma retain electrical conductivity due to the poorer electron affinity of CO_2 than compared with sulphur hexafluoride. In general, carbon dioxide has better performance in circuit breakers than air or nitrogen because of its higher value of dielectric strength [131].

5.2.2 POLYMERIC ARC IMAGING

It is not possible to develop any significant insight into the quenching effects by visual interpretation alone, however several notable characteristics of the polymer injection can be found by analysis of high-speed imagery. Visual observation shows that the interaction between the polymer and plasma can be generally divided into four phases:

1. Initial interaction – a smaller amount of polymers first react in the arc due to the lower initial flow characteristic of the propellant. At this stage the volume of polymer is not enough to extract enough energy to cause interruption
2. Main interaction – at the peak flow, 43ms after initiation, the maximum amount of polymer reacts in the arc causing the greatest amount of vapour/gasses to be formed and the maximum arc quenching reactions
3. Arc instability – starting at around the region of peak flow and continuing beyond, the arc becomes increasingly turbulent which can improve energy dissipation due to convective cooling and morphological changes
4. Extinction – the arc is forcibly interrupted if the polymer reaction is sufficient to extract enough energy, otherwise after a set duration the arc is extinguished by the apparatus

5.2.3 POLYMER CHANGE OF STATE

Images from the high-speed video showing polymer injection into the arc are shown in Figure 5-15. They have been enlarged to the region if interest shown in Figure 5-14 to show the polymer particle interaction in more detail. Close inspection shows small un-reacted peripheral particulates away from the arc core. As the density of polymer particles entering the arc increases, more irregularly shaped particles, with diameters several times larger than the un-reacted species can be seen around the arc centre, which suggests melting and the formation of vapour.

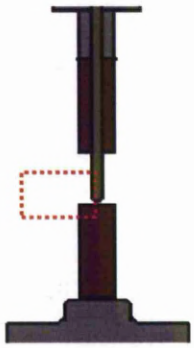

Figure 5-14: Diagram showing region of interest displayed in Fig. 5-15

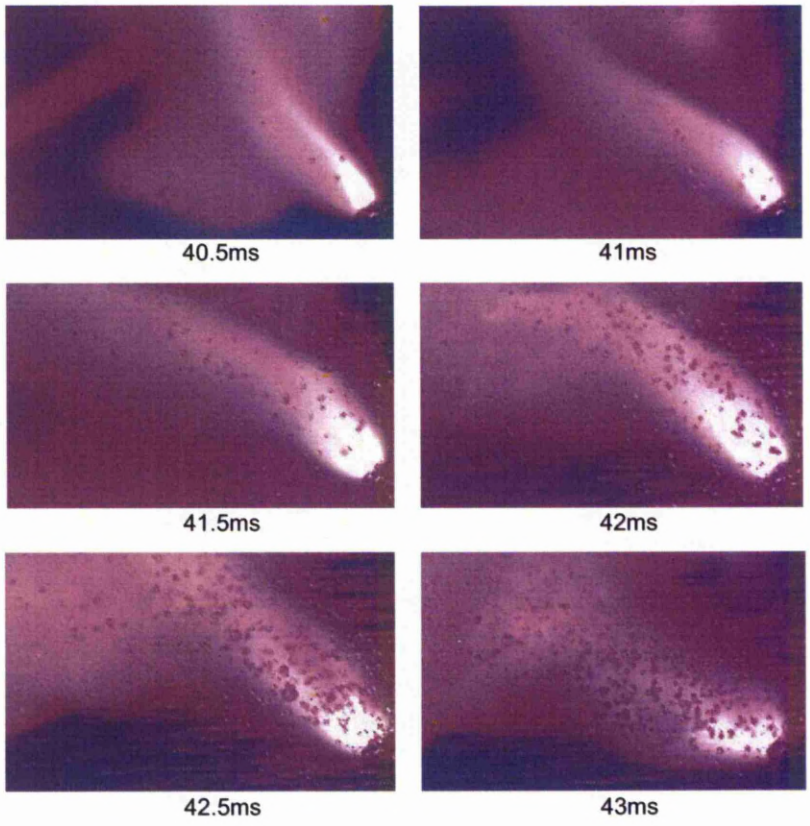

Figure 5-15: Image sequence showing polymer-arc interaction

An enlarged version of the 42.5ms image above is shown in Figure 5-16 to enable more detailed inspection. An intensity-based colour-map has been applied to the second image in the figure using a Matlab function in order to increase the information content of the figure.

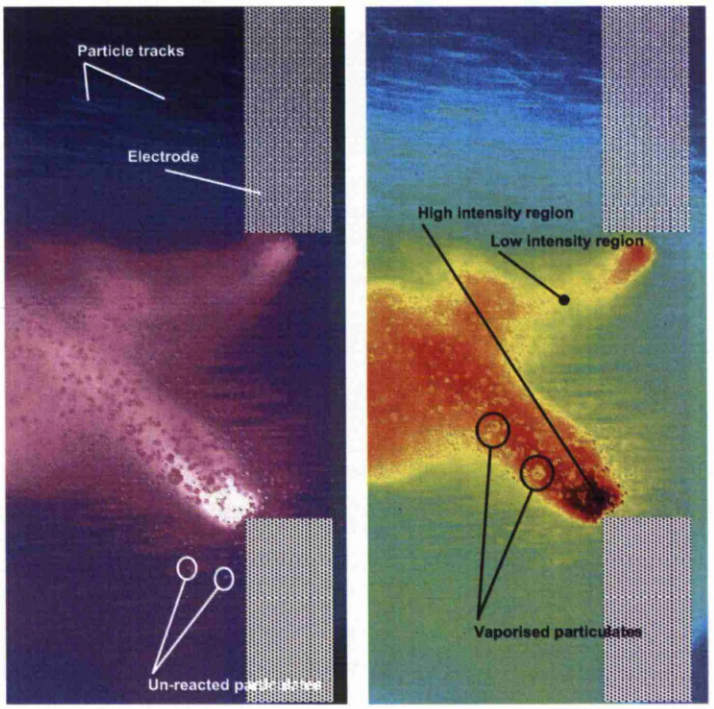

Figure 5-16: Features of polymer injection into the arc plasma

At the periphery of the arc are small white dots that are un-reacted particles in their original state; closer to the arc and particularly around the arc core, larger diameter and more irregularly shaped objects can be seen. These are likely to be localised vapour packets due to melting of the polymer in the arc. The intensity of the image is lower in the regions of vapour than the surrounding plasma, which could suggest localised cooling as a result of the particle phase change.

The cases where interruption was not achieved provide more clues as to the nature of the reaction due to the longer arc duration and resultant longer period of interaction. At the later stages of an arc with PMMA powder, randomly moving luminous shapes can be observed flowing around the arc, shown in Figure 5-17. They seem to be created when polymer particles in the vicinity of the arc interact with the plasma boundary and re-emerge, moving erratically in all directions towards and away from the electrode gap.

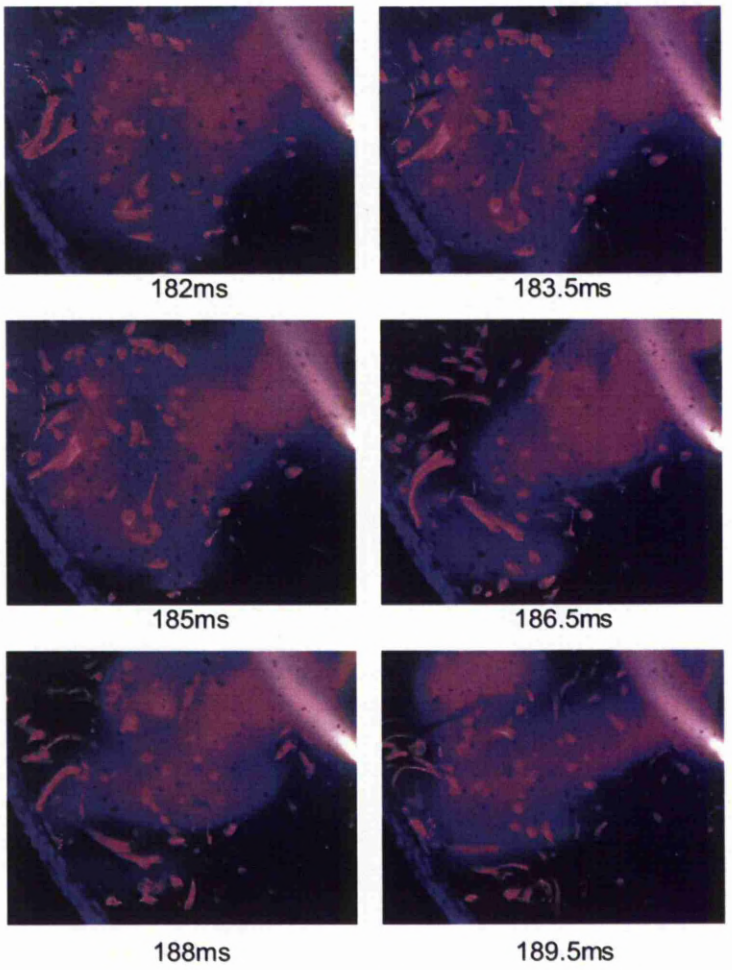

Figure 5-17: Later stage polymer vapour phenomena

The species in Figure 5-17 are luminous and so are at high temperature, which is maintained for tens of milliseconds away from the main discharge before fading. These could be charged particulates that have extracted some energetic particles from the plasma, which then exist for a short duration, or high temperature vapour formed from melting particulates.

5.2.4 INSTABILITY AND TURBULENCE

The thermal and electronegative properties of sulphur hexafluoride caused the arc to move erratically and as a consequence extract greater amounts of energy than would be the case in air. In some types of circuit breaker magnetic or gas systems deliberately introduce turbulence into the arc as it plays an important role in interruption [129]. In this case, visual investigation shows that the application of particulate polymers into the arc plasma caused instability and turbulence in the arc that could play a role in quenching. An unstable arc caused by the effect of the polymer and its vapour is shown in Figure 5-18.

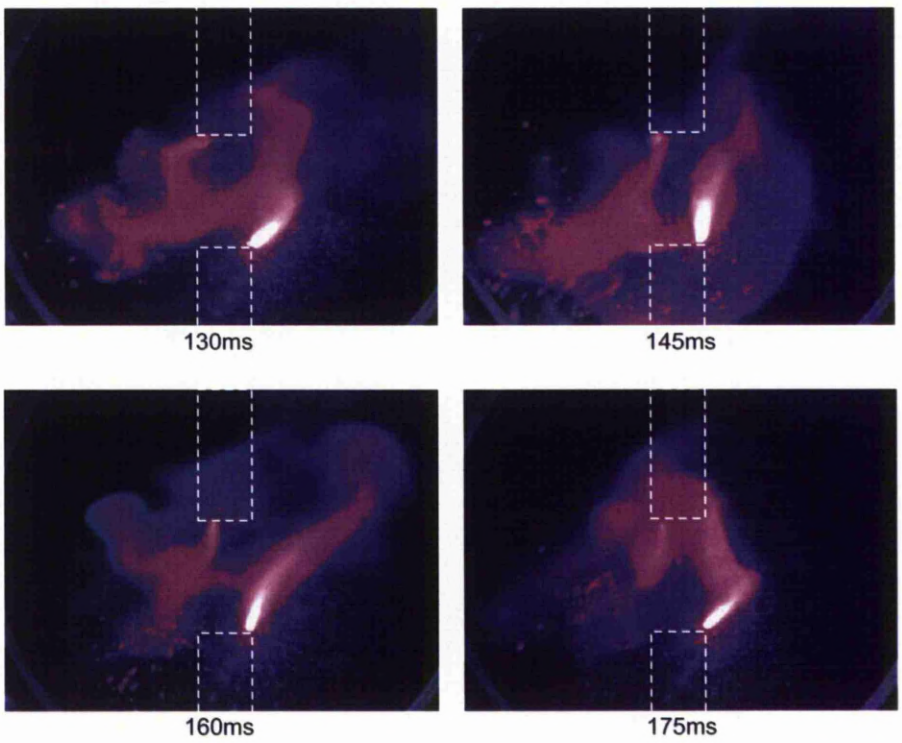

Figure 5-18: Turbulent arc formed due to polymer interaction

Turbulence is defined as fluctuations in flow field in time and space. Vigorous turbulence has been thought to result in effective arc cooling in ac systems at around the time of current zero [132] or for over a longer period of time in low current apparatus where it dominates over radiative losses [133].

It was observed through testing that different types of polymer influence different effects in terms of changes in arc morphology. The application of the polymers PTFE, PS, PVC and PE tended to cause much greater morphological changes in the arc shape and led to interruption. The less efficient arc quenchers PMMA and PA6 did not cause such significant effects in the arc and produced images that were more analogous to the nitrogen alone injection. Example image sequences from each of the polymer tests are shown in Figures 5-19 to 5-25 to allow comparison. The experiments in which the current was interrupted early show fewer images, as the arc duration was shorter.

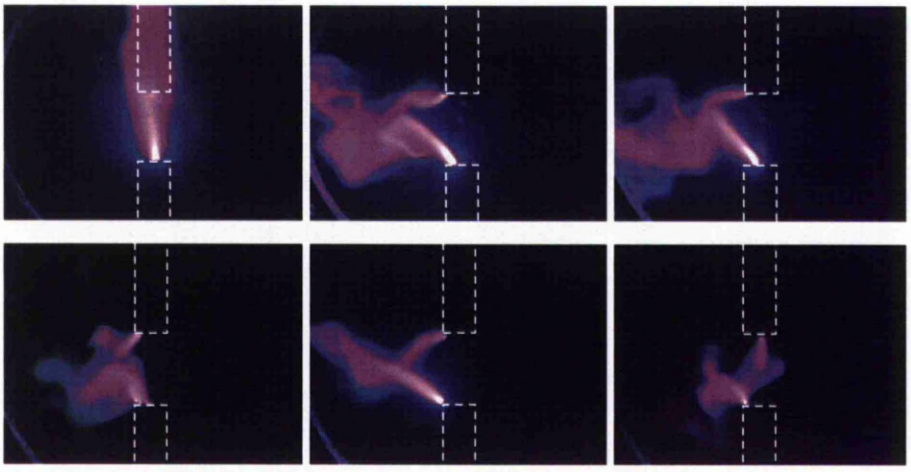

Figure 5-19: High speed imaging of nitrogen injection with no polymer

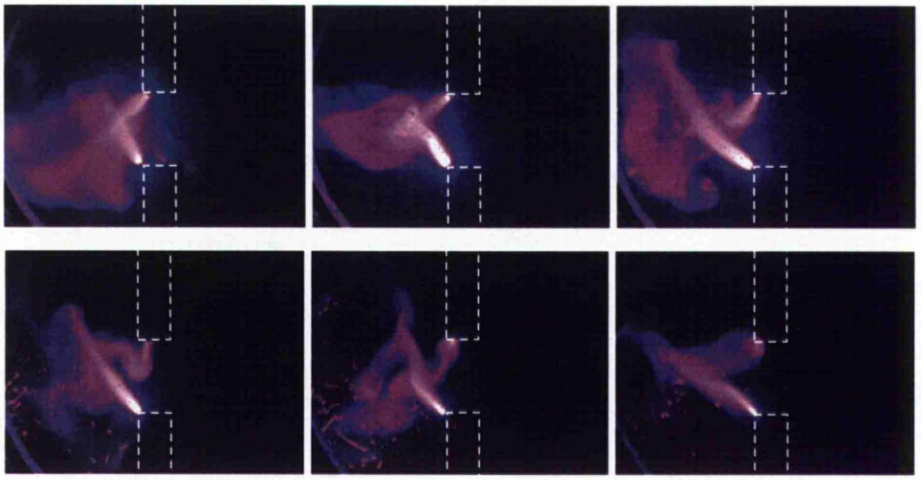

Figure 5-20: High speed imaging of injection with nitrogen and PMMA powder

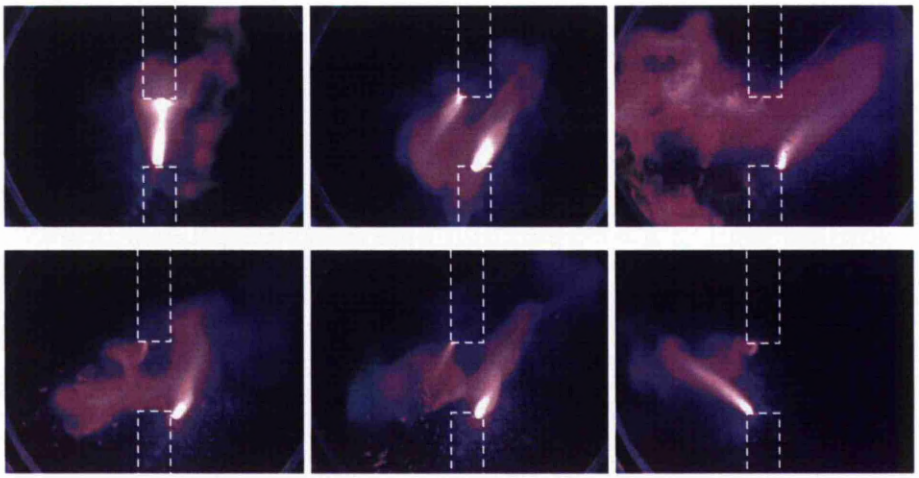

Figure 5-21: High speed imaging of injection with nitrogen and PA6 powder

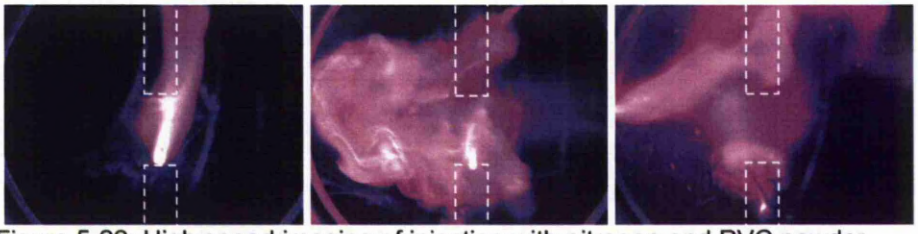

Figure 5-22: High speed imaging of injection with nitrogen and PVC powder

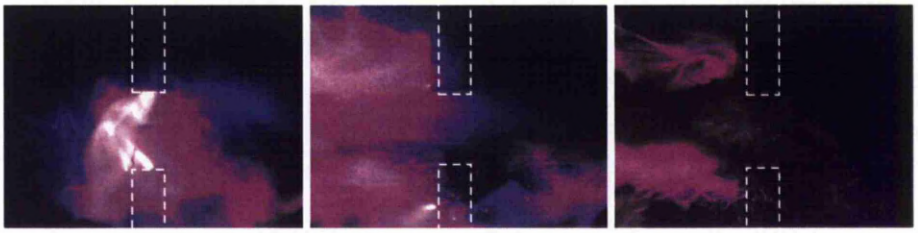

Figure 5-23: High speed imaging of injection with nitrogen and PS powder

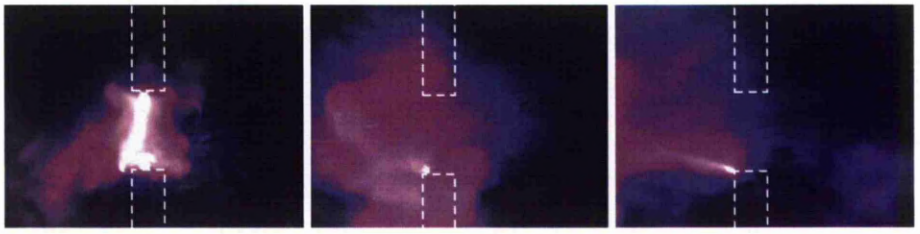

Figure 5-24: High speed imaging of injection with nitrogen and PTFE powder

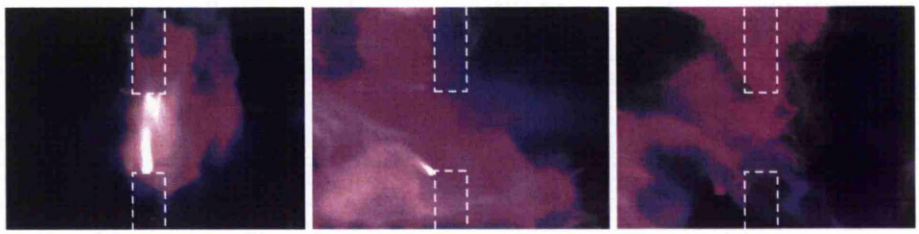

Figure 5-25: High speed imaging of injection with nitrogen and PE powder

Although inspection of the previous image sequences seem to show differences between good and poor quenchers in the way in which the polymers caused changes in the arc, the reasons for these differences, nor the interruption mechanisms themselves, can be determined by visual inspection. As a result of this, more quantifiable diagnostic tests needed to be carried out.

5.2.5 SUMMARY OF HIGH SPEED IMAGING

High speed video allowed the visual analysis of the arc as it formed in both a variety of gasses and with different polymers. Sulphur hexafluoride causes the most dramatic changes in the arc, forming loops and spirals that increase convective cooling and arc length and lead to successful interruption.

It was shown that the arc undergoes morphological changes for a long period even after the last of the polymer was injected, suggesting an active role in the polymeric quenching process for post arc gasses. Image sequences from tests with each of the polymers highlighted differences in their behaviour. The more successful polymer quenchers seemed to create more vapour and force much more changes in the arc shape then the less successful ones.

High-speed video imaging can only provide a qualitative indication of the quenching phenomena and the complex processes at play. For proper investigation diagnostic techniques such as mass spectrometry need to be used that can accurately sample the arcing environment.

5.3 PRESSURISATION CHARACTERISTICS

Forcing a gas flow by use of compressed gas, compression mechanisms ('puffers') or by use of self-pressurising units is an important part of the interruption process in circuit breakers for several reasons. Gas flow increases convective energy losses from the plasma, reducing its conductivity as well as flushing ionised gas from the electrode gap region and intermixing cooler gasses. These processes are not only important for interruption but also vital in the post-arc environment where they affect a more rapid build up of dielectric strength. With this in mind, the influence of polymer material on the overall pressure of the system was explored. The changes in arcing vessel pressure caused by the polymer reaction can aide in the understanding of the polymer-arc interaction mechanisms as well as show the effect of polymer related pressure changes on quenching gas flow.

5.3.1 BASELINE TESTS

So as to specify the extent of pressure changes in the test chamber caused by propellant alone, the change in pressure in the chamber as a result of the injection of nitrogen with no arc is shown in Figure 5-26. Any pressure changes above this value during arcing experiments with polymers could then be directly attributed to the reaction with the arc and not to the addition of propellant gas into the volume.

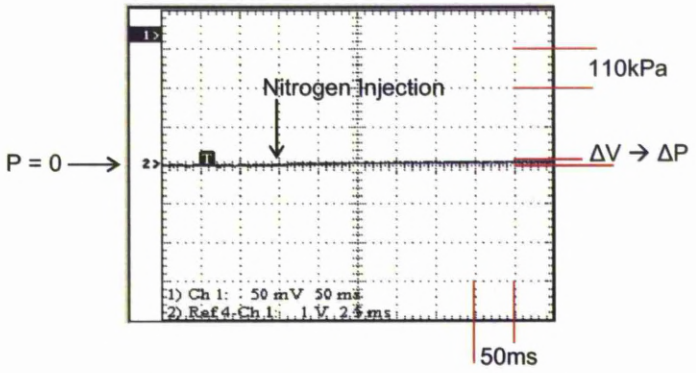

Figure 5-26 Pressure change with N_2 injection and no arc

When the same volume of nitrogen was injected into an arc a greater pressure rise was observed, shown in Figure 5-27.

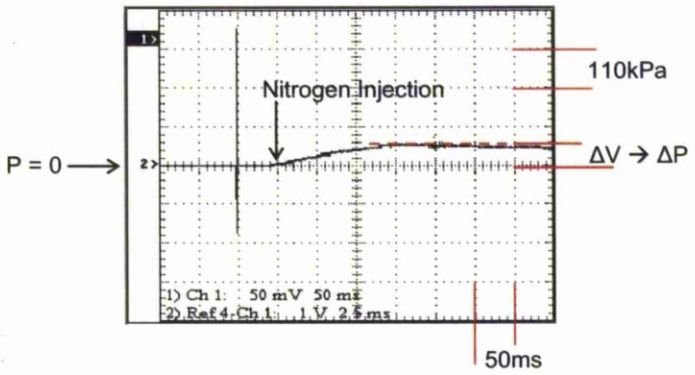

Figure 5-27: Pressure change with N_2 injection and an arc

The maximum pressure rise caused by the effect of the nitrogen injection into the arc was 55kPa. This was nearly seven times greater pressure increase than that observed without an arc. The additional pressure rise can be attributed in the most part to the heating of the gaseous volume by the arc. The transfer of thermal energy from the arc to the surrounding gas, particularly the injected nitrogen, caused the gas to gain kinetic energy which exerted a greater pressure inside the test chamber.

5.3.2 POLYMER INDUCED PRESSURE CHANGES

Representative oscilloscope traces of transducer voltage (pressure) against time for different polymeric arcs are shown in Figure 5-28. The figures highlight differences in reaction type, both between the tests with nitrogen alone and between different types of polymer material itself. Overall, the results imply different mechanisms at work for different types of polymer, which could help explain the variation in arc quenching efficiency observed previously. These differences can be assumed in the first instance to be due to the structure and composition of the polymers that mean they react in different ways in and around the arc.

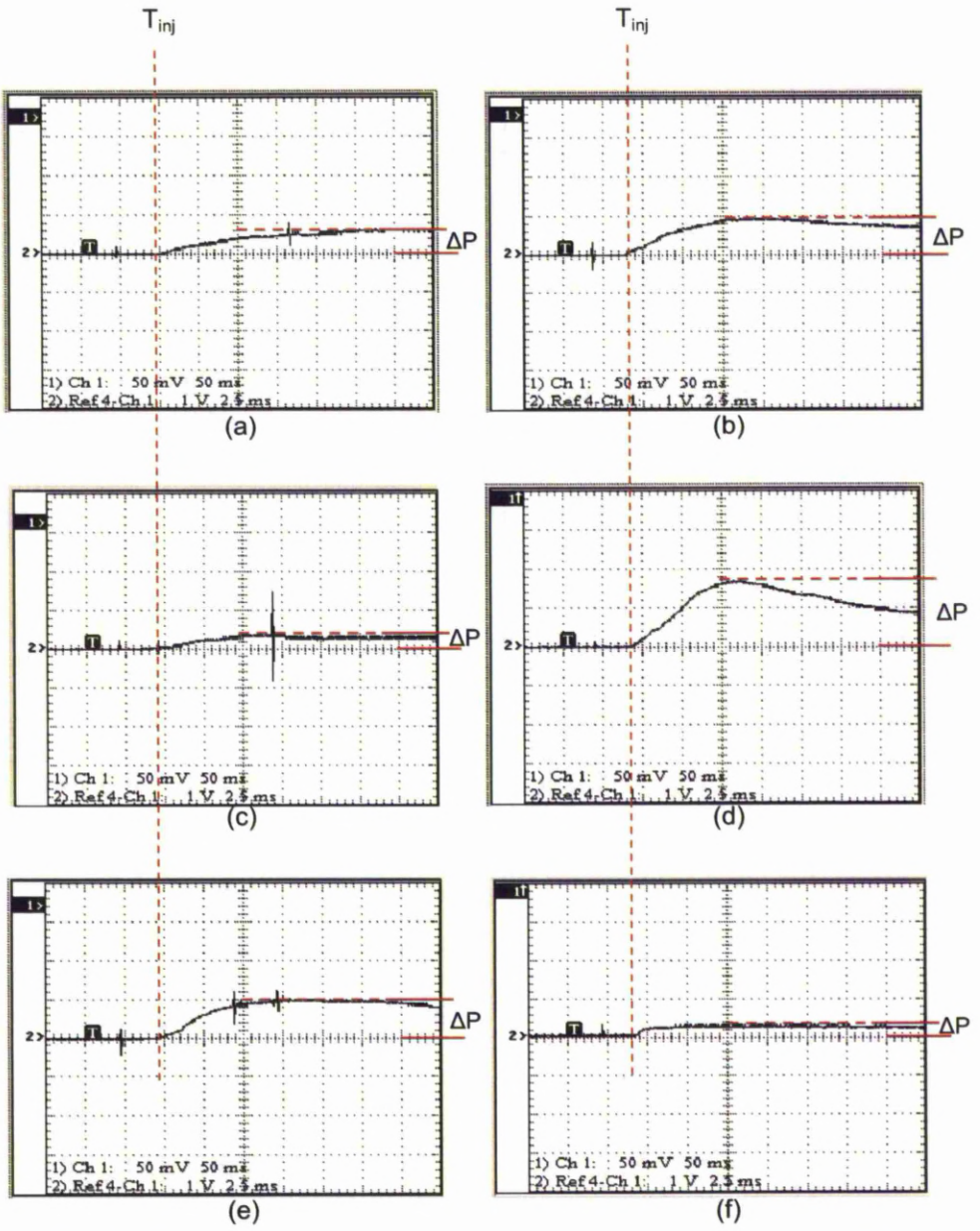

Figure 5-28: Representative pressure changes with time in different environments: (a) PMMA; (b) PVC; (c) PS; (d) PE; (e) PA6; (f) PTFE

The mean maximum pressure of the arcing vessel from a range of experimental observations is shown in Table 5-4; the mean pressure change for each polymer is shown graphically in Figure 5-29.

Table 5-4: Pressure transducer results and mean pressure

Test Environment	T1 Max. Pressure (kPa)	T2 Max. Pressure (kPa)	T3 Max. Pressure (kPa)	Mean Max. Pressure (kPa)	Standard Deviation	Standard Error
N_2 Only	8	10	6	8	2.0	0.7
N_2 + Arc	55	50	45	50	5.0	1.7
PMMA	70	67	57	64	6.8	2.3
PVC	95	56	100	83	24.1	8.0
PS	40	48	40	42	4.6	1.5
PE	190	185	180	185	5.0	1.7
PA6	105	80	100	95	13.2	4.4
PTFE	25	35	24	28	6.1	2.0

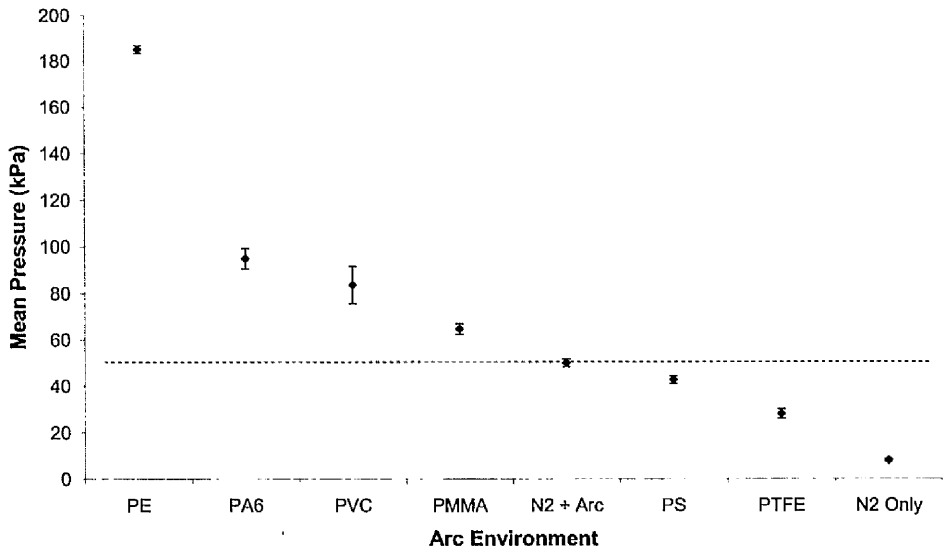

Figure 5-29: Mean pressure rise in chamber in various environments

One of the most notable features in Figure 5-29 is that the mean pressure change for PS and PTFE is actually less than that of nitrogen alone. This is suggestive of a cooling effect caused by the polymers on the arc and/or surrounding gasses which in turn limits the pressure rise in the chamber. By contrast, polyethylene causes the most significant pressure increase, over 80kPa greater than that of the next highest polymer, polyamide 6.

5.3.3 PRESSURISATION CAUSES AND EFFECTS

5.3.3.1 Causes of Pressure Variation

There are several reasons why the application of gas and polymer flow into the arc caused pressure changes in the test chamber:

1. Increase in the volume of gas – due to the addition of nitrogen propellant into the test chamber
2. Heating of the gas by the arc – transfer of thermal energy from the arc to the surrounding gas
3. Polymer change of state – polymer vapour and decomposition gasses increase the total volume of gas in chamber

As the injection of nitrogen alone caused only an 8kPa mean pressure rise, the addition of the propellant gas itself was not a major contributing factor in the pressure variation. It is most likely that the main cause of the pressure changes observed was as a result of energy transfer from the arc to the surrounding gas. This heating was greater in the cases of nitrogen and polymer flow because of the increase in power input into the arc caused by the enhanced energy losses and the tendency of the system to move to overall energy equilibrium.

There are various means by which the energy of the arc can be transferred to the surrounding gas. Most literature for arcs in various gasses [134, 135, 136] suggest that for the most part, radiation and convection are the principle effects involved in gas volume heating, with suggested values of total energy output of around 10% for convection and 50% for radiation. The remaining energy losses from the arc are from conduction and electrode heating, and are assumed to not play a significant role in the heating of surrounding gas. The fraction of arc radiation energy involved in the heating of the gas volume is dependant on the shape and size of the arc. In reality, the extent of heating would depend on the absorption cross section of the surrounding gas, which given the complexity of the polymer decomposition products would be difficult to evaluate.

Another related factor could be the composition of gas around the arc; gas mixtures with overall lower specific heat would cause greater temperature/pressure changes over other types of gas mixtures [137]. This is shown in Equation 5-1.

$$\Delta T = \frac{W_c}{C_v M_g} \Delta t \qquad (5\text{-}1)$$

Where:

ΔT – Temperature change

W_c – Power transfer to gas from arc

C_v – Constant volume specific heat

M_g – Mass of gas in the chamber

Δt – Time period

The decomposition of polymers in the arc formed a wide mix of species and it is possible that in some cases the specific heat of the products could be responsible for changes in volume heating and therefore explain quenching differences from polymer to polymer.

In the fixed volume of the chamber, the Gay-Lussac law shows that the pressure rise could be related to temperature increase of the gas volume as a result of the arc reaction, shown in Equation 5-2. This assumes the gas around the arc is homogenous and isothermal [138].

$$\frac{P_1}{T_1} = \frac{P_2}{T_2} \qquad (5\text{-}2)$$

Where:

P_1 – Pressure of chamber pre arc

P_2 – Pressure of chamber post arc

T_1 – Temperature of chamber pre arc

T_2 – Temperature of chamber post arc

This relationship means that for the fixed spatial volume of the test chamber, a given increase or decrease in internal temperature causes a corresponding increase or decrease in pressure inside the chamber. In this case, the heat of the arc and its reaction with the polymer would be responsible for the change in temperature and therefore pressure. Given this effect, the polymers PTFE and PS could have influenced a temperature reduction in the chamber by cooling the environment to a greater degree than in any other case.

In reality the pressure changes cannot be totally attributed to volume heating of the gas volume surrounding the arc. Another major factor was likely to be the production of gasses as a result of the decomposition of polymers in the arc, increasing the overall volume of gas in the test chamber. The ideal gas law shows the relationship between the variables:

$$PV = nRT \tag{5-3}$$

Where:

P – Pressure

V – Volume

n – Number of moles of gas

R – Gas constant ($8.31 JK^{-1}mol^{-1}$)

T - Temperature

In this case the volume and gas constant are fixed and the pressure is determined by both the temperature and the number of moles of gas, both of which change in response to the polymer decomposition.

The main mechanisms for increasing pressure in the chamber are all linked by the combined gas law:

$$\frac{P_1V_1}{T_1} = \frac{P_2V_2}{T_2} \tag{5-4}$$

Thus, the pressure in the chamber would be affected by the heating of the arc; heating caused by the injection of nitrogen propellant and the propellant itself; the increase in the number of moles of gas in the chamber as a result of polymer decomposition; and changes in gas temperature as a result of the thermodynamics of reactions between decomposed polymer species.

5.3.3.2 Effects of Pressurisation

There are several ways in which arc quenching can be aided by polymer induced pressure variations. These can be generally divided into three categories:

1. Arc direct effect – values of both electrical and thermal conductivity are dependent on ambient pressure, changes of which can alter the ability of the arc to carry more or less current [139]
2. Flow effects during arc phase – a pressure differential between upstream and downstream regions of the electrode gap induces intense gas flow that causes energy re-distribution by radiation, turbulence, heat convection, supersonic flows and the strong interaction between all of the above phenomena [140]
3. Flow effects in the post arc phase – after interruption the race that occurs between the cooling of the electrode gap and the re-heating by the transient recovery voltage can be shifted in favour of interruption. Flushing ionised gas away from the electrode gap by the pressure differential enables faster dielectric recovery [141].

In the configuration used in these experiments, the effect of pressure rises on arc quenching is limited due to the lack of nozzling and gas flow direction. If the pressure increase caused by the polymer particulates was constrained around the arc by the use of a nozzle, the pressure rise would cause an expansive flow through the open ends due to the negative pressure gradients towards the opening. This would cool the arc in a manner similar to a puffer design but with lower operational energy.

5.3.4 SUMMARY OF PRESSURE CHARACTERISTICS

Analysis of pressure changes in the arcing chamber as a result of polymer interactions act as a means of determining the influence of these effects on quenching and can be compared with other results to corroborate theorised quenching mechanisms and reactions. In most cases polymer induced pressure changes raise the pressure in the chamber; however PTFE and PS cause a reduction with respect to the case with a nitrogen arc alone.

The reasons for the pressure enhancement effects were in the most part due to a combination of two mechanisms: the heating of the gaseous volume by the arc; and the increase in the number of moles of gas, due to polymer decomposition and nitrogen injection. It is likely that PTFE and PS caused a particularly efficient cooling effect on the arc which resulted in a pressure reduction with respect to the baseline tests.

Chapter 6

Atomic Spectroscopy

CHAPTER 6 – ATOMIC SPECTROSCOPY

The purpose of utilising atomic spectroscopy techniques was to enable a deeper understanding of the changes in and around the arc at a fundamental level. This enables a better understanding of how the polymers react in the plasma and as a result how the quenching process works.

6.1 OPTICAL EMISSION SPECTROMETRY

The light emitted from arc plasma gives significant information on its state and composition, this information is important so as to aid in the understanding of the polymer quenching phenomena. Initially the baseline case of the plasma spectrum in the absence of polymer was tested before going on to study the differences in spectral characteristics in arcs interacting with various polymers.

6.1.1 GENERAL CONFIGURATION

In this case, the polymers were not deployed via pressurised nitrogen as was the case in other experiments; the reason for this was that the injection of N_2/polymer into the arc caused turbulence and instability. It was found that this meant the spectrum emitted was not particularly suitable for spectroscopic analysis due to the effects of line broadening, shifting and self-absorption, which could not be accounted for in post-processing due to the unpredictable nature of the arc turbulence. Instead, the polymer powders were deployed directly onto the lower electrode before initiation of the arc. In each case, the polymer powder was weighed to 2g and placed on the anode around the outside edge of the initiation electrode. When the experiment was then initiated, the polymer was ablated into the arc as it formed between the electrodes. The method did not provoke such a strong reaction as observed in the case of injection but allowed an arc with a more laminar character to be formed, which was more suitable for spectroscopic analysis.

6.1.2 BASELINE AIR SPECTRA

The spectra of arcs in air, in the absence of polymer, are shown in Figure 6-1 with the identification of the main spectral peaks is made in Table 6-1.

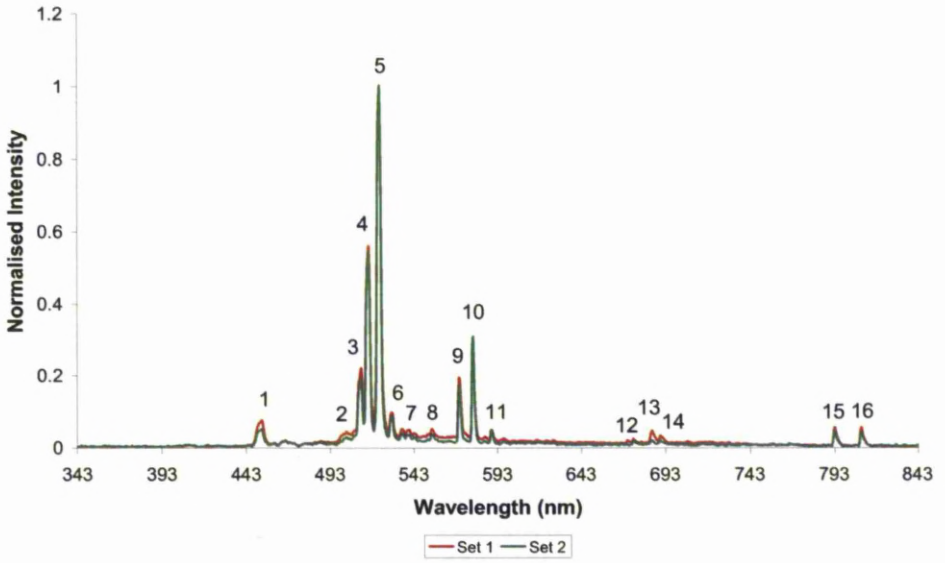

Figure 6-1: Optical emission spectrum of arcs in air

Table 6-1: Spectral lines observed from arc emission in air

Figure 1 Line Number	Figure λ (nm)	Published λ (nm)	Species	Reference
1	451.43	450.80	Cu (II)	[142]
2	502.04	501.20	Cu (II)	[142]
3	510.88	510.54	Cu (I)	[143]
4	515.28	515.32	Cu (I)	[143]
5	522.02	521.82	Cu (I)	[143]
6	529.10	529.10	Cu (I)	[142]
7	543.05	543.78	O (I)	[143]
8	553.94	553.53	N (II)	[143]
9	569.63	570.60	Cu (I)	[143]
10	578.05	579.20	Cu (I)	[143]
11	589.30	589.80	Cu (II)	[142]
12	673.78	672.26	N (I)	[143]
13	685.37	686.55	Cu (II)	[143]
14	689.80	X	unidentified	X
15	793.10	794.43	Cu (II)	[143]
16	809.15	809.40	Cu (I)	[142]

The spectrum shown in Figure 6-1 is heavily dominated by excited neutral and singly ionised copper species. There are also signs of O(I) and N(I) from the air in the chamber but these features are dominated by the Cu lines. The copper lines are formed due to the evaporation of electrode material into the arc and constitute the main conductive particles in the plasma.

The relationship between arc current and the intensity of spectral lines of some of the more significant Cu(I) peaks for an arc in air in the absence of polymers is shown in Figure 6-2. This demonstrates the association between changes in arc energy and intensity of copper spectral lines. This can be compared to the polymeric arc spectra to relate changes in intensity to changes in arc energy.

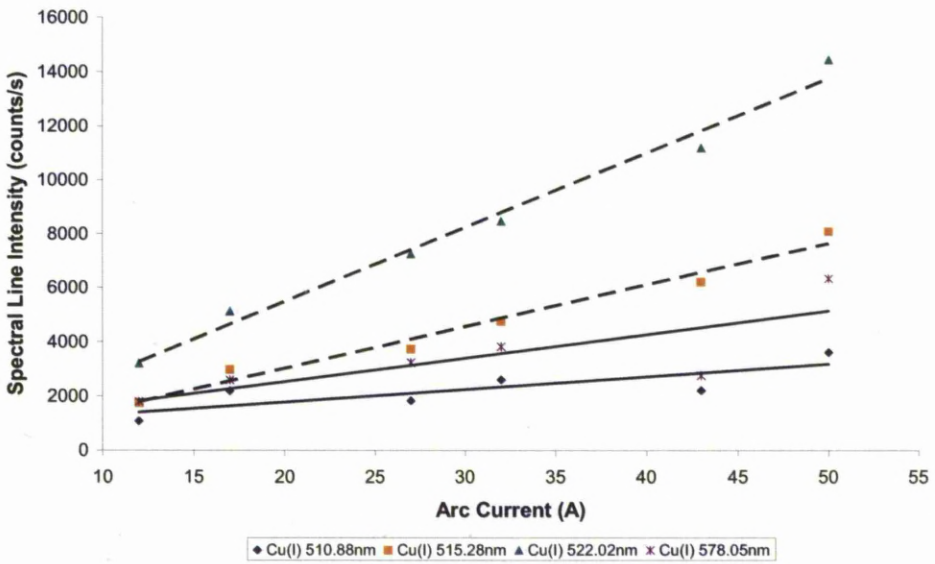

Figure 6-2: Relationship between Cu(I) intensity and arc current

Larger arc currents show an increase in emitted Cu(I) line intensity, particularly for the 515 and 522nm species. This was due to an increase in the population density of excited neutral copper species in the higher current arc. The linear dependence between arc current and copper line intensity in this current range could mean that the main excitation process was by electron impact directly from the ground state, as higher input energy allowed higher arc current and more energetic electron/neutral/ion collisions.

6.1.3 POLYMERIC ARC SPECTRA

Representative polymeric arc spectra captured from arcing tests in air and in different polymer environments is shown in Figure 6-3. Repeated tests were used to develop an accurate representation of the polymer-plasma emission from the arc and further spectra are included in the Appendix to show consistency.

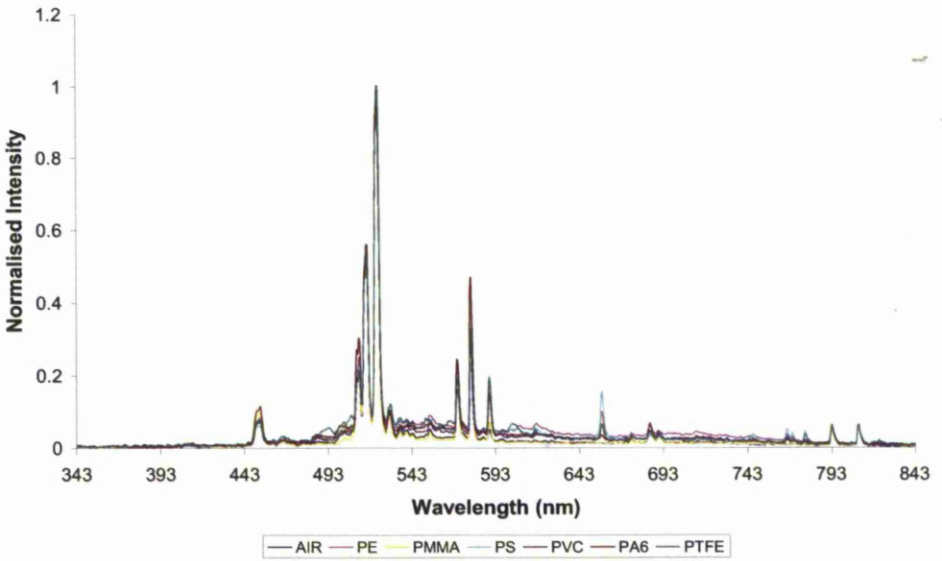

Figure 6-3: Polymeric arc spectra comparison with different polymers

As was the case previously, the spectra are dominated by Cu(I) and Cu(II) copper emissions from the evaporated electrode material, the main constituent of the plasma. However, there are also signs of new spectral features not present in the air spectra that can only be attributed to the presence of species originating from the interaction with the polymer. There are also signs of consistent changes in copper line intensity caused by certain polymers over others, suggesting some polymers caused changes in the composition and characteristics of the arc with respect to air. It is difficult to accurately observe differences in the spectra by visual interpretation due to the dominant copper lines and as a consequence more focussed interpretation of the most relevant spectral features is given in the next section.

6.1.4 PROMINENT SPECTRAL FEATURES

The most prominent changes in excited neutral and ionised copper spectral characteristics, influenced by the application of polymer to the arc, are shown in Figures 6-4 and 6-5.

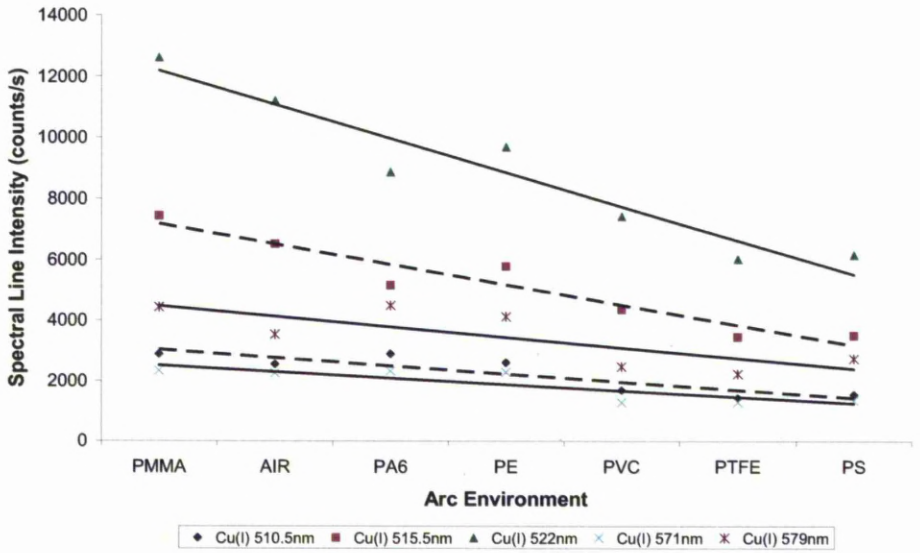

Figure 6-4: Change in arc Cu(I) line intensity with different polymers

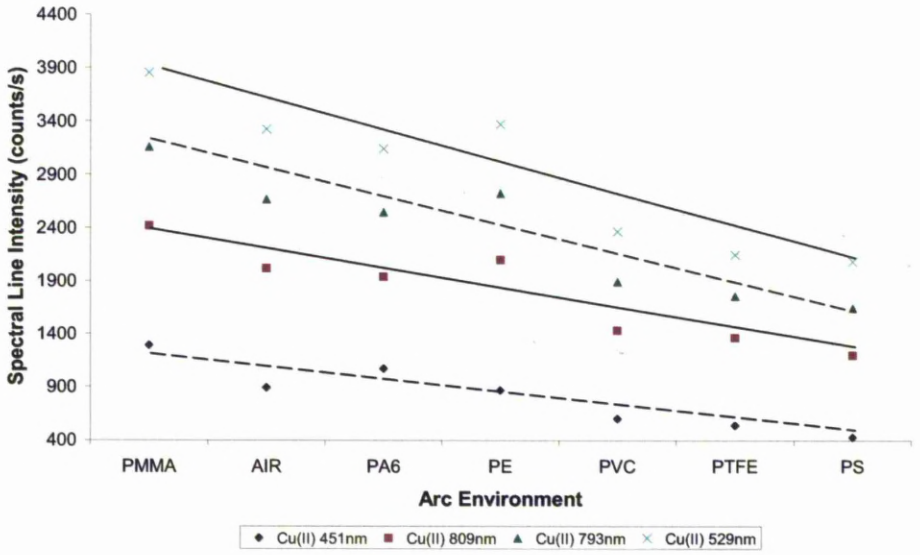

Figure 6-5: Change in Cu(II) line intensity with different polymers

The intensity of Cu(I) and Cu(II) lines reduce to different extents because of the application of certain polymers, particularly due to the influence of PS and PTFE. The reduction in radiation intensity of the copper lines could signify several effects, including: decreased plasma temperature; decreased plasma radius; decreased Cu concentration; or an increase in vapour around the arc causing attenuation of emitted light. This effect has also been observed previously, when it was shown that lower arc current caused a reduction in Cu line intensity. It is possible that the reduction in intensity observed in this case could be due to some polymers reducing the temperature of the arc sufficiently to lower the population density of the excited and ionised copper species, reducing the emission intensity.

As well as changes in copper concentration, new spectral characteristics were observed when polymers were added with respect to the no polymer case. Some of the most significant new spectral characteristics formed as a result of the polymer reaction are shown in Figure 6-6. These results indicate the dissociation of the polymer powder in the arc.

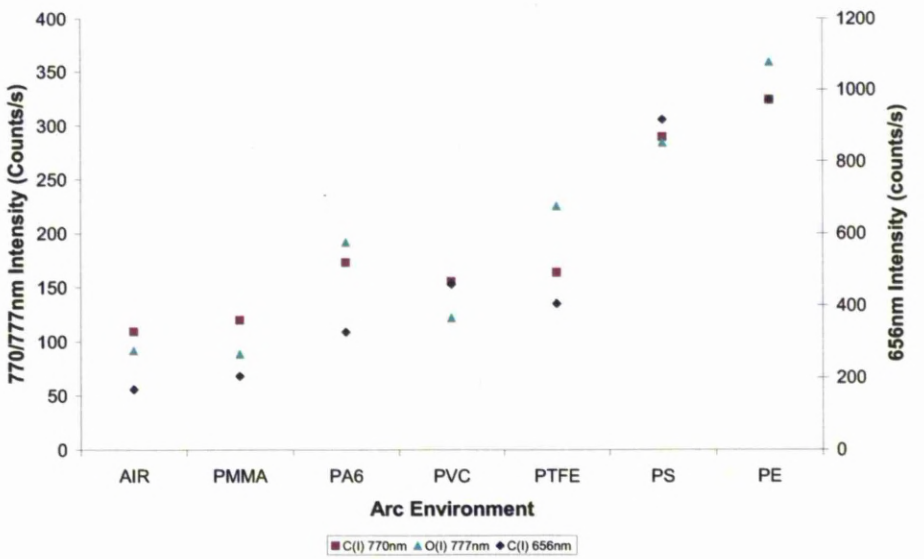

Figure 6-6: Additional spectral lines formed in arc by polymer addition

The most significant spectral line was at 656nm and attributed to excited neutral carbon, the line may be slightly influenced by the presence of the 658nm hydrogen line, which is overlapping due to Stark broadening. There was also the presence of another carbon line at 770nm. All of the polymers contained carbon and it is likely that they were formed as a result of polymer decomposition in the arc. The increase in intensity of C lines with certain polymers could indicate an increase in decomposition and a consequent increase in mass loss and ablation that could aid in the interruption process. Excited oxygen at 777nm was likely to have come from the decomposition and excitation of atmospheric oxygen. The presence of the oxygen line is a clue as to the nature of the reaction mechanism between the polymers and arc, and could be suggestive of some process of combustion type reactions. In all three cases, the lines varied in amplitude when different polymers were used showing that the polymers decomposed to different extents in the arc, this result could be important in explaining the differing abilities of the various polymers to carry out arc quenching and will be considered further in the analysis.

The results shown in the previous figures are representative results based on the test results from a set of tests. To demonstrate consistency, data from three sets of tests were used to form mean intensity values for the main species spectral lines, these are given in the Appendix and show consistency with the representative set of results described previously. A certain amount of error must be expected in this type of test due to the instability and relative unpredictability of the electric arc plasma; however the general trends can be seen and are valid to allow interpretation.

6.1.5 CHROMATIC PROCESSING

Chromatic processing was a useful tool in comparing differences in the spectra that were not easily noticed on visual inspection. Figure 6-7 demonstrates Gaussian shaped R, G, B filters applied to the spectra of an arc interacting with polyethylene, further figures showing chromatic filtering of other polymeric spectra are given in the Appendix.

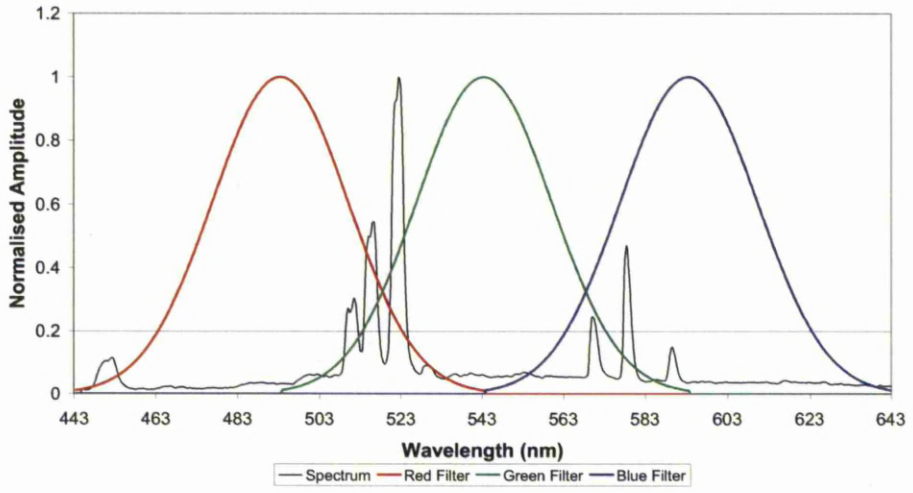

Figure 6-7: Chromatic filters applied to a spectrum of a PE arc

Although certain prominent spectral peaks have already been identified and their intensities compared, the overall relationship between peak intensity ratios can be evaluated with chromatic processing. By use of the algorithm described in Chapter 3 the chromatic parameters were found, shown in Table 6-2.

Table 6-2: Chromatic parameters from calculated from spectra

	R	G	B	H	L	S
AIR	0.312	0.423	0.179	87.12	0.30	0.58
PE	0.369	0.578	0.360	117.52	0.44	0.38
PMMA	0.296	0.403	0.173	87.90	0.29	0.57
PS	0.393	0.565	0.347	107.29	0.44	0.39
PVC	0.363	0.509	0.268	96.34	0.38	0.47
PTFE	0.411	0.542	0.272	89.25	0.41	0.50
PA6	0.433	0.587	0.346	98.31	0.46	0.41

The HLS values were converted to HS-x, HS-y, HL-x and HL-y coordinates that could be plotted on polar plots, shown in Figures 6-8 and 6-9.

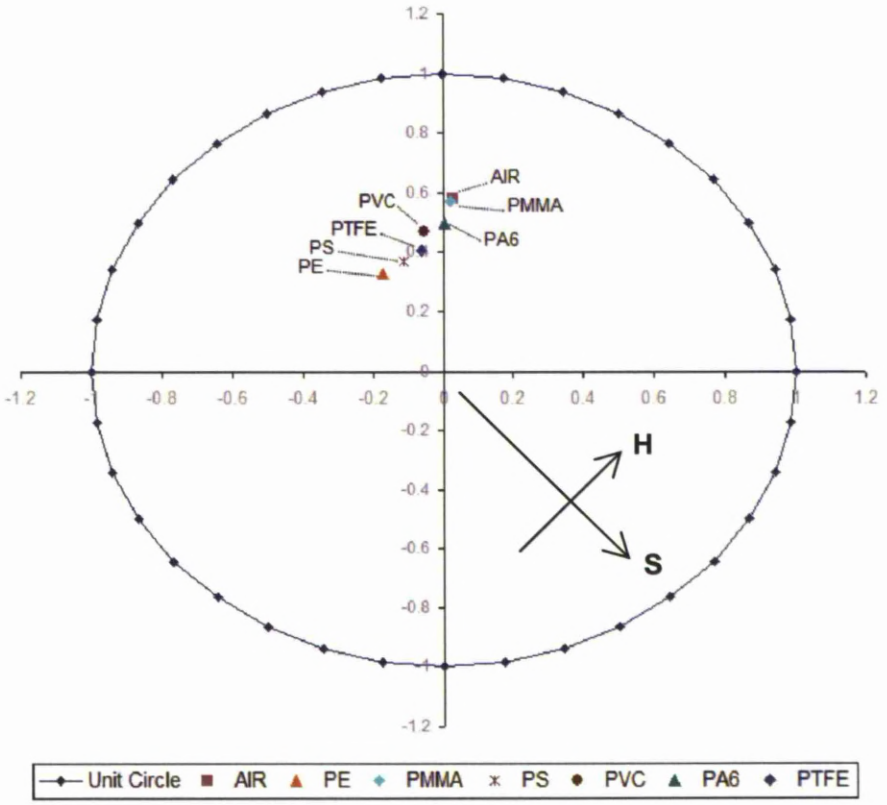

Figure 6-8: H-S polar plot of chromatically processed spectral data

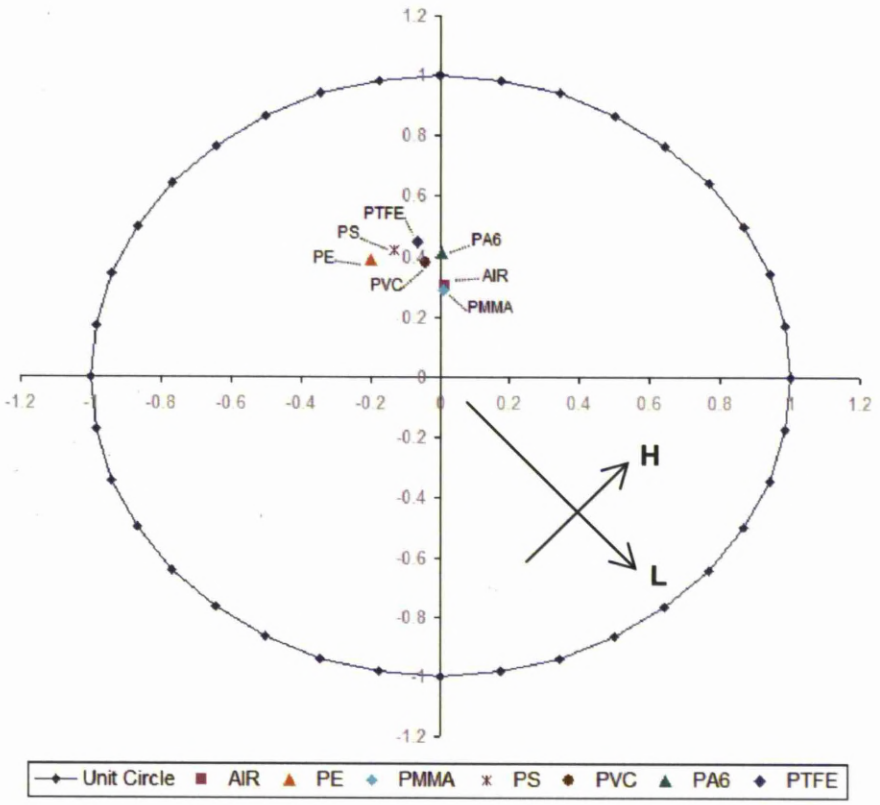

Figure 6-9: H-L polar plot of chromatically processed spectral data

The positions of the air arc and PMMA arc are close together indicating very little difference in their spectra and suggesting PMMA did not react strongly, this idea is supported by the current and voltage results in Chapter 5. In contrast to this, the position of PE on the polar plots, most noticeably on the HS chart, shows a larger translation in position with respect to the air arc and consequently the biggest change in spectral composition. This is supported by other results as it was found PE interacted with the arc plasma to a greater extent than any of the other polymers tested.

6.1.6 SPECTROSCOPIC TEMPERATURE ESTIMATION

Temperature estimation is one of the most common spectroscopic plasma diagnostic techniques available. It is used in this case to extract information from the arc that shows how the application of polymers influenced temperature change. As arc conductivity is strongly related to temperature, any cooling effect by the polymer interaction could have an important role in quenching.

There are various methods of electron temperature estimation; those used here utilise the relative spectral line intensities of peaks from the same atomic species. More detailed background information on plasma spectral temperature measurement, including the underlying theory, was given in Chapter 3. In this case, the excitation temperature was estimated by determination of the slope of a Boltzmann plot. In the first instance, LTE was assumed and then subsequently verified by analysis of the Boltzmann line fitting [144]. Instability induced in the plasma by virtue of the polymer interaction was reduced as much as possible by the experimental configuration but could not be completely eliminated. Due to this and the inherent limitation of optical emission temperature determination itself, the values obtained could only be regarded as an indicator and not absolute. However, when used in conjunction with the results from other chapters, it was hoped they would become part of a bigger picture which helps explain the overall polymer quenching mechanism.

6.1.6.1 Spectral Line Intensity

The lines selected for use in the analysis had to be positively identified species and be free from other overlapping spectral lines that would alter the intensity measurement. The intensity for each line was taken as the integral of the discrete function of the spectral line, discounting the continuous function from the continuum, integrated around the line central wavelength. The spectral lines were approximated to exhibit a Lorentzian profile due to Stark broadening and intensity was calculated by use of a least squares fit function and subsequent integration using the Matlab curve-fitting tool.

The lines chosen for analysis were from the same atomic species and ionisation stage and were selected so as to maximise the difference in upper excitation energy level which reduces error in the calculation. Spectral peaks chosen were Cu(I) lines at 515, 522, 529, 570 and 578nm. The line integral values for three sets of arc spectra in different polymeric environments are shown in Table 6-3.

Table 6-3: Intensity values of Cu(I) lines used in temperature determination

	Spectral Line (nm)				
	515.28	522.02	578.05	529.10	569.63
Set 1					
AIR	3.42	6.02	1.24	0.71	0.78
PE	3.60	6.32	1.77	0.97	0.97
PMMA	3.58	6.38	1.39	0.63	0.74
PS	3.70	6.82	1.93	0.98	0.94
PVC	3.80	6.78	1.49	0.84	0.75
PTFE	3.71	6.67	2.10	0.82	1.10
PA6	3.61	6.80	1.65	1.06	0.92
Set 2					
AIR	3.16	5.66	1.15	0.58	0.71
PE	3.44	6.13	1.43	0.99	1.15
PMMA	3.40	6.22	1.55	0.64	0.88
PS	3.76	6.91	1.79	0.83	1.04
PVC	3.83	6.83	1.79	0.80	1.04
PTFE	3.80	6.79	1.31	0.71	0.87
PA6	3.64	6.51	1.75	0.80	0.96
Set 3					
AIR	3.98	7.00	1.40	0.83	1.05
PE	3.75	6.58	1.85	1.01	1.18
PMMA	4.83	8.62	1.87	0.85	1.12
PS	2.52	4.64	1.32	0.67	0.74
PVC	3.02	5.39	1.18	0.67	0.70
PTFE	3.54	6.36	2.00	0.78	1.21
PA6	2.45	4.63	1.12	0.72	0.74

In this case Abel inversion was not performed on the integrated line intensity values and consequently the excitation temperatures calculated are the 'apparent' values [145]. It was assumed that the radial distribution of intensity was not axis-symmetric by virtue of the polymer reaction and as a consequence the Abel inversion transformation would add noise to the intensity values. The use of the apparent excitation temperature is acceptable in this case as it is the temperature change from polymer to polymer that is of more interest, rather than the absolute value, also, in similar experiments it has been found that the apparent excitation temperature is close to the highest value of temperature or radiation intensity in the observation direction [146].

6.1.6.2 Boltzmann Plot

The atomic data necessary to perform the temperature calculations are shown in Table 6-4 and were obtained from published data. Errors associated with this technique mainly arise from uncertainty about the transition probability data (A), which can have errors by as much as 25% [150].

Table 6-4: Atomic data used in temperature calculation [147]

λ (Å)	A ($10^8 s^{-1}$)	g_u	E_u (eV)
5152.8	0.6	4	6.19
5220.2	0.75	4	4.82
5291.0	0.109	8	7.74
5696.3	0.0024	4	3.82
5780.5	0.0165	2	3.79

The relative intensities of spectral lines from the same atomic species were used to estimate temperature by use of the relationship shown in Equation 6-1 [148].

$$\ln\left(\frac{I\lambda}{Ag_u}\right) = C - \frac{E_u}{kT} \qquad (6\text{-}1)$$

Where:

T = excitation temperature (K)

E_u = energy of upper level (eV)

k = Boltzmanns constant ($8.62 \times 10^{-5} eVK^{-1}$)

I = radiation intensity

g_u = statistical weight of the upper level

A = transition probability (s^{-1})

λ = wavelength (Å)

By forming a linear plot, with $\ln(I\lambda/Ag_u)$ as the ordinate and E_u as the abscissa, a straight line graph can be plotted between the points whose gradient is equal to -1/kT which subsequently allows the temperature to be found. Large deviations from linearity in the plots indicate that the condition of LTE had not been met or that the lines chosen were too strongly absorbed to be used [149].

An example Boltzmann plot for Cu(I) emissions in a polyethylene arc environment is shown in Figure 6-10. Plots in other arcing environments are included in the Appendix along with the gradient values and estimated Boltzmann temperatures. The gradients of the Boltzmann plot trend lines were formed by linear regression using Microsoft Excel and in all cases had R^2 values of higher than 0.95, which is acceptable given the nature of the polymer plasma interaction. This indicates that the assumption of LTE was valid and that the lines chosen were not too strongly absorbed to be used, meaning the subsequent apparent excitation temperature values were likely to be more representative.

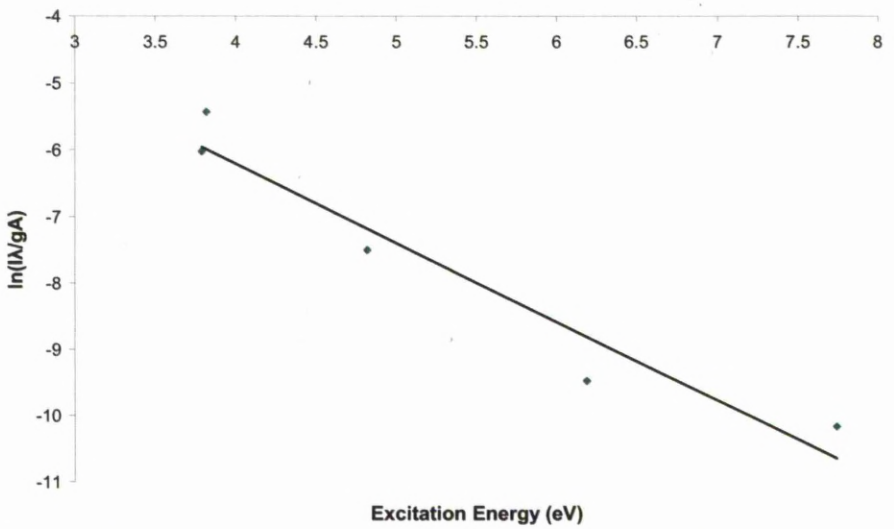

Figure 6-10: Example Boltzmann plots of Cu(I) emissions for PE

The mean excitation temperature was calculated from the results of each data set (individual results in Appendix) and is shown in Table 6-5.

Table 6-5: Boltzmann plot mean excitation temperature values

	Temperature (K)					
	Set 1	Set 2	Set 3	Mean	SD	SE
AIR	10000	9820	10000	9963	125.0	72.2
PE	9990	10100	10100	10036	38.5	22.2
PMMA	9760	9460	9760	9818	463.3	154.4
PS	9940	9630	9630	9732	183.4	105.9
PVC	10200	9590	9590	9794	358.8	207.2
PTFE	9380	10300	9380	9538	199.7	115.3
PA6	10300	9660	10300	10074	355.8	205.4

The mean arc temperature is shown graphically in Figure 6-11 and the mean temperature reduction of the polymeric arcs with respect to the air alone arc is shown in Figure 6-12.

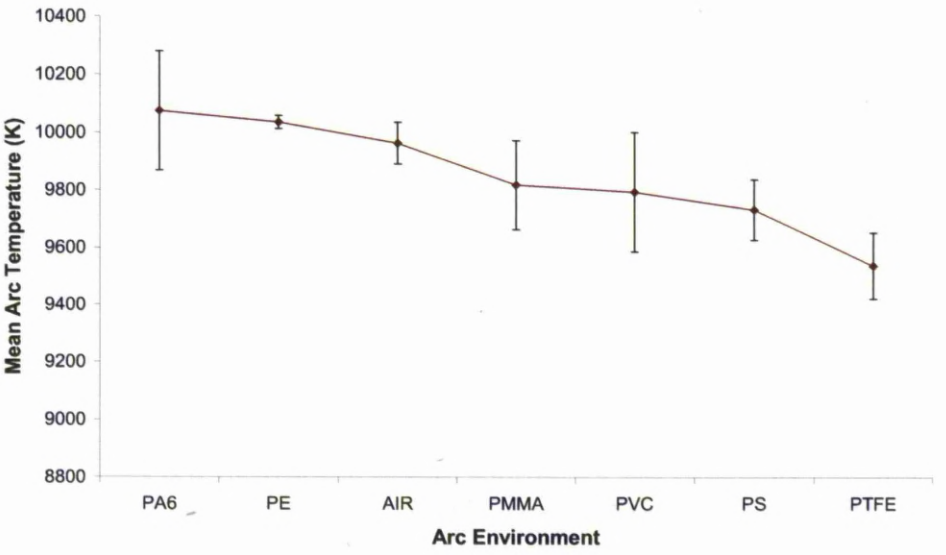

Figure 6-11: Mean arc temperature calculated using Boltzmann plot method

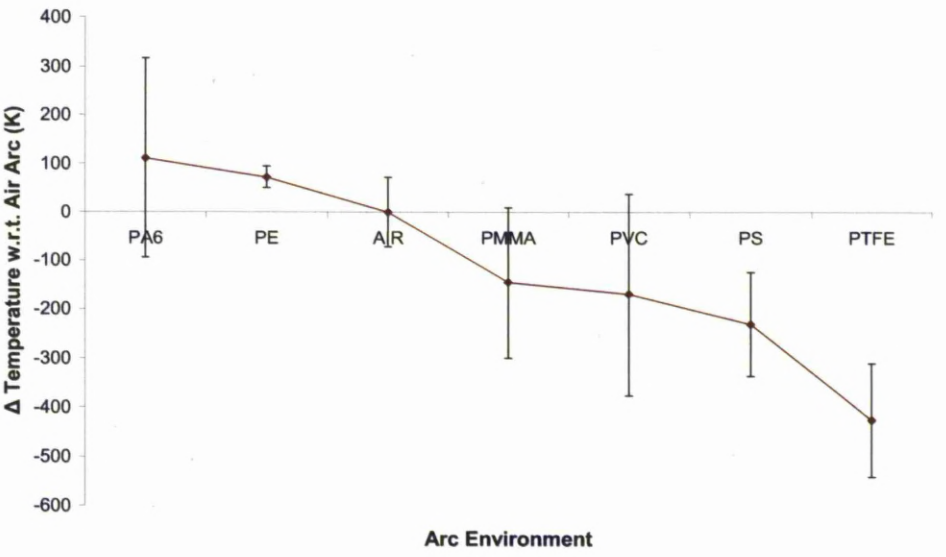

Figure 6-12: Change in mean arc temperature with polymer

The mean apparent excitation temperature shown in Figures 6-11 and 6-12 shows that in the most part, as a result of the polymer-plasma interaction, thermal energy was extracted from the arc and cooling occurred. In particular PS and PTFE were effective and this may help explain why they were considered the most efficient quenchers in the results shown in Chapter 5.

6.1.7 SUMMARY OF OPTICAL EMISSION

The spectrum of light emitted from arcs in air shows a spectrum dominated by copper lines. This is due to the emission of copper vapour into the arc from the electrodes. When particulate polymers are applied to the arc the dominant spectral characteristics are still copper due to the electrodes but more detailed analysis shows the presence of spectral characteristics that signify the complete decomposition of the polymers in the arc. Further analysis of the copper spectral lines showed a reduction in intensity when certain polymers were used, the reasons for this could have been: reduction in arc temperature, reduction in arc radius or decreased copper concentration. It could also be a sign of more vapour present around the arc, causing light attenuation. Temperature estimation showed that the polymers polystyrene and polytetrafluoroethylene cooled the arc to the greatest degree with respect to the baseline air spectrum. Reference to Chapter 5 showed that these polymers were also the ones found to seemingly have the most efficient plasma quenching ability.

6.2 MASS SPECTROMETRY

It was desirable to develop a more thorough understanding of the polymer decomposition process and of the species formed in order to understand the effect these factors had on quenching performance. By analysis of the species formed it could be determined whether the main interaction between the polymer and arc caused complete decomposition, de-polymerisation or a mixture of these. With this known, it was possible to speculate on the main reaction mechanisms and the effect that these would have on energy extraction. The second advantage of mass spectrometry was to appreciate the vapour composition, formed as a result of the arc-polymer interaction. It was thought that the species could potentially have an electron affinity that would reduce the number of conductive particles in the arc plasma and increase its resistance, aiding in extinguishment. Other properties of the vapour could also be beneficial in arc interruption, such as its thermal conductivity and specific heat capacity.

6.2.1 MASS ASSIGNMENT

To aid in the identification of species an assignment list was formed, based on the most probable gasses given the molecular compositions of the polymers. It was formed with reference to publications that performed calculations using the minimisation of the Gibbs free energy method in the context of circuit breaker nozzle ablation and plasma surface modification [152, 152, 153]. The table of assigned masses is given in Table 6-6. The m/z column indicates the mass-to-charge ratio of the ionised species in the spectrometer. More detailed background information on mass spectrometry was given in Chapter 3.

Table 6-6: Assignment of atomic mass/charge ratio to species

m/z	Species	m/z	Species
1	H^+	43	$CH_3CH_2CH_2^+$ (C_3H_7), CO_2^{+*}
2	H_2^+	44	CO_2^+, N_2O^+
11	CO_2^{3+}	45	$(CH_3)_2NH^+$
12	C^+	46	NO_2^+
13	CH^+	47	CFO^+, CCl^+
14	CH_2^+, N^+	48	C_4^+
15	CH_3^+, NH^+	49	NOF^+
16	CH_4^+, O^+, NH_2^+	50	CF_2^+, CH_3Cl^+
17	OH^+, NH_3^+	52	$C_2N_2^+$
18	H_2O^+	55	$C_4H_7^+$
19	F^+	56	$CH_3CH_2CH{=}CH_2^+$ (C_4H_8)
22	CO_2^{2+}	57	$CH_3CH_2CH_2CH_2^+$ (C_4H_9)
24	C_2^+	60	C_5^+
25	C_2H^+, CF_2^{2+}	64	$C_2H_5Cl^+$
26	$C_2H_2^+$, CN^+	65	NFO_2^+
27	$C_2H_3^+$, HCN^+	66	COF_2^+
28	CO^+, $C_2H_4^+$, N_2^+	69	$C_5H_9^+$, CF_3^+
29	$CH_3CH_2^+$ (C_2H_5), N_2H^+, CHO^+	70	$CH_3CH_2CH_2CH{=}CH_2^+$ (C_5H_{10}), Cl_2^+, CHF_3^+
30	NO^+, COH_2^+	71	$CH_3CH_2CH_2CH_2CH_2^+$ (C_5H_{11})
31	CF^+, $CH_3NH_2^+$	81	C_2F_3
32	O_2^+	82	CCl_2^+
35	Cl^+	83	$C_6H_{11}^+$
36	C_3^+, HCl^+	84	$C_6H_{12}^+$, $CH_2Cl_2^+$
38	F_2^+, C_2N^+	85	$C_6H_{13}^+$
39	C_2O^{+*}	88	CF_4^+
40	C_2O^+, CH_3CN^+	95	CF_3CN
41	$C_3H_5^+$, CH_3CN^+	100	C_2F_4
42	$CH_3CH{=}CH_2^+$ (C_3H_6)		

6.2.2 AIR MASS SPECTRUM WITH NO-POLYMER

As a baseline to allow comparison, the mass spectrum of an arc in air with N_2 propellant injection but without any polymer present is shown in Figure 6-13.

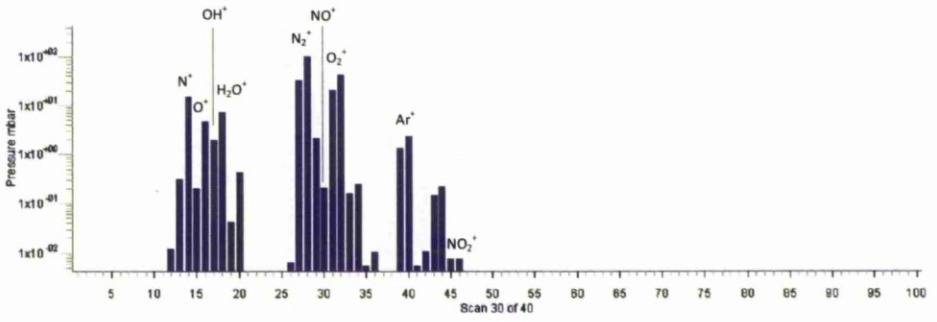

Figure 6-13: Mass spectrum of post air arc species

Examination of the baseline mass spectrum with respect to subsequent polymeric-arc mass spectra allows any differences to be attributed to the polymer reaction. A chart showing the relative abundance of each of the main species is shown in Figure 6-14.

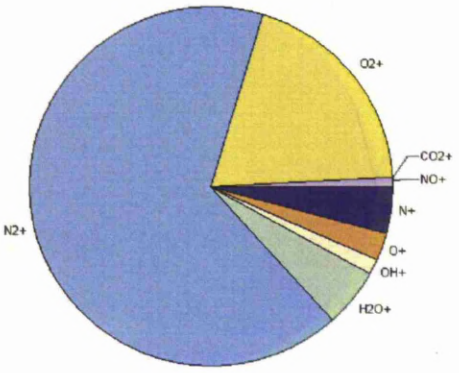

Figure 6-14: Abundance of main gaseous chemical species for an arc in air

The mass spectrum in the absence of polymer shows typical constituents that would be expected in air. Atmospheric N_2^+ and O_2^+ (m/z = 28 and 32amu) dominate with other notable species from water vapour H_2O^+, OH^+ (m/z = 18 and 17amu), possibly contaminants desorbed from the test chamber walls as a result of the arc.

6.2.3 MASS SPECTRA WITH POLYMERIC FLOW

The resultant mass spectra following the application of different polymers into the arc are shown in Figure 6-15, with the main species highlighted.

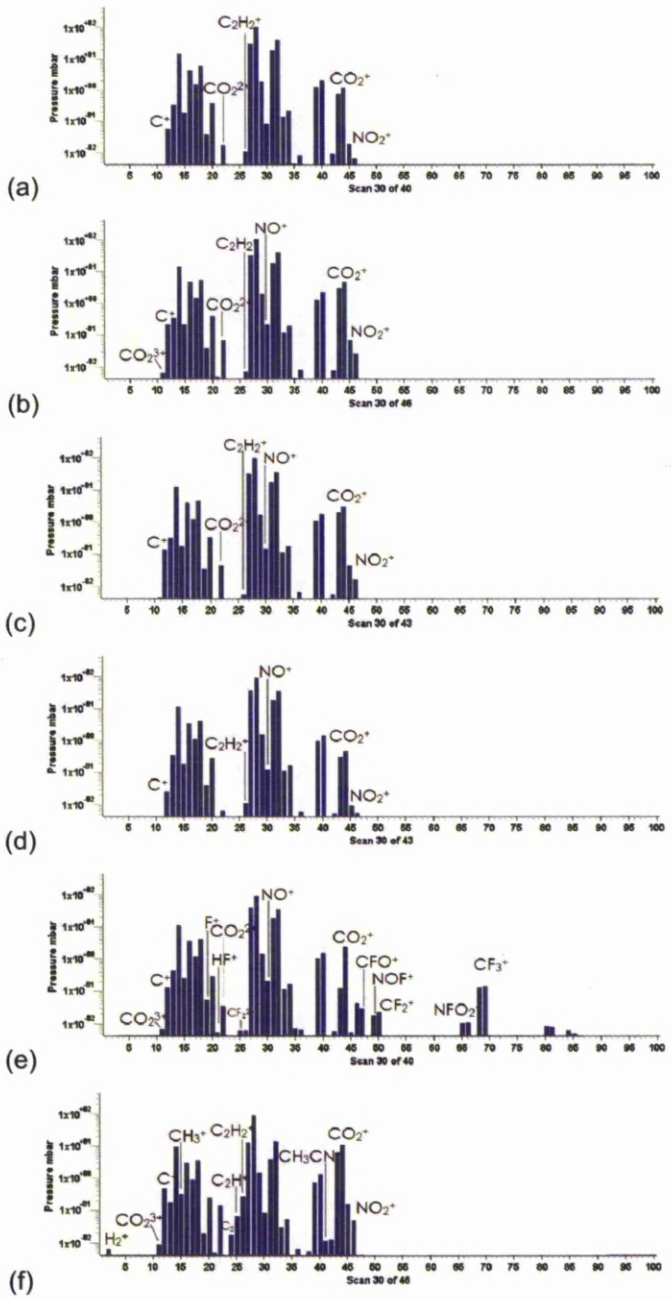

Figure 6-15: Mass spectra of polymeric arcs – results set 1: (a) PS; (b) PA6; (c) PMMA; (d) PVC; (e) PTFE; (f) PE. (Logarithmic scale)

The mass spectra in Figure 6-15 (a) – (f) generally show a richer composition of species with respect to the arc with no polymer. In order to quantify this, the total atomic mass density of the new species formed as a result of the polymer-arc interaction could be calculated by use of Equation 6-2.

$$\rho = \sum_j m_j n_j \tag{6-2}$$

Where:

m_j = atomic mass of species j

n_j = number density of species j

The mass density of different polymeric arcs is compared in Figure 6-16 for two sets of tests, so as to demonstrate consistency. In all cases the polymers formed a richer spectrum of species with respect to air due to the thermal decomposition and dissociation of the polymer material in response to the arc plasma. The heat consumption from the arc to affect melting, decomposition and dissociation of the polymers could aid in extinction by assisting in arc cooling.

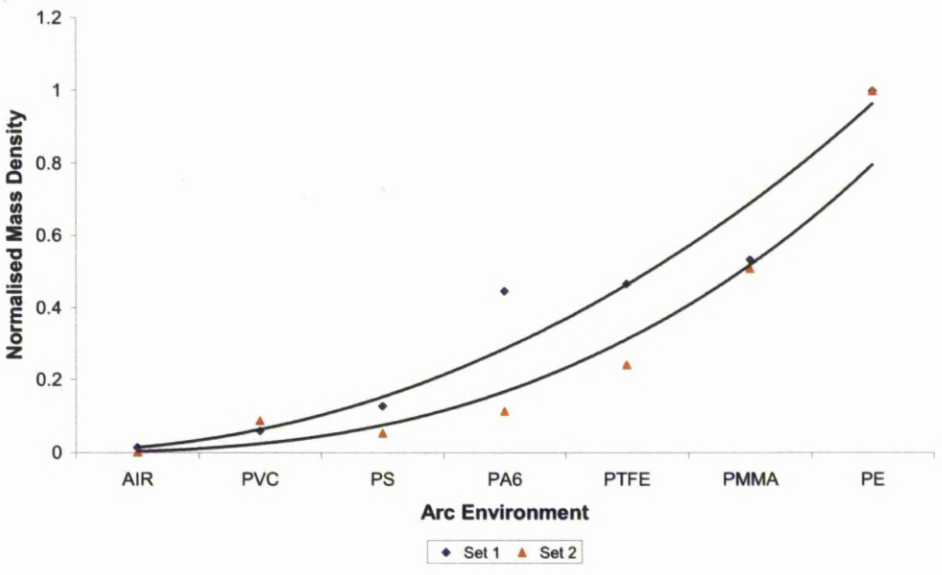

Figure 6-16: Comparison of mass density of post polymeric-arc gas

The mass spectra show that as well as normal air species such as N_2^+ and O_2^+ the polymer arc environment consists of carbon, hydrocarbons and carbon oxides such as $C_2H_2^+$ and CO_2^+ (m/z = 26 and 44amu). An increase in carbon oxides are also common by-products of the plasma treatment of polymers in the context of industrial surface modification applications [154]. The species formed as a result of the arc-polymer interaction in each case are identified in Table 6-7, they have been divided into monatomic, diatomic and polyatomic species in order to aid in the understanding of the polymer decomposition reactions.

Table 6-7: Main polymer related gas constituents from mass spectra

Polymer	Monatomic	Diatomic	Polyatomic
PS	N^+, O^+, C^+, H^+	N^+_2, O_2^+, H_2^+, C_2^+, NO^+, CH^+	CO_2^+, $C_2H_2^+$, NO_2^+, CH_3^+, C_2H^+,
PA6	N^+, O^+, C^+, H^+	N^+_2, O_2^+, H_2^+, C_2^+, NO^+, CH^+	CO_2^+, NO_2^+, C_2H^+, C_2N^+
PMMA	N^+, O^+, C^+, H^+	N^+_2, O_2^+, H_2^+, C_2^+, NO^+, CH^+	CO_2^+, $C_2H_2^+$, NO_2^+, C_2H^+, CHO^+, C_3^+, C_2O^+
PVC	N^+, O^+, C^+, Cl^+, H^+	N^+_2, O_2^+, H_2^+, C_2^+, Cl_2^+, NO^+, CCl^+, CH^+	CO_2^+, $C_2H_2^+$, NO_2^+, CCl_2^+, C_2H^+, C_3^+, C_4^+
PTFE	N^+, O^+, F^+, C^+	N^+_2, O_2^+, C_2^+, F_2^+, HF^+, NO^+	CO_2^+, CF_2^+, NO_2^+, CFO^+, NOF^+, CF_2^+, NFO_2^+, CF_3^+, $C_2F_3^+$, C_3^+, C_4^+
PE	N^+, O^+, C^+, H^+	N^+_2, O_2^+, C_2^+, H_2^+, NO^+, CH^+	CO_2^+, CH_3^+, C_2H^+, $C_2H_2^+$, CH_3CN^+, NO_2^+, $C_2N_2^+$, C_3^+, $C_3H_6^+$

The monatomic species comprised of the atomic constituents of the main atmospheric gasses in the chamber, namely N^+ and O^+ (m/z = 14 and 16amu), and the component atoms of the polymers themselves, H^+, C^+, F^+ and Cl^+ (m/z = 1, 12, 19 and 35amu respectively). Their presence indicates that in each case a proportion of the polymers underwent complete decomposition as a result of the interaction with the arc.

The main diatomic and polyatomic species were likely formed as a result of two different mechanisms. The first was de-polymerisation, where the polymers underwent chain scission leaving fragments of polymer chains, for example CH^+, CF_2^+ or CCl^+ (m/z = 13, 50 and 47amu respectively). The second process involved secondary reactions between decomposed atoms and molecules from the polymers and between existing chamber gasses, such as CH_3^+, NFO^+ and CH_3CN^+ (m/z = 15, 49 and 41amu). The most likely sources of the species detected in the test chamber following the addition of polymer to the arc are shown in Table 6-8.

Table 6-8: Probable sources of polymer vapour constituents

Polymer	Polymer Chain Fragments	Secondary Reactions	Chamber Atmosphere
PS	C^+, H^+, C_2^+, CH^+, $C_2H_2^+$, C_2H^+	H_2^+, CO_2^+, CH_3^+	N^+, O^+, N_2^+, O_2^+, NO^+, NO_2^+
PA6	C^+, H^+, C_2^+, CH^+, C_2H^+	H_2^+, CO_2^+, C_2N^+	N^+, O^+, N_2^+, O_2^+, NO^+, NO_2^+
PMMA	C^+, H^+, C_2^+, CH^+,CHO^+, $C_2H_2^+$, C_2H^+, C_3^+	H_2^+, CO_2^+, C_2O^+	N^+, O^+, N_2^+, O_2^+, NO^+, NO_2^+
PVC	C^+, Cl^+, H^+, C_2^+, CCl^+, CH^+, C_2^+, $C_2H_2^+$, C_2H^+, C_3^+, C_4^+	H_2^+, Cl_2^+, CO_2^+, CCl_2^+	N^+, O^+, N_2^+, O_2^+, NO^+, NO_2^+
PTFE	F^+, C^+, C_2^+, CF_2^+, $C_2F_3^+$, C_3^+, C_4^+	F_2^+, HF^+, CH^+, CO_2^+, CFO^+, NOF^+, NFO_2^+, CF_3^+	N^+, O^+, N_2^+, O_2^+, NO^+, NO_2^+
PE	C^+, H^+, C_2^+, CH^+, C_2H^+, $C_2H_2^+$, C_3^+, $C_3H_6^+$	H_2^+, CO_2^+, CH_3^+, CH_3CN, $C_2N_2^+$	N^+, O^+, N_2^+, O_2^+, NO^+, NO_2^+

The thermodynamics of the secondary reactions were likely to be important in the quenching mechanism: in the formation of new species, endothermic reactions would potentially aid interruption due to their extraction of thermal energy from the electrode gap, whereas exothermic reactions would release energy and diminish the effect of the temperature gradient between arc and surroundings, reducing the efficiency of convective cooling.

The full evolution of chemical species due to the plasma-polymer interaction and the subsequent reactions between them is highly complex and cannot be ascertained fully by experimentation. Atoms and molecules decomposed from the polymer could re-react with other polymer decomposition products or species from the existing gas in the chamber, and then could further react any number of times forming newer species, or could do this and then decompose back into their constituent atoms, all before reaching the mass spectrometer, following that, fragmentation in the mass spectrometer ionisation source must be considered. This means that the mass spectroscopic results can only be indicative and provide clues as to the reactions and their subsequent effect on the quenching of the plasma.

The presence of polymer constituents such as carbon and similarly, chain fragments, could only have arisen from the decomposition of polymers as there were no other sources of such species in the test chamber and they were not detected in the baseline tests. The products of secondary reactions were those species that contained mixtures of atoms from both the chamber environment and the polymer, such as CO_2^+, and those whose molecular structure precluded them from forming directly from polymer fragments. Gasses attributed to the chamber atmosphere were either those already known, or cases that suggested the reaction or decomposition of those species, such as H_2O^+ and OH^+.

The mass spectral charts are heavily dominated by nitrogen and oxygen lines from the chamber atmosphere, making it difficult to analyse the polymer decomposition mechanism alone. For that reason, the difference in abundance between the pre and post arc levels for the main polymer related gas constituents are shown subsequently in Figures 9-6 – 9-11. Species that did not change as a result of the arc, such as N_2^+, are not shown; the sub-pie charts show species that constitute the lower 15% of the total amount of new species formed. In all cases, a significant amount of CO_2 was detected which is discussed in detail separately.

6.2.3.1 Polystyrene Arc Constituents

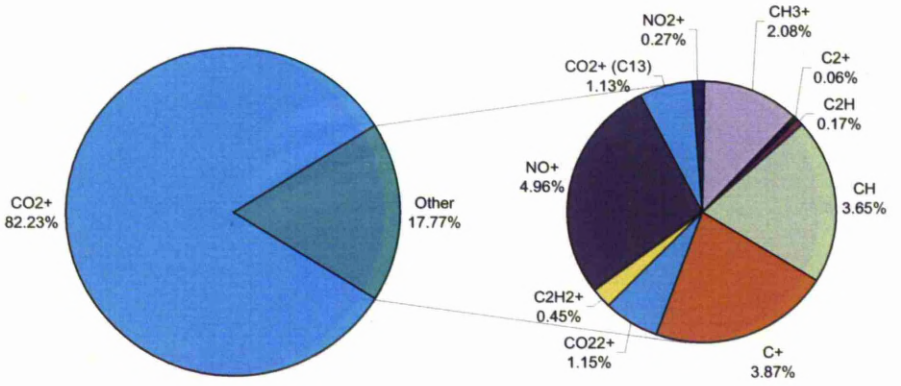

Figure 6-17: Main species following PS arc

The type and abundance of the main chemical species formed as a result of the interaction between the arc plasma and polystyrene are shown in Figure 6-17. The constituent atoms in the polystyrene monomer are carbon and hydrogen, with an additional styrene compound bonded to one of the chain carbons. Styrene is also a hydrocarbon with the structure $C_6H_5CH{=}CH_2$. Apart from CO_2, the presence of low molecular weight hydrocarbons as a result of chain scission were detected, most notably acetylene (C_2H_2, m/z = 26amu), the methyl radical CH_3 (m/z = 15amu) and CH (m/z = 13amu). These were likely formed as a result of chain scission initiated by the high temperature of the plasma but could also be remnants of higher molecular weight hydrocarbons fragmented by the mass spectrometer ionisation source. A relatively large amount of atomic carbon was formed as a result of complete dissociation of the polymer material.

6.2.3.2 Polyamide 6 Arc Constituents

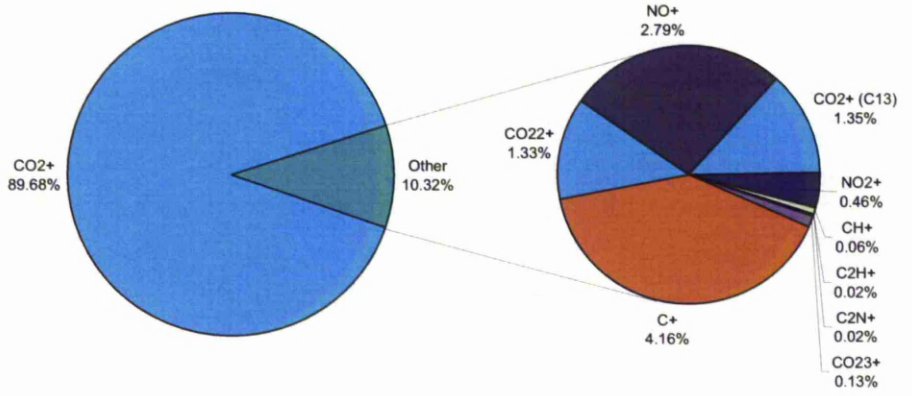

Figure 6-18: Main species following PA6 arc

The interaction between arc plasma and polyamide 6 formed new chemical species in abundances shown in Figure 6-18. The structure of polyamide 6 is a hydrocarbon backbone structure with covalently bonded C=O and N-H side branches. As a consequence of the presence of molecular oxygen and nitrogen it was necessary to distinguish if nitrogen or oxygen containing molecules formed as a result of PA6 chain scission or by the secondary reactions between the fragmented polymer species and dissociated atmospheric O_2/N_2. A relatively large amount of atomic carbon signified complete dissociation with only a small amount of low molecular weight hydrocarbon species formed, namely the ethynyl radical (C_2H, m/z = 25amu) and CH. Also detected was C_2N (m/z = 38amu), which was likely to be related to polymer dissociation by scission of the CN side branch, as opposed to secondary reactions, because it was not detected in any of the other polymers that did not contain molecular nitrogen.

6.2.3.3 Polymethylmethacrylate Arc Constituents

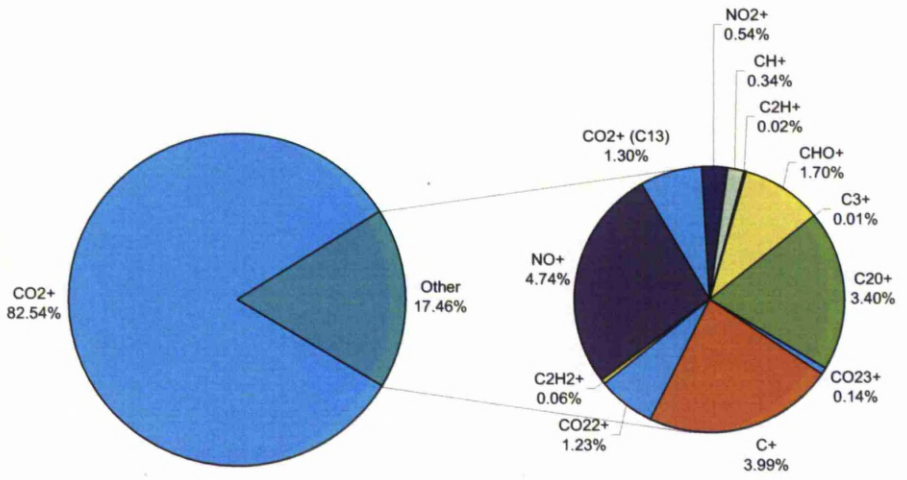

Figure 6-19: Main species following PMMA arc

Mass spectroscopic measurements of the resultant composition following an arc in the presence of PMMA shows the species indicated in Figure 6-19. The PMMA monomer consisted of carbon, hydrogen and oxygen atoms in a relatively complex structure consisting of both single and double bonds between carbon and oxygen. Due to the molecular oxygen in the PMMA structure there was a larger number of oxygen containing molecules detected as a result of the PMMA-arc interaction than in other cases. Most notably were CHO (m/z = 29amu) and ethenone (C_2O, m/z = 40amu). As was the case in the other polymers, elements of low molecular weight hydrocarbons were detected, such as acetylene (C_2H_2) and ethynyl (C_2H), as well as a relatively large amount of atomic carbon. This was indicative of complete dissociation, likely as a result of the high temperatures the polymer was exposed to.

6.2.3.4 Polyvinylchloride Arc Constituents

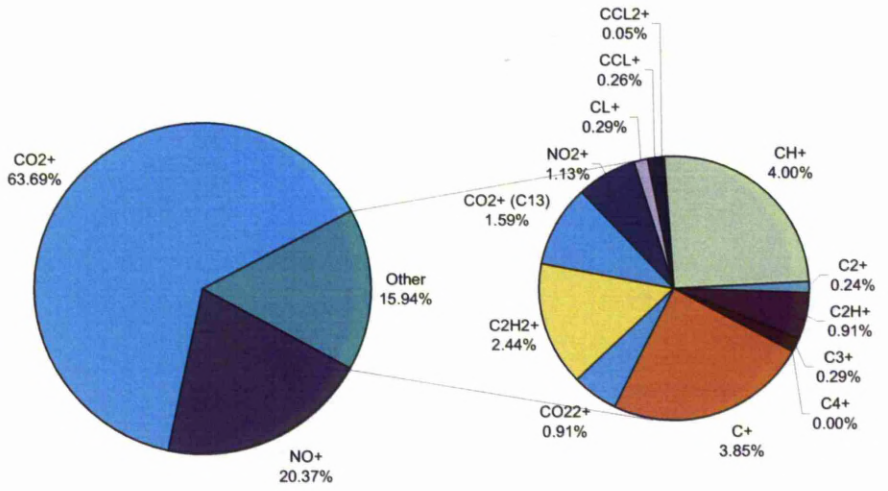

Figure 6-20: Main species following PVC arc

The interaction between arc plasma and polyvinylchloride formed new species in the abundances shown in figure 6-20. The composition of polyvinylchloride is carbon and hydrogen with side branched chlorine atoms in the chain. Low molecular weight hydrocarbons were detected, most significantly acetylene (C_2H_2) and CH, which is similar to the species formed in the other polymers tested. Again the absence of higher molecular weight species could be due to the energy of the arc or due to fragmentation by the mass spectrometer ionisation process. The largest abundance of chlorine detected was atomic chlorine (m/z = 35amu), but there were also signs of smaller amounts of CCl (m/z = 47amu) and dichloromethane (CCl_2, m/z = 82amu). This, coupled with the presence of carbon suggested that the most prevalent mechanism involved in the interaction between the arc and PVC was complete dissociation. Chlorine and chlorine containing molecules could potentially be effective around the arc in terms of quenching due to their electron affinity and the subsequent removal of conductive electrons and the formation of lower mobility ions, aiding in interruption and dielectric recovery.

6.2.3.5 Polytetrafluoroethylene Arc Constituents

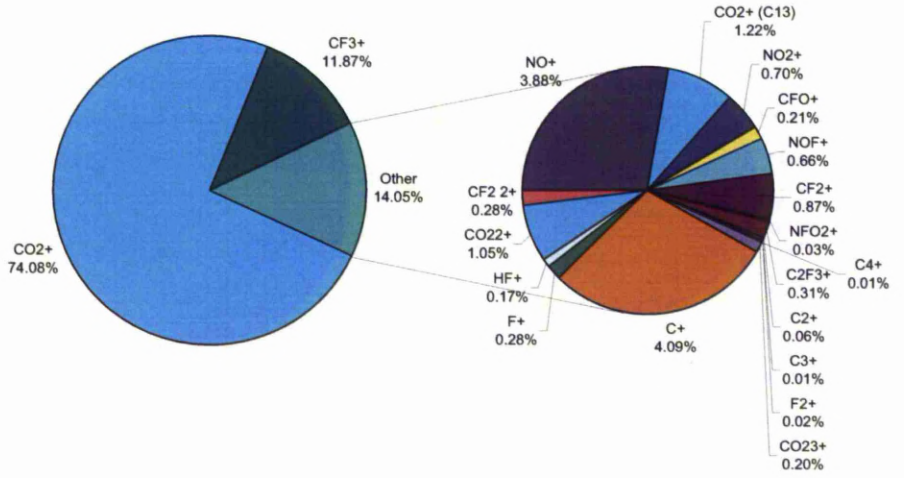

Figure 6-21: Main species following PTFE arc

Polytetrafluoroethylene reacted in the arc to form a rich composition of species, shown in Figure 6-21. The composition of PTFE is hydrogen and fluorine chains single bonded. In the case of the PTFE reaction with the arc a richer diversity of species was detected than that observed in any of the other polymers tested. A large amount of CF_3 (m/z = 69amu) was formed as a result of chain scission and interactions between dissociated chain species and is a common product of PTFE pyrolysis [155]. Other notable fluorinated molecules were formed, but as was the case previously, only low molecular weight species were detected, either as a result of de-polymerisation by the arc of by mass spectrometer fragmentation. The presence of the halogen fluorine and its molecules is positive in terms of electronegativity/electron affinity. The detected presence of F, difluoromethane (CF_2, m/z = 50amu), trifluorovinyl radical C_2F_3 (m/z = 81amu), hydrogen fluoride (HF, m/z = 20amu) and carbonyl fluoride (COF, m/z = 47amu) have positive connotations for circuit interruption. As was the case previously, a significant amount of atomic carbon was formed signifying that dissociation occurred as one of the main processes.

6.2.3.6 Polyethylene Arc Constituents

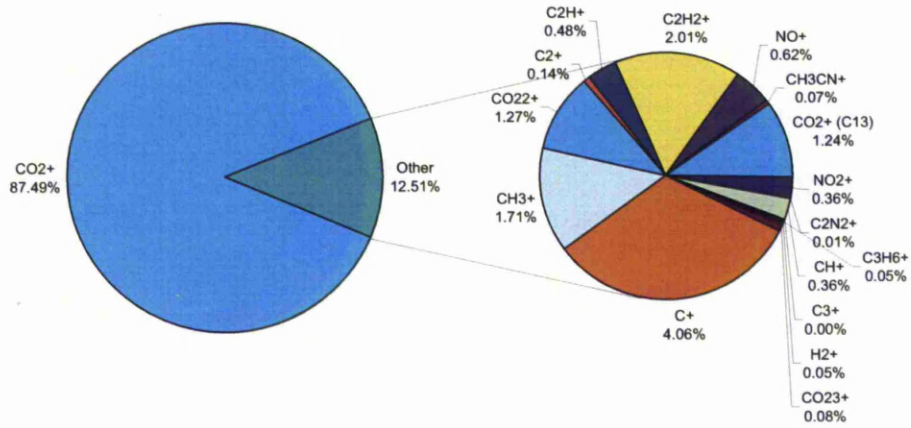

Figure 6-22: Main species following PE arc

The reaction in the arc of polyethylene formed a range of species detected by mass spectrometry and shown in Figure 6-22. Polyethylene is formed from carbon and hydrogen atoms and the reaction of PE in the arc formed a mix of polymer chain fragments and secondary reaction products. A significant amount of carbon suggested complete dissociation in the arc was likely to be the main process, with smaller amounts of hydrocarbons as a result of chain scission. The main hydrocarbon fragments were the methyl radical CH_3, acetylene (C_2H_2) and the ethynyl radical C_2H. As well as these there was the suggestion of some reaction between hydrocarbons and dissociated nitrogen with small amounts of both acetonitrile (CH_3CN, m/z = 41amu) and oxalonitrile (C_2N_2, m/z = 52amu). The presence of a small amount of C_2N_2 could be due to a 'chemical etching' reaction [156] due to the reaction between the polymer and atmospheric nitrogen reacting in the plasma.

6.2.4 REACTION KINETICS AND EVOLVED GAS PROPERTIES

6.2.4.1 Decomposition and Reaction Process

All of the polymers tested showed signs of depolymerisation, complete dissociation and subsequent reactions between decomposed polymer species. With respect to the basic air arc mass spectrum, the application of polymers to the arc caused much richer spectra, including more significant contributions of hydrocarbons, molecular carbon and carbon oxides.

The change of state and decomposition of polymers consumes thermal energy from the plasma, as arc conductivity is strongly related to temperature this process aides in interruption. To form the dissociated carbon and chain fragments observed, the covalent bonds between the constituent atoms in the polymer chains would need to be broken by utilising the energy of the arc. The amount of energy necessary to break a bond is known as the bond dissociation energy, values of bond dissociation energy for those bonds occurring in each of the polymer materials tested are given in Table 6-9; stronger bonds require more energy to dissociate.

Table 6-9: Bond dissociation energies of polymer constituents [157]

Bond	*Energy (kJ/mol)*
C – C	348
H – C	413
H – N	391
C – N	308
C – O	360
C – F	488
C = O	748
C – O	360
C = C	620
C – Cl	330

The distribution of types of bond in each polymer is shown graphically in Figure 6-23. Both the PMMA and PA6 monomers are larger and more complex molecules with a wider variety of constituents than the others, the PS molecule includes the styrene compound so has a relatively large quantity of double carbon covalent bonds. As well as decomposition of the polymers, secondary reactions were also present. The thermodynamics of the secondary reactions complicate the analysis because in terms of arc interruption they could have a positive or negative influence depending on the overall enthalpy of formation of the new species.

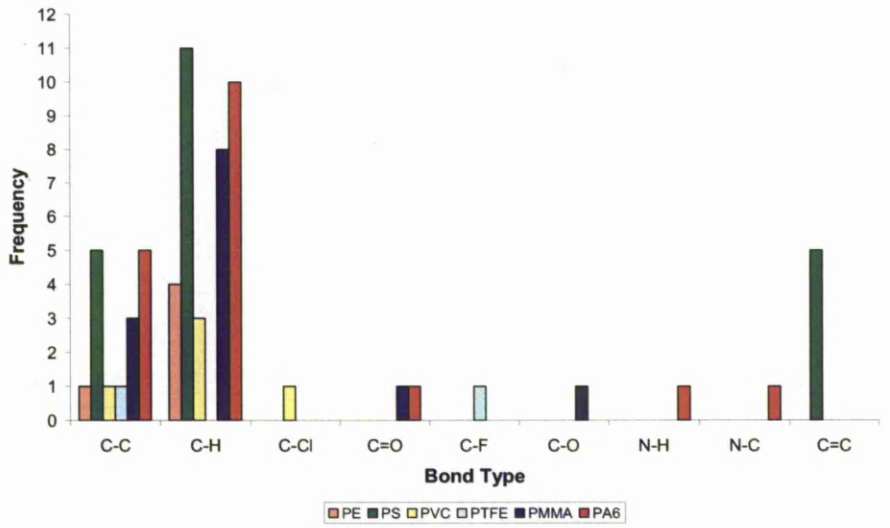

Figure 6-23: Distribution of covalent bond types in the polymer monomers

Two of the most significant contributors to the abundances of species formed in each case were carbon and carbon dioxide, which represent dissociation and secondary reaction products respectively. The change in abundance of these for a polyethylene arc are shown in Figure 6-24 as a function of time, representative scan traces for C and CO_2 for the other polymer arcs are given in the Appendix. It can be observed in Figure 6-24 that prior to the test only a negligible amount of either C or CO_2 was detected, but on arc initiation and the inception of the interaction, a large amount was generated. In all cases, a greater amount of CO_2 was formed than C by a factor of 20, which shows the magnitude of secondary reactions over dissociation.

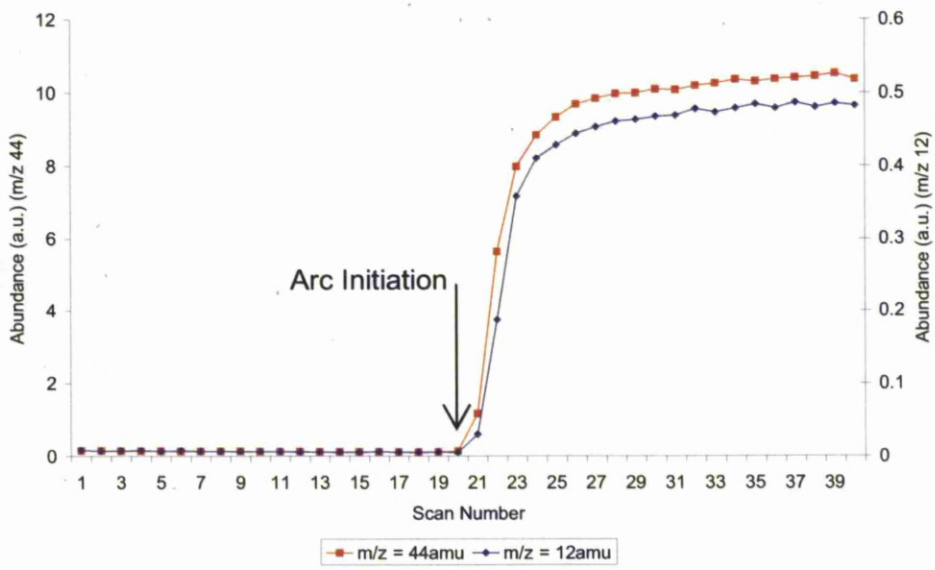

Figure 6-24: Formation of carbon and carbon dioxide as a result of the arc (PE)

Comparison of the abundance of carbon formed for each polymer is shown in Figure 6-25. The data is from the mean maximum post arc quantity detected from the mass spectral data. Carbon is the only element that is a constituent in all of polymers tested and is formed around the arc due to the complete dissociation of the polymer material.

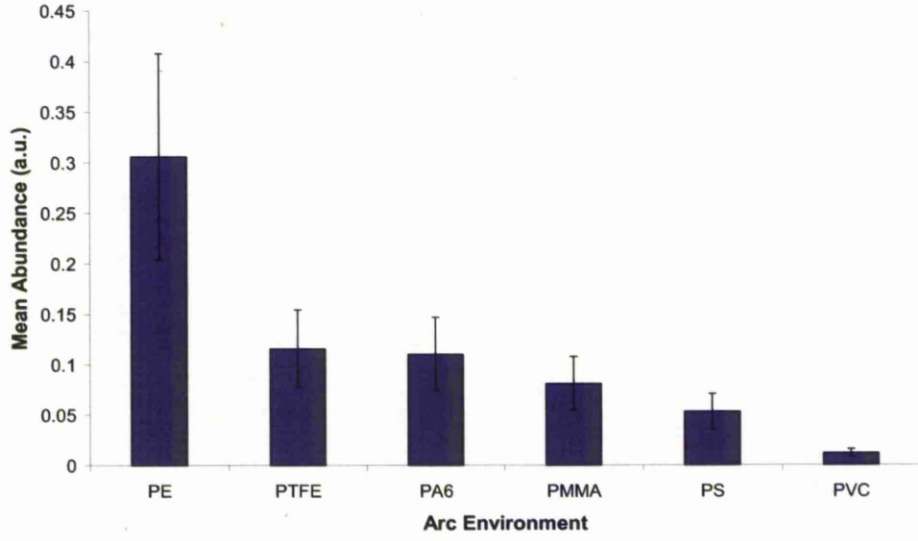

Figure 6-25: Mean abundance of carbon formed from each polymer arc

Differences in the amount of carbon released suggest differences in the degree of polymer dissociation. This is likely to be related to polymer properties such as melting point, thermal decomposition temperature and bond dissociation energy. These differences not only relate to polymer properties but also go towards helping explain the differences in arc interruption ability from polymer to polymer.

The most volumetrically significant gas formed around the arc as a result of the polymer-plasma reaction was carbon dioxide. The most likely evolution process for this amount of CO_2 was a combustion type reaction between decomposed polymer fragments with oxygen from the air as an oxidising agent. The presence of polymer combustion around the arc is likely to be a negative factor in terms of arc quenching due to the exothermic nature of the reaction and the consequent reduction in plasma cooling efficiency. A comparison of the mean abundances of carbon dioxide formed as a result of the polymer-plasma interaction with the arc for each polymer is shown in Figure 6-26. The disparity in CO_2 volume between different polymers is likely to be a result of differences in structure and composition; it is known that certain polymers resist combustion more effectively than others by virtue of their individual properties.

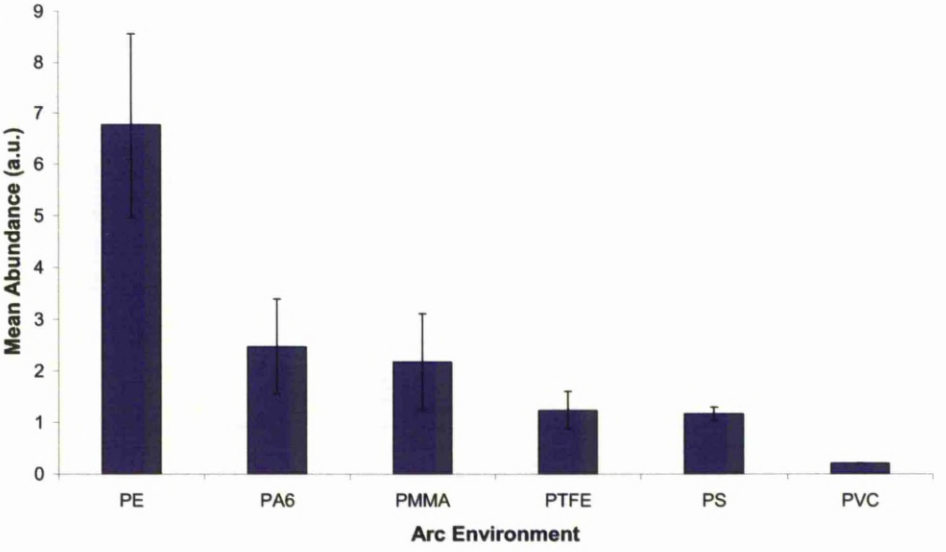

Figure 6-26: Mean abundance of carbon dioxide for different polymer arcs

By measuring the volume of each species defined as primary or secondary products, the mean quantity of species formed by primary decomposition and secondary reactions is shown in Table 6-10. The majority of species around the arc following the polymer interaction were formed as a result of secondary reactions. It is clear that in all cases most of the gasses in the post arc environment were formed as a result of secondary reactions between the dissociated polymer constituents.

Table 6-10: Source of new post arc species

Polymer	Polymer Chain Fragments (%)	*Secondary Reactions (%)*
Air	0	100
Polystyrene	13	87
Polyamide 6	8	92
Polymethylmethacrylate	5	95
Polyvinylchloride	9	91
Polytetrafluoroethylene	11	89
Polyethylene	41	59

The formation of secondary species by the interaction between decomposed polymer species could have positive or negative connotations in terms of arc quenching, depending on the thermodynamics of the reactions and the thermal and electronegative properties of the species formed. The magnitude of endothermic reactions could account for a proportional magnitude of energy dissipated prior to the extinction of a polymeric arc.

6.2.4.2 Overall Reaction Mechanisms

It is likely that the larger molecular fragments must have originated as a result of main chain scission of more then one of the polymer chain bonds. This scission is likely to have been provoked by the high temperature around the plasma coupled with the influence of energetic ions and metastables directly on the injected polymers; bombardment of which could potentially break the polymer covalent bonds.

Another potential source of chain scission could be the absorption of vacuum ultraviolet (VUV) radiation emitted from the plasma that would be likely to exceed the covalent bond energies in the polymers and liberate volatile polymer fragments. It is feasible that chain scission in most cases was due to cleavage of the single bonded C-H backbone structures and side groups creating the hydrocarbon radicals such as CH_3 and C_2H that were detected, this process would also form hydrogen but in most cases only a small amount of H_2 was detected due to low atomic mass and its volatility.

Whilst the identification of the gaseous liberated polymer fragments and dissociation products is relatively straightforward, the evaluation of the evolution kinetics of the species is more difficult due to the complex interactions, initially between the plasma and polymer as arc induced decomposition and then from the chemical reactions between species themselves. Knowledge of the way in which the species were formed, both in terms of dissociative arc energy extraction and the thermodynamics of secondary reactions were important in determining the mechanisms involved in polymeric arc quenching.

The complexity of the interactions mean it would be impossible to know precisely the process of species evolution but simple analysis of the likely source of the detected species in each case can act as an aide to understanding. A flow chart of the combination of polymer decomposition and secondary reaction processes suggested by these results is shown in Figure 6-27.

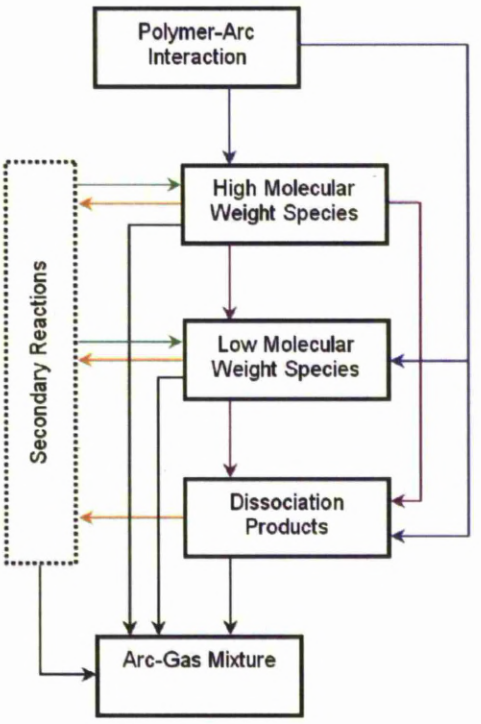

Figure 6-27: Formation routes for arc induced polymer decomposition

The block diagram in Figure 6-27 shows the complexity of the interaction between plasma and polymer and illustrates the difficulty in precisely defining the reaction mechanisms at play. Each of the high molecular weight, low molecular weight and dissociation products formed as a result of the arc interaction could stay the same, decompose/dissociate further in the arc or react with each other to form new species. The new species could potentially then undertake the same mechanisms *ad infinitum* until the arc was extinguished.

It is believed that the interaction between the polymer and the arc was the cause of the current interruption displayed in Chapter 5. In the first instance the change of state and subsequent de-polymerisation and dissociation of the polymers extracted energy in order to break the covalent bonds between the polymer constituents, resulting in volume cooling of the arc.

It is then hypothesised that in some cases the chemical reactions between dissociated species were favourable thermodynamically, which further aided energy extraction by cooling of the arc. By the same token, some of the secondary reaction thermodynamics could be exothermic overall, as was the case with combustion, and therefore negative in terms of arc cooling. In all cases the species of gas formed, the dielectric and electronegative properties and the degree of turbulent intermixing with the arc plasma was expected to have a bearing on the quenching ability of the polymer. Those polymers that were more effective at interruption are speculated to be more successful because they efficiently cooled and de-ionised the arc and electrode gap to a greater extent than the others by the processes of dissociation, secondary thermodynamics (endothermic reactions) and the properties of the gas mixture.

6.2.5 SUMMARY OF MASS SPECTROMETRY

Polymers decompose and dissociate as a result of the interaction with the arc. In all cases, low molecular weight species as well as atomic constituents of the polymers were detected, which indicated a combination of depolymerisation and dissociation reactions occurred. However, the largest abundance of species was due to secondary reactions between polymer fragments themselves and between the atmospheric gasses. Of the secondary species, carbon dioxide was formed in the greatest abundance and was speculated to be due to a combustion reaction, varying quantities were detected from polymer to polymer, indicating differences in reaction mechanism.

The thermal decomposition, dissociation and subsequent chemical reactions between species that occur during arc-induced decomposition of polymers are extremely complex. The composition of gasses around the arc formed by polymer decomposition and secondary reactions could play an important part in circuit breaker arc control. Factors such as the thermal conductivity of the gas mixture at high temperature, electronegativity/electron affinity and specific heat capacity of the polymer gas mixture could all aid or impede interruption.

Chapter 7

Discussion

CHAPTER 7 - DISCUSSION

7.1 OVERALL INTERACTIONS

The polymeric quenching effect involves a complicated interaction between plasma and polymer, as well as subsequent reactions between polymer decomposition by-products. This combination of physical and chemical effects is ultimately responsible for extracting sufficient energy from the discharge to lead to interruption. The complex interplay of mechanisms revealed during this investigation is summarised in Figure 7-1.

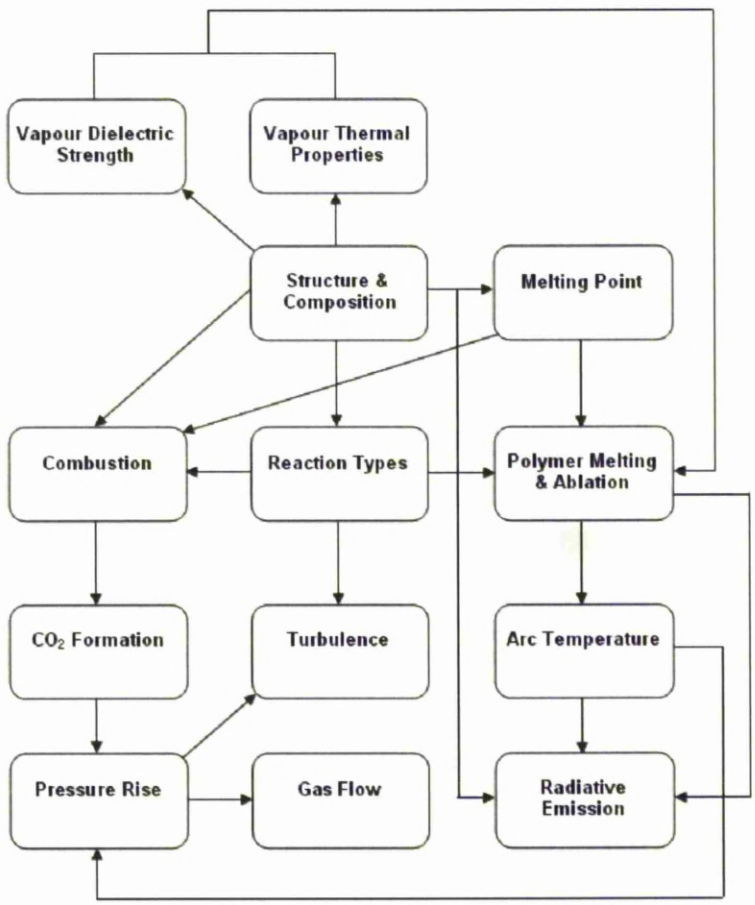

Figure 7-1: Diagram showing the complex interaction between processes

7.2 POLYMER STRUCTURE AND COMPOSITION

Differences in structure and composition of polymers are the fundamental reason why they react differently in the arc and consequently display differing quenching abilities. There are various aspects of polymer structure and composition that may have an influence on the polymeric interruption process; these include atomic constituents, monomer composition, bond dissociation energy, bond structure, and polymer family.

Experimental observations, particularly by mass spectrometry, showed that the most prevalent reaction mechanism is complete polymer dissociation in the arc. The presence of dissociated atoms around the plasma can have a positive influence on interruption, particularly during the dielectric recovery phase, and its effect is mainly dependent on the degree of electron affinity of the atoms. Of particular note are the polymers PTFE and PVC, which contain the atoms fluorine and chlorine respectively. Fluorine and chlorine have the highest electron affinity in the periodic table, with values of 328 and 349kJ/mol [158]. With respect to this, it is notable that PTFE and PVC were amongst the most effective polymers for causing current interruption. As well as halogenic species, other atomic decomposition products from the polymers: carbon (122kJ/mol) [159], hydrogen (73kJ/mol) [160] and oxygen (141kJ/mol) [161] all have greater electron affinities than air at the same temperature and pressure. This is because the main constituent of air, nitrogen, has a negative electron affinity of minus 7kJ/mol [162]. This is due to its electron configuration, which contains a stable half filled p-orbital meaning the addition of an extra electron would actually make the atom unstable. With these factors in mind, it can be taken that the complete decomposition of polymers in the arc has a positive influence on overall interruption due to the increased electron affinity of the atomic decomposition species. The electron affinity of the dissociated products reduces the number of conductive free electrons in the electrode gap by forming heavier, low mobility ions that do not conduct easily. In this aspect, polymers containing halogenated atoms, particularly fluorine and chlorine, can be considered to be effective materials to use in the arc interruption role.

As well as total dissociation, there were also signs of polymer chain cleavage leading to the presence of low molecular weight hydrocarbons around the arc; this is notable because research has shown that the presence of hydrocarbon gasses around the electrode gap can enhance dielectric strength [163]. The high temperature depolymerisation of the polymer chains in the arc negated the presence of longer chain hydrocarbons; however there were signs of low molecular weight hydrocarbon gasses. The mass spectroscopic observations showed most notably the presence of the hydrocarbons C_2H_2, C_2H and CH_3.

A greater number of carbon C-C and carbon-hydrogen C-H bonds and longer carbon chain lengths in hydrocarbon gasses cause a corresponding increase in dielectric strength [164]. Of particular note is acetylene (C_2H_2) because it contains a triple carbon-carbon bond that significantly improves dielectric strength with respect to other hydrocarbons. Highlighting the positive role of hydrocarbons in this context, research into the use of butadiene (CH_2=CH–CH=CH_2) in circuit breakers has shown a positive role for hydrocarbons in circuit breaker type applications [165,166]. Butadiene has a pair of double carbon bonds and other research has found this to be the cause of its excellent dielectric strength relative to other hydrocarbon gasses [164]. The disadvantages of the reaction of hydrocarbon gasses in circuit breakers are deposition of discharge products that could potentially settle on electrodes and alter the conductivity of the closed breaker. This is an important consideration because inefficiency caused by increased Joule heating is a significant factor in energy losses from circuit breakers and has a consequent bearing on overall electricity network costs and environmental impact [167]. It must be noted however that in this case only a relatively small proportion of the total gasses in the chamber were hydrocarbons because complete dissociation was the primary mechanism.

As well as hydrocarbons, the polymers PTFE and PVC formed a small volume of molecules that have positive electronegative properties by virtue of their halogenated constituents. Of the gasses detected, most notable were CF_2, CF_3 and CCl_2, which could aid in both the interruption and transient recovery aspects of the dielectric gas performance. The presence of these molecules would have a similar effect on interruption as the halogenic atoms, particularly with respect to dielectric recovery, and is one of the important mechanisms involved in polymeric arc quenching. In related research, experimental studies of PTFE nozzle ablation in SF_6 circuit breakers [168] has shown similar results, stating that most ablated PTFE reacts to CF_n species. This research found that the ablated polymer mass is a linear function of arc energy and the presence of these species alters the electrical and thermal conductivity, heat capacity and enthalpy of the plasma composition, which effect the arc interruption characteristics. It is not possible to directly infer that good dielectric strength equates to good interruption performance [169], however interruption is a two-stage process that involves both extinguishing the arc then recovering the dielectric strength of the electrode gap. This research and related work has shown that the presence of atoms and molecules with electronegative properties can have a positive role in both processes.

In terms of direct extinguishment of the discharge, polymer decomposition products that enhance the thermal conductivity of the surrounding gas enable more efficient arc cooling. The baseline discharge existed in an air environment; therefore any new species formed would be beneficial if they exceeded the thermal conductivity of air [0.0454W/mK (300K)]. Of all the species formed, the most effective in this respect would be CO_2. Carbon dioxide has a thermal conductivity of 0.070W/mK (300K) and therefore its production around the arc would enable more effective arc cooling. A chart of various values of thermal conductivity for some common polymer-arc by-products is shown in Figure 7-2. The presence of CO_2 around the arc was volumetrically significant in all cases and given its relative thermal conductivity with respect to air it is likely that this enhanced the interruption mechanism.

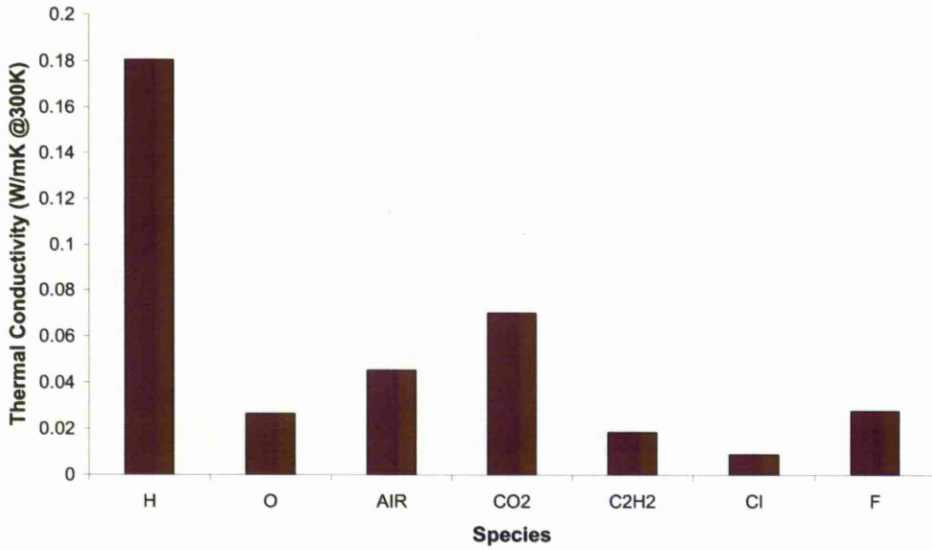

Figure 7-2: Thermal conductivity of some polymer dissociation species

Another feature related to the polymer structure and composition is bond dissociation energy. The energy required to dissociate covalent bonds in the polymer and so release atoms and chain fragments would have been extracted from the arc. The extraction of thermal energy caused volume arc cooling and as a consequence increased resistance. It was shown in Chapter 5 that the most effective polymeric arc quenchers caused significant increases in arc resistance prior to current interruption and one reason for this could be due to energy extraction to affect bond dissociation. Other research using induction coupled thermal plasma models and various polymers has corroborated this assertion and found that the application polymers to the arc plasma caused temperature degradation [170]. It was hypothesised that this occurred due to the polymers consuming energy from the thermal plasma to facilitate melting and ablation, the same processes found in this case.

The bulk properties of polymers are strongly dependant on the degree and character of the branching and cross-linkages of polymer chains. In this case, one of the most notable features was melting point. Polymer melting point is a phase change that defines the transition from crystalline to amorphous configuration and is strongly related to polymer structure.

Polymers with a higher degree of polymerisation have higher melting temperatures due to an increased number of Van der Waals forces and branch entanglement between the polymer chains. The relationship between polymer melting point (T_m) and arc temperature reduction from the optical spectral analysis in Chapter 6 is shown in Figure 7-3.

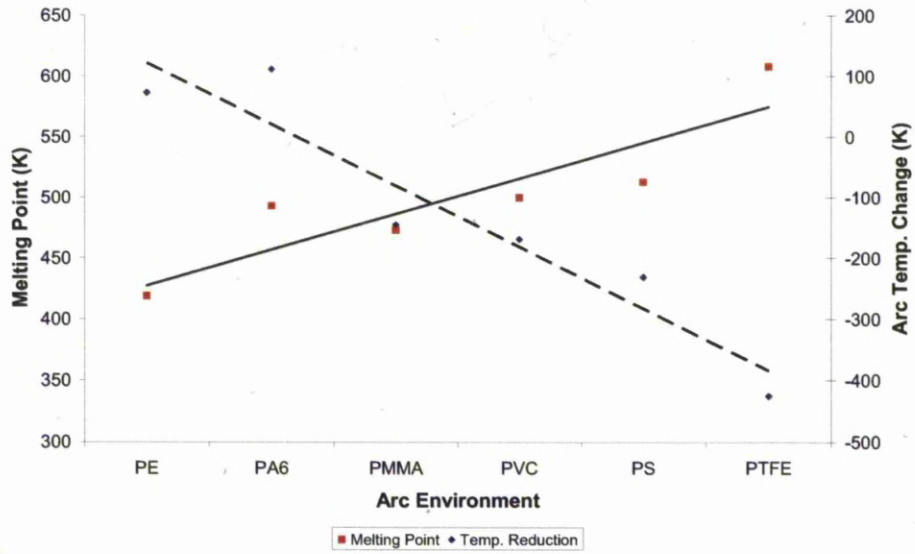

Figure 7-3: Relationship between polymer melting point and arc temperature

The relationship shown in Figure 7-3 demonstrates that polymers with higher melting point seem to cause a larger temperature reduction in the arc. This could be due to the greater energy extracted from the plasma in order to affect the change of state, which consequently cools the discharge to a larger extent. One of the main processes involved in polymeric arc quenching is thermal energy extraction from the arc by the polymer change of phase and dissociation. It has been found in other research that for arcs in narrow channels, arc induced evaporation, axial convection and radiative energy transfer to the polymeric solid wall material has a significant bearing on arc characteristics [171]. Although this cannot be directly linked with the particulate polymer reaction mechanism the parallels between the concepts provide supporting evidence.

Five different types of polymer were used in the investigation, namely polyolefines (PE), vinyl polymers (PS and PVC), fluoropolymers (PTFE), polyacrylics (PMMA) and polyamides (PA6); the distinctions are based on differences in structure and composition. Experimental investigations carried out in this project have found that polyolefines, vinyl polymers and fluoropolymers were most effective at arc quenching.

7.3 REACTION THERMODYNAMICS

Both primary and secondary reactions of the polymer in and around the arc can have a role in interruption. Primary reactions are defined in this case to be those that are directly involved in the polymer changes of state and dissociation. From the spectral data shown in Chapter 6, the strong 656nm carbon radiative emission line is a sign of the complete dissociation of the polymer in the arc and was found to occur to different magnitudes with different polymers. This result can be linked with the time period to interruption data from Chapter 5 and is shown in Figure 7-4.

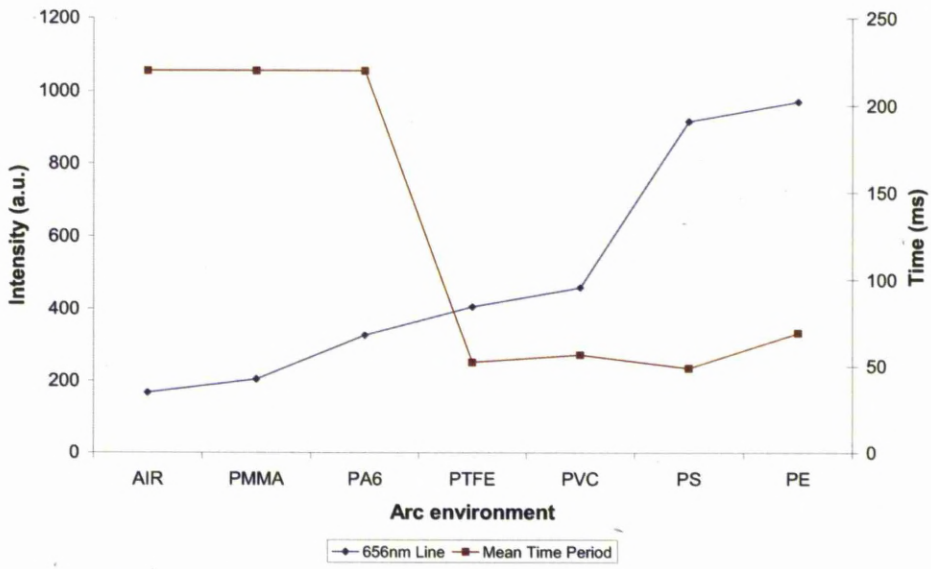

Figure 7-4: Relationship between 656nm radiative emission and interruption

The relationship in Figure 7-4 shows that the more efficient arc quenchers formed larger carbon spectral peaks that indicate more significant decomposition of the polymers in the arc. This is intuitive because a greater degree of dissociation suggests a larger energy extraction from the arc and consequent arc cooling that would lead to more efficient interruption.

Secondary reactions are defined to be those that occur between decomposition species themselves. The nature of the chemical reactions in and around the arc in terms of thermodynamics is significant with respect to the overall energy transfer mechanisms. These mechanisms can aid or impede interruption depending on the overall nature of the energy conversion. Endothermic reactions can enhance energy losses and lead to more efficient cooling of the electrode gap, improving interruption efficiency whereas exothermic reactions reduce convective energy losses and the efficiency of the temperature gradient between the arc, as well as reducing the arc cooling effect of radial gas intermixing. Related research using computer modelling of the complex polymer-arc interaction has found the thermodynamic and transport properties of ablated polymer vapour can enhance plasma energy losses [172]. Properties of the vapour such as mass density, enthalpy, thermal conductivity and specific heat could improve the temperature distribution in the plasma to aid in interruption. Further research also found that as well as the energy consumed in the change of state the resultant vapour has a role in plasma cooling [173].

Experimental observations in this case showed the most significant species formed as a result of secondary polymer interaction around the arc was carbon dioxide. The formation of carbon dioxide was most likely the result of a combustion type reaction between volatile hydrocarbon fragments decomposed from the polymer chains and atmospheric oxygen. This reaction is exothermic in nature, which could have overall positive or negative connotations for arc interruption. The positive side is that the presence of CO_2 around the arc and its intermixing due to reaction induced turbulence enhances arc cooling; the negative side is that the thermodynamics of the reaction can reduce the cooling efficiency of the temperature gradient between the arc and surrounding gasses.

Even with mass spectroscopic analysis it has proved to be extremely difficult to properly understand the complex chemical reactions between dissociated polymer chain fragments. As a consequence, it is only possible to speculate on the effect of the thermodynamic changes the reactions cause on the interruption process. With that said, the experimental results play a part in the process of more fully defining the relevant reactions that take place and their influence on interruption. The experimental observations are supported by other research that uses computer modelling to determine plasma composition in various polymer environments in the context of contact wall ablation [174, 175, 176]. It is acknowledged that the chemical reactions and thermal dissociations undertaken in this type of environment are extremely complex, and that theoretical results cannot be easily generalised into actual circuit breakers. By using the molar fraction of the polymer constituents, calculations can be made of vapour compositions at various plasma temperatures. The results in all of these investigations cohere with the mass spectrometry observations made in this research. The main species at arc temperatures are confirmed to be low molecular weight monatomic and diatomic organic species, and dissociated individual atoms. This is due to the high arc temperatures involved, which preclude the presence of molecularly heavier species.

7.4 COMBUSTION PROCESS

The formation of CO_2 around the arc as a result of the plasma-polymer interaction was a significant effect. Combustion occurred as a result of polymer degradation due to thermal energy from the arc subsequently forming combustible low molecular weight volatile gasses, which reacted to form CO_2. The fact that certain polymers/polymer by-products appeared to undergo this reaction to a lesser extent than others was indicative of the influence of combustion inhibiting factors, which are related to the structure and composition of the polymers. The combustion reaction is exothermic and the general chemical equations describing the complete and incomplete combustion of a hydrocarbon are shown below.

$$C_xH_y + \left(x + \frac{y}{4}O_2\right) \rightarrow xCO_2 + \left(\frac{y}{2}\right)H_2O$$

$$C_xH_y + \left(x + \frac{y}{2}\right)O_2 \rightarrow xCO + \left(\frac{y}{2}\right)H_2O$$

Most likely, the combustion of the hydrocarbons in the test chamber would be a mixture of complete and incomplete combustion, forming CO, CO_2, H_2O and O_2 as well as un-reacted polymer fragments. Examples of chemical reactions that may have taken place in the formation of CO_2 in the polymeric arc environments are shown in Table 7-1. The enthalpy change, ΔH, is negative for exothermic reactions due to the fact that more energy is released than absorbed.

Table 7-1: Example combustion reactions of carbon polymer products

Reaction	ΔH (KJ/mol)
C (s) + 2O (g) ↔ CO_2 (g)	-643
C (s) + O_2 (g) ↔ CO_2 (g)	-394
CO (g) + ½ O_2 (g) ↔ CO_2 (g)	-280
CO (g) + H_2O (g) ↔ CO_2 (g) + H_2 (g)	-30
CH_4 (g) + H_2 (g) ↔ CO_2 (g) +4H_2 (g)	-254

A thermodynamically similar reaction occurred as a result of the pyrolysis of C_2H_2 (acetylene) with O_2 to form C_2H, followed by the subsequent combustion of ethynyl. The ethynyl radical C_2H was likely formed in an exothermic secondary reaction and was detected in small quantities following the PE, PVC, PMMA, PA6 and PS polymeric arcs. Ethynyl radicals are observed in combustion reactions in acetylene/oxygen flames [177] and their presence in this case supports the theory that combustion of the polymers took place. Examples of some of the reaction mechanisms and their enthalpy are given in Table 7-2.

Table 7-2: Example combustion reactions of ethynyl species [178]

Reaction	ΔH (KJ/mol)
C_2H (g) + O_2 (g) → CO (g) + HCO (g)	-656
C_2H (g) + O_2 (g) → 2CO (g) + H (g)	-539
C_2H (g) + O_2 (g) → CH (g) + CO_2 (g)	-335
C_2H (g) + O_2 (g) → C_2O (g) + OH (g)	-209
C_2H (g) + O_2 (g) → C_2HO (g) + O (g)	-42

Other research has shown that a product of the combustion reaction between ethynyl and oxygen is carbon monoxide [178]. It was not possible to detect carbon monoxide (CO^+, m/z = 28amu) production by normal resolution mass spectrometry in this case due to the large quantity of nitrogen in the chamber (N_2, m/z = 28amu). The overall enthalpy of the reaction mechanisms shown in Table 7-2 mean that, as was the case previously, the exothermic nature of combustion is likely to be a negative factor in the polymeric quenching process.

The main factors that influence the combustion of polymers are: melting point, decomposition temperature and chemical composition. Polymers with higher melting points resist combustion more effectively; the relationship between polymer melting point and volume of CO_2 produced is shown in Figure 7-5.

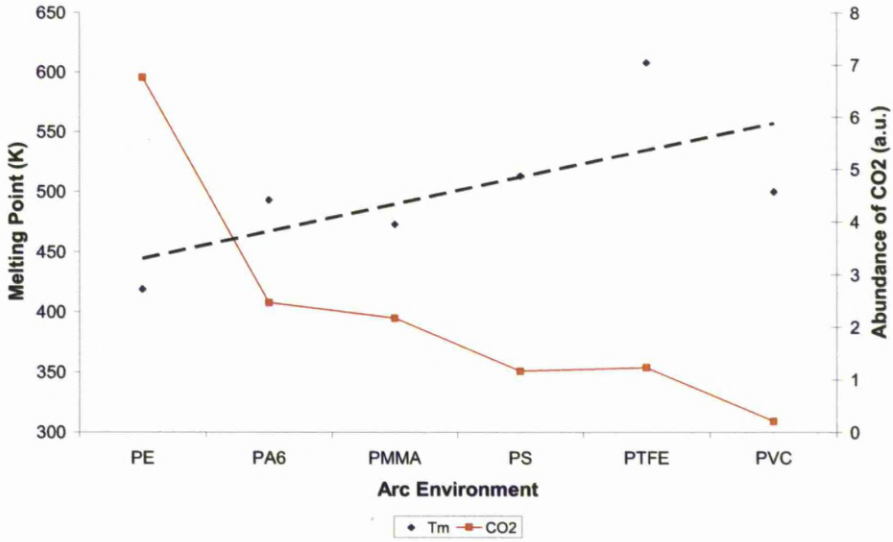

Figure 7-5: Relationship between polymer melting point and CO_2 formation

There is general relationship between polymers with larger values of T_m and the formation of CO_2 and it can be inferred that this is because they undergo less combustion. Inhibition of combustion appears in the most part to be a positive effect because the most effective arc quenching polymers, PVC, PS and PTFE, all resisted combustion relatively well and had the highest melting points with lowest volume CO_2 production. Polymer decomposition temperature refers to the point at which the polymer starts to fragment or depolymerise. The polymers that resist decomposition are more effective at inhibiting combustion and form less gaseous chain fragments; these polymers have high values of decomposition temperature.

As well as melting point and decomposition temperature, another significant inhibitor of combustion in polymers is based on structure and composition. Certain elements restrict the free-radical mechanism, which is a key part of the combustion process. In combustion reactions, when the temperature is high enough the stable oxygen radical can overcome its energy barrier and move into a highly reactive state. The reactive oxygen radical can then initiate chain reactions that lead to combustion of the material. In some circumstances termination reactions can also take place, where certain species are able to deactivate the free radicals. Halogens such as fluorine, chlorine and bromine are particularly effective at inhibiting the radical mechanism and as such are commonly used in industry for fire retardency [179]. This concept is supported by the experimental results as it was found the halogenated polymers PTFE and PVC formed the lowest quantities of CO_2. It is known that different types of polymers undergo combustion by different mechanisms depending on the structure and composition of the material. Vinyl polymers (in this case PS and PVC) degrade thermally by a free radical mechanism [180, 181]. Polystyrene also formed a relatively small quantity of carbon dioxide. This was likely to be because PS belongs in the category of vinyl polymers along with PVC and has a relatively high decomposition temperature, resisting combustion.

At the other end of the spectrum, the polymer PE formed the largest volume of CO_2 and underwent the greatest degree of combustion. This is due to its low melting and decomposition temperatures coupled with the formation of volatile hydrocarbon fragments following its decomposition. The reasons for the quenching ability of PE most likely stem from a combination of CO_2 production and violent, turbulent reactions with large pressure rises that accompany its interaction with the discharge. The presence of CO_2 itself is likely a positive effect due to its positive influence on thermal conductivity around the arc. These various factors support the assertion made previously that there are different mechanisms at work and polymers utilise different weightings of these mechanisms to quench the arc depending on their individual structure and composition. The enhancement of gas flow and pressurisation around the arc has been found in this investigation to be due in part to the formation of CO_2 from the polymer decomposition species. An assertion was made in this discussion on experimental results that the turbulence and CO_2 intermixing was one of the arc quenching mechanisms. This idea is supported by other research conducted in the context of miniature circuit breakers [182]. It was found in that case that arc mobility in the contact region is influenced by both gas flow and gas composition and is an important factor in interruption.

Given the combination of factors discussed above, combustion of polymers cannot absolutely be considered either a positive or negative quenching effect. The thermodynamics of reaction for the formation of CO_2 itself are negative because its exothermic nature reduces convective quenching efficiency and cool gas intermixing. However, the large pressure rises caused in the most part by the volume of CO_2 could be used in certain configurations to enhance gas flow and cooling of the arc. As well as this, the presence of CO_2 in the pre and post interruption electrode gap can enhance the energy extraction performance by virtue of its properties; of particular note is the increased thermal conductivity of carbon dioxide over air. These properties of CO_2 have led to the development of experimental circuit breakers that use this gas [183].

7.5 PRESSURISATION

The alteration of the overall chamber pressure as a result of the polymer-plasma interaction is both a source of quenching itself and also an indicator of the reactions taking place. As was stated in Chapter 5, conventional circuit breakers often fabricate a pressure differential in order to cause gas flow that enhances turbulent cool gas intermixing and convective cooling. The pressure changes in this case have been shown to be limited in terms of quenching due to the lack of nozzling structures around the electrode gap in this configuration. However, it is possible that the large rises in pressure caused by some polymers, particularly PE, could be utilised effectively in a circuit breaker. Also of note were the pressure changes prompted by the reactions of PTFE and PS, which reduced with respect to the baseline case.

There are three aspects of the plasma-polymer interaction that affect chamber pressure, namely: volume of injection propellant; arc heating of chamber gasses; and production of gasses as a result of polymer decomposition. Of these, the last two were considered the most significant. The mechanisms that caused the pressure changes can be better explained with reference to the results obtained in previous chapters. The analysis of optical emission spectra showed variations in apparent arc temperature caused to different extents by different polymers. Analysis of mass spectroscopic data showed evidence of the production of further gaseous species in the test chamber as a result of polymer decomposition and reactions; the most volumetrically significant species formed in all cases was CO_2. The relationship between chamber pressure and arc temperature, and chamber pressure and CO_2 production are shown in Figures 7-6 and 7-7 respectively. Analysis of Figures 7-6 and 7-7 shows a that there is a relatively close association between the chamber pressure rise and both arc temperature and CO_2 production, this corroborates the assertion that the pressure rise observed in the chamber was a result of both arc volume heating of the gas and a greater quantity of gas production in the chamber.

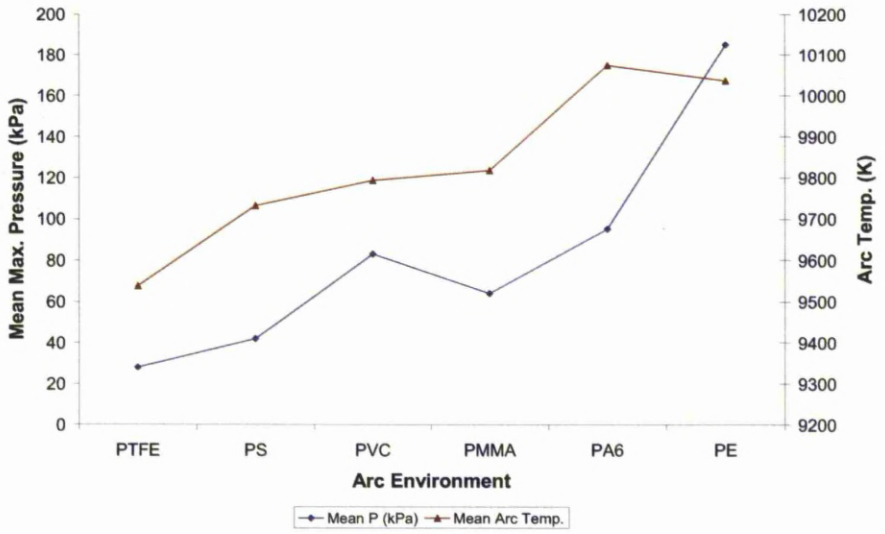

Figure 7-6: Relationship between arc temperature and chamber pressure

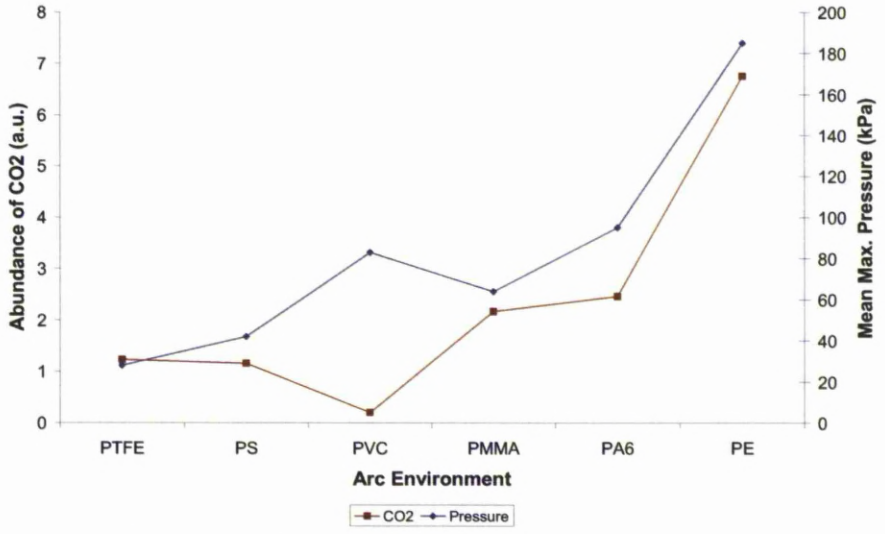

Figure 7-7: Relationship between CO_2 formation and chamber pressure

The variation in pressurisation between different polymers is due to differences in structure and composition. In operational circuit breakers these effects could be enhanced by the use of nozzles to improve pre and post interruption quenching mechanisms. By causing a pressure differential between the upstream and downstream regions, gas flow is intensified with consequent cooling and flushing effects, an example nozzle is shown in Figure 7-8.

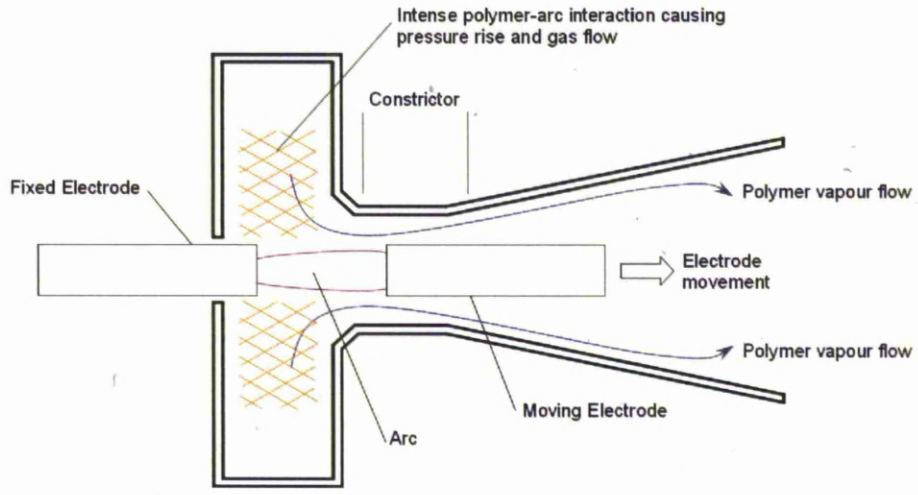

Figure 7-8: Possible nozzle design to enhance polymer induced gas flow

Of all the polymers tested, the large pressure rises and abundance of CO_2 formed by polyethylene when reacting in the arc can be best utilised in the type of self-expansion type nozzled design shown in Figure 7-8. This configuration could best exploit the large pressure rise and consequent gas flow along with the intermixing of cooler CO_2, enhancing energy losses and leading to volume arc cooling. Studies on low voltage moulded case circuit breakers [184, 185] have supported the findings in this case, showing that the gassing of the polymer wall material is an important part of the interruption process. It was found that the higher pressure caused by solid wall gassing leads to increased gas flow [186, 187]; causing a faster de-ionisation of the plasma following current zero. Similar studies on higher voltage SF_6 interrupters with PTFE nozzles have also been performed, with the motivation of understanding nozzle wear and deformation [188]. It was found that the ablation of the nozzle material was an important factor in the pressurisation of the axial blown circuit breaker methodology and it was found that in this case the rate of ablation was dependant on the material type as well as arc current and geometry.

7.6 OVERALL QUENCHING MECHANISMS

The most important mechanisms involved in the polymeric quenching process were selected by analysis of experimental data and are listed in normalised form in Table 7-3.

Table 7-3: Experimental results used in polymer comparison (normalised)

		PE	PTFE	PS	PVC	PA6	PMMA
1	Halogen Composition	0.00	1.00	0.00	1.00	0.00	0.00
2	Max. Electron Affinity	0.35	0.94	0.35	1.00	0.40	0.40
3	Time Period	0.88	0.98	1.00	0.95	0.00	0.00
4	Polymer Melting Point	0.69	1.00	0.84	0.82	0.81	0.78
5	Arc Temp Reduction	0.07	1.00	0.64	0.52	0.00	0.48
6	Degree of Turbulence	1.00	0.67	0.67	0.78	0.56	0.33
7	CO_2 Abundance	1.00	0.18	0.17	0.03	0.37	0.32
8	Max. Pressure	1.00	0.15	0.23	0.45	0.51	0.35
9	Voltage Peak	0.99	1.00	0.99	0.99	0.15	0.19

Manually comparing properties and characteristics for each polymer is complex and so is best done by utilisation of the chromatic method. In order to compare the processes involved for each polymer quantitatively, a synthetic spectrum was created for each polymer by using the experimental results. An example of the data spectrum filtering is shown in Figure 7-9.

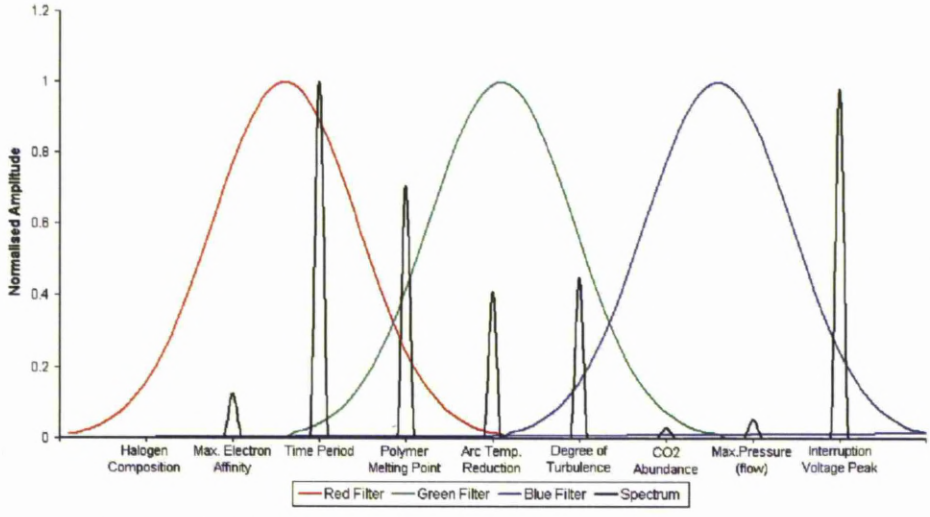

Figure 7-9: Chromatic filtering of interruption parameters (PS)

Applying the chromatic filtering and HLS algorithms allowed the plotting of single data points for each polymer on HS and HL polar plots. This meant that the gamut of information from the range of experimental data could be quantified to allow direct comparison between the quenching mechanisms. The HLS polar plots containing data from the range of polymers tested are shown in Figure 7-10.

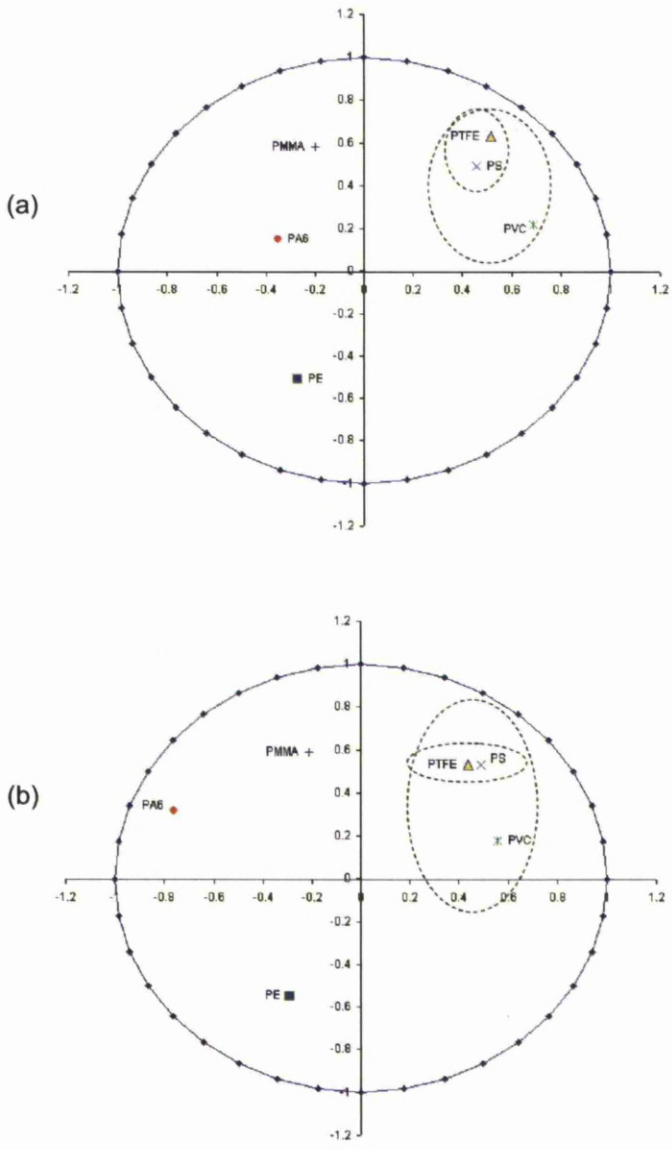

Figure 7-10: Polar plots of polymeric quenching data: (a) HS, (b) HL

The HLS polar plots shown in Figure 7-10 quantify the differences in quenching mechanisms between the different types of polymer. The most efficient polymer arc quenchers PTFE, PS and PVC occur in the upper-right quadrant of each polar plot. There is a close grouping between PTFE and PS, indicating they share a similar range and extent of quenching mechanisms. Slightly more displaced from this group is PVC, which has been shown to also be efficient at arc quenching. Its displacement was most likely due to differences in the way in which the reaction of PVC differs from that of PTFE/PS in terms of chamber pressurisation and arc temperature. Polyethylene occurs in the lower-left quadrant, which supports the assertion that its reaction with the arc and quenching mechanism is significantly different from that of PTFE, PS and PVC, most likely due to the greater effects of turbulence and cool CO_2 intermixing. The least efficient arc quenchers were PMMA and PA6, which are positioned in the upper-left quadrant of each polar plot. Most of the important quenching processes were of lesser magnitude in the cases of these polymers than in the others.

The chromatic algorithm has been shown to be a useful tool in the analysis of the complex set of data relating to the various quenching processes. The results have shown both differences and similarities in the extinguishment mechanisms between polymers in their reactions with the arc plasma.

7.7 FURTHER DEVELOPMENT

Recent development of the concept of polymeric arc quenching has utilised a prototype self-blast interrupter unit with particulate polymer assistance. This investigation utilises the high current facilities at the University of Liverpool to test the unit under a range of ac current interruption and voltage withstand conditions. The existing self-blast unit consists of a solid PTFE chamber which has been designed to harness the energy of the discharge as pressure inside the volume; this is then discharged into the arc column at around the time of current zero. This cools and de-ionises the electrode gap, aiding in interruption. A schematic of the unit is shown in Figure 7-11.

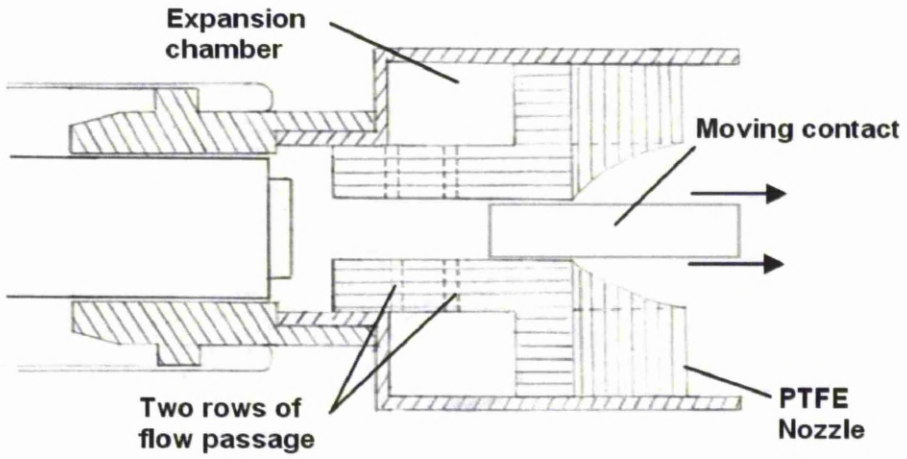

Figure 7-11: Schematic diagram of the prototype self-blast interrupter unit [197]

The use of polymer particulates inside the expansion volume enhances the interruption capability of the unit due to increased pressurisation and resultant gas flow, and because of the improved dielectric and thermal properties of the polymer ablated vapour. The design was such that the particles were confined around the electrode gap where they were needed, preventing the occurrence of particulates around other areas of the breaker leading to parasitic arcing.

In these initial stages of this development, three types of polymer were selected based on the results of the fundamental investigation; these were polyethylene, polymethylmethacrylate and polytetrafluoroethylene and were chosen so as to test polymers with differing quenching mechanisms. Probing of the expansion volume pressure during an arc was conducted at a range of currents with the intention of understanding the influence of the particulates on pressurisation and consequently gas flow around current zero. The apparatus used to do this was the Kistler sensor/charge amplifier combination described in Chapter 4 and was fitted into the expansion volume via a screw bracket. In each case, 10g of polymer were applied to the volume prior to an ac arc being formed at 2.5kA, 4kA, 6kA and 10kA. The pressurisation of the expansion volume with a range of polymers is shown in Figure 7-12.

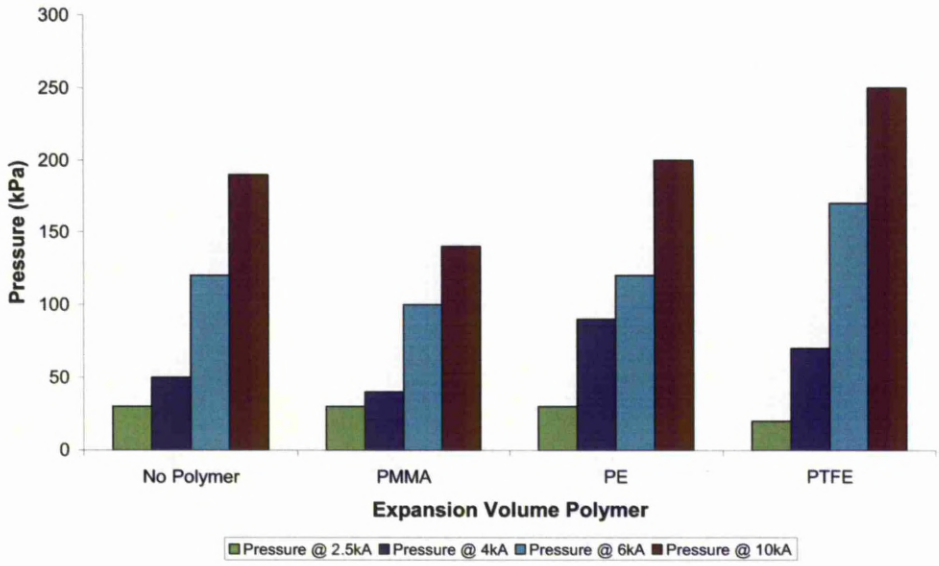

Figure 7-12: Expansion volume pressurisation with polymer particles

At 2.5kA there was no significant difference between polymeric and non-polymeric arcs, possibly because the arc energy was too low to proximally ablate the polymers in the expansion volume. At 4kA, the presence of polyethylene in the expansion volume causes an increase in pressure with respect to the no-polymer case, which subsequently led to greater gas flow at the period of current zero. At higher currents, PTFE enhances the pressurisation effect to the greatest extent, which is in contrast to the experiments where PTFE was ablated directly by the arc. Polymethylmethacrylate causes a reduction in pressure with respect to the no polymer case. This could be due to the absorption of energy without significant ablation or pressurisation, which was a characteristics of PMMA noted in the fundamental investigation.

The initial stages of this operational investigation show that the polymer effect can be utilised in full scale circuit breakers at high current. Further development is needed to as to develop practices to best exploit the polymer reaction in this environment.

7.8 SUMMARY

Experimentation has shown that polymers are able to act as arc quenching media in circuit breakers due to their ability to rapidly increase arc resistance by cooling the plasma via energy extraction due to the polymer change of state, decomposition, and the influence of turbulent flow on the arc.

Different types of polymer powders display differing characteristics, both in terms of quenching efficiency and mechanism. The fluoropolymer PTFE and vinyl polymers PS and PVC utilised energy extraction and direct arc cooling to accomplish interruption. In contrast, the polyolefin PE utilised pressurisation and strong gas flow to affect energy extraction by forced convection.

Further development has taken place to incorporate polymeric-quenching in a novel self-blast unit on a high current test rig at the University of Liverpool. To date, experimentation has found that the inclusion of polymer micro-particles enhances the interruption effect, particularly the low current performance of the device. Further operational tests are currently taking place to further develop the concept operationally.

Chapter 8
Conclusion

CHAPTER 8 - CONCLUSION

8.1 FOUNDATIONS

Climate change is an issue that in recent years has gained a large amount of interest with the public, media and politically. The release of greenhouse gasses contributes to climate change by altering the net input and output of solar radiation into the Earths atmosphere.

Sulphur hexafluoride is an extremely potent greenhouse gas that has a global warming potential tens thousands of times higher than that of carbon dioxide and a lifetime in the atmosphere of over three thousand years. The release of sulphur hexafluoride gas is an increasingly important concern to the power industry, not least due to growing political interest and legislation. Existing schemes to mitigate the losses of SF_6 from electrical transmission and distribution apparatus by utilising leak detection and repair have only been partially successful. Research has shown the level of SF_6 in the atmosphere currently increases at a rate of 5% per year [190], a reduction from 7% in 1992 [191]. Therefore, the best way in which to eradicate emissions of SF_6 from switchgear is to replace it altogether; however no viable alternatives currently exist.

The aim of this research was to play a part in the medium to long-term development of switchgear that operates free of SF_6. The project used practical experimentation in conjunction with a number of diagnostic systems to understand the fundamental interaction between polymer micro-particles and circuit breaker arc plasmas. The research was important in the development of a foundation of knowledge and experience that would allow the polymeric arc quenching phenomena to be developed.

8.2 EXPERIMENTAL RESULTS – MAIN CONCLUSION

The plasma-polymer interaction has been found to be highly complex, a number of inter-related processes occur that dissipate energy from the discharge and enable interruption. The results suggest that the more successful polymer quenchers were those that were able to rapidly and efficiently extract thermal energy from the arc, thereby reducing conductivity. The main polymer interaction mechanisms responsible for quenching have been found to be: energy extraction by ablation and decomposition; pressurisation and turbulence leading to increased convection; favourable changes in thermal and/or electrical conductivity of the gas around the arc; and the beneficial thermodynamics of chemical reactions between ablated gas species.

The structure and composition of polymers is an influential factor that affects their quenching efficiency. Polymers containing halogenated constituents dissociate in the arc leading to an electronegative gaseous environment of atoms and molecules that aids in interruption and dielectric recovery. It has also been found that polymers with a greater degree of polymerisation and cross-linking extract more energy in their change of state and cool the arc to a greater degree, increasing its resistance.

In all cases the most volumetrically abundant gaseous species formed as a result of the polymer-plasma interaction was carbon dioxide. This was formed as a result of the combustion of volatile hydrocarbon fragments that were formed by polymer decomposition; certain types of polymers inhibited combustion by virtue of their composition (halogens inhibit radical mechanism) and structure (higher melting points resist combustion). The quenching effect from CO_2 formation was mixed. The exothermic reactions in its formation reduced the efficiency of the temperature gradient between the arc and the surrounding gas, making cooling less effective. On the other hand, the presence of CO_2 around the electrode gap is a positive quenching factor given its increased thermal conductivity over air. This property of CO_2 has led to the development of circuit breakers that use CO_2 as a quenching medium [192].

Pressurisation and turbulence caused by the polymer-arc interaction was found to increase gas flow around the arc leading to improved convective cooling and de-ionisation performance. The increase in resistance could also be due to morphological changes of the plasma as a result of violent reactions between the plasma and polymer causing changes in arc length and shape, turbulence could also add to convection losses and cool gas intermixing, and has been previously considered in some research as being a significant process in arc extinction [129]. This could be further enhanced by the used of nozzling arrangements.

Tests utilising a novel self-blast interrupter in conjunction with polymer particulates has shown enhanced interruption capabilities. This ongoing development is part of the next phase of progression that will bring the principle into an operational environment; the underlying fundamental concepts developed in this investigation enable better exploitation of the polymeric quenching effect.

8.3 FUTURE WORK

The future work necessary so as to develop this concept further can be broadly divided into three categories: further development of fundamental concepts; practical research and development; and operational evaluation.

8.3.1 DEVELOPING FUNDAMENTAL CONCEPTS

To develop a deeper understanding of some of the main arc quenching mechanisms established during experimentation and to address any limitations of experimental tests, computational modelling can be used. Computer modelling cannot truly replicate reality but when used in conjunction with experimental observations it can be a powerful tool that allows the development of a deeper understanding of some of the key mechanisms involved in polymeric arc quenching.

A certain amount of computer modelling has already been carried out but the results are not in an advanced enough state to be included here. Electrostatic modelling using finite element analysis is being used to study the affect polymer powders have on the electric field between circuit breaker electrodes. Preliminary testing has shown that the presence of polymers in the electrode gap can have a depleting effect on the field. If those particles gain an electric charge, which has been shown to occur on solid walls in previous research [193, 194] then the effect is further enhanced. To develop a more detailed understanding of the chemical composition around the arc, simulations using the minimisation of the Gibbs free energy can be used. This technique has been utilised in other contexts [195, 196] and has been applied in this case because it addresses some of the inherent limitations of mass spectrometry related to the complex chemical reactions the occurred around the arc coupled with the mass spectrometer latency and fragmentation processes. Initial simulations carried out using this technique with polymer compositions at a range of arc temperatures have shown a complex mixture of low molecular weight hydrocarbons, which supports the mass spectral observations made, but requires further investigation. The pressure rises that occurred was a notable effect and can be modelled using computational fluid dynamics, which can also take into account the effect of polymer vapour on arc temperature. Computationally, it would be desirable to perform simulations of these effects and test the influence of different geometries on arc temperature. This would allow the effects to be tested and potentially optimised before more laborious practical tests.

8.3.2 PRACTICAL RESEARCH AND DEVELOPMENT

The second aspect of the further development methodology involves practically oriented studies with the intention of developing the best means of utilising particulate polymers in circuit breakers. This should involve studies into deployment methodologies, axial and radial polymer flow evaluation, and testing of the most effective host gasses, injection pressures and volumes.

In conjunction with CFD modelling, the most efficient nozzling arrangements should be researched with the aim of maximising the polymer induced gas flow conditions and hence maximising the convective cooling and de-ionisation processes.

Currently, the use of polymer micro-particles for enhancing the performance of self-blast type circuit breakers is being carried out. When the circuit approaches current zero, the expansion volume de-pressurises by flowing out and across the arc, aiding in thermal energy extraction and interruption. Polymer-induced pressurisation enhances interruption performance due to ablated polymer properties and increased pressurisation.

8.3.3 OPERATIONAL EVALUATION

The development of fundamental concepts in this research is the first stage that ultimately leads towards the design of prototype devices that could be used for research and evaluation in simulated operational conditions. By utilising the results obtained, the most efficient means of deploying polymers in circuit breakers can be developed so as to achieve arc quenching. With that, the objective is to ultimately form an interrupter design that is capable of acting as a replacement for SF_6 gas but without the environmental issues.

References

References

[1] United Nations; 'Kyoto Protocol to the United Nations Framework Convention on Climate Change'; United Nations Framework Convention on Climate Change; 1998

[2] World Nuclear Association (WNO); 'Averting the Danger of Catastrophic Climate Change: Is the Nuclear Renaissance Essential'; World Nuclear Association Century Outlook Report; 2008

[3] D.J. Telfer, J. Humphries, J.W. Spencer, GR Jones; 'Influence of PTFE on Arc Quality Using an Experimental Self Pressurised Circuit Breaker'; Proceedings from the XV International Conference on Gas Discharges and their Applications (GD2002), Volume 1; 2002

[4] IPCC; '16 Years of Scientific Assessment in Support of the Climate Convention'; Intergovernmental Panel on Climate Change; 2004

[5] Trenberth, K.E., P.D. Jones, P. Ambenje, R. Bojariu, D. Easterling, A. Klein Tank, D. Parker, F. Rahimzadeh, J.A. Renwick, M. Rusticucci, B. Soden and P. Zhai; 'Observations: Surface and Atmospheric Climate Change. In: Climate Change 2007: The Physical Science Basis. Contribution of Working Group I to the Fourth Assessment Report of the Intergovernmental Panel on Climate Change'; Cambridge University Press, Cambridge, United Kingdom and New York, NY, USA; 2007

[6] A.P.M. Baede; 'Climate Change 2007 – The Physical Science Basis – Annex I Glossary'; Cambridge University Press; p941-954; 2007

[7] V. Ramaswamy, O. Boucher, J. Haigh, D. Hauglustaine, J. Haywood, G. Myhre, T. Nakajima, G.Y. Shi, S. Solomon; 'Radiative Forcing of Climate Change' in 'Climate Change 2001: The Scientific Basis Contribution of Working Group I to the Third Assessment Report of the Intergovernmental Panel on Climate Change'; Cambridge University Press, Cambridge, United Kingdom and New York; 2001

[8] J.T. Hougton, L.G. Meiro Filho, B.A. Callander, N. Harris, A. Kattenburg, K. Maskell; 'Climate Change 1995: The Science of Climate Change: Contribution of Working Group I to the Second Assessment Report of the Intergovernmental Panel on Climate Change'; Cambridge University Press, Cambridge, United Kingdom and New York, NY, USA; 1996

[9] I.S.A. Isaksen, V. Ramaswamy, H. Rodhe, T.M.L. Wigley; 'Radiative Forcing of Climate Change'; Climate Change 1992: The Supplementary Report to the IPCC Scientific Assessment; Cambridge University Press; p47-68; 1992

[10] Massachusetts Institute of Technology Joint Program on the Science and Policy of Climate Change; 'Climate Policy Note 1: A Caution about Global Warming Potentials (GWPs)'; http://web.mit.edu/globalchange/www/pn1.html; Accessed: 14/10/08

[11] D.A. Lashof, D.R. Ahuja; 'Relative Contributions of Greenhouse Gas Emissions to Global Warming'; Nature; Volume 344; p529-531; 1990

[12] S.J. Smith, T.M.L Wigley; 'Global Warming Potentials: 1. Climactic Implications of Emissions Reductions'; Climate Change; Volume ; 2000

[13] D.A. Fisher, C.H. Hales, W.C. Wang, M.K.W. Ko, N.D. Sze; 'Model Calculations of the Releative Effects of CFCs and their Replacements on Global Warming'; Nature; Volume 344; p513-516; 1990

[14] B.C. O'Neill, M. Oppenheimer, S.R. Gaffin; 'Measuring Time in the Greenhouse'; Climate Change; Volume 37; p491-503; 1997

[15] European Database for Global Atmospheric Research (EDGAR); 'Major Trends in SF6 Emissions from 1970 to 2005'; European Commission; 2009

[16] A.R. Ravishankara, S. Solomon, A.A. Turnipseed, R.F. Warren; 'Atmospheric Lifetimes of Long-Lived Halogenated Species'; Science Magazine; Volume 259; p194-198; 1993

[17] J.T. Hougton, L.G. Meiro Filho, B.A. Callander, N. Harris, A. Kattenburg, K. Maskell; 'Climate Change 1995: The Science of Climate Change: Contribution of Working Group I to the Second Assessment Report of the Intergovernmental Panel on Climate Change'; Cambridge University Press, Cambridge, United Kingdom and New York, NY, USA; 1996

[18] P. K. Patra, S. Lal, B. H. Subbaraya, C.H. Jackman, P. Rajaratnam; 'Observed Vertical Profile of Sulphur Hexafluoride (SF_6) and its Atmospheric Applications'; Journal of Geophysical Research; Volume 102; Issue D7; p8855-8860; 1997

[19] G.J.M. Velders and S. Madronich (Lead Authors); *Chapter 2 Chemical and Radiative Effects of Halocarbons and Their Replacement Compounds* in *Safeguarding the Ozone Layer and Global Climate System;* IPCC/TEAP Special Report; 2005

[20] United Nations; 'Kyoto Protocol to the United Nations Framework Convention on Climate Change'; United Nations Framework Convention on Climate Change; 1998

[21] P. Horrocks; 'EU Proposed Legislation on Fluorinated Greenhouse Gases, The Case of SF_6'; European Commission, Environment Directorate; European Commission; 2004

[22] European Climate Change Program; 'Fluorinated Gases Working Group Report to the ECCP'; European Commission; 2003

[23] L. Niemeyer, F.Y. Chu; 'SF_6 and the Atmosphere'; IEEE Transactions on Electrical Insulation; Volume 27; No. 1; 1992

[24] C.J. Jones; 'Current Activity of CIGRE Working Group 23-10 – Metal Enclosed Substations'; IEE Colloquium on Gas Insulated Switchgear at Transmission and Distribution Voltages; 1995

[25] N. Bernard, S. Theoleyre, G. Valentin; 'How to use a Greenhouse Effect Gas while being Environmentally Friendly: SF_6 Case in Medium Voltage Distribution'; CIRED2001; IEE Conference Publication No. 482; 2001

[26] J-L. Bessede, W. Krondorfer; 'Impact of High-Voltage SF_6 Circuit Breakers on Global Warming – Relative Contribution of SF_6 Losses'; Environmental Protection Agency, San Antonio; 2006

[27] M. Maiss and I. Levin; 'Global Increase of SF_6 Observed in the Atmosphere'; Geophysical Research Letters, Vol. 21, No. 7; 1994; pp569-572

[28] United States Environmental Protection Agency; 'SF_6 Emission Reduction Partnership for Electric Power Systems'; Environmental Protection Agency Report; 2005

[29] J. Blackman; 'International Conference on SF_6 and the Environment: Electric Power Systems – Partnership Update'; 4th International Conference on SF_6 and the Environment; 2006

[30] P. Di Lillo; 'SF_6 Leak Detection and Mitigation Techniques'; Conference Presentation; 4th International Conference on SF_6 and the Environment; 2006

[31] M. Hinnrichs, P. Burke, V. Steinman, S. Moore and D. Ninedorf; 'Sherlock SF_6 Gas Imaging and Analysis Video Camera Tested at PG&E Facilities in California'; EPRI Substation Equipment Diagnostics Conference XV; 2008

[32] Ion Science Advanced Gas Sensing Technologies; *SF6 GasCheck P1 – Technical Brochure*; Ion Science; 2003

[33] National Grid United Kingdom Plc; 'Sulphur Hexafluoride'; http://www.nationalgrid.com/corporate/Our+Responsibility/Reporting+our+Performance/Environment/Sulphurhexafluoride/; Accessed: 20/10/08

[34] United Kingdom National Atmospheric Emissions Inventory; 'SF_6 Emissions Summary Data'; UK AEA; http://www.naei.org.uk/pollutantdetail.php?poll_id=26; Accessed: 15/05/09

[35] United Kingdom National Atmospheric Emissions Inventory; 'SF_6 Emissions Summary Data'; UK AEA; http://www.naei.org.uk/pollutantdetail.php?poll_id=26; Accessed: 15/05/09

[36] P. Glaubitz, F. Ploeger; 'Obtaining Low SF_6 Emissions in Germany'; Conference Presentation; 4th International Conference on SF_6 and the Environment; 2006

[37] S. Eggleston, L. Buendia, K. Miwa, T. Ngara, K. Tanabe (editors); '2006 IPCC Guidelines for National Greenhouse Gas Inventories: Volume 1 – General Guidance and Reporting'; IGES, Japan; 2006

[38] C. Cheng; 'National Policies and Programs for Climate Protection in China'; Conference Presentation; 4th International Conference on SF_6 and the Environment; 2006

[39] C. Cheng; 'SF_6 Production, Future Demand and Cooperation in China'; Conference Presentation; 4th International Conference on SF_6 and the Environment; 2006

[40] A. Pankowski; 'Improving SF_6 Management in Australia'; Conference Presentation; 4th International Conference on SF_6 and the Environment; 2006

[41] L.G. Christophorou, J.K. Olthoff, D.S. Green; 'Gases for Electrical Insulation and Arc Interruption: Possible Present and Future Alternatives to Pure SF_6'; National Institute of Standards and Technology (NIST); Techical Note 1425; 1998

[42] Y. Tanaka, T. Sakuta; 'Investigation on Plasma Quenching Efficiency of Various Gasses Using the Inductively Coupled Thermal Plasma Technique: Effect of Various Gas Injection on Ar Thermal ICP'; Journal of Physics D: Applied Physics; Volume 35; p2149-2158; 2002

[43] L.G. Christophorou and J.K. Olthoff; *Fundamental Electron Interactions with Plasma Processing Gasses*'; Springer; 2003

[44] Y.Y. Duan, L. Shi, M.S. Zhu and L.Z. Han; 'Thermodynamic Properties of Trifluoroiodomethane (CF3I)'; International Journal of Thermophysics, Vol. 21, No. 2; 2000; pp. 393 - 404

[45] H. Katagiri, H. Kasuya, H. Mizoguchi, S. Yanabu; 'BTF Interrupting Capability of CF_3I-CO_2 Mixture'; XVII International Conference on Gas Discharges and Their Applications; 2008

[46] J.C. Devins; 'Replacement Gases for SF_6'; IEEE Transactions on Electrical Insulation; Volume EI-15; No. 2; 1980

[47] M. Homma, M. Sakaki, E. Kaneko, S.Yanabu; 'History of Vacuum Circuit Breakers and Recent Developments in Japan'; IEEE Transactions on Dielectrics and Electrical Insulation; Volume 13; No. 1; 2006

[48] T. Takahshi, T. Kituta, R. Nakanishi, A. Hirakawa; '168kV Class Vacuum Circuit Breakers'; Meiden Rev.; No. 56; p9-26; 1979

[49] J. Wang; '126kV Vacuum Circuit Breaker Debuted in China'; XXII International Symposium on Discharges and Electrical Insulation in Vacuum; 2006

[50] K. Nagatake, S. Akiyama, H. Ichikawa, M. Sakaki, T. Fukai, M. Homma; 'Development of Environmentally Benign Type 72/84kV Vacuum Circuit Breaker'; Proc. 14th Annual Conference of the IEE Power & Energy Society; IEEJ; 2003

[51] S. Yanabu, S. Arai, Y. Kawaguchi, T. Kawamura; 'New Concept of Switchgear for Replacing SF_6 Gas or Gas Mixture'; Gaseous Dielectrics IX, Plenum Publishers New York; p497-504; 2001

[52] D.J. Telfer, J. Humphries, J.W. Spencer, GR Jones; 'Influence of PTFE on Arc Quality Using an Experimental Self Pressurised Circuit Breaker'; Proceedings from the XV International Conference on Gas Discharges and their Applications (GD2002), Volume 1; 2002

[53] D.J. Telfer, J.W. Spencer, G.R. Jones, J.E. Humphries; 'A Novel Approach to Power Circuit Breaker Design for Replacement of SF_6'; Acta Polytechnica; Volume 44; No. 2; 2004

[54] M. Seeger, J. Tepper, T. Christsen, J. Abrahamson; 'Experimental Study on PTFE Ablation in High Voltage Circuit-Breakers'; Journal of Physics D: Applied Physics; Volume 39; p5016-5024; 2006

[55] J.J. Shea; 'The Influence of Arc Chamber Wall Material on Arc Gap Dielectric Recovery Voltage'; IEEE Transactions on Components and Packaging Technologies; Volume 24; Issue 3; p342-348; 2001

[56] P. Andre; 'Composition and Thermodynamic Properties of Ablated Vapours of PMMA, PA6-6, PETP, POM and PE'; Journal of Physics D: Applied Physics; Volume 29; p1963-1972; 1996

[57] P. Kovitya; 'Thermodynamic and Transport Properties of Ablated Vapors of PTFE, Alumina, Perspex and PVC in the Temperature Range 5000-30000K'; IEEE Transactions on Plasma Science; Volume PS-12; No. 1; 1984

[58] Y. Tanaka, T. Numada, S. Kaneko, S. Okabe; 'Thermodynamic and Transport Properties of Ar Thermal Plasmas with Polymer Ablated Vapors and Influence of their Inclusions on Plasma Temperature'; JSME International Journal; Series B, Volume 48; No. 3; 2005

[59] J.Slepain and C.L.Denault; 'The Expulsion Fuse'; AIEE Transactions, Vol. 51; 1932; p157

[60] R.F. Wolff; 'Surge Protection and Fusing'; Electrical World; p67-68; 1979

[61] P.F. Hettwer; 'Arc Interruption and Gas Evolution Characteristics of Common Polymeric Materials'; IEEE Transactions on Power Apparatus and Systems; Volume PAS-101; No. 6; 1982

[62] J.J. Shea; 'Effect of Polymeric Gassing Walls During Arcing on AgW/AgC Contact Resistance'; Proceedings of the 45th IEEE Holm Conference on Electrical Contacts; p94-99; 1999

[63] H. Takikawa, T. Sakakibara; 'Radiative Aspects of the Ablation-Stabalized Arc on Polyethylene Tube'; IEEE Transactions on Plasma Science; Volume 19; No. 5; 1991

[64] E.Z. Ibrahim; 'The Ablation Dominated Polymethylmethacrylate Arc'; Institute of Physics, J.Phys. D: Applied Physics; Volume 13; p2045-2065; 1980

[65] H. Takikawa, T. Sakakibara, Y. Kito; 'Electrical Field Strength and Radiation Power of the Arc Burning through a Cylindrical Polyethylene Tube'; Transactions IEE Japan; Volume 106-A; p588-594; 1986

[66] H. Takikawa, T. Sakakibara; 'Radiative Aspects of the Ablation-Stabalized Arc on Polyethylene Tube'; IEEE Transactions on Plasma Science; Volume 19; No. 5; 1991

[67] C. Wang, Y. Tanaka, T. Sakuta; 'Modelling of Ar Induction Thermal Plasma with an Injection of PTFE Powder'; IEEJ Transactions on PE; Volume 124; No. 3; p440-446; 2004

[68] Y. Tanaka, T. Numada, Y. Uesugi, S. Kaneko, S. Okabe; 'Influence of Polymer Vapor Concentration on Temperature of Ar Induction Thermal Plasmas during Polymer Solid Powder Injections'; IEEJ Transactions on PE; Volume 125; No. 11; p1077-1083; 2005

[69] Y. Tanaka, Y. Takeuchi, T. Sakuyama, Y. Uesugi, S. Kaneko, S. Okabe; 'Numerical and Experimental Investigations on Thermal Interaction between Thermal Plasma and Solid Polymer Powders using Induction Thermal Plasma Technique'; Journal of Physics D: Applied Physics; Volume 41; 2008

[70] H. Azuma, T. Narita, A. Takeuchi, N. Kamiya, T Ito, M. Kato, K. Tachi and T. Motohiro; 'Surface Treatment of Polymers by Simultaneous Exposure to VUV and Nanometer Sized Particles in Helium Atmosphere'; JLMN-Journal of Laser Micro/Nanoengineering Vol. 2, No. 2; 2007

[71] Pauling, L. (1932). "The Nature of the Chemical Bond. IV. The Energy of Single Bonds and the Relative Electronegativity of Atoms". *J. Am. Chem. Soc.* 54 (9): 3570–3582. doi:10.1021/ja01348a011.

[72] David R. Lide (ed), *CRC Handbook of Chemistry and Physics, 84th Edition*. CRC Press. Boca Raton, Florida, 2003; Section 9, Molecular Structure and Spectroscopy; Electronegativity

[73] M.S. Naidu and V. Kamaraju; *High Voltage Engineering (2nd Edition)*; McGraw-Hill; 1995; p26

[74] M.P. Reece; *Physics of Circuit Breaker Arcs* in C.H. Flurscheim (Ed.); *Power Circuit Breaker Theory and Design*; Peter Peregrinus Ltd./IEE; 1982; p48

[75] J.V.R. Heberlein, C.W. Kimblin and A. Lee; *Nature of the Electric* Arc in T.E. Browne; *Circuit Interruption;* Marcel Dekker Inc.; 1984; p141

[76] Y. Yoshioka, K. Hirasawa, Y. Kurosawa, M. Tsukushi and Y. Oshita; *Overview* in K. Nakanishi (Ed.); *Switching Phenomena in High-Voltage Circuit Breakers*; Marcel Dekker Inc.; 1991; p8

[77] C.H. Flurscheim; *Development of Circuit Breakers* in C.H. Flurscheim (Ed.); *Power Circuit Breaker Theory and Design*; Peter Peregrinus Ltd./IEE; 1982; p2

[78] B. Andersen and C. Barker; 'A New Era in HVDC'; IEE Review; 2000; pp33-39

[79] A. Ekstrom, H. Hartel, H.P. Lips, W. Schultz, P. Joss, H. Holfeld and Q. Kind; 'Design and Testing of an HVDC Circuit-Breaker'; CIGRE Report 13-06; 1976

[80] M. Sakai, Y. Kato, S. Tokuyana, H. Sugawara and K. Arimatsu; 'Development and Field Application of Metallic Return Protecting Breaker for HVDC Transmission'; IEEE Transactions on Power Apparatus Systems (PAS-100); 1981; pp4860-4868

[81] A.N. Greenwood, P. Barkan and W.C. Kracht; 'HVDC Vacuum Circuit Breaker'; IEEE Transactions on Power Apparatus Systems (PAS-91); 1972; pp1575-1588

[82] A.L. Courts, J.J. Vithayathil, N.G. Hingorani, J.W. Porter, J.G. Gorman and C.W. Kimblin; 'A New Dc Breaker used as Metallic Return Transfer Breaker'; IEEE Transactions on Power Apparatus Systems (PAS-101); 1982; pp4112-4121

[83] A. Lee, J.E. Heidrich and L.S. Frost; 'A HVDC Breaker Concept based on SF_6 Puffer Technology'; 7th International Conference on Gas Discharges and their Appliactions; 1982

[84] M. Kleman, 1907, us. Patent 874,601

[85] J. Biermanns; 'High Power Circuit Breakers without Oil (Hochleistungschalter ohne Oel)'; Elektrotech Z 1929-2; 1938; pp. 1114-1119

[86] D.F. Amer; *Oil Circuit* Breakers in T.E. Browne; *Circuit Interruption – Theory and Techniques*; Marcel Dekker Inc.; 1984

[87] Environmental Protection Agency; 'Polychlorinated Biphenyl Inspection Manual'; Environmental Protection Agency Document EPA-305-X-04-002; 2004

[88] J.S. Stewart; 'Changes in Switchgear Design – A Manufacturers Experience'; IEE Colloquium in an update in SF_6 and Vacuum Switchgear at Distribution Levels'; 1996; pp. 3/1 – 3/40

[89] S.M. Gonek; *Air Blast Circuit Breakers* in C.H. Flurscheim (Ed.); *Power Circuit Breaker Theory and Design*; Peter Peregrinus Ltd./IEE; 1982; pp. 235-302

[90] W.B. Whitney, E.B. Wedmore; 'Improvements in or Relating to Electric Circuit-Breakers'; GB Patent No. 278764; 1927

[91] H. Kuwahara, Y. Yoshioka, Y. Kurosawa, K. Hirasawa, S. Yanabu and E. Kaneko; *Recent Developments in Circuit* Breakers in K. Nakanishi (Ed.); *Switching Phenomena in High-Voltage Circuit Breakers*; Marcel Dekker Inc.; 1991; p119

[92] M.S. Naidu and V. Kamaraju; *High Voltage Engineering (2nd Edition)*; McGraw-Hill; 1995; p35

[93] R.W. Sorensen and H.E. Mendenhall; 'Vacuum Switching Experiments at California Institute of Technology'; Transactions of AII, No. 45; p1102-1105; 1926

[94] H. Okummura and E. Kaneko; 'Recently Developed Vacuum Interrupter Construction and Performance Improvement'; Toshiba review No. 141; p5-10; 1982

[95] H. Kuwahara, Y. Yoshioka, Y. Kurosawa, K. Hirasawa, S. Yanabu and E. Kaneko; *Recent Developments in Circuit* Breakers in K. Nakanishi (Ed.); *Switching Phenomena in High-Voltage Circuit Breakers*; Marcel Dekker Inc.; 1991; p119

[96] P. Klasson; *Nobel Lectures, Chemistry 1901-1921*; Elsevier Publishing Company; 1966

[97] United States Environmental Protection Agency; SF_6 Emission Reduction Partnership for Electric Power systems; Environmental Protection Agency Report; 2005

[98] H.J. Lingal, A.P. Strom and T.E. Browne; An Investigation into the Arc Quenching Behavior of Sulphur Hexafluoride; AIEE Transactions 72 (III); 1953; pp242-246

[99] Air Liquide; Gas Encyclopaedia – Sulphur Hexafluoride; http://encyclopedia.airliquide.com/Encyclopedia.asp?GasID=34; Accessed 15/05/07

[100] D.J. Telfer, J.W. Spencer, G.R. Jones and J.E. Humphries; 'A Novel Approach to Power Circuit Breaker Design for Replacement of SF_6'; Acta Polytechnica Vol. 44, No. 2/2004; 2004

[101] E. Maggi and C.A. Fawdrey; *SF_6 Circuit Breakers* in C.H. Flurscheim (Ed.); *Power Circuit Breaker Theory and Design*; Peter Peregrinus Ltd./IEE; 1982; p304

[102] C.F. Cromer and R.E. Freidrich; 'A New 115kV, 1000MVA Gas Filled Circuit Breaker; AIEE Transactions 75 (III); 1956; pp1352-1357

[103] R.E. Friedrich and R.N. Yeckley; 'A New concept in Power Circuit Breaker Design Utilizing SF_6'; AIEE Transactions 78 (III); 1959; pp695-706

[104] R.E. Friedrich; *SF_6 Breaker Research and Development* in T.E. Browne; *Circuit Interruption – Theory and Techniques*; Marcel Dekker Inc.; 1984

[105] Westinghouse, United States Patent, 1953

[106] H. Kuwahara, T. Yamauchi, Y. Yoshioka, Y. Kurosawa, K. Hirasawa, S. Yanabu and E. Kaneko; *Recent Developments in Circuit Breakers* in k. Nakanishi (Ed.); *Switching Phenomena in High-Voltage Circuit Breakers*; Marcel Dekker Inc.; 1991; p123

[107] [209] K. Young; *Development of a High Voltage Rotating Arc Interrupter*; PhD Thesis, University of Liverpool; 2005

[108] U. Fantz; 'Basics of Plasma Spectroscopy'; Institute of Physics Plasma Sources Sci. Technol. 15; 2006; pS137-S147

[109] R. Kozakov, M. Kettlitz, K.D. Weltmann, A. Steffens and C.M. Franck; 'Temperature Profiles of an Ablation Controlled Arc in PTFE: I. Spectroscopic Measurements'; Journal of Physics D: Applied Physics Vol. 40; 2007; pp2499-2506

[110] A. Fridman and L.A. Kennedy; *Plasma Physics and Engineering*; Taylor & Francis; 2004

[111] H.R. Greim; *Plasma Spectroscopy;* McGraw-Hill Book Company; 1964; pp267-295

[112] J. Reader and C.H. Corliss; *Section 10 - Line Spectra of the Elements* in *CRC Handbook of Chemistry and Physics 84th Edition;* CRC Press 2003; 10/1 – 10/87

[113] J.W. Spencer, A. Deakin and G.R. Jones; 'Monitoring of Complex Systems'; Proceedings of the XVII International Conference on Gas Discharges and Their Applications; 2008

[114] G.R. Jones, A.G. Deakin and J.W. Spencer, *Chromatic Monitoring of Complex Conditions*, Taylor and Francis, 2008

[115] P.J. Flory and A.J. Vrij; 'Melting Points of Linear Chain Holologs – The Normal Parrafin Hydrocarbons'; Journal of the American Chemical Society, Vol. 85, No. 4; 1963; pp. 3548-3553

[116] W. Martienssen and H. Warlimont (Eds.); *Springer Handbook of Condensed Matter and Materials Data;* Springer; 2005; pp480-501

[117] J.E. Mark (Editor); *Polymer Data Handbook*; Oxford University Press, Inc; 1999

[118] Tektronix; 'Passive High Voltage Probes – P5100, P5102, P5120, P6015A'; Tektronix Data Sheet 56W-10262-2; 2004

[119] Stellarnet; 'EPP2000 Diffraction Grating Spectrometers'; Stellarnet Data Sheet; 2006

[120] J. Reader and C.H. Corliss; *Section 10 - Line Spectra of the Elements* in *CRC Handbook of Chemistry and Physics 84th Edition;* CRC Press 2003; 10/1 – 10/87

[121] MKS Instruments; 'MKS Cirrus^{TM} Benchtop Gas Analyer'; MKS Instruments Data Sheet; 2004

[122] T. Uchii, Y. Hoshina, T. Mori, H. Kawano, T. Nakamoto and H. Mizogushi; *Investigations on SF_6 Free Gas Circuit Breaker Adopting CO_2 Gas an an Alternative Arc-Quenching and Insulating Medium* in L.G. Christophorou and J. Kenneth; *Gaseous Dielectrics X*; Springer; 2005; pp205-210

[123] Y. Kazuma, Y. Yasunobu, M. Toshiro and S. Masatoyo; 'Interuption Tests of a Two Pressure Type of Circuit Breaker Filled with CO_2 at 0.5MPa under Short Line Fault Condictions'; IEEJ Papers of Technical Meeting on Electrical Discharges, Vol. 03, No. 70; 2003; pp23-27

[124] T. Matsumara, I. Morookaa, Y. Yokomizua and M. Suzukia; 'Arc Parameters in CO_2-Blast Quenching Chamber with a High Pressure Storage Tank'; Proceedings of the 5th International Symposium on Applied Plasma Science, Vol. 80, Iss. 11-12; 2006; pp26-30

[125] L.G. Christophorou and J. Kenneth; *Gaseous Dielectrics X*; Springer; 2005; pp205-210

[126] J.J. Lowke; Chapter *5 – Physical Theory of the Arc in a Gas Blast* in T.E. Browne; *Circuit Interruption – Theory and Techniques*; Marcel Dekker Inc.; 1984; pp157-160

[127] Y. Yoshioka and K. Hirasawa; *High Voltage Direct Current Circuit Breakers* in K. Nakanishi (Ed.); *Switching Phenomena in High Voltage Circuit Breakers;* CRC Press; 1991; pp164

[128] S. Xiu, Y. Cheng and R. Zhang; 'Experimental Investigation of a Vacuum Arc Characteristic under Axial Meagnetic Field'; Institute of Physics Journal of Physics D: Applied Physics, Vol. 41; 2008

[129] H. Hermann and K. Ragaller; 'Theoretical Description of the Current Interruption in Gas Blast Breakers'; Trans. IEEE Power Appar. Syst.' PAS-96:1546-1555; 1977

[130] E. Maggi and C.A. Fawdrey; *SF_6 Circuit Breakers* in C.H. Flursheim (Ed.) *Power Circuit Breaker Theory and Design*; Peter Peregrinous/IEE; 1982

[131] T. Uchii, Y. Hoshina, T. Mori, H. Kawano, T. Nakamoto and H. Mizogushi; *Investigations on SF_6 Free Gas Circuit Breaker Adopting CO_2 Gas an an Alternative Arc-Quenching and Insulating Medium* in L.G. Christophorou and J. Kenneth; *Gaseous Dielectrics X*; Springer; 2005; pp205-210

[132] L. Hewitson, M. Brown and R. Balakrishnan; *Practical Power System Protection*; Newnes; 2004

[133] A. Gleizes, A. Mahieddin-Rahal, S. Papadopoulos and S. Vacquie; 'Study of a Circuit Breaker Arc with Self-Generated Flow: Part II – The Flow Phase'; IEEE Transactions on Plasma Science, Vol. 16, No. 6; 1988; pp615 – 622

[134] D.C. Strachan; 'High Current Free Burning Graphite Arcs'; Proc. 12th Int. Conf. Phen. Ionised Gases; 1975; p150

[135] J.J. Lowke; 'Simple Theory of Free Burning Arcs'; Journal of Physics D: Applied Physics, Vol. 12; 1979; pp1873 – 1886

[136] D.C. Strachan, D. Ligate and G.R. Jones; 'Radiative Energy Losses from a High-Current Air Blast Arc'; Journal of Applied Physics, Vol. 48; 1977; pp2324 – 2330

[137] A. Gleizes, A. Mahieddin-Rahal, H. Delacroix and P. Van Doan; 'Study of a Circuit Breaker Arc with Self-Generated Flow: Part I – Energy Transfer in the High Current Phase'; IEEE Transactions on Plasma Science, Vol. 16, No. 6; 1988; pp606 – 614

[138] A. Gleizes, A. Mahieddin-Rahal, S. Papadopoulos and S. Vacquie; 'Study of a Circuit Breaker Arc with Self-Generated Flow: Part II – The Flow Phase'; IEEE Transactions on Plasma Science, Vol. 16, No. 6; 1988; pp615 – 622

[139] C. Luders, T. Suwanasri and R. Dommerque; 'Investigation of an SF_6 Self-Blast Circuit Breaker'; Journal of Physics D: Applied Physics, Vol. 39; 2006; pp666 – 672

[140] J.J. Shea; 'Effect of Polymeric Gassing Walls During Arcing on AgW/AgC Contact Resistance'; Proceedings of the 45th IEEE Holm Conference on Electrical Contacts; 1999; pp94 – 99

[141] L. Hewitson, M. Brown and R. Balakrishnan; *Practical Power System Protection*; Newnes; 2004

[142] B. Yotsombat, S. Davydov, P. Poolcharuansin, T. Vilaithong and I.G. Brown; 'Optical Emission Spectra of a Copper Plasma Produced by a Metal Vapour Vacuum Arc Plasma Source'; Institute of Physics, J.Phys. D: Applied Physics; Volume 34; p1928-1932; 2001

[143] J. Reader and C.H. Corliss; *Line spectra of the Elements* in D.R. Lide (Ed.) *CRC Handbook of Chemistry and Physics 84th Edition*; CRC Press 2003; pp10/1-10/81

[144] H.R. Greim; *Plasma Spectroscopy;* McGraw-Hill Book Company; 1964; pp267-279

[145] Y. Tanaka, T. Numada, Y. Uesugi, S. Kaneko, S. Okabe; 'Influence of Polymer Vapor Concentration on Temperature of Ar Induction Thermal Plasmas during Polymer Solid Powder Injections'; IEEJ Transactions on PE; Volume 125; No. 11; p1077-1083; 2005

[146] T. Uchii, Y. Hoshina, T. Mori, H. Kawano, T. Nakamoto and H. Mizogushi; *Investigations on SF_6 Free Gas Circuit Breaker Adopting CO_2 Gas an an Alternative Arc-Quenching and Insulating Medium* in L.G. Christophorou and J. Kenneth; *Gaseous Dielectrics X*; Springer; 2005; pp205-210

[147] J.R. Fuhr and W.L. Wiese; *NIST Atomic Transition Probability Tables* in D.R. Lide (Ed.) *CRC Handbook of Chemistry and Physics 84th Edition*; CRC Press 2003; pp10/1-10/81

[148] W. Lochte-Holtgreven; *Chapter 3 Evaluation of Plasma Parameters* in *Plasma Diagnostics*; North Holland Publishing Company; 1968

[149] Y. Sung and H.B. Lim; 'Plasma Temperature Measurement of a Low-Pressure Inductively Coupled Plasma using Spectroscopic Methods'; Royal Society of Chemistry, Journal of Analytical Atomic Spectrometry, Volume 18; pp 897-901; 2003

[150] O.E. Hankins, M.A. Bourham, J. Earnhart and J.G. Gilligan; 'Visible Light Emission Measurements from a Dense Electrothermal Launcher Plasma'; IEEE Transactions on Magnetics, Volume 29; pp1158-1161; 1993

[151] S. Gordon and J.M. McBride; 'Computer Program for Calculation of Complex Chemical Equilibrium Compositions, Rocket Performance, Incident and Reflected Shocks and Chapman-Jouguet Detonations'; NASA Special Publication SP-273; 1973; pp 4

[152] P. Andre; 'Composition and Thermodynamic Properties of Ablated Vapours of PMMA, PA6-6, PETP, POM and PE'; J. Phys. D: Applied Physics; Volume 29; p1963-1972; 1996

[153] P. Kovitya; 'Thermodynamic and Transport Properties of Ablated Vapors of PTFE, Alumina, Perspex and PVC in the Temperature Range 5000-30000K'; IEEE Transactions on Plasma Science; Volume PS-12; No. 1; 1984

[154] M.R. Wertheimer, L. Martinu, J.E. Klemberg-Sapieha and G. Czeremuszkin; *Adhesion Promotion Techniques in Advanced Technologies*; Marcel Dekker, New York; 1999; pp139

[155] E. Katoh, H. Sugimoto, Y. Kita and I. Ando; 'Structures of Polytetrafluoroethylene Oligomers as Studied by High-Resolution Solid-State ^{19}F NMR and their Properties'; Journal of Molecular Structure, Vol. 355, Issue 1; 1995; pp21-26

[156] J. Hong, F. Truica-Marasescu, L. Martinu and M.R. Wertheimer; 'An Investigation of Plasma-Polymer Interactions by Mass Spectrometry'; Plasmas and Polymers, Volume 7, Number 3; 2002; pp245-260

[157] J. A. Kerr; *Strengths of Chemical Bonds* in D.R. Lide (Ed.) *CRC Handbook of Chemistry and Physics 84th Edition*; CRC Press 2003; pp9/52-9/73

[158] C. Blondel, C. Delsart, C. Goldfarth; 'Electron Spectrometry at the μeV Level and the Electron Affinities'; Institue of Physics Journal of Physics B: Atomic, Molecular and Optical Physics, Vol. 34; 2001; pp. 281-288

[159] M. Scheer, R.C. Bilodeau, J. Thogresen, H.K. Haugen; 'Threshold Photodetachment of Al^-: Electron Affinity and Fine Structure'; Physical Review Letters, Vol. A57; 1998; 99. 1493-1496

[160] C.L. Pekeris; '1 ^1S, 2 ^1S, and 2 ^3S States of H^-'; Physical Review Letters, Vol. 126; 1962; pp. 1470-1476

[161] H. Hotop and W.C. Lineberger; 'Binding Energies in Atomic Negative Ions II'; Journal of Physical and Chemical Reference Data, Vol. 14; 1985; p731

[162] *CRC Handbook of Chemistry and Physics* (62nd Edn. (1981); Weast, Robert C. (ed)). Boca Raton, FL: CRC Press. "Section E, General Physical Constants; Electron Affinities".

[163] J.C. Devins and R.W. Crowe; 'Electric Strength of Saturated Hydrocarbon Gasses'; Journal of Chemical Physics, Vol. 25, No. 5; 1956

[164] A.E.D. Heylen, T.J. Lewis; 'The Electric Strength of Hydrocarbon Gasses'; British Journal of Applied Physics, Vol. 7; 1956

[165] David R. Lide (ed), *CRC Handbook of Chemistry and Physics, 84th Edition.* CRC Press. Boca Raton, Florida, 2003; Section 9, Molecular Structure and Spectroscopy; Electronegativity

[166] H. Sabuni and J.K. Nelson; 'The Electric Strength of Co-Polymers'; Journal of Materials Science, Vol. 12; 1977

[167] J. Bessede and W. Krondorfer; 'Impact of High Voltage SF_6 Circuit Breakers on Global Warming – Relative Contribution of SF_6 Losses'; United States Environmental Protection Agency (EPA);

[168] R. Meier, F.K. Kneubuhl, R. Coccioni, H. Wyss, E. Fischer and H.J. Schotzau; 'Investigations of Nozzle Materials in SF_6 Circuit Breakers'; IEEE Transactions on Plasma Science, Vol. PS-14, No. 4; 1986; pp. 390-394

[169] S. Stewart; *Distribution Switchgear*; Institution of Engineering and Technology; 2004

[170] Y. Tanaka, Y. Takeuchi, T. Sakuyama, Y. Uesugi, S. Kaneko, S. Okabe; 'Numerical and Experimental Investigations on Thermal Interaction between Thermal Plasma and Solid Polymer Powders using Induction Thermal Plasma Technique'; Journal of Physics D: Applied Physics; Volume 41; 2008

[171] L. Niemeyer; 'Evaporation Dominated High Current Arcs in Narrow Channels'; IEEE Transactions on Power Apparatus and Systems, Vol. PAS-97, No. 3; 1978; pp. 950-958

[172] Y. Tanaka, T. Numada, S. Kaneko, S. Okabe; 'Thermodynamic and Transport Properties of Ar Thermal Plasmas with Polymer Ablated Vapors and Influence of their Inclusions on Plasma Temperature'; JSME International Journal; Series B, Volume 48; No. 3; 2005

[173] Y. Tanaka; 'Two Temperature Chemically Non-Equilibrium Modelling of High Power Ar-N_2 Inductively Coupled Plasmas at Atmospheric Pressure'; Journal of Physics D: Applied Physics, Vol. 37; 2004; pp. 1190-1205

[174] P. Andre; 'The Influence of Graphite on the Composition and Thermodynamic Properties of Plasma Formed in Ablated Vapour of PMMA, PA6-6, PETP, POM and PE used in Circuit Breakers'; ; Institute of Physics, Journal of Physics D: Applied Physics, Vol. 30; 1997; pp. 475-493

[175] P. Andre; 'Composition and Thermodynamic Properties of Ablated Vapours of PMMA, PA6-6, PETP, POM and PE'; Journal of Physics D: Applied Physics; Volume 29; p1963-1972; 1996

[176] P. Kovitya; 'Thermodynamic and Transport Properties of Ablated Vapors of PTFE, Alumina, Perspex and PVC in the Temperature Range 5000-30000K'; IEEE Transactions on Plasma Science; Volume PS-12; No. 1; 1984

[177] K.H. Hormann and H.G. Wagner; Proceedings of the Royal Society: A; 1967

[178] D.R. Lander, K.G. Unfried, J.W. Stephens, G.P. Glass and R.F. Curl; 'Reaction Mechanism of $C_2H + O_2$'; American Chemical Society Journal of Physical Chemistry 93; 1989; pp4109 – 4116

[179] S.M. Lomakin, G.E. Zaikov; *Modern Polymer Flame Retardancy*; VSP Publishing; 2003

[180] Burge S.J. and Tipper C.F.H., *Combustion and Flame* 13, 495-505 (1969).

[181] Ritz W.J., Brown N.J., Sawyer R.F., *lBh International Symposium on Combustion,*pp.1871-1879 The combustion Institute, Pittsburgh (1981).

[182] J.W McBride; 'Arc Motion and Gas Flow in Current Limiting Circuit Breakers Operating with a Low Contact Switching Velocity'; IEEE Transactions on Components and Packaging Technologies, Vol. 25, No. 3; 2002; pp. 427-433

[183] T. Uchii, Y. Hoshina, T. Mori, H. Kawano, T. Nakamoto and H. Mizoguchi; '*Investigations into SF_6 Free Gas Circuit Breaker Adopting CO_2 Gas as an Alternative Arc Quenching and Insulating Medium*' in L.G. Christophorou and J.K. Olthoff; *Gaseous Dielectrics X*; Springer; 2004

[184] M. Abbaoui and B. Cheminat; 'Determination of the Characteristics of an Electric Arc Plasma Contaminated by Vapours from Insulators'; IEEE Transactions on Plasma Science, Vol. PS-15, No. 3; 1987; pp. 294-301

[185] P. Rodriguez, J. Didier, G. Bernard and S. Rowe; 'Arc Contact Insulating Wall Interactions in Low Voltage Circuit Breakers'; IEEE Transactions on Power Delivery, Vol. 13, No. 2; 1998; pp. 480-488

[186] J.J. Shea; 'The Influence of Arc Chamber Wall Material on Arc Gap Dielectric Recovery Voltage'; IEEE Transactions on Components and Packaging Technologies, Vol. 24; 2001; pp. 342-348

[187] J.J. Shea; 'Effect of Polymeric Gassing Walls during Arcing on AgW/AgC Contact Resistance'; Porceedings of the 45th IEEE Holm Conference on Electrical Contacts, Pittsburgh; 1999; pp. 94-99

[188] M. Seeger, J. Tepper, T. Christen and J. Abrahamson; 'Experimental Study on PTFE Ablation in High Voltage Circuit Breakers'; Institute of Physics, Journal of Physics D: Applied Physics, Vol. 39; 2006; pp. 5016-5024

[189] O.E. Hankins, M.A. Bourham, J. Earnhart and J.G. Gilligan; 'Visible Light Emission Measurements from a Dense Electrothermal Launcher Plasma'; IEEE Transactions on Magnetics, Volume 29; pp1158-1161; 1993

[190] G.J.M. Velders and S. Madronich (Lead Authors); *Chapter 2 Chemical and Radiative Effects of Halocarbons and Their Replacement Compounds* in *Safeguarding the Ozone Layer and Global Climate System;* IPCC/TEAP Special Report; 2005

[191] M. Maiss and I. Levin; 'Global Increase of SF_6 Observed in the Atmosphere'; Geophysical Research Letters, Vol. 21, No. 7; 1994; pp569-572

[192] U. Toshiyuki, H. Yoshikazu, M. Tadashi, K. Hiromichi and N. Tstsuya; 'Development of a 72kV Class Novel CO_2 Gas Circuit Breaker Model'; IEE Japan, Papers of Technical Meeting on Electrical Discharges; 2003

[193] W.D. Liu, J.W. Spencer, J.K. Wood, J.J. Chaaraoui and G.R. Jones; 'Effect of PTFE Dielectric Properties on High Voltage Reactor Load Switching'; IEE Proceedings – Science, Measurement and Technology, Vol. 143; No. 3; 1996; pp 195-200

[194] W.D. Liu, J. Chaaraoui, J.K. Wood, J.W. Spencer and G.R. Jones; 'Parasitic Arcing in EHV Circuit-Breakers'; IEE Proceedings A, Vol. 143, No. 6; 1993; pp 522-528

[195] P. Andre; 'Composition and Thermodynamic Properties of Ablated Vapours of PMMA, PA6-6, PETP, POM and PE'; Journal of Physics D: Applied Physics; Volume 29; p1963-1972; 1996

[196] P. Kovitya; 'Thermodynamic and Transport Properties of Ablated Vapors of PTFE, Alumina, Perspex and PVC in the Temperature Range 5000-30000K'; IEEE Transactions on Plasma Science; Volume PS-12; No. 1; 1984

[197] H.M. Looe, J.D. Yan and J.W. Spencer; 'Development of a Non-SF_6 Self-Blast Type Interrupter Unit'; Proceedings of the XVII International Conference on Gas Discharges and Their Applications, Cardiff; 2008

Appendix

APPENDIX

CONTENTS:

APPENDIX I – TEST CHAMBER DIMENSIONS

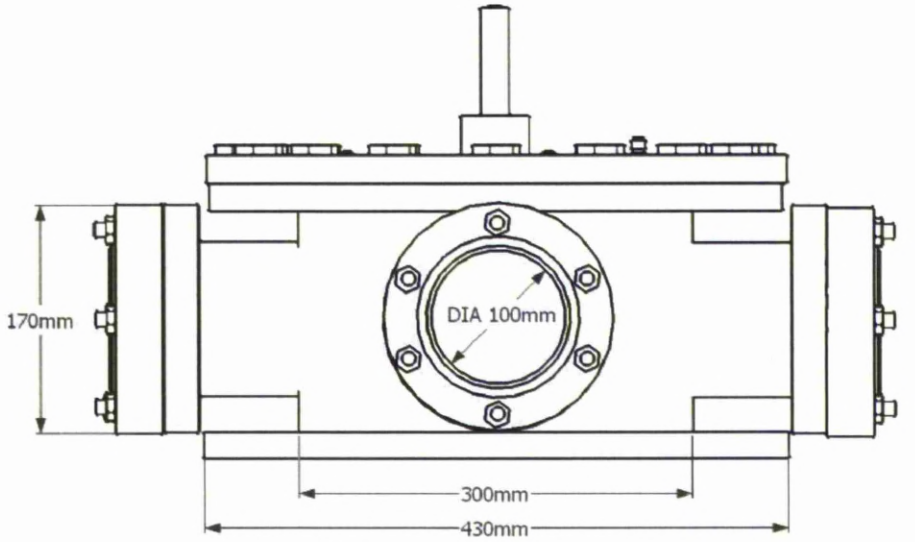

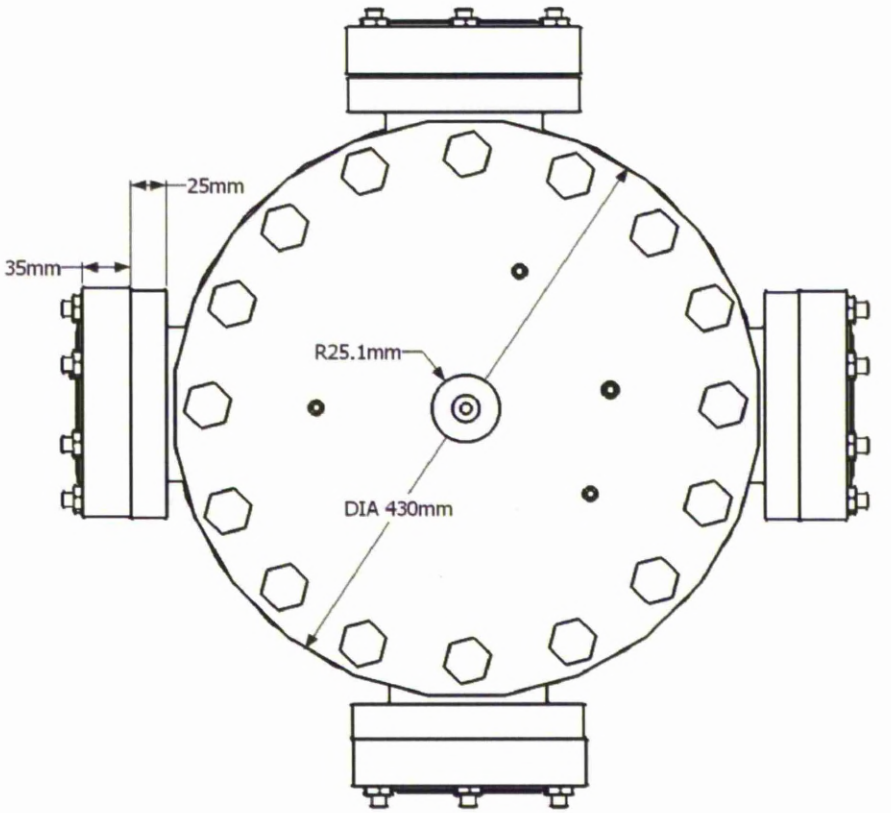

APPENDIX II – ADDITIONAL RESULTS FIGURES

POLYMERIC OPTICAL SPECTRA

Further to the results in Chapter 6, additional spectra from polymeric arcs are given here to demonstrate consistency.

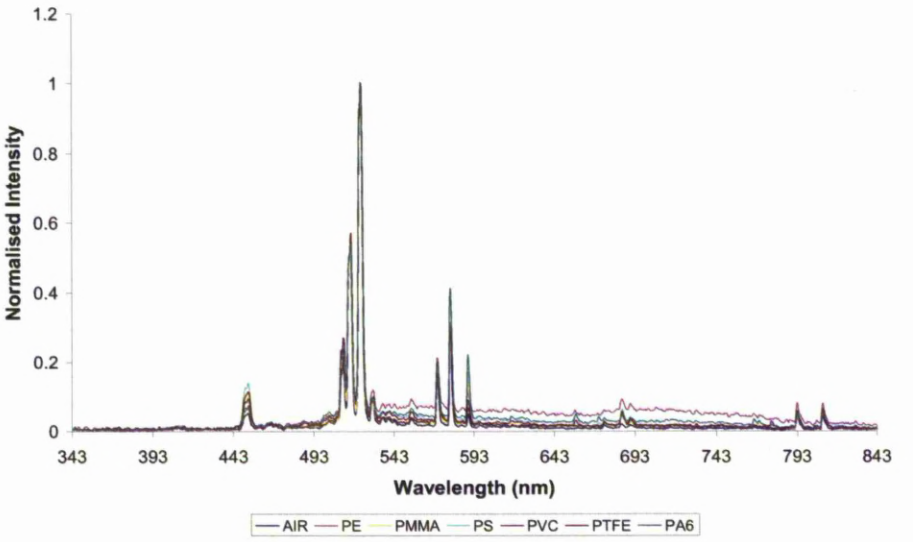

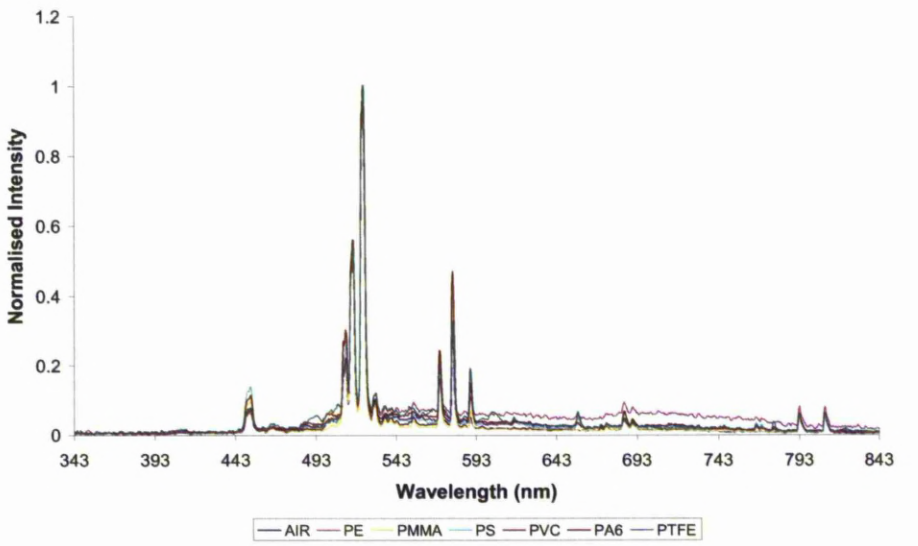

By measuring the peak intensity of the main spectral features in each polymer arc over three sets of tests and combining the results, the mean intensity of Cu(I), Cu(II) and polymer related spectral lines can be plotted, shown below respectively. Again, this demonstrates consistency between polymer arcs of the same structure and composition.

Mean intensity of Cu(I) spectral lines

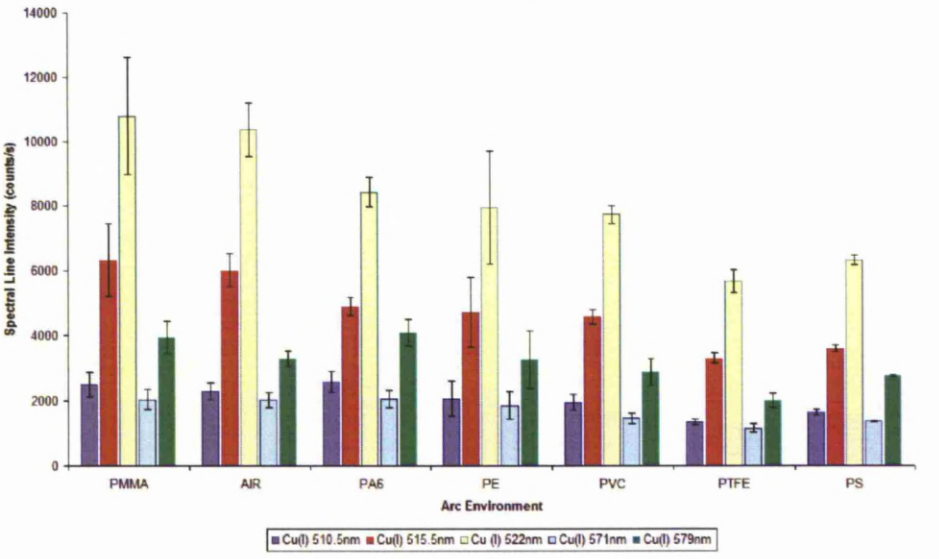

Mean intensity of Cu(II) spectral lines

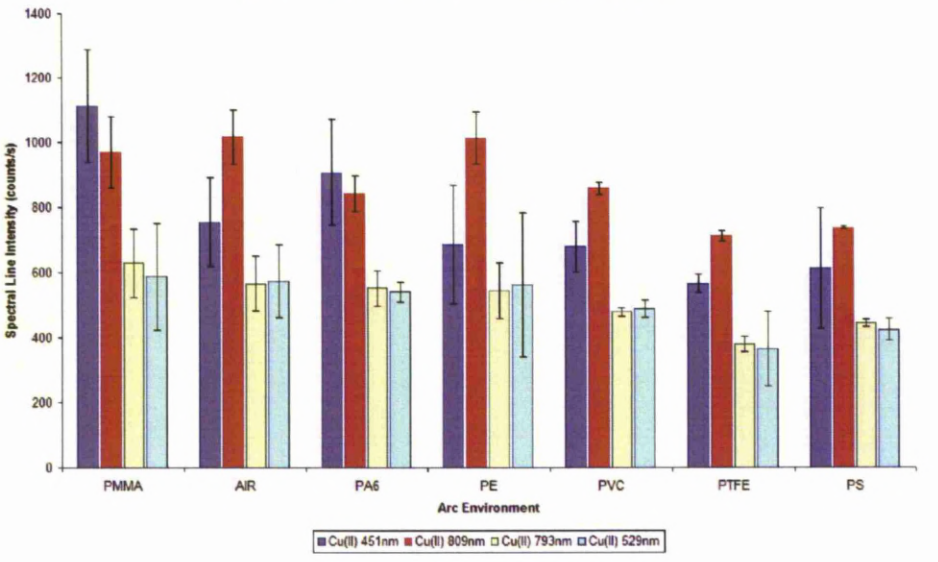

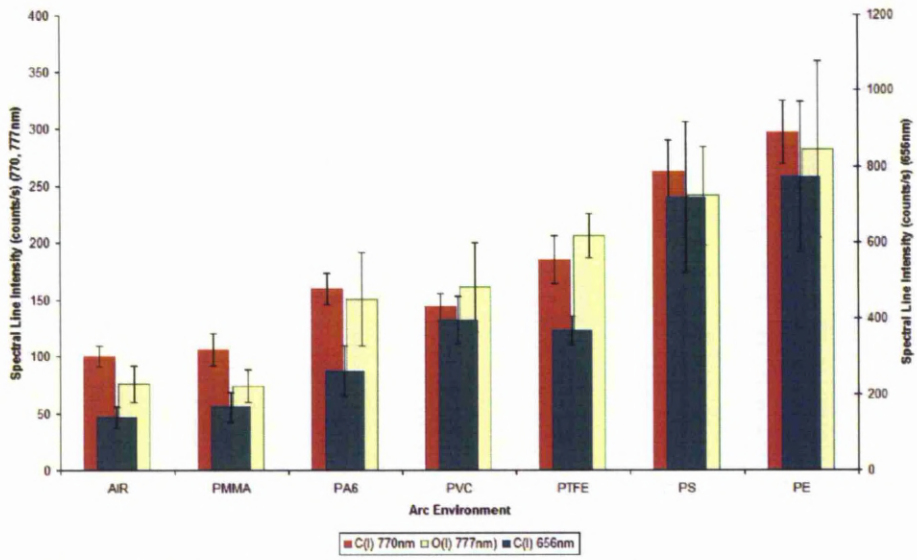

Mean intensity of the main polymer-arc related spectral lines

The results show consistency with the representative set of results described previously. A certain amount of error must be expected in this type of test due to the instability and relative unpredictability of the electric arc plasma; however the general trends can be seen and are valid to allow interpretation.

CHROMATIC FILTERING OF POLYMERIC SPECTRA

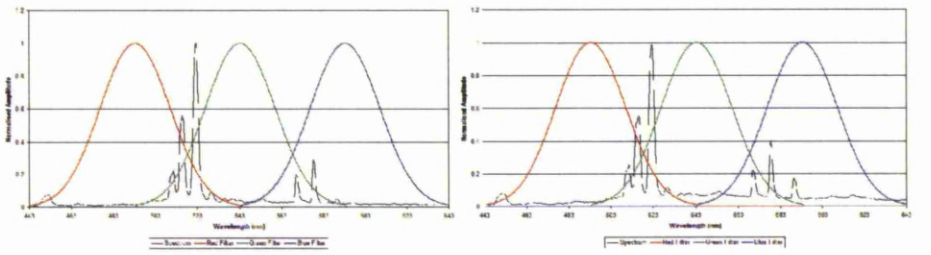

(a)

(b)

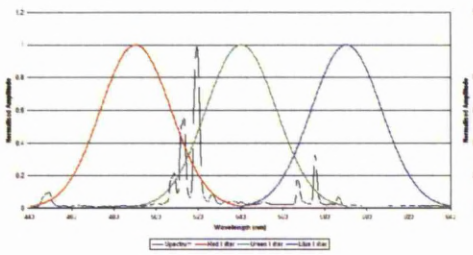

(c)

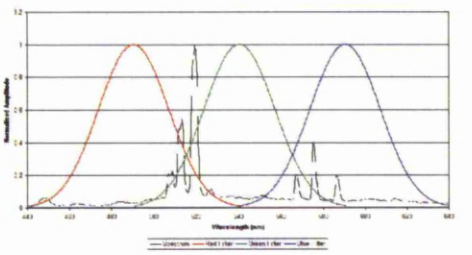

(d)

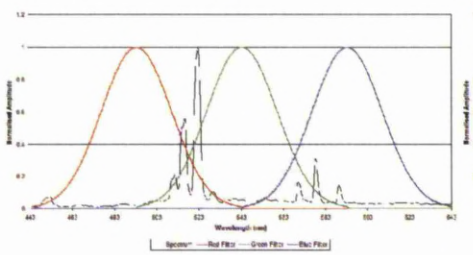

(e)

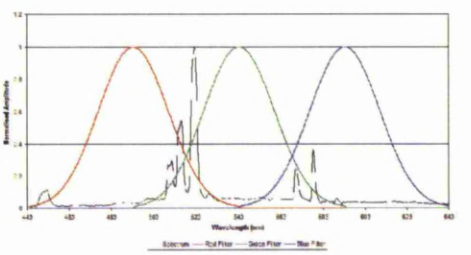

(f)

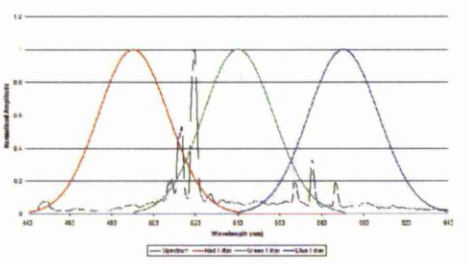

(g)

Gaussian shaped chromatic filters on different test spectra: (a) Air; (b) PE; (c) PMMA; (d) PS; (e) PVC; (f) PA6; (g) PTFE

BOLTZMANN PLOTS OF SPECTRAL INTENSITY

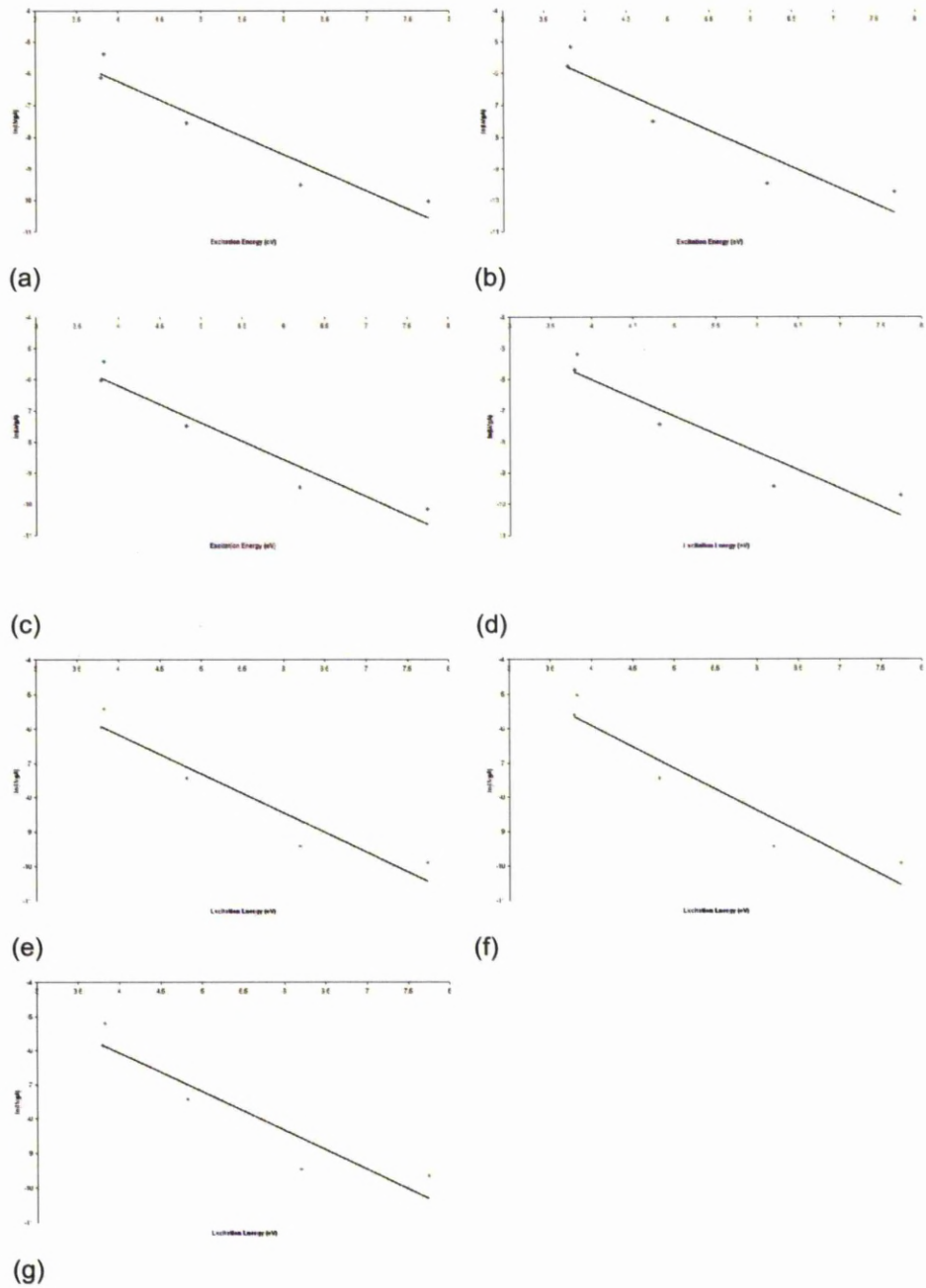

Figure 8-15: Example Boltzmann plots of Cu(I) emissions: (a) Air; (b) PE; (c) PMMA; (d) PS; (e) PVC; (f) PTFE; (g) PA6

Boltzmann plot gradient to temperature values

	Boltzmann Gradient	Temperature (K)
Set 1		
AIR	-1.1564	10000
PE	-1.1615	9990
PMMA	-1.1886	9760
PS	-1.1670	9940
PVC	-1.1368	10200
PTFE	-1.2366	9380
PA6	-1.1289	10300
Set 2		
AIR	-1.1819	9820
PE	-1.1538	10100
PMMA	-1.2261	9460
PS	-1.2055	9630
PVC	-1.2105	9590
PTFE	-1.1260	10300
PA6	-1.2009	9660
Set 3		
AIR	-1.1564	10000
PE	-1.1538	10100
PMMA	-1.1886	9760
PS	-1.2055	9630
PVC	-1.2105	9590
PTFE	-1.2366	9380
PA6	-1.1289	10300

MASS SPECTROSCOPIC RAW DATA

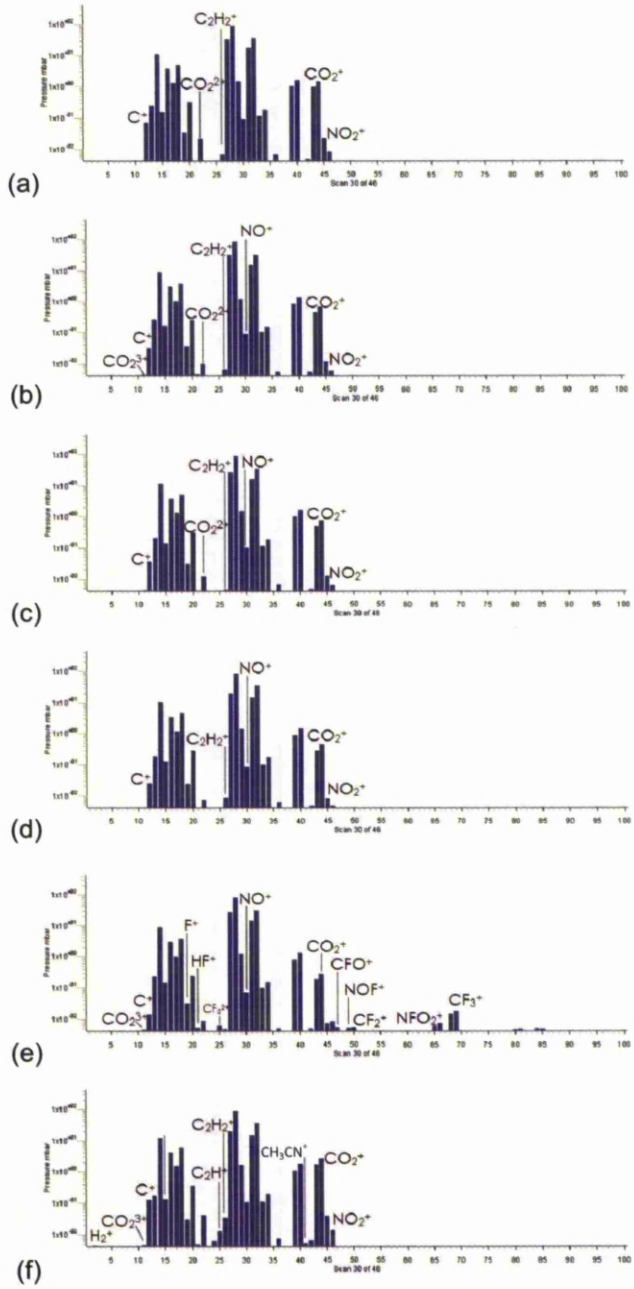

Mass spectra of polymeric arcs – results set 2: (a) PS; (b) PA6; (c) PMMA; (d) PVC; (e) PTFE; (f) PE. (Logarithmic scale)

PRE AND POST ARC ABUNDANCE OF C AND CO_2

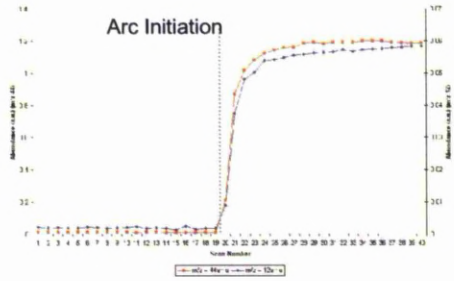

(a)

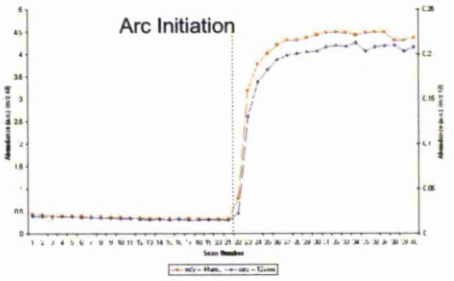

(b)

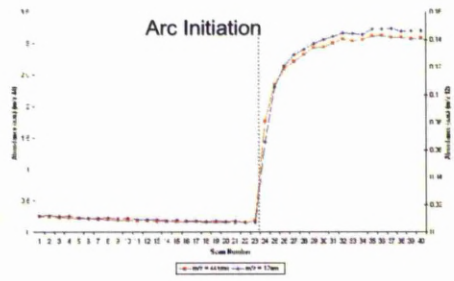

(c)

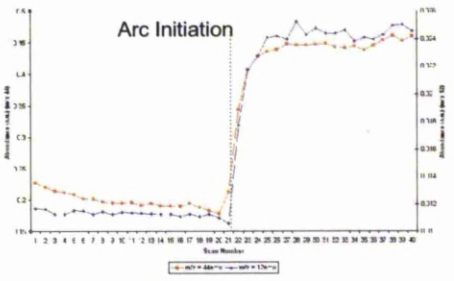

(d)

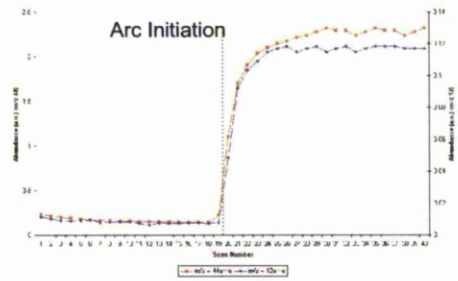

(e)

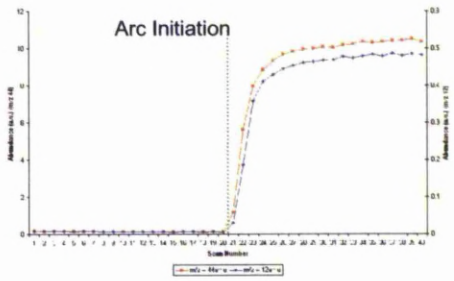

(f)

Formation of carbon and carbon dioxide as a result of the arc in the case of each polymer: (a) PS, (b) PA6, (c) PMMA, (d) PVC, (e) PTFE, (f) PE

APPENDIX III – PUBLICATIONS

This section contains publications made as a result of research conducted during this project:

- R.J. Brookes, H.M, Looe and J.W. Spencer; 'Atomic Spectroscopy for the Analysis of Switchgear Operating with Polymeric Replacements for SF_6'; XVII International Conference on Gas Discharges and Their Applications; 2008

Accepted publications not yet presented:

- R.J. Brookes and J.W. Spencer; 'Influence of Combustion of Polymer Arc Interruption'; XVIII International Conference on Gas Discharges and Their Applications; 2010

- R.J. Brookes and J.W. Spencer; 'Pressurisation Characteristics of Polymeric Interruption Media'; XVIII International Conference on Gas Discharges and Their Applications; 2010

INVESTIGATION USING ATOMIC SPECTROSCOPY FOR THE ANALYSIS OF ARC DISCHARGES IN SWITCHGEAR OPERATING WITH POLYMERIC REPLACEMENTS FOR SF_6

R J Brookes, H M Looe and J W Spencer

Department of Electrical Engineering and Electronics, The University of Liverpool, Brownlow Hill, Liverpool, L69 3GJ, United Kingdom. joe@liverpool.ac.uk

ABSTRACT

It may be possible to replace SF_6 gas in power switchgear by exploiting the arc quenching properties of common polymeric materials. In this research, the complex interactions between polymers and arc plasma have been investigated in a realistic environment using a model circuit breaker. The polymers studied were polyethylene and polymethylmethacrylate, which exhibit different processes to quench the arc involving energy removal by melting and secondary reactions respectively.

1. INTRODUCTION

Sulphur hexafluoride (SF_6) gas is one of the most potent greenhouse gasses known and is significantly more damaging to the environment than CO_2. SF_6 has been identified by the United Nations and World Meteorological Organisation (WMO) Intergovernmental Panel on Climate Change (IPCC) as having a global warming potential approximately 23,000 times higher than CO_2[1]. The increasing worldwide demand for electrical energy[2] requires more switchgear and so the amount of SF_6 potentially released into the atmosphere is forecast to continue to increase exponentially into the future[3]. This paper describes part of an investigation into the possibility of replacing SF_6 in high voltage circuit breakers by the novel use of common and readily available polymeric materials to aid in arc extinction.

Polymer ablated vapour may enhance the interruption capability of switchgear[4] but there are complex physical and chemical processes involved that are not fully understood. The polymer-arc interaction generates a number of factors that contribute to interruption, including: convective cooling from pressure changes and turbulence effects that cause increased gas flow around the arc; reducing the arc plasma temperature by energy consumption due to ablation and decomposition; dissociation and electronegative effects due to the effect of ablated vapour.

In this paper, the polymers described are polyethylene (PE) and polymethylmethacrylate (PMMA). These were chosen because of their potential to exert different quenching actions on the arc due to different molecular structures. PE is formed from the ethylene monomer C_2H_4 whereas PMMA incorporates oxygen in its molecule and has a more complex structure with the chemical formula $C_5H_8O_2$. The polymer-arc interaction was studied by the use of mass spectrometry, optical emission spectroscopy, colour high speed video and chromatic analysis.

2. EXPERIMENTAL TECHNIQUE

The apparatus consisted of a simplified model circuit breaker that embodied a pressure vessel of volume $0.015m^3$ with three glass windows set 90° from each other that allowed ease of monitoring the discharge. Inside the vessel were two copper electrodes with a moving copper initiation rod that was operated by a solenoid mechanism. During a test a DC arc was drawn from the lower electrode by means of the moving initiation rod, which retracted into the upper electrode. The apparatus is shown in Figure 1.

A capacitor bank provided the input energy for the arc. Control was provided by a variable timing unit and cam timer in order to synchronise contact separation with application of the bank energy.

Solid powder polymers were applied directly into the arc column immediately on initiation.

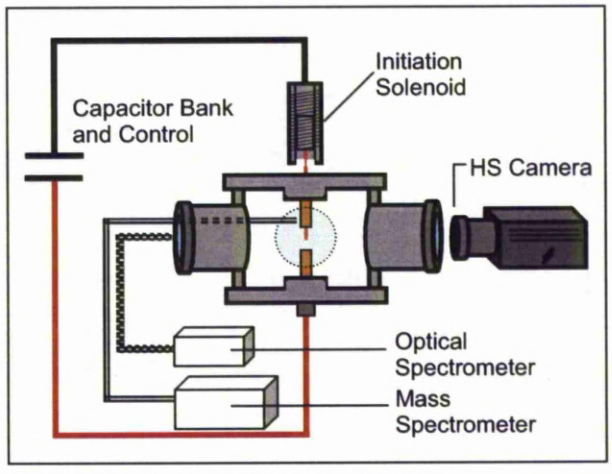

Figure 1: Test Chamber and Monitoring Apparatus

An MKS Cirrus quadrupole mass spectrometer was used to sample the gasses produced during an arcing event, its sampling tube entered the chamber and was placed 20mm away from the top electrode and 20mm above its contact surface.

For optical measurements, a Stellarnet EPP2000-LT14-VIS-10 optical spectrometer was used, which had a wavelength range of 350-1150nm and was fitted with a grating of 600g/mm and a 10μm slit that provided 0.8nm resolution.

Analysis of the optical spectra was also performed using the chromaticity method[5]. The chromatic values obtained, namely hue (H), lightness (L) and saturation (S) relate to the dominant wavelength, intensity and bandwidth of the signal respectively. These values can be plotted on polar plots that provide a measurable comparison between spectra for different arc environments.

Additionally, a Photron Fastcam SA.1.1 colour high speed camera was used to monitor the reaction between arc and polymer. This was placed 0.5m from the arc gap and used a x8 neutral density filter with a Kodak telephoto lens.

3. RESULTS

Figures 2, 3 and 4 show examples of optical spectra emitted from arcs in: air alone, air with PE and air with PMMA. It can be seen from these results that the powder reacts with the arc producing changes in the spectral lines compared to air (Fig. 2). The result for PE (Fig. 3) shows more spectral lines produced than for PMMA (Fig. 4).

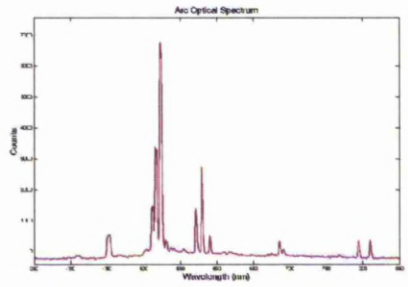

Figure 2: Optical Spectrum from Arc in Air

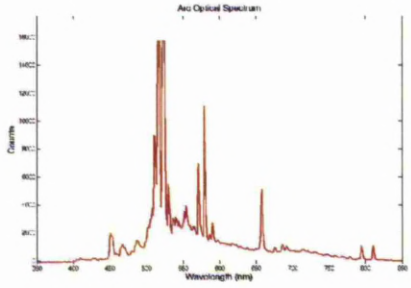

Figure 3: Optical Spectrum from Arc in Air with PE Powder

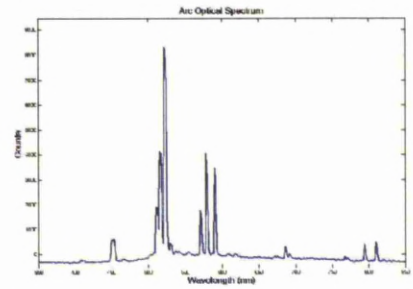

Figure 4: Optical Spectrum from Arc in Air with PMMA Powder

The chromaticity method allowed comparison between the spectral characteristics of arc plasma interactions with different polymers. The technique emphasises differences in the spectra that are not apparent from the original complex data. In this analysis, three non-orthogonal Gaussian shaped filters were used to filter each spectrum. The resulting polar plots are shown in Figures 5 and 6.

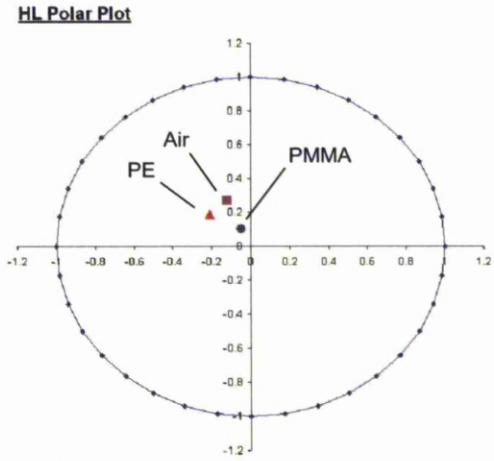

Figure 5: HL Polar Plot from Optical Spectra Emitted from Arcs in Air with Polymers

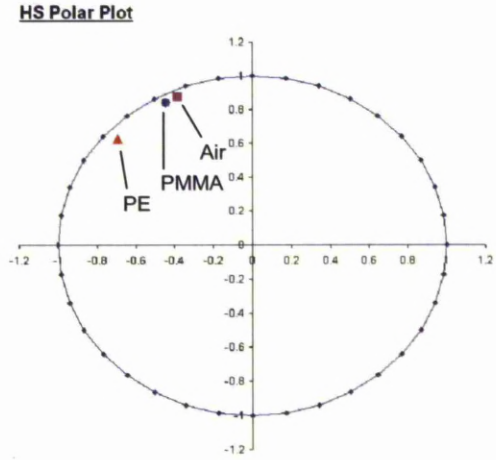

Figure 6: HS Polar Plot from Optical Spectra Emitted from Arcs in Air with Polymers

The HL Polar plot in Figure 5 shows a reduction in the luminance (intensity) of the PMMA arc. The intensity of PMMA is 63% less than that of air or PE.

Figure 6 shows that the saturation (bandwidth) of each spectrum is the same to within ±0.03 but the hue is rotated by an extra 24.6° for PE and 4.2° for PMMA compared to air. This is because of a change in the dominant emission wavelength and was caused by changes in spectral lines from PE and PMMA because of polymer decomposition products. For PE this change is particularly significant due to a strong line in the spectrum at 657nm that corresponded to singly ionised carbon[6] (Fig 3).

The relative spectral line intensities emitted from the stable arc in air were used to estimate the plasma temperature using established techniques[7]. Making the assumptions of local thermodynamic equilibrium and the plasma temperature being relatively constant over the discharge length, the average arc plasma temperature in air with no polymer was found to be approximately 5000K. This was important for later analysis, by knowing the arc plasma temperature it allowed greater understanding of the reason for the extent of polymer decomposition.

The mass spectrometer results help to confirm the differences in the reactions of the polymers in the arc. The arc temperature causes the polymers to mainly decompose into low molecular weight molecules containing carbon and hydrogen. PMMA probably forms more oxygen containing molecules due to the reaction of its molecular oxygen (Fig 8).

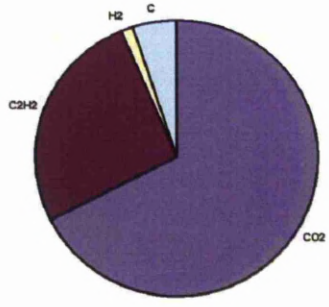

Figure 7: Comparison of Abundant Species Formed by PE Arc

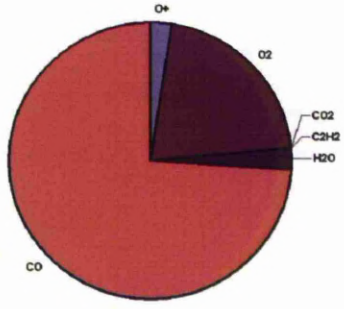

Figure 8: Comparison of Abundant Species Formed by PMMA Arc

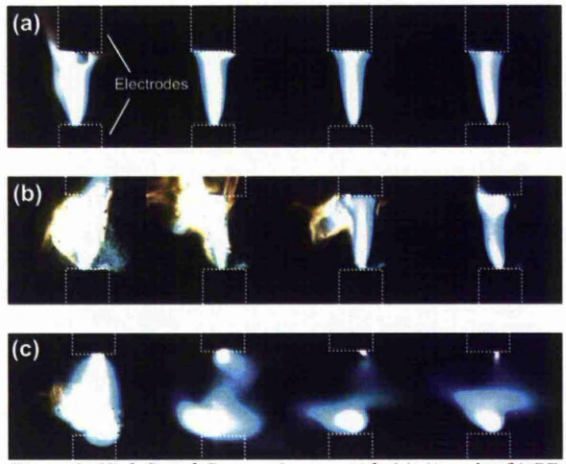

Figure 9: High Speed Camera Images with (a) Air only, (b) PE in air and (c) PMMA in air

The products formed by the arc reaction with PE and PMMA arcs are shown in Figures 7 and 8. It can be seen that polyethylene produces (in order of abundance): CO_2, C_2H_2, C^+, and H_2. Polymethylmethacrylate forms (in order): CO, O_2, O^+, H_2O, C_2H_2 and CO_2.

The high speed camera results give a visual indication of the arc-polymer interaction. Images are shown in Figure 9; each corresponding frame was taken at the same time period after arc initiation. The arc in air (Fig. 9a) is very stable, whereas the PE arc (Fig. 9b) is turbulent initially and produces a large amount of vapour, turbulence may help increase gas flow around the arc and increase convective cooling to aid in quenching. The PMMA arc (Fig. 9c) is more diffuse and less well defined, especially towards the later stages of the arc.

4. DISCUSSION

The PMMA results in Figure 5 show a reduction in intensity that suggests a reduction in the electron temperature implying that incorporating PMMA powder into the arc has a quenching effect. This effect is more significant with the incorporation of PMMA than with that of PE.

Figure 8 shows that the main species formed from the PMMA arc reaction was carbon monoxide. This is likely to be a secondary reaction between products of the initial decomposition. The formation of CO is highly endothermic and may assist in quenching the arc by removing energy. This may be formed by the following types of reaction[8]:

$C + H_2O \leftrightarrow CO\ (g) + H_2\ (g)$ ..... -135000 J/mol

$C + CO_2 \leftrightarrow 2CO\ (g)$ ..... -214000 J/mol

The implication is that the main quenching effect of PMMA is caused by secondary reactions of the dissociated PMMA vapour, which cools the arc,

reducing its conductivity. The dielectric strength of carbon monoxide is slightly higher than that of air[9] and so may have some benefit in the arc gap during dielectric recovery.

The most significant products formed by PE in the arc were CO_2 and C_2H_2 (acetylene), shown in Figure 7. In hydrocarbon gasses, the number of carbon-carbon bonds influences the electric strength of the gas[10]. Acetylene has a triple C-C bond and so has a good electric strength compared to normal air, its presence in the electrode gap may have some positive influence on reducing the conductivity of the arc and probability of re-ignition.

The results show that both PE and PMMA have arc quenching properties but do so in different ways. Polyethylene produces more vapour and seems to rely more on ablation and evaporation in order to quench the arc by removing thermal energy. PE may be more effective at this than PMMA because of the higher specific heat of PE ($1900JK^{-1}Kg^{-1}$) compared to PMMA ($1400\text{-}1500JK^{-1}Kg^{-1}$). In contrast, PMMA relies more on the resulting vapour and associated secondary reactions to quench the arc rather than the thermodynamic properties of its melting and evaporation. It can be seen by the mass spectrum that PMMA produces CO in a reaction that is highly endothermic. This could be due to the extra molecular oxygen available in PMMA that supports this reaction.

High speed imagery shows that the PMMA plasma appears diffuse and less well defined than an arc in the presence of PE. The diffuse nature may support the secondary reaction mechanism argument.

5. CONCLUSION

Both polyethylene and polymethylmethacrylate are effective at quenching arcs but do so in different ways. For polyethylene, a large amount of vapour is formed and the main quenching effect seems to be from energy removal through melting and evaporation and increased convection due to the reaction causing a turbulent arc. One of the decomposition products, acetylene, has a dielectric strength better than air[5] and so may have a positive effect in the electrode gap. Polymethylmethacrylate mainly cools the arc through highly endothermic secondary reactions producing carbon monoxide. PMMA is more effective at arc quenching than PE because of the effect of melting and evaporation coupled with its particularly effective secondary quenching processes.

ACKNOWLEGEMENTS

The authors wish to express their appreciation to the Engineering and Physical Sciences Research Council for supporting this project.

REFERENCES

[1] IPCC, "Climate Change 2001: The Scientific Basis. Contribution of Working Group I to the Third Assessment Report of the Intergovernmental Panel on Climate Change", Cambridge University Press, Cambridge, United Kingdom and New York, NY, USA, Chapter 6, p389, 2001

[2] International Energy Agency (IEA), *World Energy Outlook, 2006 Edition,* IEA, p138, 2006

[3] L. G. Christophourou, J. K. Olthoff and R. J. Van Brunt, "Sulphur Hexafluoride and the Electric Power Industry", National Institute of Standards in Technology, 1997

[4] D. Telfer, J.E. Humphries, J.W. Spencer and G.R. Jones G R, "Influence of PTFE on arc quenching in an experimental self pressured circuit breaker", Proceedings of the 14th International Conference on Gas Discharges and their Applications, University of Liverpool, UK, Vol. 1, 1-6 September, pp.91-94, 2002

[5] G.R. Jones, A.G. Deakin and J.W. Spencer, *Chromatic Monitoring of Complex Conditions*, Taylor and Francis, 2008

[6] CRC, *Handbook of Chemistry and Physics, 84th Edition*, CRC Press, p10-12, 2003

[7] W.Lochte-Holtgreven, *Plasma Diagnostics*, John Wiley and Sons, pp178-183, 1968

[8] P.F. Hettwer, "Arc-Interruption Characteristics of Common Polymeric Materials", IEEE Transactions on Power Apparatus and Systems, Vol. PAS-101, No. 6, 1982

[9] L.I.Berger, *Dielectric Strength of Insulating Materials, 84th Edition of the CRC Handbook of Chemistry and Physics*, CRC Press, pp15-34, 2003

[10] A.E.D. Heylen, T.J. Lewis, "The Electric Strength of Hydrocarbon Gasses", British Journal of Applied Physics, Vol. 7, pp411-415, 1956

INFLUENCE OF COMBUSTION ON POLYMER ARC INTERRUPTION

R J BROOKES AND J W SPENCER

Centre for Intelligent Monitoring Systems, Department of Electrical Engineering and Electronics, University of Liverpool, Brownlow Hill, Liverpool, L69 3GJ, United Kingdom. joe@liv.ac.uk

ABSTRACT

The interaction between particulate polymers and arc plasma can potentially aide in the circuit breaker interruption role. This is a complex process involving a number of physical and chemical aspects. In an air host gas, combustion of decomposed volatile hydrocarbons leads to effects that may improve the interruption process and may also lead to potentially lower operating costs of new designs.

1. INTRODUCTION

It is already known that the ablation of polymeric materials, such as PTFE nozzles, in circuit breakers can play a part in arc control [1]. In the development of new interrupter methodologies, it is desirable to investigate these complex phenomena more deeply so as to enable the effect to be exploited to the greatest extent. Previous research has shown that the application of micron scale polymer particulates in arc plasma can enhance the interruption effect by exposing a greater surface area to the plasma for reaction [2] [3]. Some of the key mechanisms that occur in these reactions are energy extraction through ablation processes, plasma turbulence and increased convective cooling and the formation of secondary gasses around the arc that improve dielectric and thermal performance. So as to reduce the cost and complexity of new gas circuit breaker designs, it is appealing to utilise air at atmospheric pressure as the main arc medium. However, conventionally this requires the arc to be extended a significant distance so as to increase arc resistance to the extent that interruption occurs, consequently air insulated circuit breakers require large outdoor spaces or high pressures in which to operate successfully. It is possible that the polymer-plasma interaction in a contained atmospheric air environment can enable more compact interrupter designs that are also of low cost and do not require the environmentally harmful SF_6 gas. This work is undertaken when it is becoming increasingly pertinent to the power industry that alternative methodologies to SF_6 are explored, as growing political [4] [5] and social pressure may lead to financial penalties being introduced related to SF_6 emissions. As the power industry uses 80% of the SF_6 manufactured each year [6], strong industrial motivation to find alternatives exists.

2. EXPERIMENTAL TECHNIQUE

This investigation utilised practical experimentation using a realistic representation of a circuit breaker environment in conjunction with a range of diagnostic apparatus. The main chamber consisted of a steel pressure vessel containing copper electrodes and a copper initiation electrode driven by a solenoid to represent contact opening; the main test chamber is shown in Figure 1.

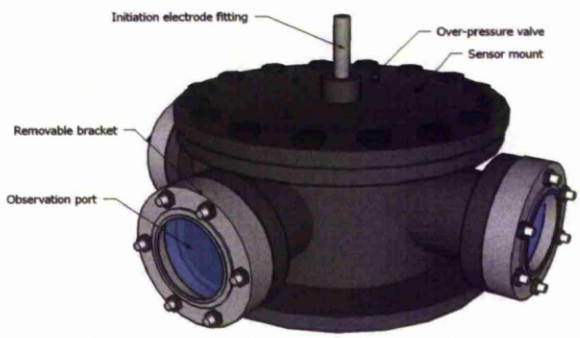

Figure 1: Experimental test chamber and fittings

The arc was formed by the discharge of a 33mF capacitor bank synchronised with the separation of the initiation electrode from the anode. When the initiation electrode was fully retracted, an arc was formed between the anode and cathode that was 30mm in length. At this point, particulate polymers were entrained to the arc plasma.

The polymer particulates under test were weighed by use of an ISO9001 compliant chemical balance and loaded into a chamber at the front of the apparatus. A storage cylinder was charged to 172kPa with nitrogen from a master cylinder. At the correct time, a signal from the timing and control unit opened the solenoid valve and discharged the N_2 seeded with polymer particulates into the plasma. The outlet of the injection mechanism was directly in line with the centre of the arc.

A suite of diagnostic apparatus was used in each test so as to monitor the changes in the discharge as a result of the interaction. As well as arc current and voltage measurements, mass spectrometry was carried out by use of an MKS Cirrus residual gas analyser in conjunction with the Process Eye Professional software. The changes in pressure inside the chamber were recorded by use of a Kystler Type 601A piezoelectric pressure sensor in conjunction with a charge amplifier and oscilloscope.

The polymers chosen for experimentation were selected to have differences in structure and composition so as to affect differing reaction mechanisms. The polymers under test and their respective structures are described in Table 1.

Table 1: Structures of polymers under test [7]

Polymer	Abr.	Structure
Polyethylene	PE	$-CH_2-CH_2-$
Polyamide 6	PA6	$-CO-(CH_2)_5-NH-$
Polytetrafluoroethylene	PTFE	$-CF_2-CF_2-$
Polymethylmethacrylate	PMMA	$CH_2-C(CH_3)(COOCH_3)-$
Polystyrene	PS	$-CH(C_6H_5)-CH_2-$
Polyvinylchloride	PVC	$-CH_2-CH(Cl)-$

3. RESULTS

A complex mixture of chemical species was detected because of the polymer decomposition process as a result of the arc. The mixture differed in composition and abundance for different polymer-arcs, highlighting the effect of the polymer compositions.

By the use of mass spectrometry, the mixture of species was determined and in all cases it was found that CO_2 comprised the greatest abundance. As an example, a pie chart is shown in Figure 4 highlighting the species formed from the interaction between PTFE and PE particulates and arc plasma respectively. Note that this only includes new species formed as a result of the plasma-polymer interaction and not existing species in the chamber, such as N_2 or O_2.

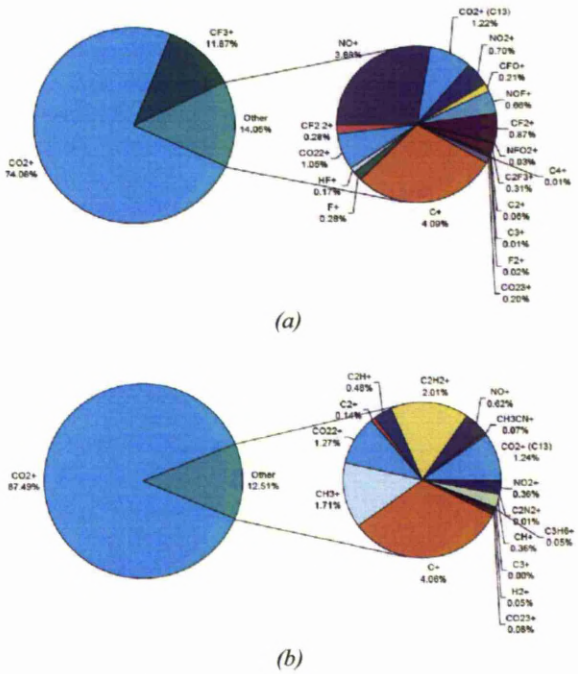

Figure 4: Abundance of chemical species formed as a result of polyethylene-plasma interaction

The formation of CO_2 can be directly associated with the interaction between the arc plasma and the polymeric particulates. A comparison between the mass spectroscopic traces taken for a polyethylene arc in comparison with an arc in air in the absence of polymers shows the distinction clearly, shown in Figure 5.

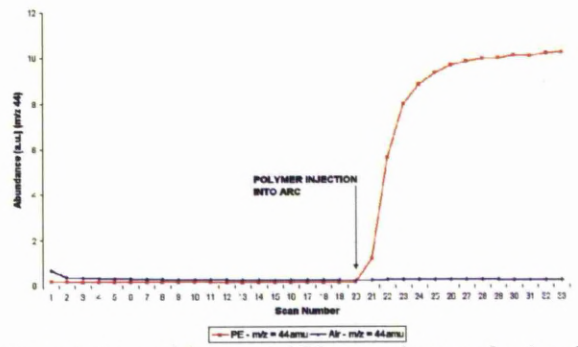

Figure 5: Temporal formation of CO_2 pre and post arc for air and polymeric arcs

In Figure 5 it can be observed that with a polymeric arc, at the point of arc formation the mass spectrometer detects the growing abundance of m/z 44 (CO_2^+), whereas in a plain air arc there is no such species detected. The production of this gas is as a result of a combustive chemical reaction between volatile hydrocarbon species dissociated from the polymers and atmospheric oxygen.

A chart showing the percentage of carbon dioxide formed in each case as a result of the polymer interaction is shown in Table 2.

Table 2: Abundance of CO_2 formed as a result of polymer plasma interaction

Polymer	% CO_2 (m/z 44)
No polymer arc	X
Polystyrene	82.23
Polyamide 6	89.68
Polymethylmethacrylate	82.54
Polyvinylchloride	63.69
Polytetrafluoroethylene	74.08
Polyethylene	87.49

The formation of carbon dioxide varies between polymer species due to differences in structure and composition that lead to a different combination of decomposed carbon species. Differences in the mean volumetric abundance of CO_2 detected by mass spectrometry after a range of experiments are shown in Figure 6; polyethylene can be observed to produce significantly more CO_2 than any of the other polymers.

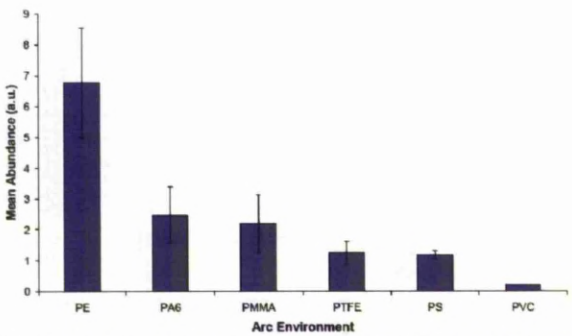

Figure 6: Abundance of CO2 formed in different polymer environments

4. DISCUSSION

The extent of the formation of volatile hydrocarbons differed between polymers due to inherent differences in their composition. Certain species act as combustion inhibitors due to their alteration of the oxygen radical mechanism. This is the case with PTFE and PVC which contain fluorine and chlorine respectively. It is also related to the structure of the polymer and the effect that this has on melting point. Polymers with higher melting temperatures resist combustion more effectively. Polyethylene formed the most volatile mixture of hydrocarbon species of those tested and was seen to form the greatest volume of carbon dioxide. This also relates to the pressure rise observed in the test chamber [8], which was highest with CO_2 and implies pressurisation was achieved in the most part by the formation of a large volume of carbon dioxide. This is shown in Figure 7.

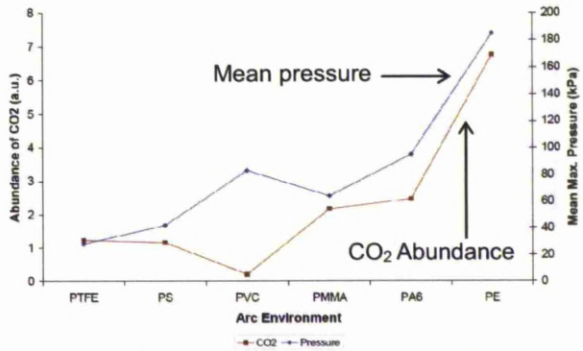

Figure 7: Formation of CO_2 compared with recorded pressurisation observed in experimentation with different polymers

In the cases of PTFE, PS and PVC a less volatile mixture of species was formed which inhibited combustion to a greater extent by virtue of those polymers inherent structure and composition. Consequently, the volume of CO_2 formed and the associated pressurisation was less pronounced in those cases.

In terms of interruption performance, the combustion reaction has both positive and negative aspects. The thermodynamics of the combustion reaction is exothermic in nature and consequently may reduce the cooling efficiency between the plasma and surrounding gas. The positive aspects are the formation of carbon dioxide, which has improved dielectric and thermal conductivity with respect to air (0.070W/mK compared to 0.045W/mk for air), and is already used in prototype interrupter units [9]. The second advantageous aspect is the pressurisation achieved due to the formation of a large volume of gas. This causes increased convective cooling and electrode gap de-ionisation, there is also evidence [8] that the reaction destabilises the arc, further enhancing cooling effects and increasing arc resistance.

The complex nature of the chemical reactions around the electrode gap between decomposed polymer species has been determined and a flow chart highlighting the different reaction routes is shown in Figure 8.

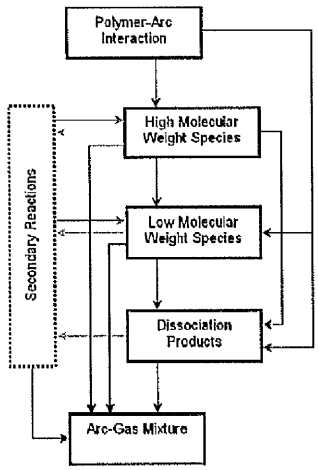

Figure 8: Polymeric arc species complex formation routes

Given the complexity of the reaction process highlighted in Figure 8, proper determination of the complex reaction mechanisms and consequently the thermodynamic processes which may aide or impede the thermal control of the arc is extremely difficult.

5. CONCLUSION

The complex interaction between micron scale particulate polymers and circuit breaker arc plasma has the potential to be exploited in practical applications. It is environmentally and economically favourable to develop new circuit breaker designs that can operate in benign environments such as in air or nitrogen, and the polymer-plasma interaction may enhance the interruption performance of such designs. In air, a combustion based reaction occurs between decomposed carbon based fragments from the polymers and atmospheric oxygen. This produces a large volume of CO_2 that can enhance energy losses from the plasma by increasing convective cooling, turbulence and enhance the gas thermal and dielectric capacity proximate to the arc.

ACKNOWLEDGMENTS

The authors with to thank the Engineering and Physical Sciences Research Council for supporting this project.

REFERENCES

[1] D.J. Telfer, J. Humphries, J.W. Spencer, GR Jones; "Influence of PTFE on Arc Quality Using an Experimental Self Pressurised Circuit Breaker"; Proceedings from the XV International Conference on Gas Discharges and their Applications (GD2002), Volume 1; 2002

[2] R.J. Brookes, H.M, Looe and J.W. Spencer; "Atomic Spectroscopy for the Analysis of Switchgear Operating with Polymeric Replacements for SF_6"; XVII International Conference on Gas Discharges and Their Applications; 2008

[3] Y. Tanaka, Y. Takeuchi, T. Sakuyama, Y. Uesugi, S. Kaneko, S. Okabe; "Numerical and Experimental Investigations on Thermal Interaction between Thermal Plasma and Solid Polymer Powders using Induction Thermal Plasma Technique"; Journal of Physics D: Applied Physics; Volume 41; 2008

[4] P. Horrocks; "EU Proposed Legislation on Fluorinated Greenhouse Gases: The Case of SF_6"; European Commission, Environment Directorate; European Commission; 2004

[5] United Nations; "Kyoto Protocol to the United Nations Framework Convention on Climate Change"; United Nations Framework Convention on Climate Change; 1998

[6] United States Environmental Protection Agency; "SF_6 Emission Reduction Partnership for Electric Power Systems"; Environmental Protection Agency Report; 2005

[7] W. Martienssen and H. Warlimont (Eds.); *Springer Handbook of Condensed Matter and Materials Data;* Springer; 2005; pp480-501

[8] R.J. Brookes, H.M. Looe and J.W. Spencer; 'Pressurisation Characteristics of Polymeric Interruption Media'; XVIII International Conference on Gas Discharges and Their Applications; 2010

[9] T. Matsumara, I. Morookaa, Y. Yokomizua and M. Suzukia; 'Arc Parameters in CO2-Blast Quenching Chamber with a High Pressure Storage Tank'; Proceedings of the 5th International Symposium on Applied Plasma Science, Vol. 80, Iss. 11-12; 2006; pp26-30

PRESSURISATION CHARACTERISTICS OF POLYMERIC INTERRUPTION MEDIA

R J BROOKES AND J W SPENCER

Centre for Intelligent Monitoring Systems, Department of Electrical Engineering and Electronics, University of Liverpool, Brownlow Hill, Liverpool, L69 3GJ, United Kingdom. joe@liv.ac.uk

ABSTRACT

The application of polymer particulates to arc plasma causes a variety of reaction effects. Some of the reactions lead to mechanisms that enhance plasma cooling and energy loss, which improves interruption quality. One such effect is pressurisation caused by the reaction and the gaseous species formed. This leads to increased arc turbulence and increased convective cooling, which improve thermal energy extraction.

1. INTRODUCTION

It is very common for gas circuit breakers to utilise a flow of gas for the purposes of arc quenching. A gas flow cools the arc and de-ionises the electrode gap, reducing conductivity and improving the recovery of dielectric strength. In all types of gas circuit breakers, a flow is caused by creating a pressure differential by some means, for example by mechanical pressurised gas injection ('puffer') or by exploiting the heating effects of the arc itself in conjunction with an expansion volume ('self-blast'). In any case, enhancement of the flow effect is often desirable so as to improve the performance of the circuit breaker; this is particularly pertinent in terms of low current operation of self-blast circuit breakers, which may struggle to achieve adequate pressurisation without the aide of additional piston based gas flow processes [1]. It is known that the ablation of polymers in different types of circuit breakers can introduce effects that aid in the task of arc control [2], but little is known of how this can be more fully exploited operationally. Previous research [3] has shown that pressurisation effects may be an important aspect of the polymeric interruption mechanism which could lead to better utilisation of polymers in circuit breaker applications. The use of particulates as opposed to larger solid pieces of material has been proposed so as to maximise the interaction between the arc and polymers and hence enhance the positive arc controlling reactions. For this investigation, micron scale polymer particulates of six different varieties were selected. They were chosen to be common and readily available at reasonable cost, which would enable future designs to be economically viable. The polymers chosen were polyethylene (PE), polyamide 6 (PA6), polytetrafluoroethylene (PTFE), polymethylmethacrylate (PMMA), polystyrene (PS) and polyvinylchloride (PVC). These polymers were selected due to their differences in structure and composition, that is, the component atoms and the way in which they were bonded together. These differences were hypothesised to lead to different reaction mechanisms and consequently differing arc control effects, which could be studied.

2. EXPERIMENTAL TECHNIQUE

Practical experimentation was carried out in a realistic approximation of a circuit breaker in conjunction with an array of diagnostic apparatus to monitor the discharge and its interaction with the polymer particulates. An arc was formed between copper electrodes by the simultaneous discharge of a 33mF capacitor bank with the opening of a solenoid driven initiation electrode, which drew an arc between the contacts. The arc was formed inside a pressure vessel which incorporated ports to allow easy diagnostic access without compromising the integrity of the chamber. For the purposes of this investigation, a pseudo-DC arc was formed so as to provide a longer duration of 200ms in order to monitor the plasma-polymer interaction and consequent arc control effect. The circuit breaker test chamber apparatus is shown in Figure 1.

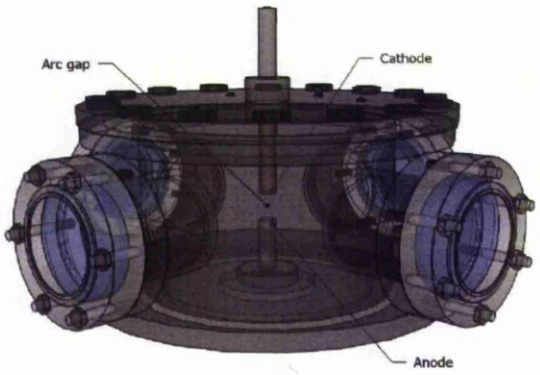

Figure 1: Experimental arc vessel and electrode configuration

Particulates were applied by means of compressed nitrogen gas propellant, triggered by a central timing and control system. Polymer particulates were applied at a precisely controlled time period such that the particulates were injected into the fully formed and stable arc, this ensured repeatability and comparable experimental conditions. The polymer injection apparatus is shown in Figure 2. In each case 4g of each polymer were weighed and applied for each test.

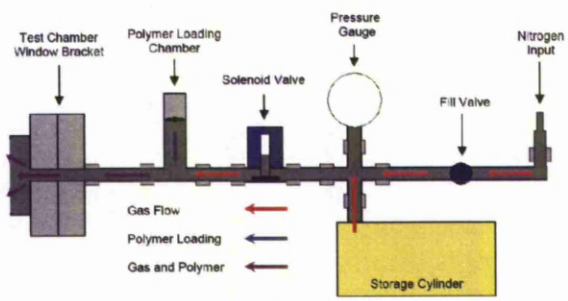

Figure 2: Polymer injection mechanism

The interaction was monitored by use of a piezoelectric pressure sensor, voltage and current probes and high speed video imaging. The sensor deployed was a Kistler 601A piezoelectric pressure sensor used in conjunction with a charge amplifier and oscilloscope. This configuration allowed fast response to dynamic changes due to arc induced pressurisation To visually record the plasma-polymer interaction a Vision Research Phantom V7 high speed video camera was used, at a resolution of 800x600 and 4700fps, with an exposure time of 200μs. This type of imaging provided a qualitative view of the changes induced in the plasma as a result of the polymer interaction, and was especially useful in developing understanding of the effect of polymer induced turbulence on the arc plasma.

3. RESULTS

Dynamic pressure measurements were carried out repeatedly for arcs in the presence of polymers. Due to the fact that nitrogen gas was used as a propellant, its effect on the overall test chamber pressure was quantified, both mathematically by using Boyles law and experimentally by injecting N_2 into the chamber alone. The propellant itself had a negligible effect on the overall pressurisation of the chamber, increasing by 8kPa. This was due to the relatively large volume of the chamber with respect to the smaller N_2 propellant volume. In the presence of an arc but without any polymer, the pressurisation of the chamber caused by the nitrogen propellant and arc heating was more pronounced and formed a baseline for comparison with polymeric tests, an example is shown in Figure 3. This was caused by the reaction between the N_2 gas flow and the arc plasma.

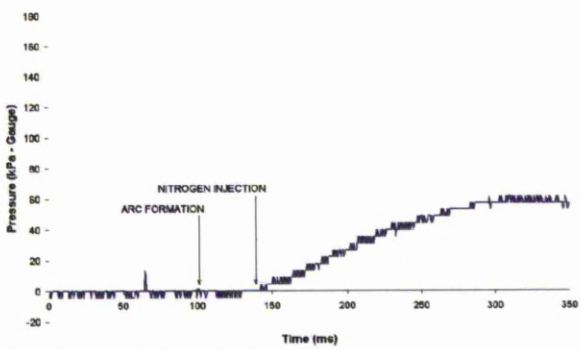

Figure 3: Temporal variation in pressure with N_2 injection

The use of N_2 injection seeded with polymeric particulates causes consistent changes to the measured pressurisation of the volume with respect to the baseline case. An example of the pressurisation caused by the application of polyethylene particulates to the arc plasma is shown in Figure 4; in the example given a pressure increase of 160kPa was observed. The inclusion of polymer caused more rapid pressurisation to a greater magnitude than was observed with N_2 alone; this was also the case with the polymers PA6, PVC and PMMA. In related research [4] it was found through mass spectrometry that those polymers form a significant volume of CO_2 due to the secondary chemical reactions between decomposed volatile hydrocarbon structures from the polymers and gaseous atmospheric oxygen in the chamber. It is likely that the rapid increases in pressurisation

were due to this effect, and were most pronounced in these polymers as a result of their composition.

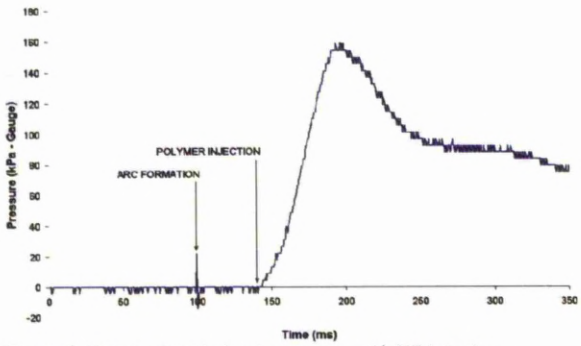

Figure 4: Temporal variation in pressure with PE injection

The situation becomes more complex however when the cases of the polymers polytetrafluoroethylene and polystyrene are considered. In those cases the pressurisation of the volume is less pronounced with respect to the baseline case, an example temporal pressure trace is shown in Figure 5.

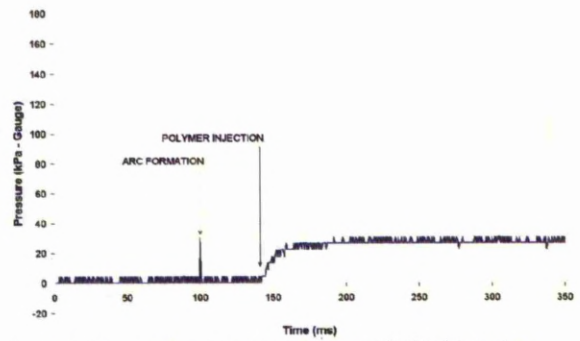

Figure 5: Temporal variation in pressure with PTFE injection

After repeated tests to ensure consistency, the mean pressure change measured in each case is shown in Figure 6.

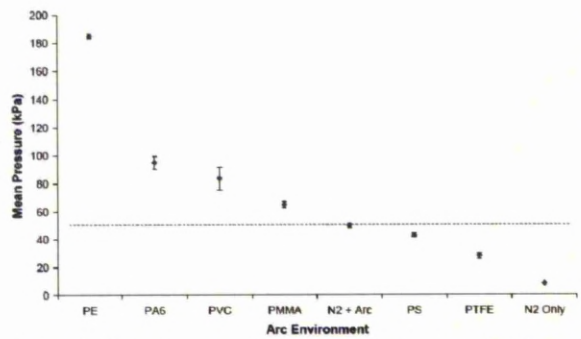

Figure 6: Mean pressure rise observed for a range of polymers when interacting with arc plasma

The variation observed from polymer to polymer shows the effect of differences in structure and composition that lead to differing reaction mechanisms and highlights the relationship between polymer structure and composition and arc control ability. It would appear that polymers which decompose into volatile hydrocarbon species are more successful due to the secondary reactions that lead to the formation of large volumes of gas.

Pressurisation due to the polymer plasma reaction causes increased gas flow around the arc which improves convective cooling of the arc, lowering its temperature and increasing its resistance. High speed imaging carried out in the absence of polymer particulates shows laminar arc plasma between the electrodes and the arc is in energy equilibrium and is stable. A representative image sequence showing this is shown in Figure 7. With the application of polymer particulates the arc becomes much more dynamic and turbulent, shown in Figure 8.

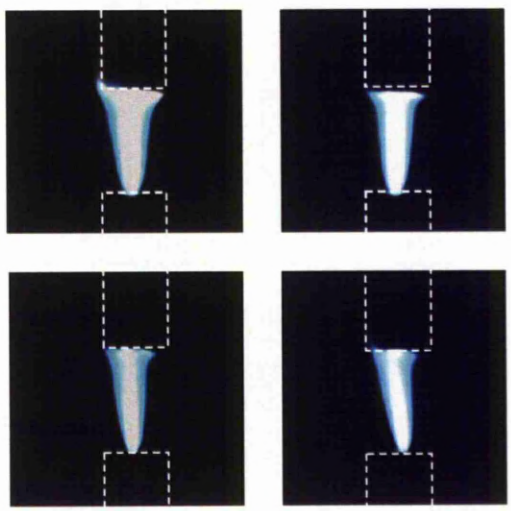

Figure 7: Laminar arc observed in air in the absence of polymer materials

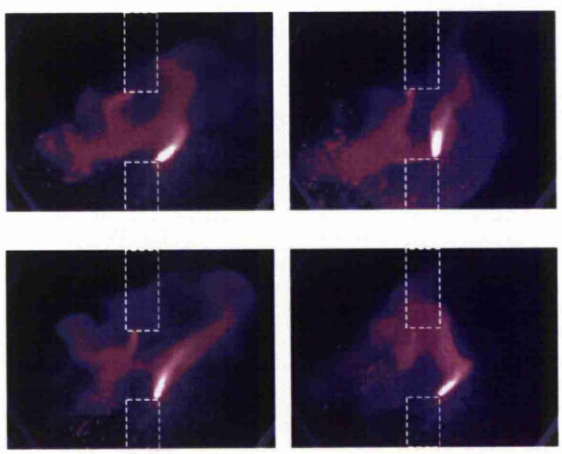

Figure 8: Instability and turbulence induced in the arc plasma as a result of polymer interaction and resulting pressurisation

From Figure 8, it can be observed that when polymer particulates are applied to the plasma the effect of the interaction was to initiate destabilisation, causing a much more turbulent and dynamic flow. The polymer induced dynamic flow can potentially be a positive effect in terms of arc control as it enhances the convective energy losses from the plasma and induces morphological changes which increase arc resistance.

4. DISCUSSION

In general there were three processes by which pressurisation was achieved in the experimental volume by use of polymers, they were: volume of injection propellant; arc heating of proximal gasses; and large volumes of gas formed related to polymer decomposition.

Pressurisation caused by the polymer interaction could benefit arc control in several ways. Firstly, changes in the ambient pressure can have a direct effect on the arc and can alter the thermal and electrical conductivity, changing the ability of the plasma to carry current. Secondly, during the arc phase a pressure differential between the upstream and downstream regions causes a flow effect which can extract energy through such mechanisms as heat convection, radiation and turbulence. Finally, in the post arc phase, interruption can be enhanced by improving the cooling of the electrode gap so as to better withstand the transient recovery voltage of the system. The enhancement of gas flow by pressurisation, caused most notably by polyethylene, is likely in the most part to be due to the formation of a large volume of CO_2. Different types of polymer caused different pressure changes due to their individual compositions which either enhanced or inhibited the reactions between decomposed polymer species.

The polymers PTFE and PS caused a reduction in arcing chamber pressure with respect to the baseline case. This is suggestive of not only a reduction in post decomposition gas production but also potentially a cooling effect on the arc gap. The difference in behaviour of the polymers highlights the complexity of the interaction and the fact that different polymers can be exploited in different roles. Of particular note is the potential for a polymer such as polyethylene be used to enhance self-blast interrupter operation at low current.

5. CONCLUSION

The interaction between particulate polymers and circuit breaker plasma is highly complex. In terms of arc control and quenching, it involves a wide variety of interrelated processes, one aspect of which is pressurisation. The additional pressurisation caused by the polymer-plasma interaction can enhance energy extraction from the arc by greater convective cooling, turbulence and post arc de-ionisation processes. Of particular note was the polymer polyethylene, which produced a significant pressurisation due to the secondary reactions between volatile decomposed polymer related hydrocarbons and the arc host gas. This process can potentially be used in operational circuit breakers to enhance the performance of self-blast configurations.

ACKNOWLEDGMENTS

The authors with to thank the Engineering and Physical Sciences Research Council for supporting this project.

REFERENCES

[1] D. Dufournet; 'Blast Off: The Latest Spring Operated Self Blast Mechanisms'; Think T&D – Winter 2009-10; Areva T&D; 2009

[2] D.J. Telfer, J. Humphries, J.W. Spencer, GR Jones; "Influence of PTFE on Arc Quality Using an Experimental Self Pressurised Circuit Breaker"; Proceedings from the XV International Conference on Gas Discharges and their Applications (GD2002), Volume 1; 2002

[3] R.J. Brookes, H.M, Looe and J.W. Spencer; 'Atomic Spectroscopy for the Analysis of Switchgear Operating with Polymeric Replacements for SF_6'; XVII International Conference on Gas Discharges and Their Applications; 2008

[4] R.J. Brookes, H.M. Looe and J.W. Spencer; 'Influence of Combustion on Polymer Arc Interruption'; XVIII International Conference on Gas Discharges and Their Applications; 2010